CENTRE FOR ECONOMIC POLICY RESEARCH

CEPR PRESS

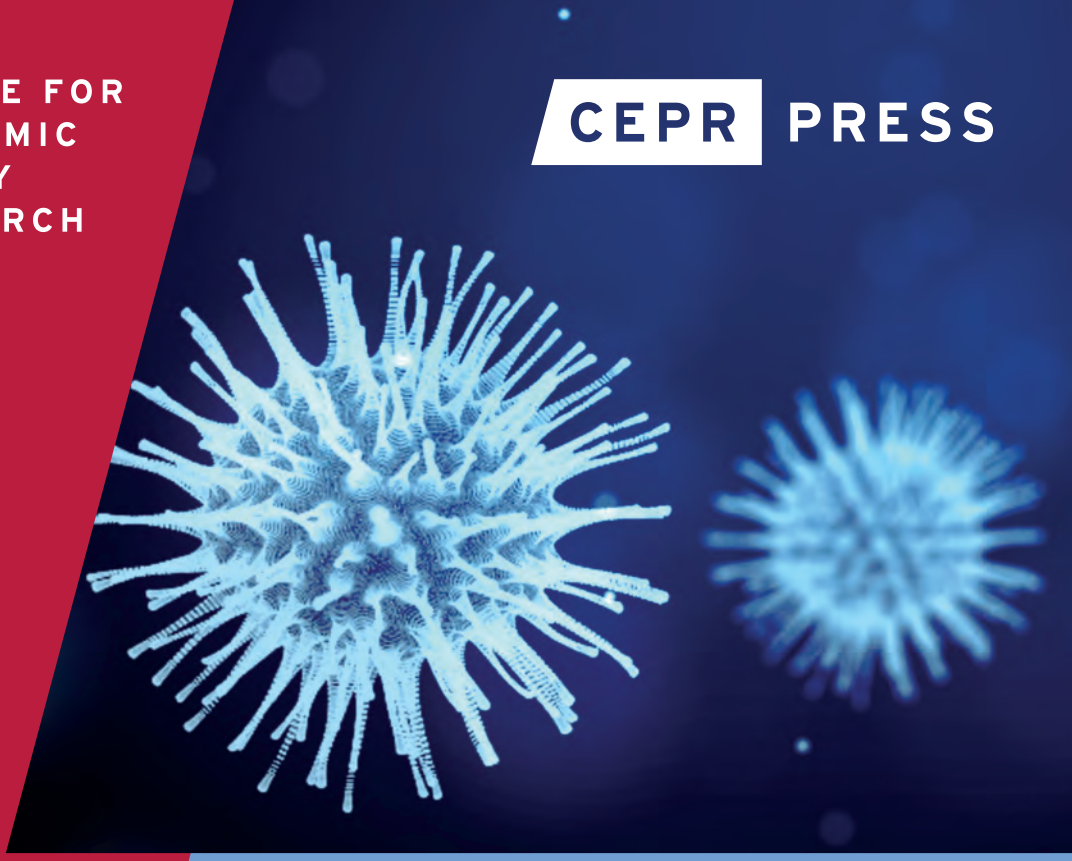

COVID ECONOMICS

VETTED AND REAL-TIME PAPERS

ISSUE 18
15 MAY 2020

Covid Economics
Vetted and Real-Time Papers

Covid Economics, Vetted and Real-Time Papers, from CEPR, brings together formal investigations on the economic issues emanating from the Covid outbreak, based on explicit theory and/or empirical evidence, to improve the knowledge base.

Founder: Beatrice Weder di Mauro, President of CEPR
Editor: Charles Wyplosz, Graduate Institute Geneva and CEPR

Contact: Submissions should be made at https://portal.cepr.org/call-papers-covid-economics. Other queries should be sent to covidecon@cepr.org.

The Centre for Economic Policy Research (CEPR)

The Centre for Economic Policy Research (CEPR) is a network of over 1,500 research economists based mostly in European universities. The Centre's goal is twofold: to promote world-class research, and to get the policy-relevant results into the hands of key decision-makers. CEPR's guiding principle is 'Research excellence with policy relevance'. A registered charity since it was founded in 1983, CEPR is independent of all public and private interest groups. It takes no institutional stand on economic policy matters and its core funding comes from its Institutional Members and sales of publications. Because it draws on such a large network of researchers, its output reflects a broad spectrum of individual viewpoints as well as perspectives drawn from civil society. CEPR research may include views on policy, but the Trustees of the Centre do not give prior review to its publications. The opinions expressed in this report are those of the authors and not those of CEPR.

Editorial Board

Ethics

Covid Economics will feature high quality analyses of economic aspects of the health crisis. However, the pandemic also raises a number of complex ethical issues. Economists tend to think about trade-offs, in this case lives vs. costs, patient selection at a time of scarcity, and more. In the spirit of academic freedom, neither the Editors of *Covid Economics* nor CEPR take a stand on these issues and therefore do not bear any responsibility for views expressed in the articles.

Submission to professional journals

The following journals have indicated that they will accept submissions of papers featured in *Covid Economics* because they are working papers. Most expect revised versions. This list will be updated regularly.

American Economic Review

American Economic Review, Applied Economics

American Economic Review, Insights

American Economic Review, Economic Policy

American Economic Review, Macroeconomics

American Economic Review, Microeconomics

American Journal of Health Economics

Economic Journal

Economics of Disasters and Climate Change

International Economic Review

Journal of Development Economics

*Journal of Econometrics**

Journal of Economic Growth

Journal of Economic Theory

*Journal of the European Economic Association**

Journal of Finance

Journal of Financial Economics

Journal of International Economics

*Journal of Labor Economics**

Journal of Monetary Economics

Journal of Public Economics

Journal of Political Economy

Journal of Population Economics

*Quarterly Journal of Economics**

Review of Economics and Statistics

*Review of Economic Studies**

Review of Financial Studies

(*) Must be a significantly revised and extended version of the paper featured in *Covid Economics*.

Covid Economics
Vetted and Real-Time Papers

Issue 18, 15 May 2020

Contents

CEPR PRESS

Covid Economics **Issue 18, 15 May 2020**

Lifting restrictions with changing mobility and the importance of soft containment measures: A SEIRD model of COVID-19 dynamics

Salvatore Lattanzio[1] and Dario Palumbo[2]

Date submitted: 11 May 2020; **Date accepted:** 12 May 2020

This paper estimates a SEIRD (susceptible-exposed-infected-recovered-deaths) epidemic model of COVID-19, which accounts for both observed and unobserved states and endogenous mobility changes induced by lockdown policies. The model is estimated on Lombardy and London – two regions that had among the worst outbreaks of the disease in the world – and used to predict the evolution of the epidemic under different policies. We show that policies targeted also at mitigating the probability of contagion are more effective in containing the spread of the disease, than the one aimed at just gradually reducing the mobility restrictions. In particular, we show that if the probability of contagion is decreased between 20% and 40% of its original level before the outbreak, while increasing mobility, the total death toll would not be higher than in a permanent lockdown scenario. On the other hand, neglecting such policies could increase the risk of a second epidemic peak even while lifting lockdown measures at later dates. This highlights the importance during the containment of the disease of promoting "soft" policy measures that could reduce the probability of contagion, such as, wearing masks and social distancing.

1 PhD Candidate, University of Cambridge.
2 Research Fellow, Ca' Foscari University of Venice, University of Cambridge.

Covid Economics 18, 15 May 2020: 1-41

Covid Economics 18, 15 May 2020: 1-41

1 Introduction

The novel coronavirus disease (COVID-19) spread quickly around the world. Many governments have adopted draconian measures to weaken its transmission among the population and some were more successful than others in containing its spread. The adoption of lockdown measures was deemed as necessary when policymakers realized that the virus was more infectious than initially thought, which brought many healthcare systems at the peak of the epidemic contagion to be under serious pressure. At some point the pressure on hospitals, and in particular on intensive care units, was so high that in some cases not all patients were treated. As a consequence, some people died without being diagnosed the infection and they did not enter the official death count. This implies that, in many countries, the official death toll considerably underestimates the true number of deaths (Villa, 2020b). This happens in addition to under-reporting of cases in official statistics. One clear example of the under-reporting of both cases and deaths is Lombardy, the region in Northern Italy where the first cases of COVID-19 appeared in late February. Lombardy is by far the most severely hit region in Italy: as of May 2, with more than 14,000 deaths, it represents 49.4% of the Italian total death toll. In some provinces, though, the true death count is at least twice the official figure, reflecting the difficulties of the healthcare system to cope with the exponential spread of the disease and of intensive care units in admitting all patients that needed medical care, as highlighted also in the media (Cancelli and Foresti, 2020). At the same time, many deaths happened in residential care homes, where many patients were not tested and, therefore, their death was not counted as COVID-19 related. The under-reporting of deaths is evident when comparing official COVID-19 death toll with death registries, available from the Italian Statistical Institute (Istat).[1] Figure 1 reports in panel (a) the daily number of "excess" deaths, defined as the difference between total deaths in 2020 relative to the average of the past 5 years, and the official coronavirus daily deaths in Lombardy in the first 3 months of 2020. To compute excess deaths, the figure uses data for a sample of municipalities in Lombardy that covers approximately 95% of the municipalities in the region and shows that, before the onset of the disease, the number of deaths in 2020 was in line – if not smaller – than the average of previous years. The series increases sharply at the end of February, when the first cases of coronavirus were registered in the region. The official death count is lower than the true number of deaths at all dates, highlighting a downward bias in official death counts. Panel (b) of the figure shows the same pattern for England and Wales, where the excess deaths are computed with the Office for National Statistics (ONS) data and COVID-related deaths are from two sources: ONS and Public Health England. The graph shows a pattern similar to Lombardy, where not all the excess mortality in 2020 is due to COVID-19. Part of this is due to under-reporting, but a part of it may also be due

[1] https://www.istat.it/it/archivio/240401

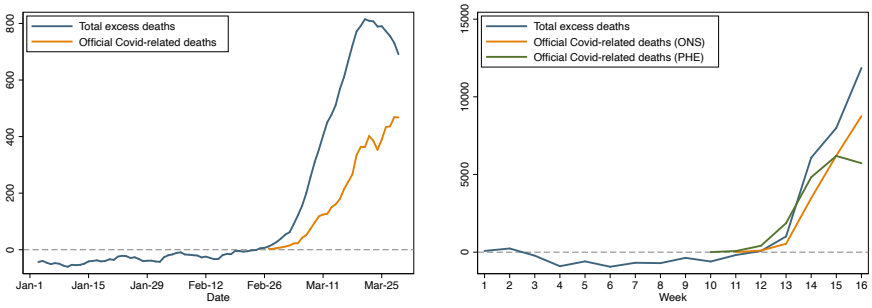

(a) Lombardy (b) England and Wales

Figure 1: Excess deaths in 2020 and official COVID-19 deaths

Notes. The figure shows excess mortality in 2020 relative to the average of previous 5 years and COVID-19 official deaths. Panel (a) reports daily data for Lombardy (averaged over a 5-day rolling window), where excess deaths are computed over a sample that comprises 95% of the municipalities in the region, whereas panel (b) reports data for England and Wales. Data: Istat, Protezione Civile, Office for National Statistics, Public Health England.

Covid Economics 18, 15 May 2020: 1-41

to deaths not directly related to coronavirus, but indirectly linked to it, if patients with other pathologies do not receive appropriate treatment because of overwhelmed hospitals.

This evidence suggests that, when trying to model the evolution of the disease, it is of utmost importance to take into account both observed and unobserved infection and death counts. This paper aims at doing so, by developing a compartmental susceptible-exposed-infected-recovered-deaths (SEIRD) model with two main compartments – observed and unobserved – of infections, recoveries and deaths, extending the classic SIR model first introduced by Kermack and McKendrick (1927). The model is estimated with Kalman filter techniques and used to forecast the evolution of the epidemic under a number of different scenarios. We calibrate the model on official data for Lombardy and London. In fact, the United Kingdom experienced an evolution of the epidemic similar to Italy and London, in particular, accounts for the majority of deaths in the country (approximately 25% of the official death toll).

Our model accounts for the underestimation of true cases, by calibrating the under-reporting intensity to time-series obtained by correcting the observed case fatality rate with the infection fatality rate estimated in the literature (Ferguson et al., 2020; Villa, 2020a). Moreover, it accounts for the under-estimation of total deaths by explicitly modeling observed and unobserved deaths and calibrating the true mortality rate to be proportional to the number of excess deaths recovered from death registries. Finally, we account for mobility restrictions in the estimation of the infection probability, one key parameter that governs the rate at which susceptible individuals get exposed to the disease. We use mobility trends in Lombardy from Pepe et al. (2020) and in London from Google Community Mobility Reports and estimate the initial contact rate, given the rate of change of mobility. Therefore, we explicitly model lockdown by accounting for the decrease in

mobility of individuals after its imposition.

Our model suggests that at the end of the fit period used to estimate the parameters (9 April in Lombardy, 15 April in London), the prevalence of the disease is approximately 5.7% in Lombardy and 2% in London. The number of unobserved infected cases is at least twice as large as observed cases in both regions, whereas the number of unobserved recoveries is between 20 and 26 times larger than observed recoveries. The true death count is underestimated by 35% in Lombardy and 17% in London.

We use our model to forecast the evolution of the disease under different policy scenarios. Specifically, we consider a number of policy measures that go from lifting immediately all lockdown measures to maintaining them until mid-summer, with different intermediate scenarios, where restrictions are gradually lifted over time. Our forecasts suggest that with appropriate measures that reduce the probability of contagion by 20% to 40% of its pre-lockdown level, lifting restrictions would not entail a second epidemic peak, even in the presence of increased mobility, both in Lombardy and London. In other terms, with appropriate policies that reduce the probability an individual is infected – e.g. social distancing, using masks, increasing hygiene standards, isolating infected cases –, we show that gradually and carefully lifting lockdown measures does not imply a resurgence of the epidemic curve. This result may provide guidance to policymakers when deciding how and when lifting lockdowns. Our model suggests that the trade-off between economic recovery and saving lives can be balanced by implementing soft containment measures that could reduce the spread of the virus, even in the presence of increased mobility.

The rest of the paper is organized as follows. Section 2 details the methodology for modeling the evolution of the pandemic. Section 3 details the estimation results. Section 4 provides model forecasts and the predictions about policy counterfactuals. Finally, section 5 concludes.

2 Methodology

We base our modeling on a susceptible-exposed-infected-recovered-deaths (SEIRD) model with two compartments – detected or observed and undetected or unobserved – of infected, recovered and deaths. From the beginning of the epidemic, many researchers have highlighted the severe under-reporting of cases in official statistics. As tests are conducted on symptomatic individuals only, there is a large fraction of asymptomatic and mildly sympomatic cases that are not reported in official statistics (Lavezzo et al., 2020; Li et al., 2020a; Russo et al., 2020). Moreover, the stress on hospitals has led to a severe underestimation of deaths, too (Bucci et al., 2020). For this reason we augment the classic SIR model (Kermack and McKendrick, 1927), by accounting for both observed and unobserved states.

SIR models have been used extensively in the modeling of the COVID-19 spread

Covid Economics 18, 15 May 2020: 1-41

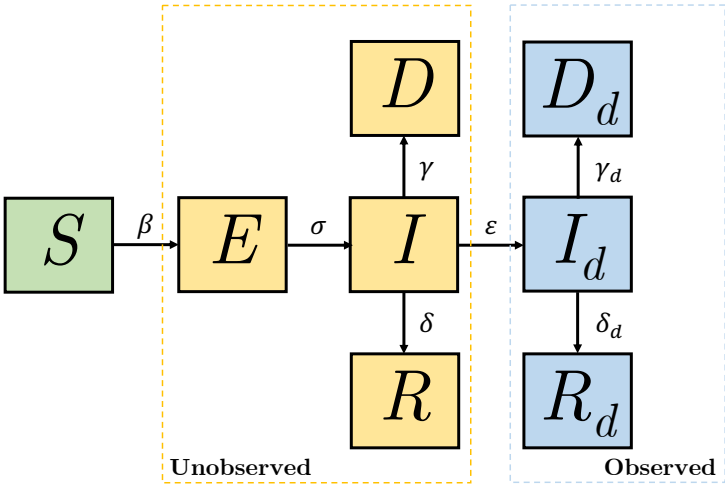

Figure 2: SEIRD model with unobserved and observed compartments

(Favero, 2020; Giordano et al., 2020; Russo et al., 2020; Toda, 2020; Toxvaerd, 2020). The version here proposed assumes the existence of 8 states, summarized in Figure 2: susceptible S_t, exposed E_t, infected unobserved I_t, infected observed I_{dt}, recovered unobserved R_t, recovered observed R_{dt}, deaths unobserved D_t and deaths observed D_{dt}. Every individual in the population at every point in time belongs to one of these categories. The discrete dynamics of the system are described as follows,

$$
\begin{aligned}
S_t &= \left(1 - \frac{\beta}{N - D_{t-1} - D_{dt-1}} I_{t-1}\right) S_{t-1} \\
E_t &= (1-\sigma)\, E_{t-1} + \frac{\beta}{N - D_{t-1} - D_{dt-1}} S_{t-1} I_{t-1} \\
I_t &= (1 - \delta - \epsilon - \gamma)\, I_{t-1} + \sigma E_{t-1} \\
I_{dt} &= (1 - \delta_d - \gamma_d)\, I_{dt-1} + \epsilon I_{t-1} \\
R_t &= R_{t-1} + \delta I_{t-1} \\
R_{dt} &= R_{dt-1} + \delta_d I_{dt-1} \\
D_t &= D_{t-1} + \gamma I_{t-1} \\
D_{dt} &= D_{dt-1} + \gamma_d I_{dt-1}
\end{aligned}
$$

where N is total size of the population,[2] β, σ, ϵ, δ, δ_d, γ, γ_d are the static parameters which determine the transitions between the states in the dynamics. In particular, we have that all parameters are strictly positive, then $0 < \sigma < 1$, $0 < \delta + \epsilon + \gamma < 1$ and

[2]We do not allow for variations in population size which might have occurred in the time periods considered. For the purpose of our study we assume them to be marginal in respect to total population.

$0 < \delta_d + \gamma_d < 1$. The subscript d indicates detected variables or parameters referred to detected variables.

Given that the observed variables are only $\mathbf{y}_t = (I_{dt}, R_{dt}, D_{dt})'$ and are observed with noise, we can represent this dynamic system with a non-linear state space

$$\begin{aligned} \mathbf{y}_t &= \mathbf{Z}\boldsymbol{\alpha}_t + \boldsymbol{\varepsilon}_t & \boldsymbol{\varepsilon}_t &\sim N(\mathbf{0}, \Omega_\varepsilon) \\ \boldsymbol{\alpha}_t &= \mathbf{T}(\boldsymbol{\alpha}_{t-1}) + \boldsymbol{\eta}_t & \boldsymbol{\eta}_t &\sim N(\mathbf{0}, \Omega_\eta) \end{aligned}$$

where $\boldsymbol{\alpha}_t = (S_t, E_t, I_t, I_{dt}, R_t, R_{dt}, D_t, D_{dt})'$ is the unobserved state vector, $\mathbf{Z}$ is the time invariant matrix

$$\mathbf{Z} = \begin{pmatrix} 0 & 0 & 0 & 1 & 0 & 0 & 0 & 0 \\ 0 & 0 & 0 & 0 & 0 & 1 & 0 & 0 \\ 0 & 0 & 0 & 0 & 0 & 0 & 0 & 1 \end{pmatrix}$$

and $\mathbf{T}(.)$ is the multivariate function describing the linear and non-linear relations between the state vector relating $t-1$ and t. Following Harvey (1989), the estimation of the sequence $(\boldsymbol{\alpha}_t)_{t=1}^T$ is obtained through an Extended Kalman Filter, and the estimation of the unknown parameters by maximizing the likelihood obtained by the resulting prediction error decomposition.[3]

As showed by Diekmann et al. (1990) and Heffernan et al. (2005), the basic reproductive ratio (R_0) for continuous time SEIR compartmental epidemic models is defined as the dominant eigenvalue of the "next generation operator," which is the matrix that describes the rates at which infected individuals in one infected state can produce new infected individuals from another state, times the average length of time period that an infected individual spends in her own compartment. In a state-space SIR model Kucinskas (2020) shows that it can be identified from the daily growth rate in the number of infected individuals at time 0. On the other hand, Tibayrenc (2007) shows it can be approximated by $R_0 = \beta\tau$, where τ is the duration of the infectivity. Following Diekmann et al. (1990) the R_0 of our model reads as[4]

$$R_0 = \frac{\beta}{\epsilon + \delta + \gamma} \tag{1}$$

This result coincides with Russo et al. (2020) where R_0 is obtained from the necessary condition for convergence on the Jacobian matrix of the subsystem of the three infected states E_t, I_t, I_{dt}.

For the model to be valid we need that at each time t the sum of all the states is equal to N. In order to impose this restriction while using the Kalman Filter we follow the

[3]For details on the state equation specification under the Extended Kalman Filter see Appendix A.
[4]For the details on the derivation see Appendix B.

Covid Economics 18, 15 May 2020: 1-41

approach of Doran (1992) and augment the cross-section of each observation vector $\mathbf{y}_t$ of an additional observation set constant as N for every t. Then the transition equation for this series becomes $\sum_j \alpha_{jt} = N$ at every t. While assuming that this additional series has a Gaussian uncorrelated measurement error with $E[\varepsilon_{0t}] = 0$ and $E[\varepsilon_{0t}^2] = 0$, the constraint is guaranteed to hold in both the updating and smoothing equations of the Kalman Filter.

3 Calibration and Estimation

3.1 Data and Initial Conditions

The current study is based on the COVID-19 contagion data for Lombardy and London. The data for Lombardy are obtained from the Github repository of Protezione Civile Italiana.[5] We collect daily data on the current total number of COVID-19 infected positively tested, number of recovered and total number of COVID-19 deaths in the region from 24/02/2020 to 09/04/2020. The data provided by Protezione Civile are reported before being confirmed by the Italian National Institute of Health (ISS). Due to this delay there might be reporting differences with the actual number of detected individual and this certainly is one of the contributors to the noise in the measurment of the true detected variables.

In regards to London, we have collected daily data on the total number of COVID-19 infected from the UK Government COVID-19 data dashboard[6] and on the total number of COVID-19 hospital deaths from the NHS website[7] from 01/03/2020 to 17/04/2020. The data on recovered patients are not publicly available for the London area, and the total number of infected TI_{dt} is now a sum of I_{dt}, R_{dt} and D_{dt}. Therefore in the case of London we modify the transition equation for an observed vector of $\mathbf{y}_t = (TI_{dt}, D_{dt})'$ where $\mathbf{Z}$ is now redefined as

$$\mathbf{Z}_{Lon} = \begin{pmatrix} 0 & 0 & 0 & 1 & 0 & 1 & 0 & 1 \\ 0 & 0 & 0 & 0 & 0 & 0 & 0 & 1 \end{pmatrix}$$

In estimating the model on the two datasets, we set the total population in the two regions equal to $N_{Lom} = 10,060,574$ for Lombardy,[8] and $N_{Lon} = 9,050,506$ for London.[9]

To partly solve the identification problem we assume that there is no correlation in the cross-section between the disturbances of the state equation and that they are homoschedastic, i.e. $\Omega_\eta = \sigma_\eta^2 \mathbf{I}$. On the other hand, measurement errors in the transition

[5] https://github.com/pcm-dpc/COVID-19
[6] https://coronavirus.data.gov.uk
[7] NHS, COVID-19 Daily Deaths.
[8] Istat, Resident population on the 1st of January, 2019.
[9] ONS, Subnational population projections, 2018.

Covid Economics 18, 15 May 2020: 1-41

equation can be due to different sources. Therefore, while we still assume no correlation in the cross-section, we assume that the variances are heteroschedastic

$$\Omega_{\varepsilon Lom} = \begin{pmatrix} \sigma^2_{1\varepsilon} & 0 & 0 \\ 0 & \sigma^2_{2\varepsilon} & 0 \\ 0 & 0 & \sigma^2_{3\varepsilon} \end{pmatrix} \qquad \Omega_{\varepsilon Lon} = \begin{pmatrix} \sigma^2_{1\varepsilon} & 0 \\ 0 & \sigma^2_{2\varepsilon} \end{pmatrix}$$

In SEIR models the initial conditions imply that all states should equal 0 at $t = 0$. In our specification we assume that $S_0 = N$. However, given that in both settings data on COVID-19 infections begin to be reported after the outbreak has already started, we cannot have initial states starting at 0. For this reason, we set I_{d0}, R_{d0}, D_{d0} at their values at the beginning of the datasets. Among the remaining state variables we set $D_0 = Y_{d0} \times 0.015$ and we estimate the other initial conditions, imposing that $S_0 > E_0 > I_0 > I_{d0} > R_0$ and that $\sum_j \boldsymbol{\alpha}_{j0} = N$. Finally, the standard errors of the estimated parameters are computed by bootstrap following Stoffer and Wall (1991).

3.2 Parameter Description

The introduced SEIRD model has 8 time-invariant parameters which describe the evolution of the disease over time, β, σ, ϵ, δ, δ_d, γ, γ_d. The estimation of all the parameters, including the elements of the covariance matrices Ω_ϑ and Ω_η, creates an issue of identification. We address this problem by calibrating some of the parameters.[10]

σ is the rate at which the exposed individuals become infected. This is usually set equal to the inverse of the incubation period of the disease. Li et al. (2020b) collected data on the first 425 confirmed cases in Wuhan and found that the median incubation period was 5.2 days with 95% confidence intervals between 4.1 and 7 days. These results are also also consistent with the findings of Lauer et al. (2020). Another study by Li et al. (2020a) assessed the prevalence of the novel coronavirus for the reported cases in China with a Bayesian Networked Dynamic Metapopulation Model with data on mobility. The study estimates the fraction of undocumented infections and their contagiousness finding a mean latency period in the transmission of the disease of 3.42 days with 95% confidence intervals between 3.30 and 3.65 days. We have estimated our model on the samples selected for a range of values of $1/\sigma$ between $[3, 7]$ finding that the estimates of β, and as a consequence R_0, where practically unchanged. We ultimately set $1/\sigma = 3$, using the lower bound of the range.

ϵ, δ and γ are, respectively, the proportion of the infected unobserved I_t which become detected, recovered, and die at each time period t. According to the guidelines of the

[10] As highlighted by Russo et al. (2020), the actual transition of the individuals across these states is reported with a time delay. Therefore these parameters are not exactly the average daily transition rates.

Covid Economics 18, 15 May 2020: 1-41

WHO, a normal flu should go away between a week or two.[11] Symptoms of fever should disappear between 4 to 5 days but cough might still be present. On the other hand, according to Day (2020), from the data available from Wuhan we also have that 4 out 5 cases are asymptomatic. For these reason we calibrate the average recovery period to 5 days resulting in a $\delta = 1/5$.

δ_d and γ_d are the proportions of the infected observed I_{dt} which recover or ultimately die, respectively. Among detected infected, few of the individuals are positively tested with mild symptoms and home-isolate, whereas the majority are those with severe symptoms who are hospitalized. According to a recent WHO report, patients with severe or critical symptoms take between 3 to 6 weeks to recover (WHO, 2020). In light of this, we assume the recovery time for detected infected to be the lower bound of this range. Therefore we set $\delta_d = 1/21$.

3.3 Including Mobility Data

In SEIR models the parameter β describes the infection rate of susceptible individuals, or the "effective" daily transmission rate of the disease. The possibility of temporal heterogeneity in the transmission rate has been extensively studied in the literature to explain the amplitude in the variation in the outbreaks of diseases, from Soper (1929) to Grassly and Fraser (2006). In our context the possible variation in the transmission rate of COVID-19 is mainly related to changes in mobility of the population. The impact of mobility on the transmission rate can be appreciated given its approximate decomposition in the product $\beta \approx \bar{n} p_c$, where $\bar{n}$ is the daily average number of contacts that an individual has in the population and p_c is the actual probability of contracting the disease in a single contact. Alteration in p_c can be due to many factors, among which how each individual actively take precautions to prevent the contagion in each contact. Della Valle et al. (2007), among others, estimates $\bar{n}$ at a given point in time and taking into account heterogeneity between age groups and lifestyles. However, rather than estimating a single value for $\bar{n}$, we are mostly interested in observing its variation over time, which crucially depends on individuals' mobility.

To measure mobility changes during the COVID-19 outbreak, we use data from the Google Community Mobility Reports[12] for London, and from Pepe et al. (2020) for Lombardy. Google reports collect information from smartphones of Google users who opted-in for their location history in their Google Accounts, and calculate the variation in the average visits and length of stay at different places compared to a baseline. Google provides this data for 6 categories of places: retail and recreation, grocery and pharmacy, parks, transit stations, workplace and residential. There are no further information, though, on how the measures are computed, the sample size and if it varies over time.

[11] Q&A: Similarities and differences – COVID-19 and influenza

[12] https://www.google.com/covid19/mobility/

Covid Economics 18, 15 May 2020: 1-41

Covid Economics 18, 15 May 2020: 1-41

On the other hand, the study of Pepe et al. (2020) also collects location data from users who have opted-in to provide access to their location data anonymously through agreeing to install partner apps on their smartphones. This app allows to collect geographical coordinates with an estimated accuracy level of about 10 meters. Their dataset is composed of a panel of about 167,000 users in Italy who were active during the week 22-28 February and for whom there was at least one stop collected during the same week. Individuals are then followed over the next 8 weeks. The study provides data on the average contact rate over time by constructing a proximity network between individuals, where proximity between any two users is assessed within a circle of radius 50 meters. Despite being potentially a more selected sample they compute the daily average relative degree of the network at the province level, thus providing more detailed data than Google reports.[13]

For our purposes, we have collected the average degree of the network for each of the provinces of Lombardy between 24 February and 21 March and computed a weighted average by population of each province.[14] We then compute the daily rate of change of the relative degree of the network with respect to its value on 24 February. Since after 11 March the values tend to vary little, we assume that the rate of change from the 21 March to 9 April remains unchanged.

Finally, we incorporate in our model the data on mobility obtained by these sources assuming that the rates of changes r_{mt} in mobility are proportional to the rates of changes in the average daily contact rate $\bar{n}$. In particular, assuming that p_c remains constant we have that $\beta_t = \bar{n} p_c (1 + r_{mt}) = \beta_0 (1 + r_{mt})$, which is in line with works on deterministic variation in effective daily transmission rate in SEIRD model, such as the recent Piccolomini and Zama (2020) on the Italian COVID-19 outbreak.

This alteration ultimately makes the multivariate function $\mathbf{T}_t(\boldsymbol{\alpha}_t)$ time varying. However, given that the time path of r_{mt} is completely defined beforehand, the time variation in $\mathbf{T}_t(\boldsymbol{\alpha}_t)$ is deterministic and the standard Kalman Filter equations are still valid.

3.4 Under-reporting of Cases – ϵ_t

In the same fashion as for β, we calibrate ϵ_t on the rate of change of under-reporting estimated from real data, following Villa (2020a). Specifically, let ξ_t be the adjusted daily case fatality rate of the disease, computed as the number of cumulative deaths divided by the number of cumulative official cases lagged by 6 days[15] and ι be the true infection

[13] Our analyses are robust to the use of Google mobility reports for Lombardy, too. Results are available upon request.

[14] The weighting does not have a large effect on the outcome.

[15] We choose to divide the current number of deaths by 6-day lagged cases because there is a lag between the onset of symptoms and death. The Italian Health Institute (Istituto Superiore di Sanità, ISS) quantifies this lag in a median time of 10 days. However, since there is a lag between the infection and the onset of symptoms, we rescale this factor to 6 days, following Villa (2020a).

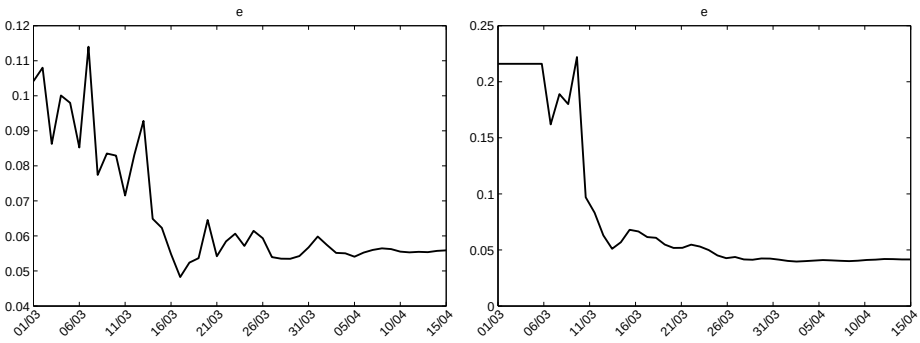

(a) Lombardy (b) London

Figure 3: Estimated values of $\tilde{\epsilon}_t$

fatality rate, which, following Ferguson et al. (2020) and Villa (2020a), is estimated to be 0.9% (95% CI: 0.4%-1.4%) for the United Kingdom and 1.14% for Italy (95% CI: 0.51%-1.78%).[16] Therefore, a proxy for ϵ_t is computed as:

$$\tilde{\epsilon}_t = \frac{\iota}{\xi_t}$$

Although the magnitude of $\tilde{\epsilon}_t$ estimated with this methodology might not exactly match the ϵ_t parameter in our SEIRD model, because of measurement error, we still believe that its variation over time might be closely related to the one that our parameter should experience if it were to be time varying. The variation in ϵ_t would represent the ability that the healthcare system has to detect infected individuals and this ability should be decreasing as the system is under stress, as we see from the results presented in Figure 3. In order to incorporate this feature, as already done for mobility, we compute the daily rate of change of $\tilde{\epsilon}_t$, $r_{\tilde{\epsilon}t}$ and we assume that $\epsilon_t = \epsilon_0 (1 + r_{\tilde{\epsilon}t})$.

3.5 Per-day Mortality Rates – γ and γ_d

We calibrate the per-day mortality rate to match the unobserved mortality computed from Istat mortality statistics for Lombardy. Specifically, we compute excess mortality as the difference between daily deaths in 2020 and average daily deaths in the previous 5 years, as in Figure 1, panel (a). The difference between excess mortality and COVID-19 official deaths represents deaths that occured in 2020 in excess relative to previous years but not officially attributed to COVID-19. Only a subset of the excess mortality in Istat data is directly or indirectly related to COVID-19. Indeed, the difference may represent: (*i*) deaths that are directly caused by COVID-19, but not reported in official statistics; (*ii*)

[16] The estimate is obtained by correcting the age-stratified infection fatality rate in Verity et al. (2020) for the demographic structure of Italy and the United Kingdom.

Covid Economics 18, 15 May 2020: 1-41

deaths for other causes indirectly related to COVID-19 (for example, if healthcare systems could not provide appropriate care to patients for other diseases because of overwhelmed hospitals); (*iii*) deaths from other causes unrelated to COVID-19. Following Bucci et al. (2020), and using one of their most conservative scenarios, we assume that only 36% of the mortality in excess to official statistics is directly related to COVID-19, but *unobserved*.[17] To this end, we set the per-day mortality rate to be $\gamma = 0.0011$. This choice ensures that we are able to match unobserved deaths in the model to the true excess mortality series, derived empirically from the data. We then assume that the per-day *detected* mortality rate is equal to three times the mortality rate for unobserved cases, i.e. $\gamma_d = 0.0033$. We make this choice, based on the fact that observed cases are generally more severe (because symptomatic) and therefore are more likely to cause complications which may result fatal.

4 The Impact of the Lockdown

4.1 Permanent Lockdown, Unmitigated Scenario and Gradual Lifting of Restrictions

Lombardy The results of our estimation are reported in Figure 4, where we assume that the restrictions in place in Lombardy remain the same until July. The top panel reports the evolution of infected, recovered and deaths in the fit window (24 February - 9 April), observed (solid lines) and unobserved (dashed lines). The middle panel reports the same set of variables, adding a forecasting window that ends in the first week of July.[18] The bottom panel reports the evolution of exposed individuals, the reproduction number R_t and the fatality rate, computed as the ratio of total deaths (observed and unobserved) over total cases, computed as the sum of infected, recovered and deaths (observed and unobserved).

The model estimates a $\hat{\beta}_0 = 0.744$ and suggests that at the end of the in-sample period there are at least twice as many infected individuals as those observed (63,202 undetected and 29,067 detected), whereas the number of recoveries is 26 times higher than those actually observed in the data: this suggests that the prevalence of the disease among the population is approximately 5.7% (computed as the sum of total recoveries and infected over the total population in Lombardy). The number of unobserved deaths – those caused by COVID-19 but unreported – is 3,470, meaning that the official death count would be underestimating the true number of deaths by as much as 35%, being the number of detected deaths 10,022. By the end of July, our model forecasts that the total number of cases is close to 1 million, the majority of which is composed of undetected recoveries.

[17] See Appendix C for a more detailed discussion on the calibration of this parameter.

[18] Figure D.1 in the Appendix plots detected infected, recovered and deaths alongside 95% bootstrapped forecasting bounds.

Covid Economics 18, 15 May 2020: 1-41

Covid Economics 18, 15 May 2020: 1-41

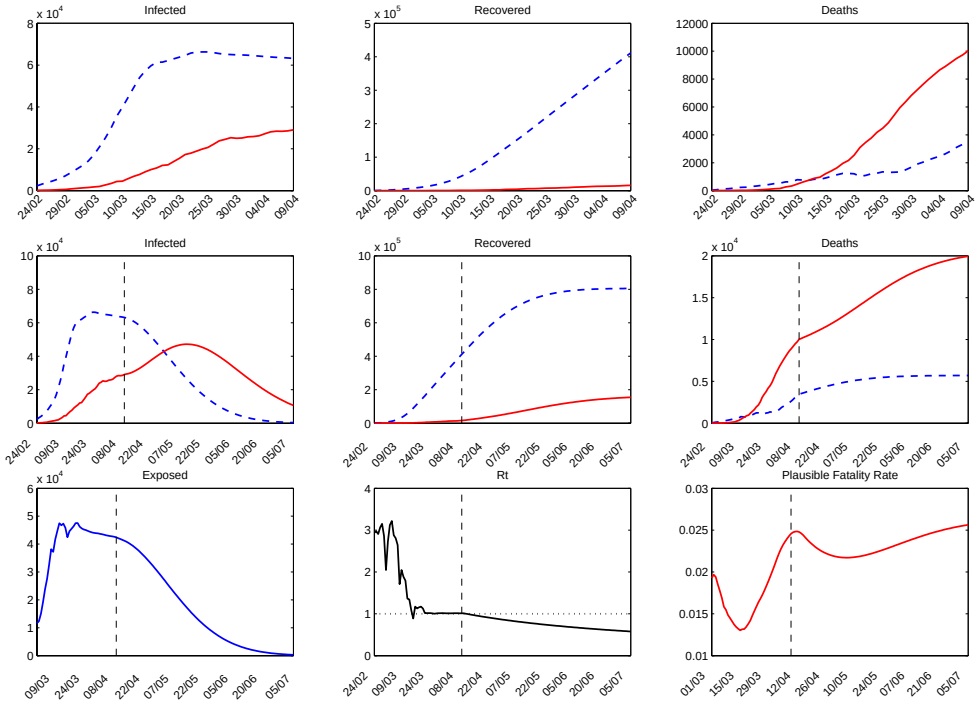

Figure 4: Baseline scenario Lombardy: permanent lockdown.

Notes. The figure shows the fitted (top panel) and forecasted (middle panel) curves of undetected (blue dashed lines) and detected (red solid lines) infections, recoveries and deaths. The bottom panel shows exposed individuals, the reproduction rate R_t and the "plausible" fatality rate. This scenario assumes that the lockdown stays in place until the end of the forecast window (5 July).

The number of observed and unobserved infected individuals fades out by the end of the forecasting period, whereas the total number of deaths equals 25 thousand, 5.7 of which unobserved.

The lockdown measures considerably reduce the number of exposed individuals, which become close to 0 by July. The reproduction rate of the disease, summarized by the variable R_t, reaches a level of 1.01 (95% CI: 0.90-1.12) by the end of the fit period and keeps decreasing until the end of the forecast window to a level of 0.58 (95% CI: 0.51-0.64).[19] The plausible fatality rate oscillates between 1.5% and 2.5% in the fit window and it stabilizes around 2-2.5% in the forecast period. Our estimate is thus in the upper bound of those found in the literature for the Italian case (Rinaldi and Paradisi, 2020; Villa et al., 2020). However, this seems plausible given the severity of the disease in the case of Lombardy and may reflect the overwhelming pressure under which the healthcare systems has been operating.

[19]Figure D.2, panel a, plots the evolution of R_t in Lombardy over time, alongside 95% bootstrapped confidence intervals, under the permanent lockdown scenario.

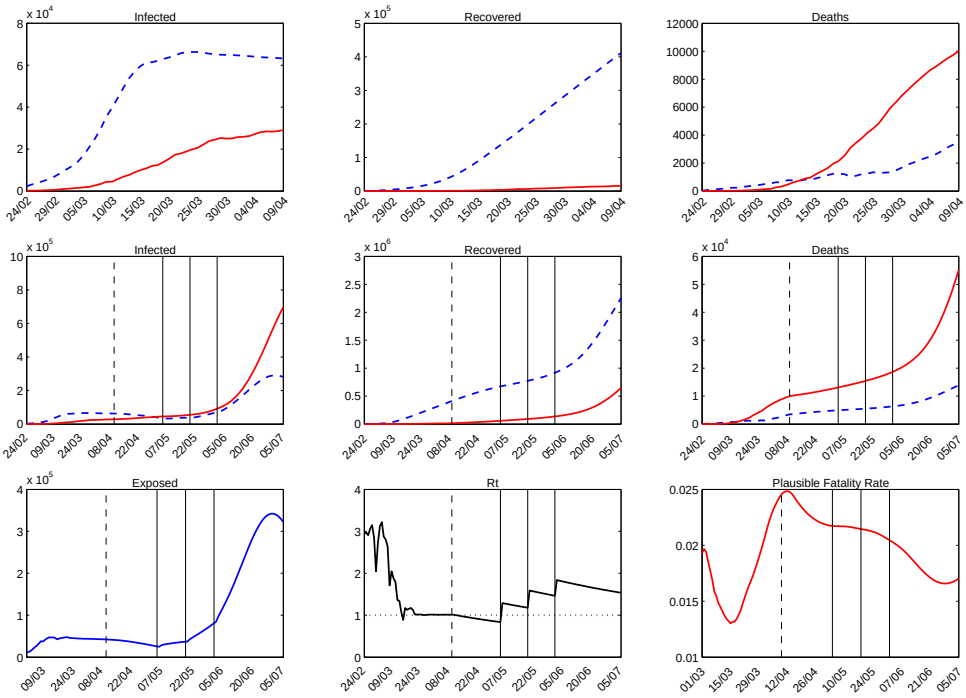

Figure 5: Current Scenario Lombardy

Notes. In this scenario, the government lifts the lockdown gradually on three dates 04/05, 18/05 and 01/06 bringing the mobility at 25%, 50% and 75% of the baseline of 24/02. The probability of contagion is unchanged.

We compare these results to a scenario where we assume that no restrictions take place, i.e. an unmitigated scenario, reported in Figure D.3. In this scenario we assume that mobility remains at the levels observed in the two weeks *before* the first cases were officially recorded in Italy.[20] In an unmitigated scenario the number of deaths is predicted to reach a level around 125,000, of which 48,000 would not be detected. The high number of undetected deaths reflects the stress under which hospitals would be put if no containment measures were adopted. The reproduction rate in this scenario fluctuates around 3.

Both these scenarios (the permanent lockdown and the unmitigated case) are only benchmarks. They show what would happen in the absence of policy interventions to lift restrictions in one case and to impose them in the other. Therefore, we also evaluate what would happen under the current policy implemented by the Italian government. Specifically, the lockdown measures have been partly lifted starting from May 4. The Italian government announced a further lifting of restrictions in the coming days, if the epidemic proves to be under control. We forecast the evolution of the epidemic under

[20]Specifically, we replicate the mobility pattern of the two weeks prior to the beginning of the epidemic until the end of the forecast window.

Covid Economics 18, 15 May 2020: 1-41

the plan of re-openings of the government under different assumptions on the evolution of mobility changes.

The current government plan entails a gradual re-opening of economic activities on three dates: May 4, May 18 and June 1. On each of these dates, we assume that mobility increases up to a fraction of its level before that any restriction was imposed. Specifically, we assume that mobility goes back to 25%, 50% and 75% of its pre-lockdown level at each subsequent date. However, we assume that the probability of contagion remains unaffected, i.e. we set p_c to be equal to its pre-lockdown level.[21] The evolution of the epidemic under this scenario, according to our model, is reported in Figure 5. The model suggests that we can expect a second peak of infections by mid-summer (middle panel of Figure 5) and a surge in deaths, both observed and unobserved. Therefore, in the current policy scenario for Lombardy, our model predicts 978,000 infected, 2.9 million recovered and 69,100 deaths, of which 280,700, 649,000 and 13,900, respectively, are undetected.

The cumulative numbers of exposed, infected, recovered and deaths under these scenarios for Lombardy are reported in Table 1, panel A, rows 1-5.

London In this case the model estimates a $\hat{\beta}_0 = 0.474$, while Figure 6 reports the forecasts of the evolution of the epidemic assuming a permanent lockdown until mid-July. Exposed individuals reach a peak in early May and then fade out, as well as infected, with a delay between detected and undetected cases. By the end of the forecast period on July 19, our model predicts a total of 13,827 detected deaths and 3,124 undetected deaths. We can compare these numbers to those that would be observed if no restrictions were imposed. Results are reported in Figure D.4. The total number of detected deaths under the no lockdown policy would reach a level of 43,754, whereas unreported deaths would be 39,295. Thus, we would observe approximately 83 thousand deaths, i.e. around 1% of the total population living in London as also measured by the case fatality rate (which in this case would coincide with the mortality rate of the disease).

The UK government has only very recently announced a plan of re-opening of economic activities, but precise dates are yet unavailable. For our purposes, we assume that the dates at which the government lifts lockdown measures are set two weeks later than Italy (i.e. on 18/05, 01/06, 15/06). We also assume, as we did for Lombardy, that on these dates mobility goes back to 25%, 50% and 75% of the baseline level. The forecasted states under this scenario are reported in Figure 7. Under this policy, the total number of deaths would be considerably reduced, even assuming that the probability of contagion remains unaffected. The cumulative number of deaths equals 23,494, whereas unobserved deaths are 5,062. The reproduction rate R_t equal 1.16 (95% CI: 1.02-1.31) at the end of the fit

[21] Since we do not have an exact measure of the average number of daily contacts among the individuals at the beginning of our sample, $\bar{n}$, we cannot disentangle p_c from β_0. However, we assume it to be close to the average of the results provided by Della Valle et al. (2007) – roughly 16 –, so that the probability of contagion estimated by our model is $p_c = 0.046$.

Covid Economics 18, 15 May 2020: 1-41

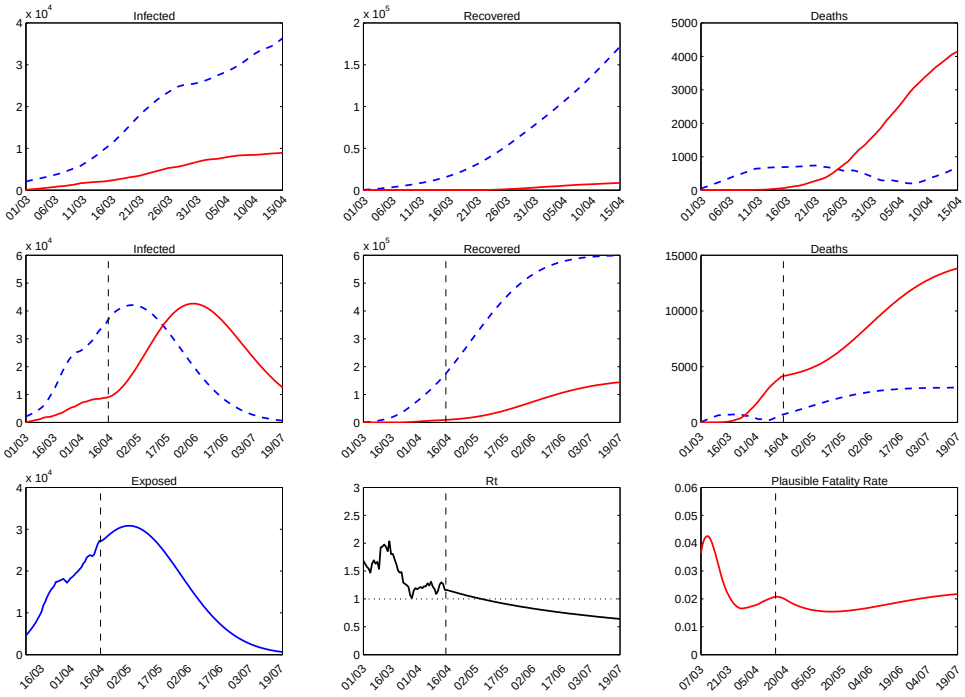

Figure 6: Baseline scenario London: permanent lockdown.

Notes. The figure shows the fitted (top panel) and forecasted (middle panel) curves of undetected (blue dashed lines) and detected (red solid lines) infections, recoveries and deaths. The bottom panel shows exposed individuals, the reproduction rate R_t and the "plausible" fatality rate. This scenario assumes that the lockdown stays in place until the end of the forecast window (19 July).

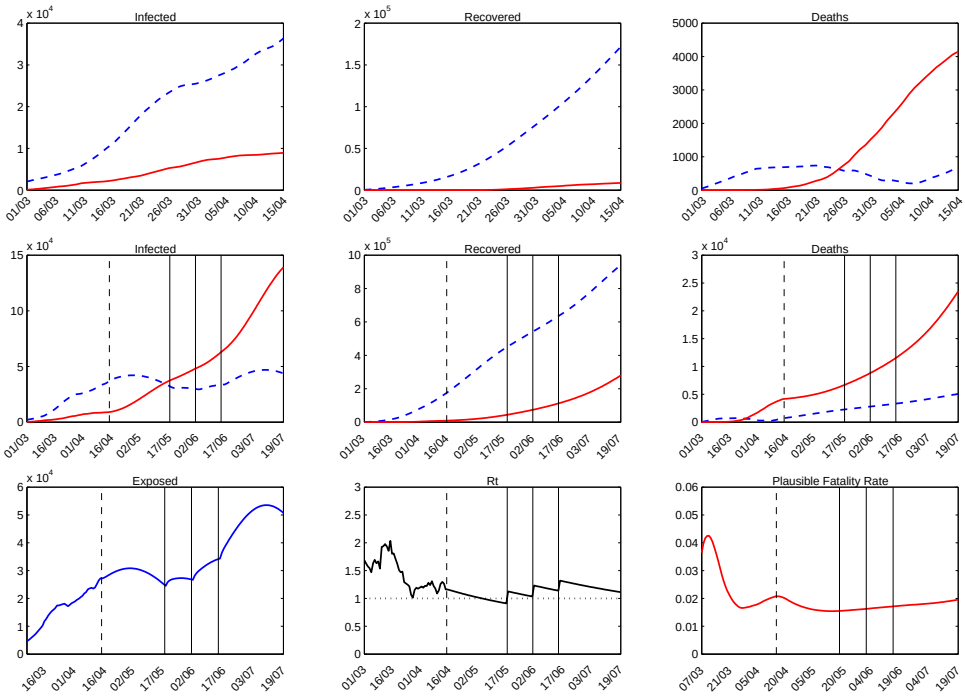

Figure 7: Current plausible scenario, London

Notes. In this scenario, the government lifts the lockdown gradually with a two weeks delay with respect to Lombardy on three dates – 18/05, 01/06 and 15/06 – bringing the mobility at 25%, 50% and 75% of the baseline of the 24/02. The probability of contagion is unchanged.

period and declines to 0.64 (95% CI: 0.56-0.72).[22]

The cumulative numbers of exposed, infected, recovered and deaths under these scenarios for London are reported in Table 1, panel B, rows 15-19.

4.2 Policy Counterfactuals

Changing mobility and opening dates We run counterfactual scenarios where we change mobility levels and dates of re-opening. Specifically, for Lombardy only,[23] we look at 5 different counterfactual policies:

1. the lockdown is gradually lifted on the three aforementioned dates, but mobility increases at 33%, 66% and 100% of its pre-lockdown level;

2. the lockdown is lifted earlier on three dates: April 27, May 11, May 25 and mobility increases at 25%, 50%, 75% of the baseline;

[22]Figure D.2, panel b, plots the evolution of R_t in London over time, alongside 95% bootstrapped confidence intervals, under the permanent lockdown scenario.

[23]Results for London are qualitatively similar and available upon request.

Covid Economics 18, 15 May 2020: 1-41

Table 1: Cumulative states at the end of fit and forecast period under different policy scenarios

		(1) E	(2) I	(3) I_d	(4) R $\times 10^3$	(5) R_d	(6) D	(7) D_d	(8) R_t	(9) R_t^{LB}	(10) R_t^{UB}
						Panel A: Lombardy					
						Fit - End date: 9 April					
1.	Baseline	42.4	63.2	29.1	411.5	15.7	3.5	10.0	1.01	0.90	1.12
2.	Unmitigated	955.2	1,804.8	493.5	5,031.3	196.8	28.5	14.1	3.36	2.99	3.73
						Forecast - End date: 5 July					
3.	Baseline	0.3	0.3	10.6	805.1	154.8	5.7	20.0	0.58	0.51	0.64
4.	Unmitigated	0.0	0.0	13.0	8,401.7	1,084.6	47.6	77.4	3.36	2.99	3.73
5.	$p_c = 100\%$	322.0	280.7	697.3	2,254.9	649.0	13.9	55.2	1.54	1.37	1.71
6.	$p_c = 90\%$	190.9	158.1	369.5	1,580.2	421.3	10.1	39.0	1.38	1.23	1.54
7.	$p_c = 80\%$	76.5	63.3	163.0	1,157.9	281.3	7.7	29.0	1.23	1.09	1.36
8.	$p_c = 70\%$	22.6	19.4	64.3	938.6	205.0	6.5	23.5	1.07	0.96	1.19
9.	$p_c = 60\%$	5.2	4.8	24.9	834.4	165.6	5.9	20.7	0.92	0.82	1.02
10.	Scenario 1	318.1	336.4	1,311.1	3,717.0	1,208.8	22.2	95.2	1.85	1.65	2.06
11.	Scenario 2	212.1	213.0	915.9	3,251.9	1,117.9	19.6	88.7	1.54	1.37	1.71
12.	Scenario 3	241.4	188.5	351.2	1,447.1	353.3	9.3	34.1	1.54	1.37	1.71
13.	Scenario 4	231.5	183.2	369.4	1,579.0	416.4	10.1	38.6	1.54	1.37	1.71
14.	Scenario 5	492.4	423.7	903.6	2,593.7	733.9	15.8	61.3	1.85	1.65	2.06
						Panel B: London					
						Fit - End date: 15 April					
15.	Baseline	27.2	36.4	8.9	171.8	8.7	0.7	4.1	1.16	1.02	1.31
16.	Unmitigated	309.5	331.6	39.4	579.4	18.6	3.3	1.3	2.23	1.95	2.51
						Forecast - End date: 19 July					
17.	Baseline	0.6	0.7	12.5	599.3	144.2	3.1	13.8	0.64	0.56	0.72
18.	Unmitigated	0.1	0.3	14.2	6,934.3	612.8	39.3	43.8	2.23	1.95	2.51
19.	$p_c = 100\%$	50.7	43.8	139.1	941.4	279.6	5.1	23.5	1.11	0.97	1.25
20.	$p_c = 90\%$	19.1	16.9	65.6	751.7	206.3	4.0	18.3	1.00	0.88	1.13
21.	$p_c = 80\%$	6.0	5.5	29.9	645.3	162.9	3.4	15.2	0.89	0.78	1.00
22.	$p_c = 70\%$	1.6	1.6	14.1	586.5	137.4	3.1	13.3	0.78	0.64	0.91
23.	$p_c = 60\%$	0.4	0.4	7.4	552.9	122.2	2.9	12.3	0.67	0.55	0.78

Notes. Columns 1-7 report the cumulative number (in thousands) of exposed (E), infected (I), detected infected (I_d), recovered (R), detected recovered (R_d), deaths (D), detected deaths (D_d). Columns 8-10 report the reproduction rate (R_t) and its 95% confidence interval (R_t^{LB} and R_t^{UB}). Panel A reports the numbers for Lombardy and panel B for London. The *Baseline* scenario assumes the presence of the lockdown until the end of the forecast period. The *Unmitigated* scenario is one where no restriction measures are taken. *Scenario 1* assumes the government gradually lifts lockdown on three dates – 04/05, 18/05, 01/06 – bringing mobility at 33%, 66% and 100% of its baseline on 24/02. *Scenario 2* anticipates the aforementioned dates by one week, whereas *Scenario 3* delays the dates by one week, both assuming mobility goes back to 25%, 50% and 75% of its baseline. *Scenario 4* and *Scenario 5* assume a slower lifting of restrictions on three dates (04/05, 25/05, 15/06) bringing mobility to 25%, 50%, 75% and 33%, 66% 100% of its baseline, respectively. The row labelled $p_c = x\%$, with $x = \{100, 90, 80, 70, 60\}$, uses the current plan of the Italian government: lifting restrictions on 04/05, 18/05, 01/06, with mobility going back to 25%, 50% and 75% of its baseline and assuming the probability of contagion is only a fraction $x\%$ of its baseline in the pre-lockdown period. For London, we assume the government lifts restrictions two weeks after Italy: 18/05, 01/06, 15/06.

Covid Economics 18, 15 May 2020: 1-41

3. the lockdown is lifted later on three dates: May 11, May 25, June 8, and mobility increases at 25%, 50%, 75% of the baseline;

4. the lockdown is lifted over a longer time horizon on three dates: May 4, May 25, June 15, and mobility increases at 25%, 50%, 75% of the baseline;

5. the lockdown is lifted over a longer time horizon on three dates: May 4, May 25, June 15, and mobility increases at 33%, 66%, 100% of the baseline;

Results for counterfactual scenarios 1-5 are reported in Figures D.5-D.9 and rows 10-14 of Table 1, panel A. The model suggests that a faster return to the mobility of the pre-lockdown period (scenario 1, Figure D.5) is associated with a second and more severe peak of the epidemic during the summer, with increases in infections and deaths, both observed and unobserved. Anticipating (scenario 2, Figure D.6) or delaying (scenario 3, Figure D.7) the lifting of restrictions has the expected effect on the number of cases: an earlier re-opening would anticipate the second peak and a later re-opening would further delay the peak. Spreading the lifting of restrictions on a longer time horizon and increasing mobility (Scenario 4 and 5, shown in Figure D.8 and D.9) makes little difference with respect to the current policy if mobility increases only up to 75% of its baseline level, but it entails more cases and deaths if mobility increases up to 100% of its baseline.

Reducing the probability of contagion p_c All these scenarios rest on the assumption that the probability of contagion remains the same throughout the whole period under analysis. However, many prevention measures will be in place and, in some cases, will be mandatory, such as, wearing masks in public, social distancing, avoid gatherings of people, higher hygienic standards, sanitizing public and private spaces. Moreover, the virus could mutate over time (although the consensus on this is not unanimous). We can nonetheless expect that "soft" containment measures reduce the probability of contagion, therefore compensating for the increased mobility. We therefore run a second set of counterfactual scenarios where we fix the dates at which the government lifts restrictions to the baseline (i.e. to the actual plan implemented by the government), but we assume different values for the probability of contagion, from 100% to 60% of its pre-lockdown levels,[24] assuming mobility increases to 25%, 50% and 75% of its pre-lockdown levels on May 4, May 18 and June 1 in Lombardy (May 17, June 1 and June 15 in London). We compare these counterfactuals to the scenario where the lockdown is maintained until the end of the period under analysis. Figures 8 and 9 show the results for detected and undetected infections and deaths in Lombardy and London, respectively.[25] The line where the probability of contagion is held constant to 1 is the same as the current policy scenario

[24]For the purpose of our model, given a deterministic path of $\bar{n}_t$, a percentage change Δ in p_c would result in an equal percentage change in β_t since $\Delta p_c \bar{n}_t \approx \Delta \beta_t$.

[25]Figure D.10 provides results for the number of exposed individuals.

Covid Economics 18, 15 May 2020: 1-41

Covid Economics 18, 15 May 2020: 1-41

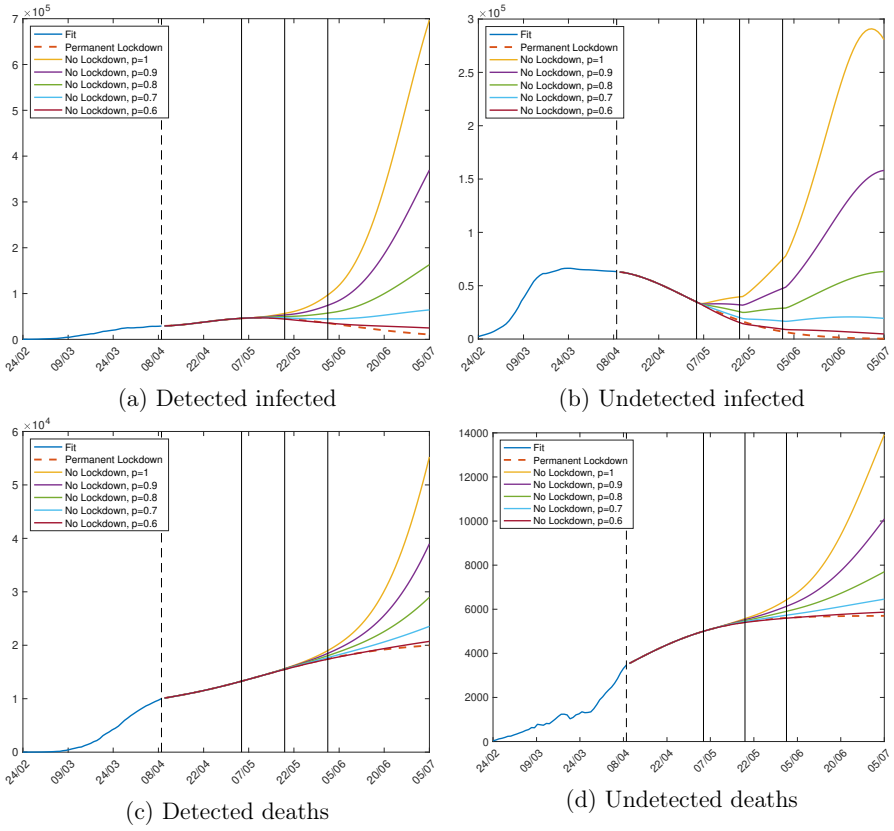

(a) Detected infected

(b) Undetected infected

(c) Detected deaths

(d) Undetected deaths

Figure 8: Detected and undetected deaths under different policy scenarios, Lombardy

Notes. The figure shows the evolution of infected and deaths under a set of counterfactual policies in Lombardy. We assume that the government lifts restrictions on three dates: 04/05, 18/05, 01/06. Vertical solid lines highlight these dates, vertical dashed line highlight the end of the fit window. On each date mobility increases at 25%, 50% and 75% of the pre-lockdown level. The counterfactuals assume different probability of contagion from 100% to 60% of its baseline. As a comparison, we also report the evolution under the permanent lockdown scenario (dashed line).

Covid Economics 18, 15 May 2020: 1-41

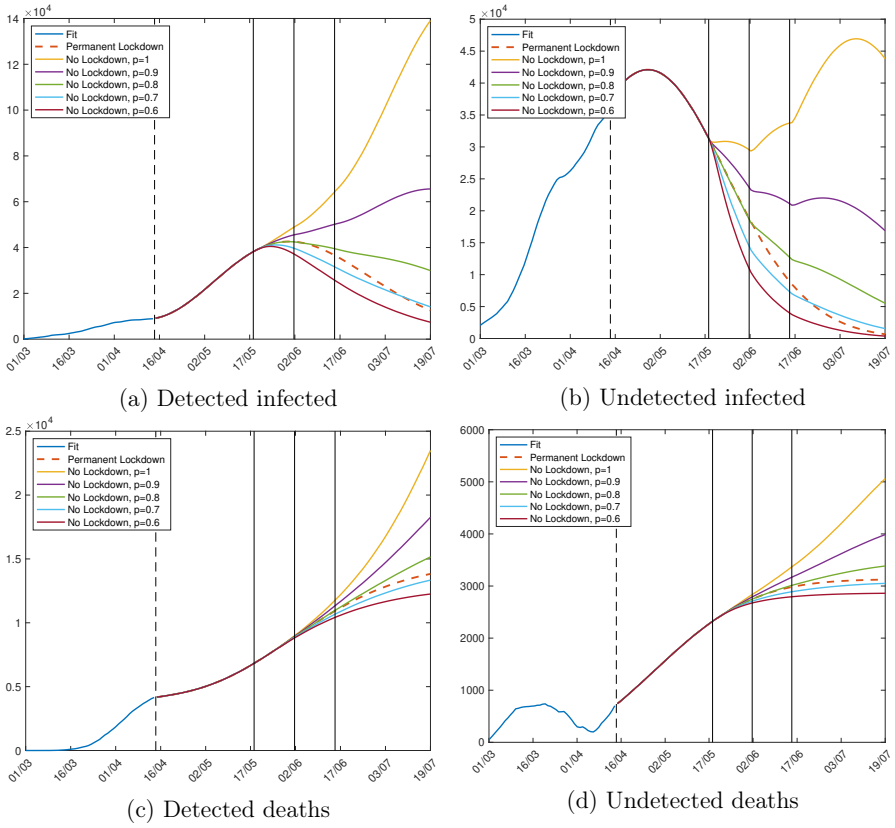

(a) Detected infected

(b) Undetected infected

(c) Detected deaths

(d) Undetected deaths

Figure 9: Detected and undetected deaths under different policy scenarios, London

Notes. The figure shows the evolution of infected and deaths under a set of counterfactual policies in London. We assume that the government lifts restrictions on three dates: 18/05, 01/06, 15/06. Vertical solid lines highlight these dates, vertical dashed line highlight the end of the fit window. On each date mobility increases at 25%, 50% and 75% of the pre-lockdown level. The counterfactuals assume different probability of contagion from 100% to 60% of its baseline. As a comparison, we also report the evolution under the permanent lockdown scenario (dashed line).

of the previous section. As highlighted already, in this scenario our model suggests that increases in mobility that are not offset by a reduced probability of contagion likely end up in a second epidemic peak. Reducing the probability of contagion makes the appearance of a second peak less likely and, as a consequence, considerably decreases the death toll. If the probability of contagion decreases at 60% of its baseline level we can expect in Lombardy a number of deaths that is very close to the permanent lockdown scenario: 20,700 detected and 5,900 undetected deaths in this counterfactual as opposed to 20,000 and 5,700, respectively, in the permanent lockdown, as shown in Table 1, row 9. In London a similar result is achieved when the probability of contagion is set between 70% and 80% of its baseline level.

Table 1 also shows that if the probability of contagion p_c does not increase to its level before the introduction of restriction measures the reproduction rate of the virus, R_t remains below 1. In the scenario where the probability of contagion is 60% of its pre-lockdown level, the forecast of R_t at the end of the forecast window is 0.92 (95% CI: 0.82-1.02) in Lombardy and 0.67 (95% CI: 0.55-0.78) in London. This evidence could provide some useful insights for policymakers when lifting restrictions and highlights the importance of adopting "soft" containment measures that could reduce the probability of infection, even when mobility goes back to its baseline levels as economic activities re-open.

5 Conclusion

This paper estimates a SEIRD epidemic model of COVID-19, by accounting for both observed and unobserved states in modeling infections, recoveries and deaths. We calibrate our model on data for Lombardy and London, two of the hardest hit regions in the world by the epidemic. We explicitly account for mobility changes due to the lockdown. We show that the under-reporting of cases and deaths is a quantitatively relevant phenomenon. Furthermore, we use the model to predict the evolution of the epidemic under different policy scenarios of lockdown lifting. We show that the lockdown has a considerable impact on total cases and deaths relative to an unmitigated scenario where the whole population would have been infected. Furthermore, we show that a gradual lifting of restrictions, in both Lombardy and London, would likely cause a second epidemic peak, which would be more severe if the return to the pre-lockdown mobility is faster. Anticipating, delaying or spreading the dates of re-opening on a longer time horizon would not change the main conclusion that a second peak is likely. However, we further show that reducing the probability of contagion to 60% of its baseline pre-lockdown level in Lombardy and between 70% and 80% in London – even in the presence of increased mobility – implies an evolution of the epidemic similar to that under a permanent lockdown scenario. Therefore, this paper provides evidence in favor of soft policies for the so called

Covid Economics 18, 15 May 2020: 1-41

"second phase," such as social distancing, wearing masks, sanitizing public and private spaces and increasing hygienic standard and, in general, all measures that can reduce the probability of infection. We see our results as a starting point, which could help policymakers in balancing the trade-off between imposing stricter measures and harming economic activity and campaigning in favor of softer measures whose efficacy ultimately depends on citizens' active collaboration. Nonetheless, more research is needed on which policy is most effective in cutting the transmission of the virus as more governments lift restrictions around the world.

References

Bucci, E., Leuzzi, L., Marinari, E., Parisi, G., and Ricci-Tersenghi, F. (2020). Un'analisi dei dati ISTAT sui decessi legati all'epidemia Covid-19 in Italia: verso una stima del numero di morti dirette ed indirette, anche grazie allo sbilanciamento di genere. Technical report, Mimeo.

Cancelli, C. and Foresti, L. (2020). The real death toll from Covid-19 is at least 4 times the official numbers. *Corriere della Sera*.

Day, M. (2020). Covid-19: four fifths of cases are asymptomatic, China figures indicate. *BMJ*, 369.

Della Valle, S., Hyman, J., Hethcote, H., and Eubank, S. (2007). Mixing patterns between age groups in social networks. *Social Networks*, 29(4):539–554.

Diekmann, O., Heesterbeek, J. A., and Metz, J. A. (1990). On the definition and the computation of the basic reproduction ratio R0 in models for infectious diseases in heterogeneous populations. *Journal of mathematical biology*, 28(4):365–382.

Doran, H. (1992). Constraining Kalman Filter and Smoothing Estimates to Satisfy Time-Varying Restrictions. *Journal of Economics and Statistics*, 74(3):568–572.

Favero, C. (2020). Why is Covid-19 mortality in Lombardy so high? Evidence from the simulation of a SEIHCR model. *Covid Economics: Vetted and Real Time Papers*, 4:47–61.

Ferguson, N., Laydon, D., Nedjati Gilani, G., Imai, N., Ainslie, K., Baguelin, M., Bhatia, S., Boonyasiri, A., Cucunuba Perez, Z., Cuomo-Dannenburg, G., et al. (2020). Report 9: Impact of non-pharmaceutical interventions (NPIs) to reduce COVID19 mortality and healthcare demand.

Covid Economics 18, 15 May 2020: 1-41

Giordano, G., Blanchini, F., Bruno, R., Colaneri, P., Filippo, A. D., and andMarta Colaneri, A. D. M. (2020). Modelling the COVID-19 epidemic and implementation of population-wide interventions in Italy. *Nature Medicine*.

Grassly, N. C. and Fraser, C. (2006). Seasonal Infectious Disease Epidemiology. *Proceedings: Biological Sciences*, 273(1600):2541–2550.

Harvey, A. (1989). *Forecasting structural time series models and the Kalman filter*. Cambridge University Press, 1 edition.

Heffernan, J. M., Smith, R. J., and Wahl, L. M. (2005). Perspectives on the basic reproductive ratio. *Journal of the Royal Society, Interface*, 2(4):281–293.

Kermack, W. O. and McKendrick, A. G. (1927). A contribution to the mathematical theory of epidemics. *Proceedings of the royal society of london. Series A, Containing papers of a mathematical and physical character*, 115(772):700–721.

Kucinskas, S. (2020). Tracking R of COVID-19. *Available at SSRN 3581633*.

Lauer, S. A., Grantz, K. H., Bi, Q., Jones, F. K., Zheng, Q., Meredith, H. R., Azman, A. S., Reich, N. G., and Lessler, J. (2020). The Incubation Period of Coronavirus Disease 2019 (COVID-19) From Publicly Reported Confirmed Cases: Estimation and Application. *Annals of Internal Medicine*, 172(9):577–582.

Lavezzo, E., Franchin, E., Ciavarella, C., Cuomo-Dannenburg, G., Barzon, L., Del Vecchio, C., Rossi, L., Manganelli, R., Loregian, A., Navarin, N., Abate, D., Sciro, M., Merigliano, S., Decanale, E., Vanuzzo, M. C., Saluzzo, F., Onelia, F., Pacenti, M., Parisi, S., Carretta, G., Donato, D., Flor, L., Cocchio, S., Masi, G., Sperduti, A., Cattarino, L., Salvador, R., Gaythorpe, K. A., Brazzale, A. R., Toppo, S., Trevisan, M., Baldo, V., Donnelly, C. A., Ferguson, N. M., Dorigatti, I., and Crisanti, A. (2020). Suppression of COVID-19 outbreak in the municipality of Vo, Italy. *medRxiv*.

Li, D., Lv, J., Botwin, G., Braun, J., Cao, W., Li, L., and McGovern, D. P. (2020a). Estimating the scale of COVID-19 Epidemic in the United States: Simulations Based on Air Traffic directly from Wuhan, China. *medRxiv*.

Li, Q., Guan, X., Wu, P., Wang, X., Zhou, L., Tong, Y., Ren, R., Leung, K. S., Lau, E. H., Wong, J. Y., Xing, X., Xiang, N., Wu, Y., Li, C., Chen, Q., Li, D., Liu, T., Zhao, J., Liu, M., Tu, W., Chen, C., Jin, L., Yang, R., Wang, Q., Zhou, S., Wang, R., Liu, H., Luo, Y., Liu, Y., Shao, G., Li, H., Tao, Z., Yang, Y., Deng, Z., Liu, B., Ma, Z., Zhang, Y., Shi, G., Lam, T. T., Wu, J. T., Gao, G. F., Cowling, B. J., Yang, B., Leung, G. M., and Feng, Z. (2020b). Early Transmission Dynamics in Wuhan, China, of Novel Coronavirus-Infected Pneumonia. *New England Journal of Medicine*, 382(13):1199–1207. PMID: 31995857.

Covid Economics 18, 15 May 2020: 1-41

Pepe, E., Bajardi, P., Gauvin, L., Privitera, F., Lake, B., Cattuto, C., and Tizzoni, M. (2020). COVID-19 outbreak response: a first assessment of mobility changes in Italy following national lockdown. *medRxiv*.

Piccolomini, E. L. and Zama, F. (2020). Preliminary analysis of covid-19 spread in italy with an adaptive seird model.

Rinaldi, G. and Paradisi, M. (2020). An empirical estimate of the infection fatality rate of COVID-19 from the first Italian outbreak. *medRxiv*.

Russo, L., Anastassopoulou, C., Tsakris, A., Bifulco, G. N., Campana, E. F., Toraldo, G., and Siettos, C. (2020). Tracing DAY-ZERO and Forecasting the Fade out of the COVID-19 Outbreak in Lombardy, Italy: A Compartmental Modelling and Numerical Optimization Approach. *medRxiv*.

Soper, H. E. (1929). The Interpretation of Periodicity in Disease Prevalence. *Journal of the Royal Statistical Society*, 92(1):34–73.

Stoffer, D. S. and Wall, K. D. (1991). Bootstrapping State-Space Models: Gaussian Maximum Likelihood Estimation and the Kalman Filter. *Journal of the American Statistical Association*, 86(416):1024–1033.

Tibayrenc, M. (2007). *Encyclopedia of Infectious Diseases: Modern Methodologies*. John Wiley & Sons, Inc., 1 edition.

Toda, A. A. (2020). Susceptible-infected-recovered (SIR) dynamics of Covid-19 and economic impact. *Covid Economics: Vetted and Real Time Papers*, 1:47–61.

Toxvaerd, F. (2020). Equilibrium Social Distancing. *Cambridge working papers in Economics No: 2020/08*.

Verity, R., Okell, L. C., Dorigatti, I., Winskill, P., Whittaker, C., Imai, N., Cuomo-Dannenburg, G., Thompson, H., Walker, P., Fu, H., Dighe, A., Griffin, J., Cori, A., Baguelin, M., Bhatia, S., Boonyasiri, A., Cucunuba, Z. M., Fitzjohn, R., Gaythorpe, K. A. M., Green, W., Hamlet, A., Hinsley, W., Laydon, D., Nedjati-Gilani, G., Riley, S., van Elsand, S., Volz, E., Wang, H., Wang, Y., Xi, X., Donnelly, C., Ghani, A., and Ferguson, N. (2020). Estimates of the severity of COVID-19 disease. *medRxiv*.

Villa, M. (2020a). Covid-19 and Italy's Case Fatality Rate: What's the Catch? Technical report, Istituto per gli Studi di Politica Internazionale.

Villa, M. (2020b). Fase 2: morti sommerse, "eccesso" di zelo? Technical report, Istituto per gli Studi di Politica Internazionale.

Covid Economics 18, 15 May 2020: 1-41

Villa, M., Myers, J. F., and Turkheimer, F. (2020). COVID-19: Recovering estimates of the infected fatality rate during an ongoing pandemic through partial data. *medRxiv*.

WHO (2020). Report of the WHO-China Joint Mission on Coronavirus Disease 2019 (COVID-19). Technical report.

Covid Economics 18, 15 May 2020: 1-41

CEPR PRESS

Appendix

A Extended Kalman Filter State Space Representation for the SEIRD Model

Our SEIRD model can be represented in non-linear state space form as

$$\mathbf{y}_t = \mathbf{Z}\boldsymbol{\alpha}_t + \boldsymbol{\varepsilon}_t \qquad \boldsymbol{\varepsilon}_t \sim N(\mathbf{0}, \Omega_\varepsilon) \tag{A.1}$$

$$\boldsymbol{\alpha}_t = \mathbf{T}(\boldsymbol{\alpha}_{t-1}) + \boldsymbol{\eta}_t \qquad \boldsymbol{\eta}_t \sim N(\mathbf{0}, \Omega_\eta) \tag{A.2}$$

where $\boldsymbol{\alpha}_t = (S_t, E_t, I_t, I_{dt}, R_t, R_{dt}, D_t, D_{dt})'$ is the unobserved state vector. The non linearity comes from the presence of multivariate vector function $\mathbf{T}(\boldsymbol{\alpha}_{t-1})$, which can be decomposed in the sum of its linear and non linear components $\mathbf{T}(\boldsymbol{\alpha}_{t-1}) = \mathbf{T} \cdot \boldsymbol{\alpha}_{t-1} + \mathbf{t}(\boldsymbol{\alpha}_{t-1})$, where

$$\mathbf{T} = \begin{pmatrix} 1 & 0 & 0 & 0 & 0 & 0 & 0 & 0 \\ 0 & (1-\sigma) & 0 & 0 & 0 & 0 & 0 & 0 \\ 0 & \sigma & (1-\epsilon-\delta-\gamma) & 0 & 0 & 0 & 0 & 0 \\ 0 & 0 & \epsilon & (1-\delta_d-\gamma_d) & 0 & 0 & 0 & 0 \\ 0 & 0 & \delta & 0 & 1 & 0 & 0 & 0 \\ 0 & 0 & 0 & \delta_d & 0 & 1 & 0 & 0 \\ 0 & 0 & \gamma & 0 & 0 & 0 & 1 & 0 \\ 0 & 0 & 0 & \gamma_d & 0 & 0 & 0 & 1 \end{pmatrix}$$

$$\mathbf{t}(\boldsymbol{\alpha}_{t-1}) = \begin{pmatrix} -\frac{\beta}{N-D_{t-1}-D_{dt-1}} S_{t-1} I_{t-1} \\ \frac{\beta}{N-D_{t-1}-D_{dt-1}} S_{t-1} I_{t-1} \\ \mathbf{0}_{6\times 1} \end{pmatrix}$$

Following Harvey (1989) the approximate Extended Kalman Filter can be applied to a non-linear state space model approximating $\mathbf{T}(\boldsymbol{\alpha}_{t-1})$ through its Tailor Expansion as $\mathbf{T}(\boldsymbol{\alpha}_{t-1}) \simeq \mathbf{T}(\hat{\boldsymbol{a}}_{t-1}) + \hat{\mathbf{T}} \cdot (\boldsymbol{\alpha}_{t-1} - \hat{\boldsymbol{a}}_{t-1})$, where $\hat{\boldsymbol{a}}_{t-1}$ is the updated state vector obtained from the updating recursions of the Kalman Filter and $\hat{\mathbf{T}} = \mathbf{T} + \hat{\mathbf{t}}$, where

Covid Economics 18, 15 May 2020: 1-41

$$\hat{\mathbf{t}} = \left.\frac{\partial \mathbf{t}\left(\boldsymbol{\alpha}_{t-1}\right)}{\partial \boldsymbol{\alpha}_{t-1}'}\right|_{\boldsymbol{\alpha}_{t-1}=\hat{\boldsymbol{a}}_{t-1}} =$$

$$= \begin{pmatrix} -\hat{I}_{t-1} & 0 & -\hat{S}_{t-1} & 0 & 0 & 0 & -\frac{\beta}{\left(N-\hat{D}_{t-1}-\hat{D}_{dt-1}\right)}\hat{S}_{t-1}\hat{I}_{t-1} & -\frac{\beta}{\left(N-\hat{D}_{t-1}-\hat{D}_{dt-1}\right)}\hat{S}_{t-1}\hat{I}_{t-1} \\ \hat{I}_{t-1} & 0 & \hat{S}_{t-1} & 0 & 0 & 0 & \frac{\beta}{\left(N-\hat{D}_{t-1}-\hat{D}_{dt-1}\right)}\hat{S}_{t-1}\hat{I}_{t-1} & \frac{\beta}{\left(N-\hat{D}_{t-1}-\hat{D}_{dt-1}\right)}\hat{S}_{t-1}\hat{I}_{t-1} \\ & & & & & & \mathbf{0}_{6\times 8} & \end{pmatrix} \times$$

$$\times \frac{\beta}{\left(N-\hat{D}_{t-1}-\hat{D}_{dt-1}\right)}$$

Here $\hat{S}_{t-1}$, $\hat{I}_{t-1}$, $\hat{D}_{t-1}$ and $\hat{D}_{dt-1}$ are the updated quantities obtained form the updated vector $\hat{\boldsymbol{a}}_{t-1}$.

Then the state equation (A.2) can be rewritten as

$$\boldsymbol{\alpha}_t = \left(\mathbf{t}\left(\boldsymbol{a}_{t-1}\right) - \hat{\mathbf{t}} \cdot \boldsymbol{a}_{t-1}\right) + \hat{\mathbf{T}} \cdot \boldsymbol{\alpha}_{t-1} + \boldsymbol{\eta}_t$$

Covid Economics 18, 15 May 2020: 1-41

Covid Economics 18, 15 May 2020: 1-41

B Derivation of R_0

Following Diekmann et al. (1990), the R_0 of our SEIRD model can be computed from the leading eigenvalue of the Next Generation Matrix. In our model, we have three states that describe the dynamics between the infected and non infected individuals, E_t, I_t and I_{dt}. The first difference of these three states reads as follows

$$\begin{aligned}
\Delta E_t &= -\sigma E_{t-1} + \frac{\beta}{N - D_{t-1} - D_{dt-1}} S_{t-1} I_{t-1} \\
\Delta I_t &= -\left(\delta + \epsilon + \gamma\right) I_{t-1} + \sigma E_{t-1} \\
\Delta I_{dt} &= -\left(\delta_d + \gamma_d\right) I_{dt-1} + \epsilon I_{t-1}
\end{aligned}$$

Then we need to identify the vectors $\mathcal{F}$ and $\mathcal{V}$ at the steady state of the system, which are the terms describing respectively the evolution of the new infections from the susceptible equation and the outflows from the infectious states. At the steady state we have that $S^* = N - D^* - D_d^*$, then

$$\mathcal{F} = \begin{pmatrix} \beta I^* \\ 0 \\ 0 \end{pmatrix} \qquad \mathcal{V} = \begin{pmatrix} \sigma E^* \\ \left(\epsilon + \delta + \gamma\right) I^* - \sigma E^* \\ \left(\delta_d + \gamma_d\right) I_d^* - \epsilon I^* \end{pmatrix}$$

From this we can compute their Jacobian matrices with respect to the exposed and infected states

$$F = \nabla \mathcal{F} = \begin{pmatrix} 0 & \beta & 0 \\ 0 & 0 & 0 \\ 0 & 0 & 0 \end{pmatrix} \qquad V = \nabla \mathcal{V} = \begin{pmatrix} \sigma & 0 & 0 \\ -\sigma & \left(\epsilon + \delta + \gamma\right) & 0 \\ 0 & -\epsilon & \left(\delta_d + \gamma_d\right) \end{pmatrix}$$

The Next Generation Matrix is the product FV^{-1} which describes the expected number of secondary infections in compartment i produced by individuals initially in state j. In our case we have

$$FV^{-1} = \begin{pmatrix} \frac{\beta}{\epsilon+\delta+\gamma} & \frac{\beta}{\epsilon+\delta+\gamma} & 0 \\ 0 & 0 & 0 \\ 0 & 0 & 0 \end{pmatrix}$$

From this we can compute the dominant eigenvalue (or spectral radius) from the characteristic equation of its eigendecomposition

$$\left|FV^{-1} - \lambda I_3\right| = \lambda^2 \left(\frac{\beta}{\epsilon + \delta + \gamma} - \lambda\right) = 0$$

which has two repeated solutions at $\lambda = 0$ and one at

$$\lambda = \frac{\beta}{\epsilon + \delta + \gamma}$$

which is our R_0.

Covid Economics 18, 15 May 2020: 1-41

CEPR PRESS

Covid Economics 18, 15 May 2020: 1-41

C Calibration of the Per-day Mortality Rate γ

As highlighted in the main text, we calibrate the per-day mortality rate γ so to estimate a number of unobserved deaths that equals a fraction of the excess mortality calculated from Istat data. Specifically, Bucci et al. (2020) exploit the gender unbalance in the number of deaths to decompose the excess mortality observed in Istat statistics into: deaths directly caused by COVID-19, but unreported in official data; deaths indirectly linked to COVID-19 (because of the pressure on hospitals at the peak of the epidemic); deaths unrelated to COVID-19. They provide estimates for various Italian regions and provinces and, among them, Lombardy. They show that, under different assumptions about the gender-specific mortality rate of COVID-19, the fraction of unreported deaths can range between 16% and 57% of the excess mortality with respect to the official death toll.[1] We therefore calibrate γ in order for our model to estimate a number of unobserved deaths that is equal to the simple average of these values, i.e. 36%. We find that $\gamma = 0.0011$ provides a series that resembles closely the cumulative deaths from Istat data, rescaled by this factor, as shown in Figure C.1.

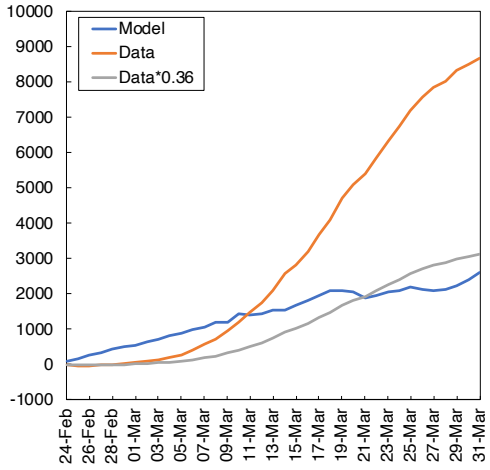

Figure C.1: Unobserved deaths, model and data

Notes. The figure reports the cumulative unobserved deaths from the SEIRD model and the excess mortality from Istat death registries, computed as the excess mortality in 2020 relative to the average of previous 5 years *minus* the official COVID-19 death toll. The latter is shown in levels and scaled by a factor of 0.36, following Bucci et al. (2020).

We also assume that the observed per-day mortality rate is three times larger than the unobserved one, i.e. $\gamma_c = 0.0033$, based on the fact the detected infections are usually symptomatic and more severe cases that are more likely to end up in critical conditions. The same parameters are used also when estimating the model on data for London.

[1] They also provide an estimate where the number of undetected deaths is higher than those detected, but we deem this as an extreme scenario.

D Additional Figures

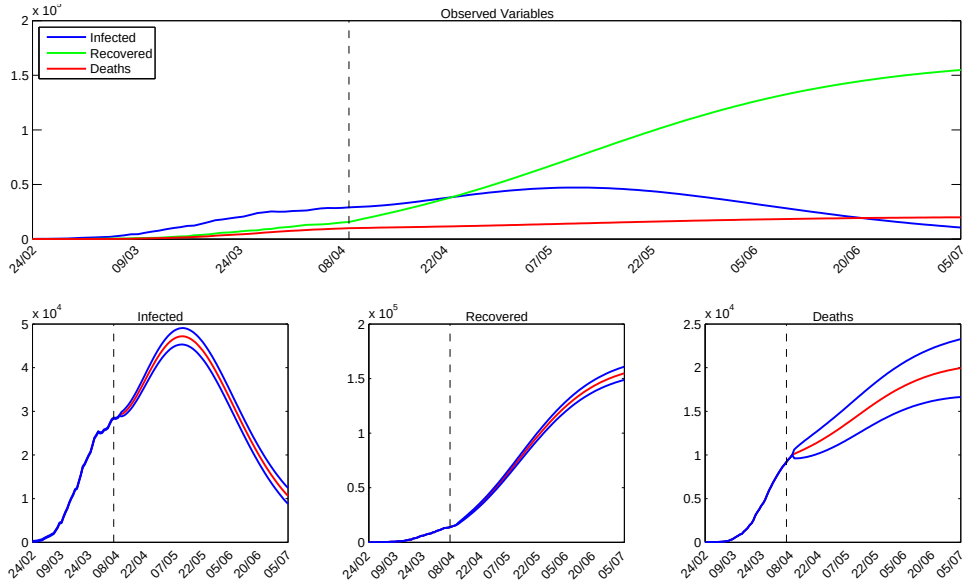

Figure D.1: Baseline scenario Lombardy: permanent lockdown.

Notes. The top panel shows fitted values and forecasts of detected infections, recoveries and deaths. The bottom panel shows the same quantities, alongside the inefficient 95% forecasting confidence bounds.

Covid Economics 18, 15 May 2020: 1-41

Covid Economics 18, 15 May 2020: 1-41

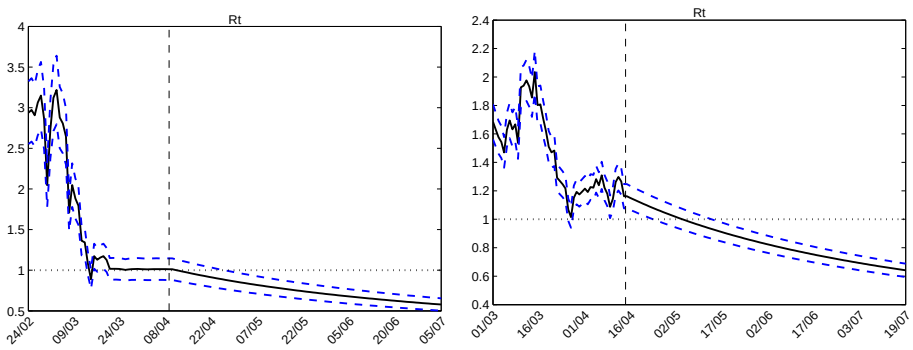

(a) Lombardy (b) London

Figure D.2: Estimated and forecast values of R_t in the baseline scenario of permanent lockdown, with the 95% bootstrapped confidence intervals.

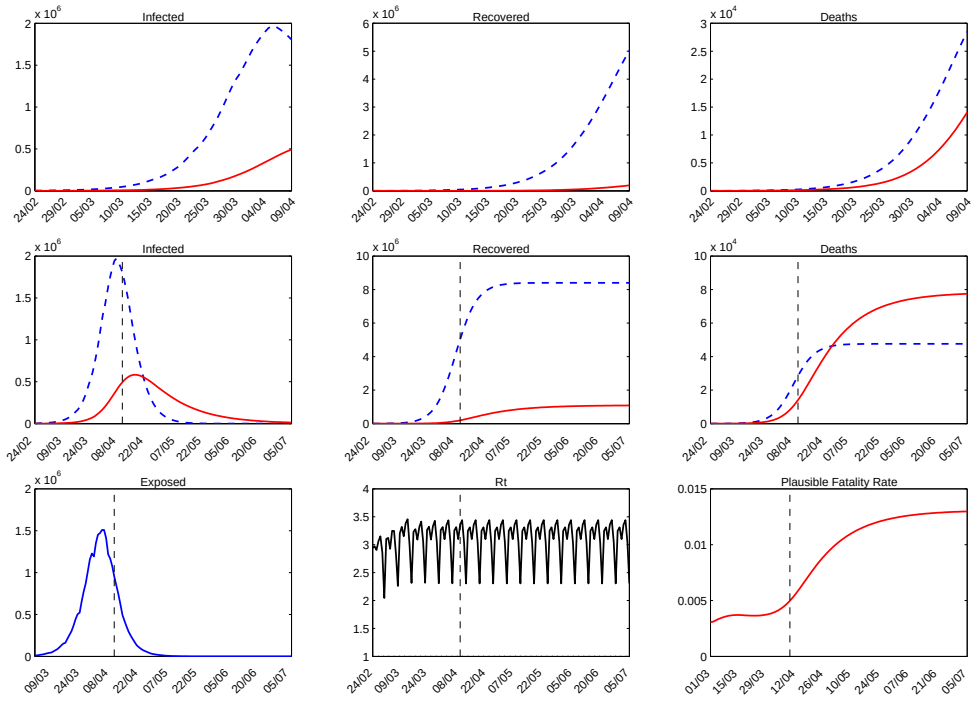

Figure D.3: Worst case scenario Lombardy: no lockdown.

Covid Economics 18, 15 May 2020: 1-41

Covid Economics 18, 15 May 2020: 1-41

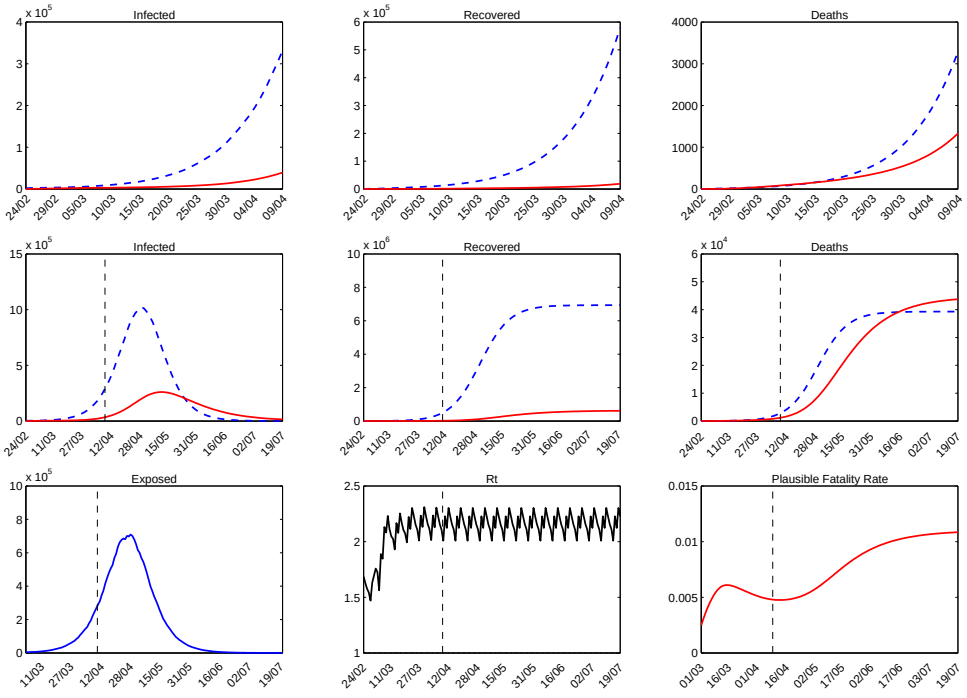

Figure D.4: Worst case scenario London: no lockdown.

Covid Economics 18, 15 May 2020: 1-41

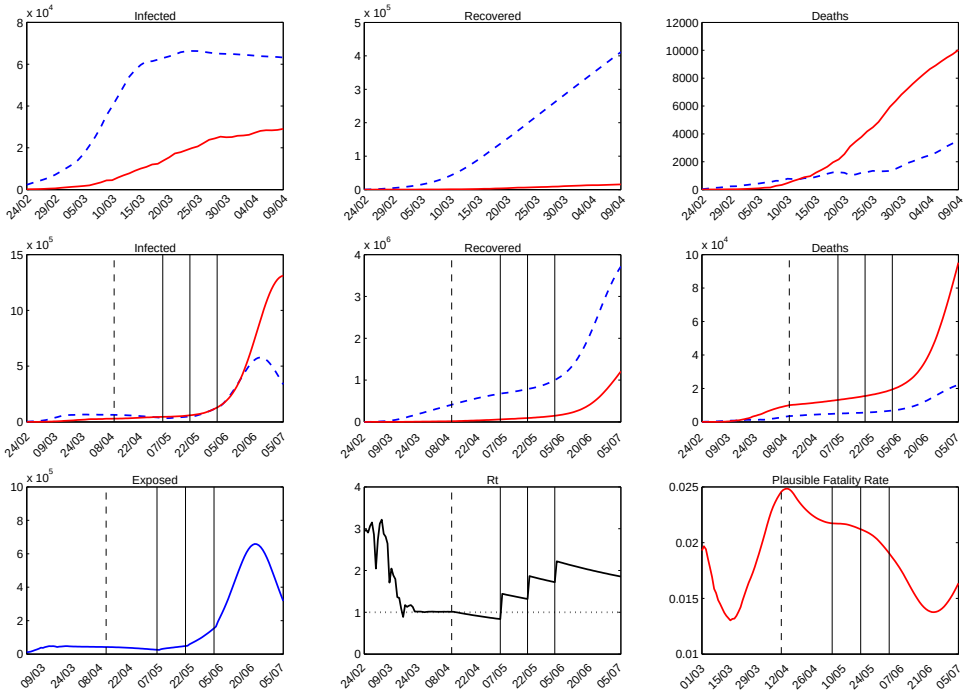

Figure D.5: Counterfactual scenario 1, Lombardy

Notes. In this scenario, the government lifts the lockdown gradually on 04/05, 18/05 and 01/06 bringing the mobility at 33%, 66% and 100% of the baseline of the 24/02.

Covid Economics 18, 15 May 2020: 1-41

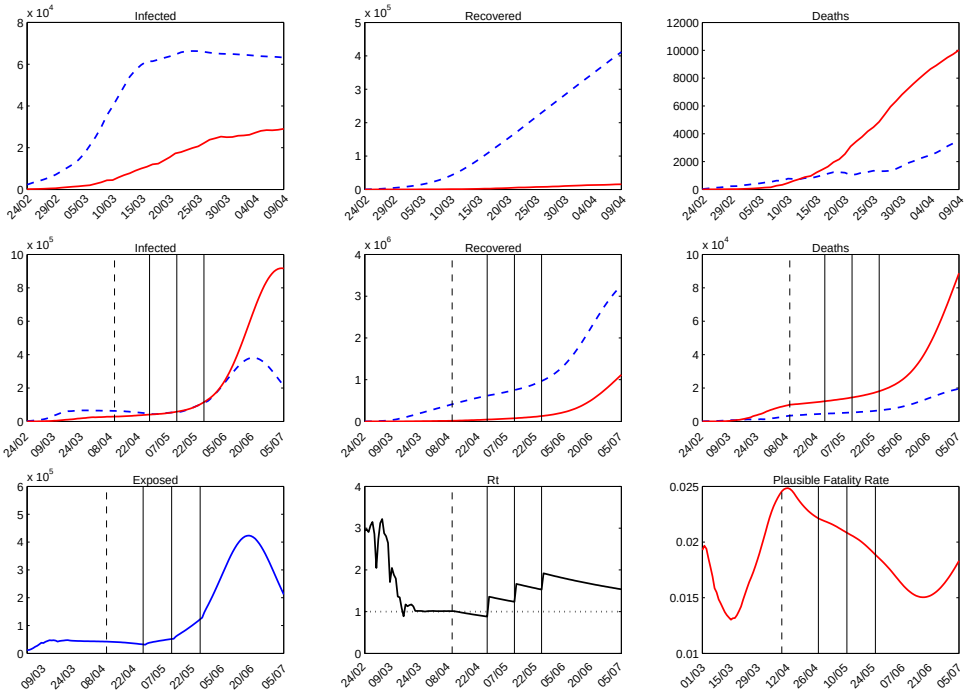

Figure D.6: Counterfactual scenario 2, Lombardy

Notes. In this scenario, the government lifts the lockdown gradually early on 27/04, 11/05 and 25/05, bringing the mobility at 25%, 50% and 75% of the baseline of the 24/02.

Covid Economics 18, 15 May 2020: 1-41

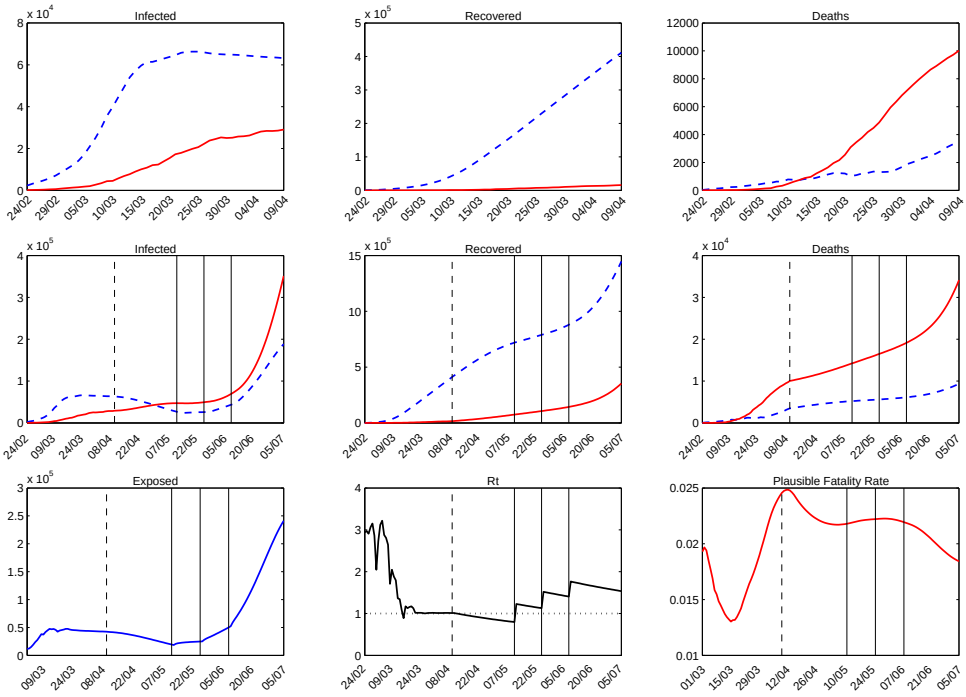

Figure D.7: Counterfactual scenario 3, Lombardy

Notes. In this scenario, the government lifts the lockdown gradually later on three dates 11/05, 25/05 and 08/06 bringing the mobility at 25%, 50% and 75% of the baseline of the 24/02.

Covid Economics 18, 15 May 2020: 1-41

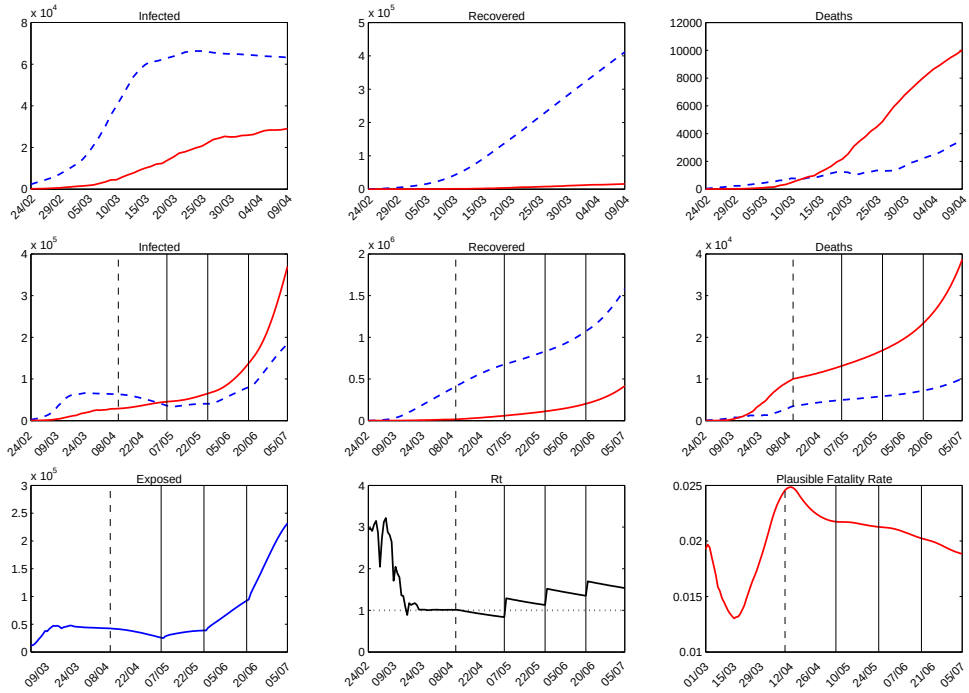

Figure D.8: Counterfactual scenario 4, Lombardy

Notes. In this scenario, the government lifts the lockdown gradually later on three dates 04/05, 25/05 and 15/06 bringing the mobility at 25%, 50% and 75% of the baseline of the 24/02.

Covid Economics 18, 15 May 2020: 1-41

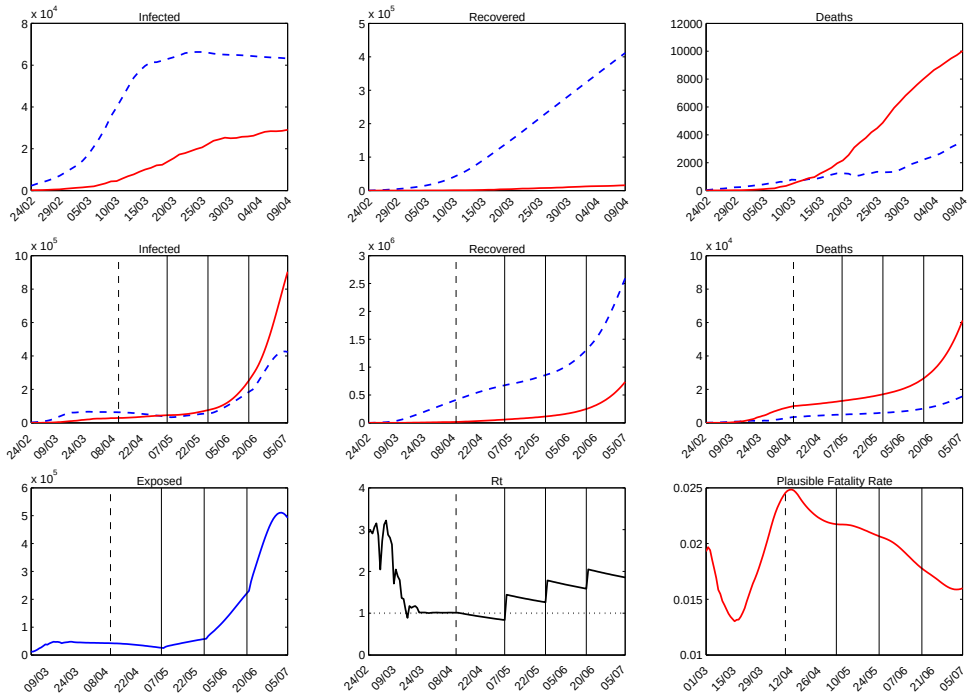

Figure D.9: Counterfactual scenario 5, Lombardy

Notes. In this scenario, the government lifts the lockdown gradually later on three dates 11/05, 25/05 and 08/06 bringing the mobility at 33%, 66% and 100% of the baseline of the 24/02.

Covid Economics 18, 15 May 2020: 1-41

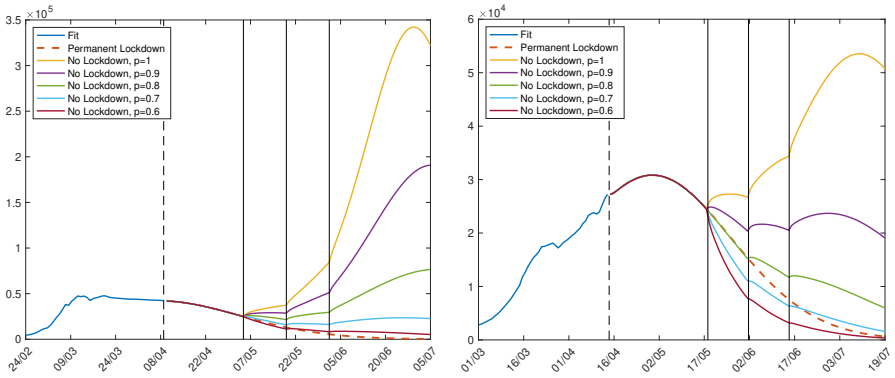

(a) Exposed, Lombardy (b) Exposed, London

Figure D.10: Exposed individuals in Lombardy and London under different probabilities of contagion

Notes. The figure shows the evolution of exposed individuals under a set of counterfactual policies in Lombardy (panel a) and London (panel b). We assume that the government lifts restrictions on three dates: 04/05, 18/05, 01/06 in Lombardy and 18/05, 01/06 and 15/06 in London. Vertical solid lines highlight these dates, vertical dashed line highlight the end of the fit window. On each date mobility increases at 25%, 50% and 75% of the pre-lockdown level. The counterfactuals assume different probability of contagion from 100% to 60%. As a comparison, we also report the evolution under the permanent lockdown scenario (dashed line).

Covid Economics Issue 18, 15 May 2020

Social distancing, quarantine, contact tracing and testing: Implications of an augmented SEIR model[1]

Andreas Hornstein[2]

Date submitted: 7 May 2020; Date accepted: 9 May 2020

I modify the basic SEIR model to incorporate demand for health care. The model is used to study the relative effectiveness of policy interventions that include social distancing, quarantine, contact tracing, and random testing. A version of the model that is calibrated to the Ferguson et al. (2020) model suggests that permanent, high-intensity social distancing reduces mortality rates and peak ICU demand substantially, but that a policy that relaxes high-intensity social distancing over time in the context of a permanent efficient quarantine regime is even more effective. Adding contact tracing and random testing to this policy further improves outcomes. For the policies considered, employment outcomes are determined by their respective social distancing components, not their quarantine component or health outcomes. Given the uncertainty surrounding the disease parameters, especially the transmission rate of the disease, and the effectiveness of policies, the uncertainty for health outcomes, however, is very large.

1 I would like to thank Alex Wolman and Zhilan Feng for helpful comments and Elaine Wissuchek for research assistance. Any opinions expressed are mine and do not reflect those of the Federal Reserve Bank of Richmond or the Federal Reserve System.

2 Senior Advisor, Federal Reserve Bank of Richmond.

Covid Economics 18, 15 May 2020: 42-72

Covid Economics 18, 15 May 2020: 42-72

1 Introduction

So far the primary response to the coronavirus pandemic, high-intensity social distancing, has been extremely disruptive for any economy where it has been applied. The question becomes whether the response can be maintained for an extended time without large negative effects for social, economic, and health outcomes. If high-intensity social distancing cannot be a permanent response to limit the spread of the coronavirus, then it is likely that the fallout of the pandemic might be dampened now but ultimately only delayed. Or are there alternative policy options that would be less disruptive for the economy but still contain the spread of the disease?

Ferguson et al. (2020) study the possible containment of the virus in a large-scale pandemic model emphasizing social distancing. Shen, Taleb and Bar Yam (2020) argue that this approach omits effective methods, such as testing for the virus and tracing contacts of known infected individuals. Modeling these methods could reduce the number of predicted deaths. To evaluate this criticism, I modify a simple susceptible-exposed-infected-recovered (SEIR) model to provide a stylized version that abstracts from all the demographic detail of the model of Ferguson et al. (2020). The model includes asymptomatic and symptomatic individuals who spread the disease and hospitalized individuals who require more or less intensive medical care. Symptomatic individuals are assumed to be known and can be quarantined. Furthermore, previously infected contacts of newly symptomatic individuals can be traced, and some can be quarantined too. Finally, random tests can be performed on the general population to find asymptomatic but infectious individuals. As in the standard SEIR model, health-state changes follow Poisson processes. The model is calibrated based on information in Ferguson et al. (2020).

With a baseline infection fatality rate of about 1 percent, the consequences from no intervention are dire: about 1 percent of the population is at risk of dying. For the UK that means about 600 thousand deaths, and for the US it means about 3.25 million deaths. I consider various interventions that involve social distancing, quarantine, contact tracing, and random testing to ameliorate this outcome. For the calibrated stylized model, I find that

- high-intensity social distancing (SD) is effective in the sense that it lowers cumulative deaths to less than 0.1 percent of the population, but it is only effective if it is permanent;
- permanent efficient quarantine is less effective than SD, it lowers cumulative deaths to 0.25 percent of the population, but when augmented with an efficient tracing process for previous contacts of newly symptomatic individuals, it is about as effective as permanent high-intensity SD;
- combining permanent high-intensity quarantine with a gradual relaxation of high-intensity SD is noticeably more effective than a policy of permanent high-intensity SD;
- adding contact tracing or random testing to the combination of permanent quarantine and gradual relaxation of SD further improves outcomes, but more for tracing than for testing;

- employment outcomes for the policies considered are determined by the SD component, that is, employment losses due to illness or quarantine of infectious individuals are negligible relative to employment losses due to SD.

To summarize, for a simple SEIR model that is calibrated to the Ferguson et al. (2020) study, there are alternative policies to permanent SD that provide health outcomes that are at least as good and potentially less disruptive. All of these policies attempt to reduce the rate at which the disease spreads, a summary statistic of which is the basic reproduction rate. Independent of whether the simple SEIR model is appropriate, there is a large degree of uncertainty associated with the effectiveness of any of these policies in the model. Most of this uncertainty is related to what we do (not) know about the parameters that characterize the spread of the disease. In a robustness analysis, I find that

- the model cannot match the sharp increase in cumulative deaths observed for the US and UK from late March to mid-April 2020 if it is parameterized to widely used estimates of the basic reproduction rate;
- the model can match the sharp increase in cumulative deaths if more recent estimates of higher reproduction rates are used, but for this case all policies become correspondingly less effective;
- more generally, given the large uncertainty surrounding parameter estimates for the disease process, the uncertainty about health outcomes predicted by the model is equally large. In the model the main driver of this outcome uncertainty is the uncertainty surrounding the basic reproduction rate.

One can have well-founded reservations on the use of the kind of model described here for policy analysis, and Jewell, Lewnard and Jewell (2020) provide an extensive list of these reservations. On the other hand, short of running actual 'experiments' on an economy, models like the one described here provide some guidance on possible outcomes for these policy interventions. Nevertheless, predictions on the relative efficiency of policy measures should be interpreted in the context of other work and past experience.

1.1 Related work in epidemiology

We work with an augmented version of the standard SEIR model of disease diffusion with Poisson arrival rates for health-state changes and implied exponential distributions for stage duration. While analytically convenient, the assumption of constant hazard rates for transitioning between disease stages in a SEIR model leads to outcomes that do not match the actual spread patterns for many infectious diseases. For example, Wearing, Rohani and Keeling (2005) and Feng, Xu and Zhao (2007) argue that relative to the observed diffusion of infectious diseases, standard SEIR-type models for which health-state transitions follow Poisson processes understate peak infection periods and overstate the duration of the process. They suggest that SEIR-models with gamma distributions for the stage distributions provide a better match of actual disease diffusion. But Feng (2007) also argues that in the presence of policy interventions, like quarantine, this simple ranking of the disease process

Covid Economics 18, 15 May 2020: 42-72

for exponential and gamma distributions may no longer hold. These qualifications should be kept in mind when interpreting the numerical results from our SEIR model.

Most epidemiological work on quarantine and contact tracing models these interventions as setting aside a fraction of newly infected individuals and gradually moving them to a quarantine state, similar to the transition between health states. The effectiveness of these interventions is then determined by the share and speed parameters, see for example Wearing et al. (2005) or Feng (2007). Lipsitch et al. (2003) use a similar approach to study the issue of contact tracing in the context of the SARS epidemic.

Compared to this epidemiological work, the approach taken here to model quarantine and tracing is more reduced form: a share of infected individuals is identified, and they are immediately quarantined, but only a fraction of quarantined individuals can be excluded from the infectious pool.

Covid Economics 18, 15 May 2020: 42-72

1.2 Related recent work by economists using SIR-type models

Eichenbaum, Rebelo and Trabandt (2020) study the impact of SIR-type dynamics on employment and output in a simple macro model with some endogenous response of meeting rates to the disease. Atkeson (2020) studies the impact of SD on deaths in a simple SIR-model. Alvarez, Argente and Lippi (2020) and Farboodi, Jarosch and Shimer (2020) study the optimal application of social distancing measures in a SIR model without and with an endogenous response of individuals to the emergence of the disease. Fernandez-Villaverde and Jones (2020) estimate time-varying transmission rates in a SIR-model by matching observed time paths of cumulative deaths in different localities.

Piguillem and Shi (2020) and Berger, Herkenhoff and Mongey (2020) are closest to this paper. They study optimal quarantine and testing in a SEIR-type model but do not include contact tracing. Berger et al. (2020) use a time-delayed quarantine model similar to the standard epidemiological literature, whereas the quarantine model in Piguillem and Shi (2020) is similar to the one we are using. The calibration in neither paper is tied as closely to Ferguson et al. (2020) as this paper is. Stock (2020) discusses the limitations of random testing of the general population to obtain better estimates of the asymptomatic share in the population.

New papers on the implications of the coronavirus for the economy are appearing daily, so this survey is already outdated.

2 The basic SEIR model

Define the stock of susceptible population S, infected and infectious population I, and recovered population R. Total population is

$$N = S + I + R.$$

Individuals transition sequentially between the states determined by Poisson processes with given arrival rates. Assume that the disease transmission rate for a given encounter is α, that the recovery rate from the disease is γ, and that recovered individuals are immune to the disease. See Figure 1 for a graphic representation.

Figure 1: The SIR Model

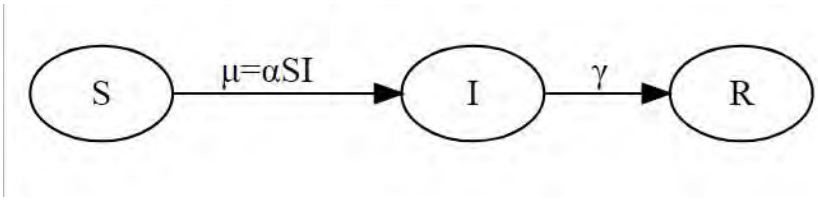

Total disease transmission, M, following from meetings between the susceptible and infected population is then,

$$M = \alpha \frac{IS}{N}.$$

The dynamics of $x = (S, I, R)$ are described by the differential equations

$$\begin{aligned} \dot{S} &= -\alpha \frac{IS}{N} \\ \dot{I} &= \alpha \frac{IS}{N} - \gamma I \\ \dot{R} &= \gamma I. \end{aligned}$$

The growth rate of the infectious group is

$$\hat{I} = \left(\frac{\alpha}{\gamma} \frac{S}{N} - 1 \right) \gamma.$$

Assume that the initial value for the population share of susceptible individuals when the process starts is essentially one, $S(0) \approx N$. Therefore the number of infected people is initially increasing if

$$\mathcal{R}_0 = \frac{\alpha}{\gamma} > 1.$$

The ratio $\mathcal{R}_0$ is called the basic reproduction number because it is approximately the average number of new infections before recovery from an infected individual at time zero,

$$\int_0^\infty \left[\alpha \frac{S(\tau)}{N} \tau \right] \gamma e^{-\gamma \tau} d\tau \approx \frac{\alpha}{\gamma} = \mathcal{R}_0,$$

where the first term in the integral is the average number of infections over a time interval τ and the second term is the probability of staying infectious for that time.

A standard extension of the SIR model places an exposed state that is not infectious, E, between the susceptible and the infectious group. This is called the SEIR model. Introducing the exposed state changes the dynamics of the model, e.g., it tends to change peak infection rates, but it usually does not affect terminal outcomes much. Let ϕ denote the rate at which exposed individuals become infectious, normalize the population at one, $N = 1$, and interpret the variables $x = (S, E, I, R)$ as population shares. Then the modified SEIR system is

$$\begin{aligned} \dot{S} &= -\alpha ES \\ \dot{E} &= \alpha ES - \phi E \\ \dot{I} &= \phi E - \gamma I \\ \dot{R} &= \gamma I. \end{aligned}$$

Covid Economics 18, 15 May 2020: 42-72

The system of differential equations is straightforward to solve, e.g., using MATLAB's ode45 routine starting with an initial condition $x_0 = (S_0, E_0, I_0, R_0)$.

3 An extended SEIR model with hospitalizations and death

I now extend the basic SEIR model to provide a stylized representation of the pandemic model in Ferguson et al. (2020). The pandemic model of Ferguson et al. (2020) contains a detailed description of the demographics of the population, its age distribution, locations, etc. Our stylized model will not contain any of that detail. What the model takes from Ferguson et al. (2020) is the basic mechanics of how the disease spreads from exposure to asymptomatic infection to symptomatic infection, hospitalization, and finally recovery or death. This abstraction makes it easy to explore the relative merits of various policy measures, such as social distancing, quarantine, contact tracing, and random testing in a unified framework.

We start with the SEIR model. Susceptible individuals are exposed to the infection but are not immediately infectious. Exposed individuals become infectious, but they initially do not show any symptoms. After some time, asymptomatic infected individuals do show symptoms of the disease and are triaged depending on their condition. Most do not require hospitalization, but some do, in severe cases in ICUs. All infected individuals either recover over time and become immune, or they die.

Figure 2: The Extended SEIR Model

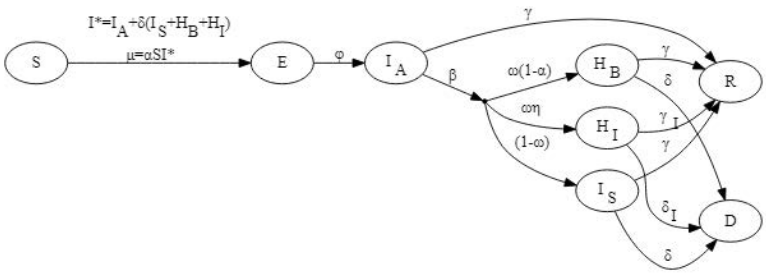

Figure 2 provides a graphic representation of this process. The stock of exposed individuals is E, the inflow of newly exposed individuals is M, and the rate at which exposed individuals become infectious without symptoms is ϕ. Asymptomatic individuals recover at rates γ, and they become symptomatic at rate β. For a fraction ω of newly symptomatic individuals, the condition is serious enough to be hospitalized. In addition, a fraction η of the hospitalized individuals require ICU treatment. Hospitalized individuals recover at rates γ respectively γ_{ICU}, and they die at rates δ respectively δ_{ICU}. Asymptomatic and

Covid Economics 18, 15 May 2020: 42-72

Covid Economics 18, 15 May 2020: 42-72

symptomatic individuals who are not hospitalized also recover or die at rates γ respectively δ.[1]

The following system of differential equations provides the formal representation of the process dynamics.

$$\begin{aligned}
\dot{S} &= -M \\
\dot{E} &= M - \phi E - q_{TE} - q_{FE} \\
\dot{I}_A &= \phi E - (\beta + \gamma) I_A - q_{TA} - q_{FA} \\
\dot{E}_T &= q_{TE} + q_{FE} - \phi E_T \\
\dot{I}_{AT} &= q_{TA} + q_{FA} + \phi E_T - (\beta + \gamma) I_{AT} \\
\dot{I}_S &= (1-\omega)\beta(I_A + I_{AT}) - (\gamma + \delta) I_S \\
\dot{H}_B &= (1-\eta)\omega\beta(I_A + I_{AT}) - (\gamma + \delta) H_B \\
\dot{H}_{ICU} &= \eta\omega\beta(I_A + I_{AT}) - (\gamma_{ICU} + \delta_{ICU}) H_{ICU} \\
\dot{R} &= \gamma (I_A + I_{AT} + I_S + H_B) + \gamma_{ICU} H_{ICU} \\
\dot{D} &= \delta (I_S + H_B) + \delta_{ICU} H_{ICU}
\end{aligned}$$

The flow terms q_{TE}, q_{TA}, q_{FE}, and q_{FA}, and the stocks E_T and I_{AT} refer to the identification of exposed and asymptomatic individuals through tracing and/or random testing discussed below.

Policy interventions, such as social distancing and quarantining known infected individuals, are modeled through their impact on the flow of new infections. As in the basic SIR model, the flow of new infections is proportional to the product of susceptible individuals and infectious individuals, but quarantine can reduce the number of infected individuals who can meet the susceptible population. We assume that symptomatic individuals are always known and that tracing and random testing can identify some of the exposed and asymptomatic individuals, E_T and I_{AT}. Let ε_i denote the effectiveness of quarantine for the known infected population groups, $i \in \{S, B, ICU, AT\}$, and also assume that symptomatic infected are more infectious than asymptomatic infected at the rate σ, then the effective pool of infectious individuals that meets the susceptible population and the inflow of newly infected individuals are[2]

$$\begin{aligned}
I^* &= I_A + (1-\varepsilon_{AT}) I_{AT} + \sigma \left[(1-\varepsilon_S) I_S + \sum_{i=B,ICU} (1-\varepsilon_i) H_i \right], \\
M &= \alpha S I^*.
\end{aligned}$$

Social distancing is assumed to directly reduce the rate at which individuals, infectious and susceptible, contact each other. Let ψ denote the relative contact rate for an individual,

[1] Total deaths are small enough such that the implicit assumption of a constant population is not too distorting.

[2] This is a simplified version of the quarantine model used in the epidemiological literature in the sense that identified people are added instantaneously to the quarantine pool, but some infections seep out of that pool. The epidemiological literature I am aware of assumes that infected individuals join the quarantine pool gradually following a Poisson process, but then quarantine is perfect. For example, Feng (2007).

Covid Economics 18, 15 May 2020: 42-72

that is, $\psi \leq 1$ and $\psi = 1$, in the absence of SD. Then the transmission flow is

$$M = \alpha_0(\psi S)(\psi I^*) = \alpha_0 \psi^2 S I^*,$$

where α_0 is the disease transmission rate without any SD measures. In the following we will use $\alpha = \alpha_0\psi^2$ as the effective transmission rate.

Social distancing is thus potentially a very effective way to contain the spread of the disease since a reduction of contact rates applies to all individuals, infectious and non-infectious. Therefore a reduction of contact rates implies a squared reduction of transmission rates. Social distancing is also 'easy' to implement since all individuals are supposed to reduce their contact rates, that is, no particular information is required. This indiscriminate reduction of contact rates also makes SD very disruptive for the economy.

Quarantine methods on the other hand target individuals who are infectious, that is, they require information on an individual's health status. As long as the health status is observable, that is, for symptomatic individuals, it is relatively straightforward to implement, though not costless. The problem with a disease like COVID-19 is that a large share of infectious individuals, current estimates are around 50 percent, may never show symptoms. Thus even if one were able to quarantine all symptomatic individuals, one would only be able to reduce the pool of infectious individuals by 50 percent. On the other hand, quarantine is somewhat more efficient than that since symptomatic individuals are presumably more infectious than asymptomatic individuals. Contact tracing and random testing are attempts to reduce the pool of infectious individuals even more.

Tracing of asymptomatic infected individuals is modeled as follows. The average number of people an asymptomatic individual has infected and who are still in the exposed resp. asymptomatic state when he or she becomes symptomatic is $\mathcal{R}_{ATE}$ resp. $\mathcal{R}_{ATA}$, derived in the Appendix. If ε_T is the efficiency of tracing, then the inflow of newly identified exposed and asymptomatic individuals through tracing is

$$q_{TE} = \varepsilon_T \mathcal{R}_{ATE} \beta I_S \text{ and } q_{TA} = \varepsilon_T \mathcal{R}_{ATA} \beta I_S.$$

We essentially assume that tracing does not require time, but is instantaneous.[3]

Testing is modeled as follows. Let f be the flow rate at which not yet identified asymptomatic people are randomly tested. Assume that asymptomatic infected can be identified through tests, but not merely exposed individuals. Also assume that recovered individuals are not tested. Then the share of identified asymptomatic in a random test is[4]

$$p_F = \frac{I_A}{S + E + I_A}.$$

The inflow of newly identified exposed and asymptomatic individuals through random testing is

$$q_{FA} = p_F f \left(1 + \varepsilon_T \mathcal{R}_{ATA}\right) \text{ and } q_{FE} = p_F f \varepsilon_T \mathcal{R}_{ATE},$$

where we allow for the possibility that previous contacts of newly identified asymptomatic individuals are then also traced.

[3] It is straightforward to introduce a time delay for the recovery of tracked individuals. Again, we model the efficiency of tracing not through the rate at which potentially traceable individuals enter the quarantine pool, but through the size of the captured pool, see footnote 2.

[4] This potentially overstates the effectiveness of random testing with incomplete quarantine to the extent that the infectious pool also contains symptomatic individuals.

Covid Economics 18, 15 May 2020: 42-72

4 Calibration

I parameterize the model following Ferguson et al. (2020) as much as possible, that is, unless otherwise noted all listed statistics are from Ferguson et al. (2020). The unit time interval is a year.

- The basic reproduction rate is $\mathcal{R}_0 = 2.4$. This estimate is consistent with the assessment of Fauci, Lane and Redfield (2020).
- The incubation period is 5.1 days, $\phi = 1/(5/365)$.
- Symptomatic infections are 50% more infectious than asymptomatic infections, $\sigma = 1.5$
- 4.4 percent of newly symptomatic infected are hospitalized, $\omega = 0.044$
- 30 percent of hospitalized infected require ICU, $\eta = 0.3$
- The mean duration of a hospital stay is 10.4 days
  - Non-ICU for 8 days, $\gamma_B = 1/(8/365)$
  - ICU for 16 days, of which 10 days are on ICU. We set $\gamma_{ICU} = 1/(16/365)$, which overstates the time ICU requirement by about 50 percent.
  - We set the recovery rates of non-hospitalized infected to the same as the one of non-ICU hospitalized, $\gamma = \gamma_B$
- 50 percent of infected in ICU die, $p_{D,ICU} = 0.5$. In the appendix we derive the probability for death in ICU, $P_{D,ICU}(\delta_{ICU}, \gamma_{ICU})$. We can solve $p_{D,ICU} = P_{D,ICU}(\delta_{ICU}, \gamma_{ICU})$ for δ_{ICU}.
- 40 percent to 50 percent of infected are never identified, mainly because they are asymptomatic, $p_{AR} = 0.5$. In the Appendix we derive the probability that an asymptomatic infected recovers before showing symptoms as a function of the rate of becoming symptomatic, and the recovery and death rates, $P_{AR}(\beta, \gamma, \delta)$. We can solve $p_{AR} = P_{AR}(\beta, \delta, \gamma)$ for β.
- The unconditional infection fatality ratio (IFR) is 0.9 percent, $p_I = 0.009$. We adjust the death rate for non-ICU infected, δ, such that the overall terminal fatality rate without intervention is close to p_I.
- Two-thirds of I_S self-isolate after one day, with a mean delay of five days. Since our quarantine does not involve any time delay, we assume that the baseline quarantine rate for non-hospitalized I_S is $\varepsilon_S = 1/3$.
- Quarantine: Baseline effectiveness for policy intervention is $\varepsilon_S = 0.5$, which is an average of the two options listed
  - Case isolation at home (CI): I_S stay home for seven days, reduce contacts with non-household members by 75%. Compliance is 75%. $\varepsilon = 0.75 \times 0.75 = 0.6$

Covid Economics 18, 15 May 2020: 42-72

  - Voluntary quarantine at home (VQ): All household members stay home for 14 days. Infection rate within households doubles, community contacts reduced by 75%. Compliance is 50%.

- Social distancing (SD) is assumed to reduce contact rates for workplace interactions by 25 percent and for social interactions by 75 percent. I use the 2018 American Time Use survey together with data on US employment rates to calculate the implications of these assumed reductions in contact rates for the average contact rate in the economy, Appendix A.2. The average contact rate ψ declines by about 60 percent, depending on what assumptions we make on the relative intensity of social and workplace interactions. This means that SD can reduce the transmission rate α and the reproduction rate $\mathcal{R}_0$ by about 80 percent.

- Finally, I made up the quarantine rate for hospitalized infected, $\varepsilon_i = 0.95$ for $i \in \{B, ICU\}$. These quarantine rates should be high, but medical staff gets infected.

5 Experiments

I consider various time-varying interventions affecting the basic reproduction rate, $\mathcal{R}_0$, that is, infection rate α, the quarantine efficiency for non-hospitalized symptomatic infected, ε_S, and the tracing efficiency, ε_T. For SD and quarantine policies, we consider a permanent intervention, that is, a permanent change in the policy parameter, and a temporary intervention that returns the policy parameter to its initial value after some time. I then consider joint policies of SD and quarantine, augmented by tracing and testing.

We seed the initial condition following Ferguson et al. (2020) and assume that the first infection occurs January 1, 2020, and that infections double every five days. Taking the case fatality rate of 0.9%, we then match the number of deaths at the starting date of the simulation. For the UK and the USA, we take the starting date to be March 24, when the UK imposed a national lockdown.[5] Up to that day, 335 deaths and 5,654 infections were reported in the UK. According to the seeding method, reported infections represented 9 percent of imputed infections in the UK.[6] We also assume that initially there are one and a half times as many exposed individuals as there are imputed infected individuals.

The baseline outcome from the spread of the disease without any policy intervention is about 1 percent of the population dead since the assumed case fatality rate is about 1 percent. That means 600 thousand deaths in the UK and 3.25 million deaths in the USA. By how much can the various policy interventions reduce the total number of deaths?

The model specification assumes that ICU units are available for any infected individuals requiring intensive care. Fatality rates will be higher if demand for ICU units exceeds the number of available ICU units. So the impact of policies on the number of infected requiring

[5] In the US, 21 states had issued stay-at-home orders by March 24, including California and the north-eastern states. An additional 19 states issued these orders by April 1. These orders cover most of the US population. Source: https://www.kff.org/coronavirus-policy-watch/stay-at-home-orders-to-fight-covid19/

[6] We could also seed the model with US data. On March 24, there were 471 cumulative deaths and 42,164 reported infections in the USA. Reported infections represent 43 percent of imputed infections in the USA. Peak infection rates and terminal conditions do not depend on the two initial conditions.

ICU units is also important. There are about 4 thousand ICU units in the UK, about 0.006 percent of UK population, and 63 thousand ICU units in the US, about 0.095 percent of US population.[7]

In the following section, we consider the impact of variations in social distancing and the effectiveness of quarantine, tracing, and random testing measures to reduce cumulative deaths and peak ICU demand. These experiments are performed for the UK seeding, but the seeding does not make a big difference. We report the outcomes for population shares and occasionally compare the absolute numbers with Ferguson et al. (2020).

5.1 Effectiveness of social distancing

High-intensity SD, that is, large permanent reductions in the basic reproduction rate, has a large impact on fatalities and peak ICU usage. But even high-intensity SD interventions have to be permanent to be effective.

- We consider permanent SD interventions and SD interventions that are limited to six months, after which the reproduction rate returns to its base value. The results are displayed in Table 1 and Figure 3.[8]
- A permanent reduction of the reproduction rate by 75 percent reduces total deaths by a factor of 150, from 1 percent to 0.006 percent of the population, top panel of Table 1, column 5. In addition it cuts the peak demand for ICU units by a factor of more than 50 to 0.001 percent of the population, Table 1, column 4. This peak ICU demand is below ICU capacity for either the UK or the US.
- SD interventions need not necessarily have to bring the basic reproduction rate below one to be effective. For example, a 50 percent reduction of the reproduction rate still leaves it above one, but it reduces total deaths by a factor of twenty.
- Temporary reductions of the basic reproduction rate have a minor impact on total deaths and peak ICU demand, they mostly delay them, see bottom panel of Table 1, columns 4 and 5, and Figure 3. Essentially, most people are still susceptible to the virus at the time SD is lifted, and the spread of the disease starts anew, Table 1, column 6.[9]
- It is not obvious how much of a reduction in the reproduction rate can be attained through SD. Using the assumptions of Ferguson et al. (2020), the reproduction rate can be reduced by about 80 percent, depending on the assumptions on the relative intensity of social and workplace interactions, Appendix A.2. But even a 75 percent reduction of the reproduction rate reduces total deaths to about 4 thousand in the UK and brings

[7]For the UK, *Daily Telegraph*, March 25, 2020, https://www.telegraph.co.uk/global-health/science-and-disease/hospitals-could-need-75-times-number-critical-care-beds-treat/. For the US, medical intensive care and other ICUs for adults from https://www.aha.org/statistics/fast-facts-us-hospitals for the US.

[8]Recall that the percentage reduction of the reproduction rate is the squared percentage reduction of the contact rate.

[9]In Piguillem and Shi (2020), a temporary SD policy is effective because they assume that a critical mass of infected individuals is needed for the disease to spread.

Covid Economics 18, 15 May 2020: 42-72

Table 1: Effectiveness of Social Distancing ψ

Model	(1) Max I_A	(2) Max I_{AT}	(3) Max I_S	(4) Max H_{ICU}	(5) Term D	(6) Term S
			Permanent Change			
$\mathcal{R}_0$=2.40	4.294	0.000	3.871	0.054	0.912	23.665
$\mathcal{R}_0$=1.80	1.556	0.000	1.444	0.020	0.627	47.476
$\mathcal{R}_0$=1.20	0.101	0.000	0.070	0.001	0.040	96.684
$\mathcal{R}_0$=0.60	0.100	0.000	0.056	0.001	0.006	99.521
			Transitory Change			
$\mathcal{R}_0$=2.40	4.294	0.000	3.871	0.054	0.912	23.665
$\mathcal{R}_0$=1.80	1.656	0.000	1.529	0.021	0.802	32.813
$\mathcal{R}_0$=1.20	3.932	0.000	3.556	0.050	0.901	24.594
$\mathcal{R}_0$=0.60	4.179	0.000	3.768	0.053	0.907	23.977

Note. The rows list the replication rate $\mathcal{R}_0$ implied by reduction of contact rates ψ through SD. The first four columns are the peak shares of (1) asymptomatic infected, (2) known asymptomatic infected, (3) symptomatic at home, and (4) ICU units required. The last two columns are the terminal values after one and a half years for (5) cumulative deaths and (6) susceptible population. All variables are percent of total population. A temporary intervention reduces the basic reproduction rate for a six month period and then returns it to its baseline value of 2.4.

peak ICU demand below capacity. These numbers for deaths and ICU demand in the UK are substantially smaller than the numbers in Ferguson et al. (2020), who report cumulative deaths of 80 thousand to 100 thousand for policies that emphasize SD. Since we are interested in the impact of policy alternatives to SD for a calibration that starts with an SD policy whose implications are comparable to the ones discussed in Ferguson et al. (2020), from now on we assume that the impact of SD is more limited. In particular, we assume that SD reduces the reproduction rate only by 45 percent, resulting in cumulative deaths of about 80 thousand in the UK.

5.2 Effectiveness of quarantine

Efficient permanent quarantine on its own reduces fatalities and peak ICU demand substantially. When quarantine is combined with contact tracing, it yields results comparable to SD.

- We allow for the possibility of quarantining a fraction, ε_S, of the known symptomatic non-hospitalized individuals, and possibly trace previous contacts of newly symptomatic individuals. We only display results for a permanent quarantine regime, since transitory quarantine policies are as ineffective as are transitory SD policies. The results are displayed in the top panel of Table 2 and Figure 4.

- Permanent strict quarantine that removes up to 90 percent of the known symptomatic infected individuals from the infectious pool reduces total deaths by 75 percent and

Covid Economics 18, 15 May 2020: 42-72

Covid Economics 18, 15 May 2020: 42-72

Figure 3: Effectiveness of Social Distancing $\mathcal{R}_0$

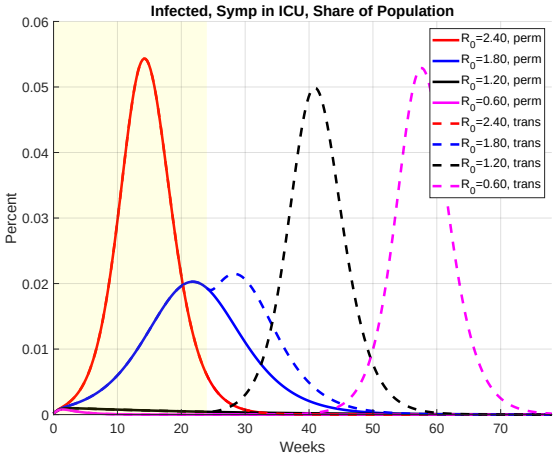

(a) ICU Hospital Beds

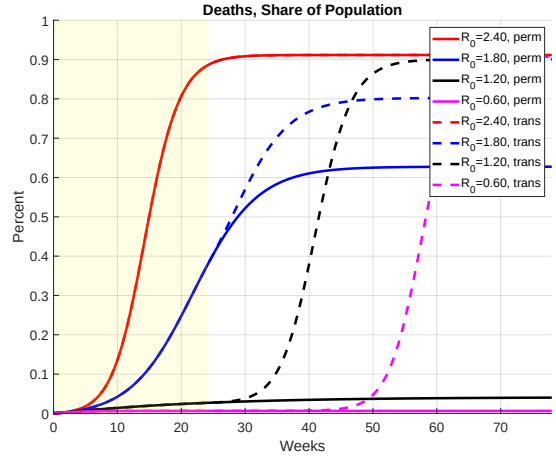

(b) Deaths

Note: See notes for Table 1. Solid lines represent permanent policies and dashed lines represent temporary policies. The shaded area denotes the first six months for which a temporary policy is in place.

Table 2: Effectiveness of Quarantine ε_S and Tracing ε_T

Model	(1) Max I_A	(2) Max I_{AT}	(3) Max I_S	(4) Max H_{ICU}	(5) Term D	(6) Term S
No Contact Tracing $\varepsilon_T = 0$						
ε_S=0.33	4.294	0.000	3.871	0.054	0.912	23.665
ε_S=0.50	3.085	0.000	2.817	0.040	0.804	32.718
ε_S=0.70	1.571	0.000	1.456	0.020	0.599	49.830
ε_S=0.80	0.858	0.000	0.801	0.011	0.448	62.507
ε_S=0.90	0.293	0.000	0.274	0.004	0.247	79.293
Perfect Contact Tracing $\varepsilon_T = 1.0$						
ε_S=0.33	3.674	0.402	3.679	0.052	0.899	24.698
ε_S=0.50	2.421	0.297	2.490	0.035	0.772	35.326
ε_S=0.70	0.910	0.134	0.972	0.014	0.509	57.402
ε_S=0.80	0.303	0.050	0.331	0.005	0.290	75.677
ε_S=0.90	0.101	0.016	0.092	0.001	0.058	95.211

Note. See Notes for Table 1.

brings peak ICU demand below capacity in the UK and US, top panel of Table 2, columns 4 and 5.

- Combining efficient quarantine with perfect contact tracing reduces the infectious pool by another factor of three, column 1 of Table 2. Quarantining traced asymptomatic individuals then cuts peak ICU demand and total deaths by another factor of four, Table 2, columns 4 and 5.

5.3 Effectiveness of combined policies

We now consider the impact on total deaths and peak ICU demand of four policy interventions that to various degrees combine elements of SD, quarantine, tracing, and testing, Table 3. As a reference point, we list the outcomes from no intervention in the first row of Table 3. The baseline policy is one of permanent high-intensity SD and temporary medium efficient quarantine based on Ferguson et al. (2020). We then consider alternative policies that combine a relaxation of SD over time with more efficient permanent quarantine regimes, augmented with efficient tracing and/or random testing. We find that in our calibrated stylized model, the alternative policies that combine efficient quarantine with tracing do equally well as SD in terms of reducing peak ICU demand and imply significantly lower total deaths than the baseline SD policy.

For our stylized version of the policy studied in Ferguson et al. (2020), we interpret the baseline policy as a permanent 45 percent reduction of the transmission rate α, combined with a temporary three-month increase of quarantine efficiency to $\varepsilon_S = 0.5$.[10] Relative to no

[10]See sections 4, 5.1, and Ferguson et al. (2020), Table 4, for the cases with general quarantine and SD. Ferguson et al. (2020) propose SD for at least five months, with subsequent relaxation and tightening contingent on ICU demand triggers. Effectively SD is in place for 80 percent of the time.

Covid Economics 18, 15 May 2020: 42-72

Figure 4: Effectiveness of Quarantine ε_{IS}

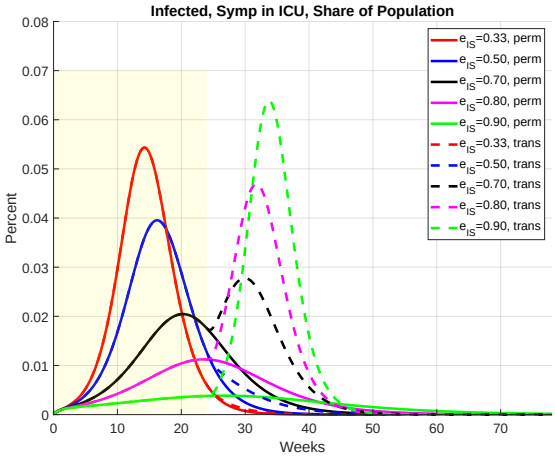

(a) ICU Hospital Beds

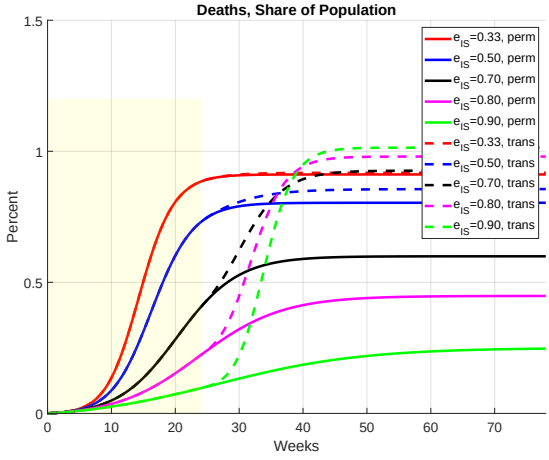

(b) Deaths

Note: See notes for Table 1. Solid lines represent permanent policies and dashed lines represent temporary policies. The shaded area denotes the first six months for which a temporary policy is in place.

Covid Economics 18, 15 May 2020: 42-72

Table 3: Effectiveness of Alternative Policies

Model	(1) Max I_A	(2) Max I_{AT}	(3) Max I_S	(4) Max H_{ICU}	(5) Term D	(6) Term S
Policy 0	4.301	0.000	3.879	0.054	0.912	23.645
Policy 1	0.116	0.000	0.083	0.001	0.076	93.464
Policy 2	0.115	0.000	0.074	0.001	0.013	98.976
Policy 3	0.112	0.007	0.074	0.001	0.009	99.261
Policy 4	0.114	0.001	0.074	0.001	0.012	99.008
Policy 5	0.111	0.008	0.073	0.001	0.009	99.277

Note. The policies are defined on the intervals covering the first two months, the third through fifth month, and the remaining time. Policy 0 is the no-intervention case. The parameters for policy interventions are as follows
Policy 1: $\alpha = 0.55$, $\varepsilon_S = (0.5, 1/3, 1/3)$, $\varepsilon_{AT} = \varepsilon_T = f = 0$
Policy 2: $\alpha = (0.55, 0.75, 0.95)$, $\varepsilon_S = \varepsilon_{AT} = 0.9$, $\varepsilon_T = 0$, $f = 0$
Policy 3: $\alpha = (0.55, 0.75, 0.95)$, $\varepsilon_S = \varepsilon_{AT} = 0.9$, $\varepsilon_T = 0.9$, $f = 0$
Policy 4: $\alpha = (0.55, 0.75, 0.95)$, $\varepsilon_S = \varepsilon_{AT} = 0.9$, $\varepsilon_T = 0$, $f = 1.0$
Policy 5: $\alpha = (0.55, 0.75, 0.95)$, $\varepsilon_S = \varepsilon_{AT} = 0.9$, $\varepsilon_T = 0.9$, $f = 1.0$

intervention, this policy reduces total deaths by a factor of ten and peak ICU demand by a factor of 50, Table 3, Policies 0 and 1. In absolute numbers, for the UK this means about 50 thousand deaths and 800 peak ICU demand. Recall that UK ICU capacity is estimated to be about 5 thousand. These projected numbers are lower than those projected in the Ferguson et al. (2020) study.[11]

We now consider alternative policies that relax SD over time, in the context of a permanent and efficient quarantine policy, backed up by efficient contact tracing and/or random testing. For this policy, we start with a two-month, 45 percent reduction of the transmission rate α through SD, followed by another three months with a 25 percent reduction of the transmission rate, and finally a permanent 5 percent reduction. All reductions are relative to the base level. Quarantine efficiency is permanently increased to 90 percent.

The first alternative policy combines a gradual relaxation of SD with an efficient quarantine regime, Table 3, Policy 2. For this policy, we assume that 90 percent of newly symptomatic individuals are known and quarantined. This policy reduces total deaths relative to the baseline SD policy by a factor of seven and yields similar peak ICU demand. As we now show, contact tracing and random testing yield only marginal improvements over this policy.

The second alternative policy backs up the efficient quarantine policy with an efficient tracing regime, Table 3, Policy 3. For this policy, we assume that 90 percent of previous contacts that a newly symptomatic individual has infected are traced and quarantined. This policy reduces total deaths relative to the baseline SD policy by a factor of eight and yields similar peak ICU demand.

[11] Ferguson et al. (2020), Table 4, for the cases with general quarantine and SD predicts total deaths of 100 thousand and peak ICU demand of 10 thousand. These numbers are predicted to be lower if additional policies targeting particular demographic groups are implemented.

Covid Economics 18, 15 May 2020: 42-72

Covid Economics 18, 15 May 2020: 42-72

We have not discussed how tracing is actually implemented. The contact-tracing process for a newly confirmed symptomatic patient consists of a detailed interview with the patient to find out where they have been and then reaching out to those people or the heads of organizations responsible for places, such as airlines, hotels, or religious organizations, that may have been affected. High-risk/close contacts are monitored by public health authorities and low-risk contacts are asked to self-monitor for symptoms in the process laid out by the CDC.[12] As far as we can tell, even among traced individuals only the ones showing symptoms are tested.

No matter how contact tracing is implemented, our assumptions that tracing is efficient and that individuals who have been identified through tracing can be quarantined the same way as symptomatic individuals are highly optimistic. Furthermore, contact tracing has been mainly used for less prevalent diseases and not for large-scale pandemics.

Consider now the alternative of backing up quarantine through random testing of asymptomatic individuals at a rate that would test the complete population within a year. For comparison, the US has been able to increase its testing rate from 50 thousand a day to 100 thousand a day from the middle of March to the middle of April. At that rate the US can test 10 percent of its population in a year. So our assumption on the testing rate would require another ten-fold increase. Table 3, Policy 4, displays the impact of high-intensity random testing. In our stylized model, adding random testing to quarantine, at least for the rate considered here, is somewhat less effective than contact tracing, but total deaths are reduced by a similar magnitude as with tracing, and peak ICU demand is reduced as much as with tracing. Finally, adding random testing to tracing with quarantine has a negligible impact, Table 3, Policy 5.

The main reason why random testing is not very effective is that with an efficient quarantine policy in the background, the share of infectious asymptomatic individuals in the general population is not very large. The peak value of that share is less than 0.1 percent, Table 3, column 1, and the probability of finding an asymptomatic infectious individual through a random test is less than 0.01 percent. Testing every newly symptomatic individual alone would require testing less than 0.5 percent of the population in a year, well within the current capacity constraints for testing.

To summarize, the stylized model predicts that a policy with gradual relaxation of SD, combined with permanent high-efficiency quarantine and possibly tracing of infectious individuals reduces total deaths more and has the same impact on peak ICU demand as a policy of high-intensity permanent SD. A by-product of the successful reduction of new infections by all of these policies is that after more than a year almost all of the population remains susceptible to the virus, Table 3, last column. Thus, in the absence of a vaccine or effective treatment, these policies need to remain permanently in place.

5.4 Implications for employment

The purpose of this paper is to study the impact of policy alternatives to a high-intensity SD policy that are less disruptive for the workings of the overall economy. If we view current policy in the UK or US as representing high-intensity SD as described in the preceding

[12] Landman (2020), Armbruster and Brandeau (2007)

CEPR PRESS

Figure 5: Employment Impact

Note: The solid lines denote the population available for work, that is, not hospitalized and not quarantined. In terms of health outcomes all policies are about equally effective. The dashed lines denote the additional employment reduction associated with SD. For the policies see notes for Table 3. SD1Q1 is Policy 1, SD2Q2T2 is Policy 3, SD2Q2F2 is Policy 4, and SD2Q2T2F2 is Policy 5.

exercises, that is, a reduction of individual contact rates by 25 percent with a corresponding reduction of the transmission rate by 45 percent, then this policy has been disruptive. Employment has declined by about 12 percent, and current estimates are for a total decline of 25 percent in the second quarter of 2020, see Appendix A.2.

In Figure 5, we plot 'guesses' of the impact of the policy alternatives on employment in the economy. The solid lines represent the population available for work in the economy, relative to normal at one. The dashed lines represent employment consistent with the available workforce and the extent of SD.

The available workforce consists of those who are healthy and not quarantined.[13] For none of the policies we consider, the pure health effect on workforce availability is noticeable, and the pure health effect on employment is dwarfed by the disruptions of high-intensity SD.

The dashed lines in Figure 5 represent the joint impact of SD and other policies on employment. We take as given that a 25 percent reduction of contact rates reduces employment relative to available workforce by 25 percent. We then assume that smaller reductions of the transmission rates through SD reduce employment proportionally to the corresponding reduction in the contact rate. More or less by assumption (or interpolation), the alternative policies result in substantially better employment outcomes than the permanent high-intensity SD policy.

[13]We essentially assume a representative worker or that employed and non-employed are equally affected by the spread of the disease.

Covid Economics 18, 15 May 2020: 42-72

6 Caveats

I have used a stylized model to evaluate the relative efficiency of four policy interventions to contain the spread of the coronavirus: SD, quarantine, contact tracing, and random testing. The qualitative features of the relative efficiency of these policies are intuitive enough to expect that they would hold in more general models. How much one should trust the quantitative implications is a different issue.

The first thing to note is that the model was intentionally parameterized to replicate the Ferguson et al. (2020) model. To the extent that there is uncertainty about the 'stylized facts' in Ferguson et al. (2020), we will do a robustness exercise below. Second, and possibly more important, the disease does not spread as fast in the model as we observe in the data.

6.1 Higher basic reproduction rate

We have seeded the model to the 335 cumulative deaths in the UK on March 24. Three weeks later on April 14, cumulative deaths in the UK were 11,329. The model predicts, however, that after three more weeks, cumulative deaths without an intervention should have been about 4,600, and under a high-intensity SD policy they should have been about 3,300. The corresponding numbers for the US are actual cumulative deaths of 673 on March 24 and 21,972 on April 14. Seeding the model to the March 24 deaths, the model predicts 8,700 deaths for April 14 with no intervention and 5,800 deaths with a high-intensity SD policy. For both countries, the predicted increase of cumulative deaths is substantially below the actual increase of reported deaths.[14]

One way to account for the large increase of cumulative deaths from March 24 to April 14 is to work with a larger basic reproduction rate. Sanche, Lin, Xu, Romero-Severson, Hengartner and Ke (2020), for example, reconsider the emergence of COVID-19 in Wuhan and argue that it is twice as infectious as previous estimates suggested. They estimate the basic reproduction rate to be 5.7 and that infections double within 2.7 days. Similarly, Fernandez-Villaverde and Jones (2020) estimate a time-varying effective transmission rate α by matching cumulative deaths to the predictions of a SIR model. They find reproduction rates in excess of 4 for some US cities and European countries.[15]

We now replicate the comparison of alternative policies when we seed the model to the higher basic reproduction rate estimated by Sanche et al. (2020), keeping all other parameters unchanged. Again, we match the cumulative deaths on March 24. For the UK, the model now predicts cumulative deaths on April 14 of about 26,000 with no intervention and about 11,400 with the high-intensity SD policy. The corresponding cumulative deaths for the US on April 14 are now about 56,000 with no intervention and 20,200 with the high-intensity

[14]The data are from the WHO website https://covid19.who.int/region/euro/country/gb and ../usa, April 22, 2020.

[15]Another reason why the stylized model might understate the increase in cumulative deaths could be related to the assumption that disease state changes follow a Poisson process. As mentioned in Section 1.1, a number of authors in the epidemiological literature argue that SEIR-type models with duration-dependent transition rates provide a better match for the dynamics of diseases like SARS, delivering a bigger peak and shorter duration, for example, Wearing et al. (2005) and Feng et al. (2007). But then Feng (2007) also argues that this simple ranking of models with duration (in)dependent transition rates may depend on the particular way policy interventions like quarantine are modeled.

Covid Economics 18, 15 May 2020: 42-72

Table 4: Effectiveness of Alternative Policies for High $\mathcal{R}_0$

Model	(1) Max I_A	(2) Max I_{AT}	(3) Max I_S	(4) Max H_{ICU}	(5) Term D	(6) Term S
Policy 0	15.089	0.000	11.711	0.164	1.180	1.193
Policy 1	6.679	0.000	5.857	0.082	1.050	12.107
Policy 2	5.115	0.000	4.522	0.063	0.932	21.980
Policy 3	3.114	0.551	3.305	0.046	0.877	26.600
Policy 4	4.940	0.097	4.443	0.062	0.921	22.870
Policy 5	2.941	0.592	3.194	0.045	0.865	27.541

Note. The basic reproduction rate is $\mathcal{R}_0 = 5.7$. All policies are defined as in Table 3.

SD policy. Recall that we chose March 24 as a starting date because the UK adopted a national lockdown policy on that day, and a substantial share of US population was already subject to stay-at-home policies by March 24. The predicted increase in cumulative deaths associated with the high-intensity SD policy is then remarkably close to actual outcomes for both the UK and the US.

Table 4 displays the outcomes for the same policies we considered previously when the reproduction rate is twice as high as in the baseline analysis. If there is no intervention, peak infections and ICU demand triple, and deaths increase by 30 percent relative to the lower reproduction rate; Table 4, Policy 0. The main result for all policy interventions is that their ability to reduce the spread of the disease is greatly diminished. Permanent high-intensity SD now reduces cumulative deaths by only 10 percent, rather than a factor of ten as before. The alternative policies still improve on the high-intensity SD policy but by less. For example, they reduce cumulative deaths by an additional 10 percent, rather than a factor of seven. Finally, peak ICU demand now exceeds capacity for the UK, but it remains below capacity for the US.

With a higher reproduction rate, policies not only cannot reduce cumulative deaths that much, they also cannot slow down the rate at which deaths accumulate. The substantial run-up in cumulative deaths that the model generates for late March is only the precursor of more future deaths to come in the near future. Given the high rate at which the disease spreads, cumulative deaths attain their terminal value within 15 to 25 weeks, depending on the policy, Figure 6. This seems inconsistent with European countries and US states being able to flatten the path for cumulative deaths substantially. One way to account for this observation in the model might be further adjustments to the social distancing parameter.

6.2 Uncertainty

As we just saw, estimates of the basic reproduction rate are being revised upward, but estimates of other parameters, such as the incident fatality rate, also vary substantially. We do not really know what the share of exposed or asymptomatic individuals in the population is, etc. On the policy side, we do not really know what the implemented SD policies mean for the transmission rate of the disease. For example, if we target a 50 percent reduction of the transmission rate through such a policy, how do we know that that's what we get? To address some of these questions, we perform the following simulation study.

Covid Economics 18, 15 May 2020: 42-72

Covid Economics 18, 15 May 2020: 42-72

Figure 6: Deaths with Large $\mathcal{R}_0$

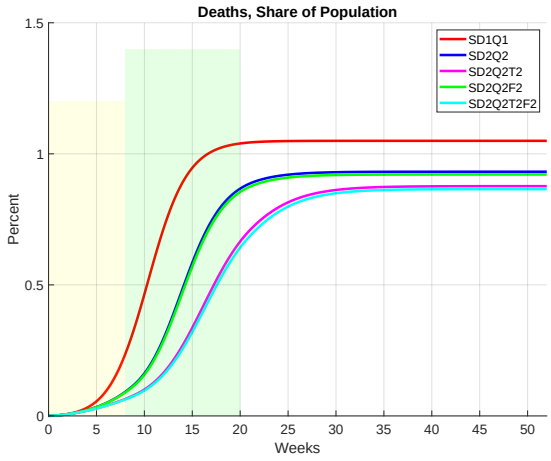

Note: The reproduction rate is $\mathcal{R}_0 = 5.7$. The policies correspond to the policies in Table 3: SD1Q1 is Policy 1, SD2Q2 is Policy 2, SD2Q2T2 is Policy 3, SD2Q2F2 is Policy 4, SD2Q2T2F2 is Policy 5. Some of the policies vary over time, and the shaded areas cover the first two months, and the third through fifth month for which the policies change.

Covid Economics 18, 15 May 2020: 42-72

We classify parameters from our baseline calibration as being subject to low, medium, or high uncertainty. This means that percentage deviations of a parameter from its baseline value have a 5 percent, 10 percent, or 15 percent coefficient of variation. The classification is subjective but informed by the literature as summarized by the Robert Koch Institut, see Appendix A.4.[16] For example, we consider the uncertainty surrounding the basic reproduction rate and the effectiveness of SD as large, but the uncertainty surrounding the mean recovery periods as small. That being said, the alternative basic reproduction rate we just discussed is very unlikely, even for the high uncertainty case. We then generate one million joint random draws on the parameters from gamma distributions, keep 5,000 of them, and calculate the implied time paths. As an illustration, in Figure 7 we plot for the above-discussed high-intensity SD policy the time path of cumulative deaths for the fixed parameter values and the mean, median, and the symmetric ranges containing 33 percent and 66 percent of all realizations. We do this for four cases. The first case displays the joint uncertainty surrounding disease and policy parameters. The second case considers only uncertainty related to policy parameters, that is, we take all parameters but ε as fixed. The third case considers only uncertainty related to disease parameters, that is, we take the policy parameters ε as fixed. Finally, the fourth case illustrates the main source of outcome uncertainty, the basic transmission rate α_0.

Figure 7 shows that for the stylized model and the particular SD policy the uncertainty surrounding outcomes for total deaths is large, and almost all of it can be attributed to the uncertainty surrounding the disease parameters, in particular, the basic transmission rate α_0. Panel (a) of Figure 7 shows that the outcome uncertainty associated with uncertainty in all parameters is large, the 66 percentage coverage area for total deaths after a year ranges from 0.02 percent to 0.9 percent. The latter is the no-intervention outcome for the baseline parameters. Even though the median outcome is close to but below the fixed-parameter path, the mean outcome is substantially larger than the fixed parameter path. In other words, the risks associated with uncertainty are weighted to the upside. Comparing panels (b) and (c) of Figure 7, we see that almost all of the outcome uncertainty is associated with the disease parameter uncertainty rather than the uncertainty about policy parameters.[17] Finally, comparing panels (c) and (d) of Figure 7 shows that uncertainty in the basic transmission rate is the main driver of outcome uncertainty.

7 Conclusion

I have studied the effectiveness of alternative policies to contain the spread of a pandemic in a stylized model of the SEIR variety that is calibrated to the Ferguson et al. (2020) study. I find that a policy that combines a gradual relaxation of social distancing with an efficient quarantine, possibly augmented by contact tracing, improves noticeably on a policy of permanent high-intensity SD.

We should qualify the stylized model's ability to make quantitative predictions on the spread of the disease. First, cumulative deaths in the model do not increase as fast as

[16] https://www.rki.de/DE/Content/InfAZ/N/Neuartiges_Coronavirus/Steckbrief.html, as of April 30, 2020.

[17] Note the different scales for panels (b) and (c).

Covid Economics 18, 15 May 2020: 42-72

Figure 7: Impact of Parameter Uncertainty on Projected Deaths

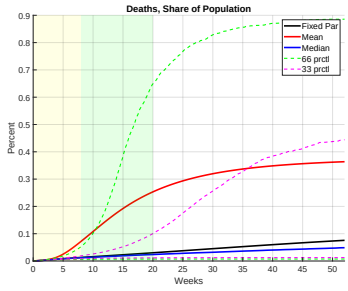

(a) All Parameters

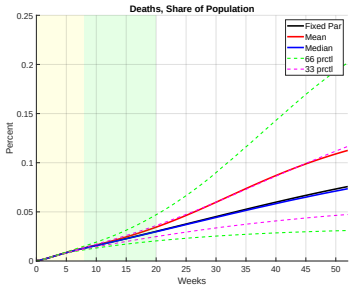

(b) Policy Parameters

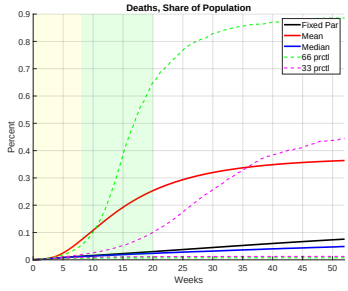

(c) Disease Parameters

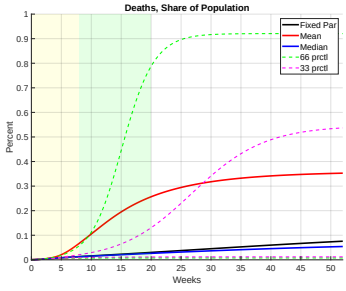

(d) Contagiousness α_0

Note: Baseline policy is permanent high-intensity SD, combined with temporary medium-intensity quarantine. Solid black line is the outcome for the calibrated parameter values. Solid red and blue lines are the mean and median from the Monte Carlo simulations. The area between the dashed purple and green lines reflect the symmetric ranges that contain 33 percent, respectively 66 percent, of the realizations from the Monte Carlo simulations. Panel (a) allows for uncertainty in policy and disease parameters, panel (b) keeps the disease parameters fixed, panel (c) keeps the policy parameters ε fixed, and panel (d) keeps all parameters fixed except the disease transmission rate α_0.

we observe for the UK and the US from late March to mid-April 2020. The model better matches this increase in cumulative deaths for a higher basic reproduction rate, consistent with recently revised estimates. But if COVID-19 is much more infectious than what we have assumed until now, then the effectiveness of all policies will be greatly reduced. More generally, the uncertainty surrounding all parameter estimates used to calibrate the model is large, and so is the implied uncertainty for policy outcomes. The most important contributor to outcome uncertainty, at least as it relates to cumulative deaths, appears to be the uncertainty about the disease transmission rate.

Covid Economics 18, 15 May 2020: 42-72

References

Alvarez, Fernando, David Argente, and Francesco Lippi, "A Simple Planning Problem for COVID-19 Lockdown," *Covid Economics*, May 2020, *14*, 1–32.

Armbruster, B. and ML Brandeau, "Contact Tracing to Control Infectious Disease: When Enough is Enough," *Health Care Manag Sci.*, 2007, *10* (4), 341–355.

Atkeson, Andrew, "What Will Be the Economic Impact of COVID-19 in the US? Rough Estimates of Disease Scenarios," Working Paper 26867, National Bureau of Economic Research March 2020.

Berger, David W., Kyle F. Herkenhoff, and Simon Mongey, "An SEIR Infectious Disease Model with Testing and Conditional Quarantine," Working Paper 26901, National Bureau of Economic Research March 2020.

Eichenbaum, Martin S., Sergio Rebelo, and Mathias Trabandt, "The Macroeconomics of Epidemics," Working Paper 26882, National Bureau of Economic Research March 2020.

Farboodi, Maryam, Gregor Jarosch, and Robert Shimer, "Internal and External Effects of Social Distancing in a Pandemic," *Covid Economics*, April 2020, pp. 22–58.

Fauci, Anthony S., H. Clifford Lane, and Robert R. Redfield, "Covid-19 — Navigating the Uncharted," *New England Journal of Medicine*, 2020.

Feng, Zhilan, "Final and Peak Epidemic Sizes for SEIR Models with Quarantine and Isolation," *Mathematical Biosciences and Engineering*, 2007, *4*, 675–686.

___ , Dashun Xu, and Haiyun Zhao, "Epidemiological Models with Non-Exponentially Distributed Disease Stages and Applications to Disease Control," *Bulletin of Mathematical Biology*, 2007, *69* (5), 1511–1536.

Ferguson, Neil M et al., "Impact of Non-Pharmaceutical Interventions (NPIs) to Reduce COVID-19 Mortality and Healthcare Demand.," Technical Report 2020.

Fernandez-Villaverde, Jesus and Charles Jones, "Estimating and Simulating a SIRD Model of COVID-19," *Working Paper*, 2020.

Jewell, Nicholas P., Joseph A. Lewnard, and Britta L. Jewell, "Predictive Mathematical Models of the COVID-19 Pandemic: Underlying Principles and Value of Projections," *JAMA*, April 2020.

Landman, Keren, "How The Painstaking Work of Contact Tracing Can Slow the Spread of an Outbreak," *National Public Radio*, 2020.

Lipsitch, Marc et al., "Transmission Dynamics and Control of Severe Acute Respiratory Syndrome," *Science*, 2003, *300* (5627), 1966–1970.

Covid Economics 18, 15 May 2020: 42-72

Piguillem, Facundo and Liyan Shi, "Optimal COVID-19 Quarantine and Testing Policies," EIEF Working Papers Series 2004, Einaudi Institute for Economics and Finance (EIEF) 2020.

Sanche, Steven, Y.T. Lin, C. Xu, E. Romero-Severson, N. Hengartner, and R. Ke, "High Contagiousness and Rapid Spread of Severe Acute Respiratory Syndrome Coronavirus 2," *Emerg Infect Dis.*, July 2020.

Shen, Chen, Nassim N. Taleb, and Yaneer Bar Yam, "Review of Ferguson et al 'Impact of non-pharmaceutical interventions...'," Technical Report 2020.

Stock, James H., "Data Gaps and the Policy Response to the Novel Coronavirus," *Covid Economics*, April 2020, pp. 1–11.

Wearing, Helen J., Pejman Rohani, and Matt J. Keeling, "Appropriate Models for the Management of Infectious Diseases," *PLOS Medicine*, July 2005, *2* (7).

Covid Economics 18, 15 May 2020: 42-72

Covid Economics 18, 15 May 2020: 42-72

A Appendix

A.1 Reproduction rates

We now calculate the average new infections caused by a newly infectious agent. We start with the basic reproduction rate in the SIR model, then the basic reproduction rate in the SEIR model, and then calculate average new infections from an asymptomatic individual until he becomes symptomatic and is quarantined.

A.1.1 Basic reproduction rate $\mathcal{R}_0$ for SIR model

The individual is infectious at rate $S(\tau)\alpha$ until recovery or death ($\tilde{\gamma} = \gamma + \delta$).

$$\begin{aligned}\mathcal{R}_0 &= \int_0^\infty \left[S(\tau)\alpha\tau\right]\left[\left(\gamma e^{-\gamma\tau}\right)e^{-\delta\tau} + \left(\delta e^{-\delta\tau}\right)e^{-\tilde{\gamma}\tau}\right]d\tau \\ &\approx S(0)\int_0^\infty (\alpha\tau)\left(\tilde{\gamma}e^{-\tilde{\gamma}\tau}\right)d\tau \\ &\approx \alpha\tilde{\gamma}\int_0^\infty \tau e^{-\tilde{\gamma}\tau}d\tau\end{aligned}$$

For the first approximation, we assume that changes in the measure of susceptible individuals S are small over the time of an individual infection. For the second approximation, we assume that initially the share of susceptible individuals is close to one.

Note that

$$\int_0^t \tau e^{\alpha\tau}d\tau = \frac{1}{\alpha^2}\left[1 + e^{\alpha t}(\alpha t - 1)\right] \text{ and } \lim_{t\to\infty}\int_0^t \tau e^{-\gamma\tau}d\tau = \frac{1}{\gamma^2}$$

Therefore

$$\mathcal{R}_0 = \frac{\alpha}{\tilde{\gamma}}$$

A.1.2 Basic reproduction rate in $\mathcal{R}_0$ for SEIR model

We consider the progression from an asymptomatic infectious individual to a symptomatic infectious one, working backwards.

The average number of new infections caused by a symptomatic individual, ignoring hospitalization, is

$$\begin{aligned}\mathcal{R}_{0S} &= S(t)\int_0^\infty \left[\sigma\alpha\tau\right]\left(\tilde{\gamma_S}e^{-\tilde{\gamma_S}\tau}\right)d\tau \\ &= S(t)\alpha\frac{\sigma}{\tilde{\gamma_S}}\end{aligned}$$

with $\tilde{\gamma}_S = \gamma_S + \delta$

The average number of new infections caused by an asymptomatic individual is

$$\begin{aligned}\mathcal{R}_{0A} &= S(t)\int_0^\infty \left[\alpha\tau + \mathcal{R}_{0S}\right]\left(\beta e^{-\beta\tau}\right)\left(e^{-\gamma_A\tau}\right)d\tau + S(t)\int_0^\infty (\alpha\tau)\left(\gamma_A e^{-\gamma_A\tau}\right)\left(e^{-\beta\tau}\right)d\tau \\ &= S(t)\alpha\frac{1}{(\beta+\gamma_A)}\left[1 + \frac{\sigma\beta}{\gamma_S(\beta+\gamma_A)}\right]\end{aligned}$$

A.1.3 New infections with quarantine

We consider an asymptomatic infectious individual, $(\alpha, \beta, \gamma_A)$, who is quarantined once he becomes symptomatic. For this case, we calculate the average number of exposed and infectious asymptomatic individuals that this individual has created.

By the time an asymptomatic individual becomes symptomatic, the average number that individual has infected is

$$\begin{aligned}\mathcal{R}_{AQ} &= S(t)\left[\int_0^\infty (\alpha\tau)\left(\beta e^{-\beta\tau}\right)\left(e^{-\gamma_A\tau}\right)d\tau\right] \\ &= S(t)\alpha\frac{\beta}{(\beta+\gamma_A)^2}\end{aligned}$$

The average number of individuals that the infectious agent has infected and who are not yet infectious at the time the agent becomes symptomatic is

$$\mathcal{R}_{ATE} = S(t)\int_0^\infty \left[\alpha\int_0^\tau e^{-\phi s}ds\right]\left[\left(\beta e^{-\beta\tau}\right)\left(e^{-\gamma_A\tau}\right)\right]d\tau$$

The term in the first square bracket denotes the total who have been infected by the infectious individual at τ and who have not yet become infectious at that time. This can be rewritten as

$$\mathcal{R}_{ATE} = S(t)\alpha\frac{\beta}{(\beta+\gamma_A)(\beta+\gamma_A+\phi)}.$$

The average number of individuals that an infectious agent has infected and who are infectious but asymptomatic at the time the agent becomes symptomatic is

$$\mathcal{R}_{ATA} = S(t)\int_0^\infty \left[\alpha\int_0^\tau \left[\int_0^s \phi e^{-\phi v}e^{-\gamma_A(s-v)}dv\right]ds\right]\left[\beta e^{-(\beta+\gamma_A)\tau}\right]d\tau$$

The innermost integral is the probability that an individual who has been infected time s ago has become infectious in the meantime but also has not yet recovered at the time the original infectious individual becomes symptomatic. This can be rewritten as

$$\mathcal{R}_{ATA} = \alpha\frac{\beta\phi}{2(\beta+\gamma_A)^2(\beta+\gamma_A+\phi)}$$

A.1.4 Probability of recovery without developing symptoms

The probability of recovering while asymptomatic before becoming symptomatic

$$p_{AR} = \int_0^\infty \left(\gamma_A e^{-\gamma_A\tau}\right)e^{-\beta\tau}d\tau = \frac{\gamma_A}{\gamma_A+\beta}$$

A.2 Social distancing

- According to the American Time Use Survey for 2018, an employed person spends on average 6.3 hours working and 5.13 hours on social activities (purchasing, helping non-household members, education, participating in organizations, and leisure and sports). A non-employed person spends on average 0.12 hours on work related activities and 9.36 hours on social activities.

Covid Economics 18, 15 May 2020: 42-72

- Social interactions may be more or less intense than workplace interactions. Given the reports on super spreader events related to soccer games in Italy and churches in South Korea, social interactions may well be more intense than workplace interactions, suppose 50 percent more. This is the opposite of Eichenbaum et al. (2020) for which workplace infections dominate infections related to consumption or unspecified social interactions.

- Assume that 60 percent of the population are working. This corresponds to US employment rates.

- In the last two weeks of March and the first week of April, new unemployment insurance claims increased by about 18 million. On a payroll employment base of 151 million, this means that employment probably decreased by about 12 percent, and the employment rate declined to about 53 percent. Current estimates are for additional employment declines with a total employment decline of 25 percent. Taking this into account reduces social contacts per person by about 63 percent, an additional 2 percentage points.

- The following table lists the implied average contact rates and social reproduction factors for various assumptions on the relative intensity of social interactions, with and without taking into account changes in the employment rates. Contact rates may decline by about 60 percent, and implied reproduction rates may decline by about 80 percent.

	Individual Contact Rate ψ Percent relative to normal		Reproduction Rate Factor α_S Fraction relative to normal	
S/W	ω fixed	ω declines	ω fixed	ω declines
0.75	46.4	42.1	0.22	0.18
1.00	43.0	39.6	0.18	0.16
1.50	38.6	36.5	0.15	0.13

A.3 Seeding the initial condition

We start with initial cumulative deaths, $D(0)$. Assuming a seeding rate σ, such that infections are doubling every five days, and an unconditional case fatality rate δ, consistent with an unconditional case fatality probability $p_D = 0.009$, total cumulative deaths starting from $-\Delta$ are

$$D(0) = I(0)\,\delta\left(\frac{1-e^{-\sigma\Delta}}{\sigma}\right)$$

We assume that infections start two and half months before the initial date, $\Delta = 2.5/12$.

Covid Economics 18, 15 May 2020: 42-72

A.4 Representing parameter uncertainty

Consider a parameter p and assume that the uncertainty about the parameter is represented by the following form

$$\begin{aligned} \ln p &= \ln \bar{p} + \ln X - E[\ln X] \\ \ln X &\sim \Gamma(k, \theta) \end{aligned}$$

where Γ denotes the Gamma distribution. Then

$$\begin{aligned} E[\ln p] &= \ln \bar{p} \\ Var(\ln p) &= Var(\ln X) \end{aligned}$$

The mean and variance of the gamma distribution are

$$\begin{aligned} \mu &= E[\ln X] = k\theta \\ \sigma^2 &= Var(\ln X) = k\theta^2 \end{aligned}$$

and the median ν is bounded by

$$\mu - 1/3 < \nu < \mu$$

So to get a symmetric distribution we need μ to be large. Let

$$S = k\theta$$

Suppose we fix the coefficient of variation for the observed variable

$$CoV = \frac{Std(\ln p)}{E[\ln p]} = \frac{Std(\ln X)}{\ln \bar{p}} = \frac{\sqrt{k}\theta}{\ln \bar{p}} = \frac{\sqrt{k}S/k}{\ln \bar{p}} = \frac{S}{\sqrt{k}\ln \bar{p}}$$

So the parameters of the gamma distribution are

$$\begin{aligned} k &= \left(\frac{S}{CoV \ln \bar{p}}\right)^2 \\ \theta &= \frac{S}{k} = S\left(\frac{CoV \ln \bar{p}}{S}\right)^2 = \frac{(CoV \ln \bar{p})^2}{S} \end{aligned}$$

The MATLAB usage of the gamma function is

$$\Gamma(a, b) = \Gamma(k, \theta)$$

We represent uncertainty through the CoV. The Robert Koch Institut (RKI) summarizes the available evidence on various characteristics of the coronavirus.[18] For example, estimates of the basic reproduction rate $\mathcal{R}_0$ range from 2.4 to 3.3. If we interpret the range as representing a 2 standard deviation band around a mean of 2.8, then the CoV for percentage deviation is 13%. We interpret this CoV as representing the uncertainty surrounding the basic transmission rate α_0, but we should note that $\mathcal{R}_0$ not only depends on the transmission

[18] https://www.rki.de/DE/Content/InfAZ/N/Neuartiges_Coronavirus/Steckbrief.html, April 30, 2020.

Covid Economics 18, 15 May 2020: 42-72

rate, but also on the incubation time, recovery time, and relative infectiousness of symptomatic individuals. Since the RKI excludes studies with significantly higher values than 3.3 from its summary of the evidence, assuming a CoV of 15% for the basic transmission rate α_0 may not overstate its uncertainty by much. We classify uncertainty as high, $CoV = 15\%$, medium, $CoV = 10\%$, and low, $CoV = 5\%$ for the parameters

High:	α, α_S, ϕ, β, σ, ε_i for $i \in \{AT, S, B, ICU\}$, ε_T
Medium:	δ, δ_{ICU}, ω, η,
Low:	γ, γ_{ICU}

Covid Economics 18, 15 May 2020: 42-72

How does household spending respond to an epidemic? Consumption during the 2020 COVID-19 pandemic[1]

Scott R. Baker,[2] Robert A. Farrokhnia,[3] Steffen Meyer,[4] Michaela Pagel[5] and Constantine Yannelis[6]

Date submitted: 8 May 2020; **Date accepted:** 9 May 2020

We explore how household consumption responds to epidemics, utilizing transaction-level household financial data to investigate the impact of the COVID-19 virus. As the number of cases grew, households began to radically alter their typical spending across a number of major categories. Initially spending increased sharply, particularly in retail, credit card spending and food items. This was followed by a sharp decrease in overall spending. Households responded most strongly in states with shelter-in-place orders in place by March 29th. We explore heterogeneity across partisan affiliation, demographics and income. Greater levels of social distancing are associated with drops in spending, particularly in restaurants and retail.

Covid Economics 18, 15 May 2020: 73-108

1 The authors wish to thank Sylvain Catherine, Caroline Hoxby, Ralph Koijen, Jonathan Parker, Amir Sufi, Pietro Veronesi, Rob Vishny and Neil Ning Yu for helpful discussions and comments. Constantine Yannelis is grateful to the Fama Miller Center for generous financial support. R.A. Farrokhnia is grateful to Advanced Projects and Applied Research in Fintech at Columbia Business School for support. We are grateful to Suwen Ge, Sypros Kypraios, Sharada Sridhar, George Voulgaris and Jun Xu for excellent research assistance sand SaverLife for providing data. This draft is preliminary and comments are welcome.
2 Northwestern University, Kellogg.
3 Columbia Business School.
4 University of Southern Denmark and Danish Finance Institute.
5 Columbia Business School and CEPR.
6 University of Chicago Booth School of Business.

Covid Economics 18, 15 May 2020: 73-108

1 Introduction

Disease epidemics have plagued human societies since at least the earliest days of recorded history. This paper presents the first study of how households' consumption and debt respond to an outbreak using transaction-level household data. As COVID-19 began to spread across the United States in March 2020, households across the country were faced with drastic changes in many aspects of their lives. Large numbers of businesses were closed by government decree and in many cities and states, Americans were required to limit trips outside and exposure to others following shelter-in-place orders.

While Americans adjusted how they lived and worked in response to uncertainty about how the future would play out, they also rapidly altered how and where they spent their money. This paper works to deploy transaction-level household financial data to provide a better and more comprehensive understanding of how households shifted spending as news about the virus spread and the impact in a given geographic area became more severe and far-reaching.

The extent to which both individual households as well as the economy at large have been upended is without recent precedent. Entire industries and cities were largely shut down, with estimates of the decline in economic activity hitting all-time records. Policymakers at all levels of government and across a wide range of institutions have worked to mitigate the economic harm on households and small businesses. However, the speed at which the economic dislocation is occurring has made it difficult for policymakers to properly target fiscal stimuli to households and credit provision to businesses. After all, little is known about how households respond in their spending to a pandemic on a scientific basis and across a larger number of households and geographies.

This paper aims to close this gap by utilizing transaction-level household financial data to analyze the impact of the COVID-19 outbreak on the spending behavior of tens of thousands of Americans. We use transaction-level data from linked bank-accounts from SaverLife that works with individuals to sustain savings habits. Transaction-level financial data of this type is a useful tool for understanding household financial behavior in great detail. In the context of the current COVID-19 outbreak, it can allow for a high speed, dynamic and timely diagnosis of how households have adjusted their spending, when they began to respond, and what the characteristics are

of the households who have responded the fastest and strongest.[1]

News media reported that customers emptied supermarket shelves in an effort to stock-pile durable goods.[2] Furthermore, as advice flowed from federal and state governments to households, one common refrain was that households should prepare to mostly stay inside their homes for multiple weeks with minimal trips outside. Home production is thus a source of savings that households can engage in which should also increase their spending at certain stores as opposed to others.

We find that households substantially changed their spending as news about the COVID-19's impact in their area spread. Overall, spending increased dramatically in an attempt to stockpile needed home goods and also in anticipation of the inability to patronize retailers. Household spending increases by approximately 50% overall between February 26 and March 11. Grocery spending remains elevated through March 27, with a 7.5% increase relative to earlier in the year. We also see an increase in card spending, which is consistent with households borrowing to stock-pile goods. As the virus spread and more households stayed home, we see sharp drops in restaurants, retail, air travel and public transport in mid to late March.

Restaurant spending declined by approximately one third. The speed and timing of these increases in spending varied significantly across individuals depending on their geographic location as state and local governments reacted to outbreaks of different sizes and with different levels of urgency. The overall drop in spending is approximately twice as large in states that issued shelter-in-place orders, however the increase in grocery spending is three times as large for states with shelter-in-place orders.

We explore heterogeneity among partisan affiliations and demographics, which are closely tied to stated beliefs about the impacts of the new virus. Republicans generally reported less concern about the new virus. For example, an Axios Poll between March 5 and 9 found that 62% of Republicans thought that the COVID-19 threat was greatly exagerated, while 31% of Democrats and 35% of Independents thought the same. A Quinnipac poll between March 5 and 8 also found that 68% of Democrats were concerned, while only 35% of Republicans were concerned. Barrios

[1]Researchers have previously utilized a range of transaction-level household financial datasets to answer questions about household consumption, liquidity, savings, and investment decisions. See Baker (2018), Baker and Yannelis (2017), Olafsson and Pagel (2018), Baker, Kueng, Meyer and Pagel (2020), and Meyer and Pagel (2019).

[2]For example, see USA Today, CNN, and FoxNews.

Covid Economics 18, 15 May 2020: 73-108

Covid Economics 18, 15 May 2020: 73-108

and Hochberg (2020) find that partisanship played a significant role in shaping risk perceptions to the new pandemic. Contrary to much of what was seen in the press, and despite lower levels of observed social distancing, Republicans actually spent more than Democrats in the early days of the epidemic. We see some significant differences in categorical responses, with Republicans spending more at restaurants and in retail shops, which is consistent with lower levels of concern about the virus or differential risk exposure.

We see significant heterogeneity along demographic characteristics, but little along household income. Households with children stockpiled more, and men stockpiled less in early days as the virus was spreading. We find more spending in later periods by the young. We see little heterogeneity across income, which is largely consistent with work by Kaplan, Violante and Weidner (2014) and Kaplan and Violante (2014) and the "wealthy-hand-to-mouth."

This paper joins a large literature on household consumption. Early empirical work, such as Zeldes (1989), Souleles (1999), Pistaferri (2001), Johnson, Parker and Souleles (2006), Blundell, Pistaferri and Preston (2006) and Agarwal, Liu and Souleles (2007) used survey data or studied tax rebates. Gourinchas and Parker (2002), Kaplan and Violante (2010) and Kaplan and Violante (2014) provide theoretical models of household consumption responses. Recent work uses administrative data (Fuster, Kaplan and Zafar, 2018; Di Maggio, Kermani, Keys, Piskorski, Ramcharan, Seru and Yao, 2017) and Baker (forthcoming), Pagel and Vardardottir (forthcoming) and Baker and Yannelis (2017) have studied income shocks and consumption using financial aggregator data. Jappelli and Pistaferri (2010) provide a review of this literature.

This paper is the first to study how household spending reacts in an epidemic, where there are anticipated income shocks as well as the threat of supply chain disruption, but all combined with significant uncertainty. In early March, there was little direct effect of COVID-19 in the United States, but significant awareness of potential damage in the future. We see significant stockpiling and spending reactions, which is consistent with expectations playing a large role in household consumption decisions.

This paper also relates to a literature on how crises impact the economy, and policy responses to those crises. In the aftermath of the 2008 Great Recession, a large body of work studied how credit supply shocks (**?**Mian and Sufi, 2011; Mian, Rao and Sufi, 2013) and securitization (Keys, Mukherjee, Seru and Vig, 2008; Keys, Seru and Vig, 2012) led to the financial crisis. Several

Covid Economics 18, 15 May 2020: 73-108

papers also study the effect of government policies aimed at mitigating the effects of the financial crisis. (Bhutta and Keys, 2016; Di Maggio, Kermani, Keys, Piskorski, Ramcharan, Seru and Yao, 2017; Ganong and Noel, 2018). This paper provides a first look at the impacts of the new epidemic on households, which will be key in evaluating any future policy response.

Additionally, the paper joins a growing literature in finance on the impacts of how belief heterogeneity shaped by partisan politics affects real economic decisions. Malmendier and Nagel (2011) show the individuals growing up in the Great Depression exhibited more risk averse behavior relative to others. The literature on how partisanship affects economic decisions has had mixed findings. Some papers have found large effects of partisanship on economic decision-making. For example, Kempf and Tsoutsoura (2018) explore how partisanship affects financial analysts decisions and Meeuwis, Parker, Schoar and Simester (2018) find large effects of the 2016 US Presidential election on portfolio rebalancing. Mian, Sufi and Khoshkhou (2018) study how US presidential elections affect consumption and savings patterns, and find little effect. Baldauf, Garlappi and Yannelis (2020) study how beliefs about climate change impact home prices, and find large differences between political groups. This paper studies differences in partisan behavior in the face of a major crisis where survey evidence indicates large differences in beliefs among people belonging to different political parties, which have been attributed to statements made by policymakers.[3]

Finally this paper joins a rapidly growing body of work studying the impact of the COVID-19 epidemic on the economy. Eichenbaum, Rebelo and Trabandt (2020), Barro, Ursua and Weng (2020) and Jones, Philippon and Venkateswaran (2020) provide macroeconomic frameworks for studying epidemics. Coibion, Gorodnichenko and Weber (2020) document a strong impact of the epidemic on labor markets. Gormsen and Koijen (2020) study the stock price and dividend future reactions to the epidemic, and use these to back out growth expectations for a potential recession caused by the virus. In a related paper, Barrios and Hochberg (2020) find the political partisanship played a large role in shaping risk perceptions towards COVID-19. Our paper is the first to study the household spending and debt responses to COVID-19, or any major epidemic, given that detailed high-frequency household financial data did not exist during previous pandemics.

[3] A NBC/Wall Street Journal Poll found more Democrats than Republicans were worried about family members catching the virus, while 40% of Republicans were worried, and that twice as many Democrats thought the virus would change their lives.

The remainder of this paper is organized as follows. Section 2 describes the main transaction data used in the paper, as well as ancillary datasets. Section 3 discusses the spread of the novel coronavirus in the United States. Section 4 presents the main results, new facts about household spending during an epidemic. Section 5 discusses heterogeneity in spending responses, particularly by partisan affiliation. Section 6 concludes.

2 Data

2.1 Transaction Data

We analyze de-identified transaction-level data from a non-profit Fintech company called SaverLife. SaverLife encourages households to increase savings through targeted information and rewards. Users can use the platform to sign up for an account with SaverLife and link their main bank account including their checking, savings, and credit card accounts. Users have two main incentives for linking accounts. First, SaverLife can provide them with information, provides tools to aid personal financial decision making and offers financial advice. Second, SaverLife offers targeted rewards and lotteries to individuals who link their accounts to achieve savings goals.

Figure 1 shows two screenshots of the SaverLife online interface. It shows the screenshots of the main linked account as well as a screenshot of the savings and financial advice resources that the website provides.

The primary data used in this paper consists of de-identified daily data on each user's spending and income transactions from all linked checking, savings, and credit card accounts. In addition, for a large number of users, we are able to link financial transactions to demographic and geographic information. For instance, for most users, we are able to map them to a particular 5-digit zip code. Many users self-report demographic information such as age, education, family size, and the number of children they have. In Panel A of Figure 2, we can see how many users we observe in each US zip code. In Panel B of Figure 2, we show the users' average annual household income by zip code that they report upon signing up with SaverLife.

Using data from August 2016 to March 2020, we observe bank-account transactions for a total sample of 44,660 users. For each transaction in the data, we observe a category (such as Groceries and Supermarkets or Pharmacies), parent category names (such as ATM), and grandparent category

Covid Economics 18, 15 May 2020: 73-108

names (such as Shopping and Food). Looking only at the sample of users who have updated their accounts reliably in March of 2020, we have complete data for 4,735 users. These users each are required to have several transactions per month in 2020 and have transacted at $1,000 in total during these three months of the year.

Table 1 shows summary statistics for users spending in a few select categories as well as their income at a monthly level. We can see that payroll income is relatively low for the median user of SaverLife, though many users get income from a range of other non-payroll sources. Additionally, we can see the number of linked accounts and number of monthly transactions of users in all linked accounts. The number of total transactions and weekly observations are also noted. We run regressions at a weekly level to examine more precisely the high frequency changes in behavior brought about by the fast-moving news about the COVID-19 outbreak and the policy responses to the outbreak.

Spending transactions are categorized into a large number of categories and subcategories. For instance, the parent category of 'Shops' is broken down into 53 unique sub-categories including 'Convenience Stores', 'Bookstores', 'Beauty Products', 'Pets', and 'Pharmacies'. For most of our analysis, we examine spending across a majority of categories, excluding spending on things like bills, mortgages, and rent. We also separately focus on a number of individual categories including 'Grocery Stores and Supermarkets' as well as 'Restaurants'.

2.2 Gallup Daily Tracker Data

We predict partisanship from 2018 Gallup Daily Tracker Data. Gallup randomly samples 1,000 Americans daily each year via landlines and cellphones. Individuals are asked questions about their political beliefs, expectations about the economy, and demographics. The sample is restricted to individuals 18 and over. We estimate a linear probability model, predicting whether a respondent identifies as a Republican using variables common to both datasets: (i) county (ii) income (iii) gender (iv) marital status (v) presence of children in the household (vi) education and (vii) age. Older people, men, married individuals and individuals with children are more likely to be Republicans. Identifying as a Republican is monotonically increasing in income bins.[4] The rela-

[4]The Gallup data provides income in bins, rather than in a continuous fashion. We observe self-reported continuous income for the majority of the individuals in the transaction data, for those for whom income is observed in a range we take the midpoint. We standardized the income and education bins in the transaction data to match Gallup to construct

Covid Economics 18, 15 May 2020: 73-108

tionship between education and partisan affiliation is non-monotonic, with individuals without a high school diploma strongly leaning Democrat, and individuals with only a high school degree, a vocational degree, or an associates degree being most likely to identify as Republicans.

For each individual we construct a predicted coefficient of partisan leaning, using the coefficients estimated from the Gallup data, and predicting partisan learning using demographics in the transaction data. In cases where demographics are missing in the transaction data, we replace the predicted Republican political affiliation with the 2016 Republican vote share, using data from the MIT Election Lab. We classify individuals predicted to be in the top quartile of the highest propensity to be Republicans, and those in the bottom quartile to be Democrats. The remaining individuals in between are classified as Independents.

2.3 Social distancing data

We also collect data on the effectiveness of social distancing from unacast.com Unacast social distancing-scoreboard. Unacast provides a daily updated social distancing scoreboard. The scoreboard describes the daily changes in average mobility, measured by change in average distance travelled and the change in non-essential visits using data from tracking smartphones using their GPS signals. The data is available on a daily basis and by county on their website. We use the data of average mobility, because the data on non-essential visits is less reliable as many people have re-located and moved to areas out of a city or kids have moved to parents' homes or vice versa. Therefore, unacast reports the average distance travelled (difference in movement) as the most accurate measure in times of the pandemic. We downloaded the data from their website by day and county and merged it to our consumption data.

3 Geographic Spread of COVID-19

COVID-19 was first identified in Wuhan, China before spreading worldwide. This new coronavirus spread very rapidly, and had a mortality rate approximately ten times higher than the seasonal flu and at least twice its infection rates.[5] The first case in the United States was identified on

out measure of predicted partisanship.

[5]See the ADB study referenced by WHO

Covid Economics 18, 15 May 2020: 73-108

Covid Economics 18, 15 May 2020: 73-108

January 21, 2020 in Washington State, and was quickly followed by cases in Chicago and Orange County, California. All these early cases were linked to travel in Wuhan. Throughout January and February, several cases arose which were all linked to travel abroad. Community transmission was first identified in late February in California. The first COVID-19 linked death occurred on February 29, in Kirkland, Washington. In early March, the first case was identified in New York, which by the end of the month would account for approximately half of all identified cases in the United States. In early and mid-March the virus began to spread rapidly.

The federal and many state governments responded to the COVID-19 pandemic in a number of ways. The first state to declare a state of emergency was Washington, which did so on January 30. The following day the US restricted travel from China. Initially, the President made many statements suggesting that the COVID-19 virus was under control. For example, on January 22 President Trump said that the virus was "totally under control" and on February 2nd the President noted that "We pretty much shut it down coming in from China." Statements that the virus was under control continued throughout February, and on February 24 the President said that "The Coronavirus is very much under control in the USA."

This pattern even continued into early March, with the President saying on March 6 that "in terms of cases, it's very, very few." On February 24, President Trump asked Congress for $1.25 billion in response to the pandemic. General concern and statements from policymakers changed sharply in mid-March as new cases increased rapidly. On March 11, following major outbreaks in Italy and much of Europe, President Trump announced a travel ban on most of Europe. Two days later on March 13, President Trump declared a national emergency. Many states followed by closing schools, restaurants, and bars or issuing shelter-in-place orders.

The fact that the initial public messages about the COVID-19 pandemic were relatively mild and suggested that the panic was under control led to suggestions of a partisan divide on the dangers of the new virus. For example, a NBC/Wall Street Journal Poll between March 11 and 13 found that 68% of Democrats were worried that someone in their family could catch the virus, while 40% of Republicans were worried. The same poll found that 56% of Democrats thought their day-to-day lives would change due the virus, while 26% of Republicans held the same view. A Pew Research Center Poll between March 10 and 16 found that 59% of Democrats and 33% of Republicans called the virus a major threat to US health.

We also worked to obtain data that might predict the extent to which locations are affected by the COVID-19 outbreak as the timing of any household response may differ substantially across geographic regions. As the outbreak has progressed, numerous governments have enacted orders, begun testing regimes, closed schools, and made other statements regarding the extent to which residents of an area should adjust their expectations and behavior. Rather than construct a timeline of explicit events, we construct a proxy for the extent to which COVID-19 has impacted a given location at a point in time.

In particular, we gather counts of articles that discuss COVID-19 (or several other related terms like 'corona' or 'coronavirus') across approximately 3,000 US newspapers at a daily level using the Access World News's Newsbank service. We aggregate this data at a state level and look at the ratio of articles related to COVID-19 to the total number of newspaper articles in that state on a given day. This data is displayed for a subset of states in Figure 7. Figure 7 illustrates differential intensity in reporting on COVID-19 over time across different states. In particular, we see notable increases in reporting in states like Washington prior to other states yet to see major outbreaks.

4 Household Financial Response to Coronavirus

While there were media reports of stockpiling, it was not ex ante clear whether consumption would go up or down in the early days of the COVID-19 outbreak. As James Stock notes: *"For the week ended March 14, there were two countervailing effects. Consumer confidence plummeted and new claims for unemployment insurance jumped sharply, but same-store sales surged as a result of the run on groceries and supplies."*

Figure 3 shows the aggregate response in terms of all daily spending, and grocery spending. The left panel shows average daily spending each week, while the right panel shows average daily grocery spending. After an initial seasonal increase in the first week of the new year, spending is largely flat for most of January and February. There is a sharp spike in spending between February 26 and March 10, as COVID-19 cases begin to spike in the United States. This initial spike in spending is followed by depressed levels of general spending by approximately 50%, but higher levels of grocery spending followed by a sharp drop. This is consistent with stockpiling behavior as it increasingly became clear that there would be a significant number of virus cases in the US.

Covid Economics 18, 15 May 2020: 73-108

This large and persistent drop is also in line with estimates from surveys conducted by the French Statistical Service, which found a 35% drop in total consumption.

Figure 4 shows that this initial spike in spending is large and consistent across all categories, however later on there is significant heterogeneity across categories. For some categories, like restaurants, retail, air travel, public transport and card spending. The initial sharp increase in credit card spending is consistent with households borrowing to smooth consumption. Food delivery spending increases and remains elevated, not dropping as sharply as other categories.

Figure 5 provides a visualization of the changes in spending between three time periods. The figure shows the percentage change in daily spending across categories, relative to a baseline of January 1 through February 26, 2020. The top panel shows evidence of stockpiling and an increase in consumer spending during the time period when it became clearer that the virus was spreading in the United States. The middle panel shows the change in spending between March 11 and March 17, when a national emergency was initially declared. During this time period, there is a sharp decrease in public transit spending, and continued high levels of elevated spending on groceries and retail.

The bottom panel shows spending between March 18 and March 27, well into shelter-in-place orders in many states. The bottom panel indicates very sharp declines in restaurant spending, air travel, and public transport. There is a significant increase in food delivery spending, consistent with households substituting meals at restaurant with meals at home.

4.1 Response Across States

In Table 2, we examine the pattern of user spending in a regression framework, concentrating on the periods of highest interest surrounding the periods between February 26 and March 10, before a national emergency was declared, the period between March 11 and march 17 following the imposition of a national emergency and the period between March 18 and March 27 when states and cities issued shelter-in-place orders. That is, when users seemed to be increasing spending in advance of a 'shelter-in-place' order and when those orders began to take effect.

In each column, we regress users' spending on indicators for the weekly periods indicated: February 26th to March 10, March 11 to March 17, and March 18 to March 27. These periods roughly coincide with observed patterns of behavior among households across the country. In the

Covid Economics 18, 15 May 2020: 73-108

first period, households tended to be stocking up on goods across a number of categories and also still patronizing entertainment venues and restaurants. The third period, in late March, corresponds to a period in which many cities and states were under 'shelter-in-place' advisories or orders, often with schools closed, non-essential businesses closed, and restaurants forced to only serve take-out food.

In each column, we present results on user spending with differing samples and types of spending. In columns (1)-(3), we measure user spending using a wide metric that includes services, food and restaurants, entertainment, pharmacies, personal care and transportation. Columns (4)-(6) include only spending on restaurants, while the final set of columns include spending only at grocery stores and supermarkets. In addition, we vary the sample across each column. 'All' represents all users in our sample. 'Shelter' indicates that the sample is limited to users in states that, as of March 27th, had a shelter-in-place order in place. 'No Shelter' restricts to users in states without such an order. All regressions utilize user-level fixed effects and all standard errors are clustered at the user level.

Several clear patterns emerge from this analysis. Overall, we see a stark pattern consistent with the figures presented above. Households tended to stock up substantially at the end of February into the beginning of March, then begin to cut spending dramatically. We also note that the number of transactions followed a similar though less extreme pattern. That is, the number of transactions in the stocking up period increased by about 15% while spending soared by around 50%. Thus, the *size* of transactions in the stocking up period was substantially higher than a household's average transaction size.

Comparing users that live in states that have had shelter-in-place orders put in place, we tend to see more negative coefficients in the third row for non-grocery spending (eg. comparing columns (2) and (3) as well as (5) and (6). That is, users in these states tended to decrease spending across categories at a much more rapid pace. This is especially seen within restaurant spending, with users in shelter-in-place states decreasing restaurant spending by about 31.8%, while users in other states decreased restaurant spending by only an insignificant 12.3%.[6]

In addition, we see more evidence for stocking up on groceries in states that have been put

[6]This decline in restaurant spending is much more muted if we restrict to Fast Food restaurants. Coefficients for these stores are approximately half the size as for non-Fast Food restaurants. This is likely driven by the fact that Fast Food restaurants serve a large portion of their customers via drive through and take out.

Covid Economics 18, 15 May 2020: 73-108

under a shelter-in-place order. Looking at columns (8) and (9), we see that grocery spending has been consistently higher among users in shelter-in-place states, likely reflecting a shift away from eating at restaurants or at office cafeterias and towards eating at home.

4.2 Response by Social Distancing

We also link the spending decisions of households to the Unacast data on social distancing, which comes from cell phone records. We create bin scatters (Figure 6) relating the difference in movements to the different spending categories. On the horizontal axis we plot the difference in movement and on the vertical axis we show the log-spending by different categories. In general, we find that across all spending categories a reduction in movement is related to a reduction in spending. The effect size, however, varies by spending category. The less people move the less they spend in restaurants, groceries or on buying at retailers. For public transport we also observe a reduction as less people travel and if they travel they are presumably more likely to use the car. The least reduction is observed for credit card spending. We conjecture this is because the credit card can still be used for online shopping or paying for subscriptions services like Netflix or Apple TV. The data on social distancing underscores the robustness of our findings and clearly relates them to the shelter-in-place orders.

5 Heterogeneity in Response by Political Views, Demographics, and Financial Indicators

In Table 3, we split users according to their predicted political orientation and examine how users' spending adjusted during these same periods. In particular, we utilize the Gallup polling data to map demographic and geographic characteristics of these households to form a predicted political score. We split users into the highest and lowest quartiles that are most likely to be Republicans and Democrats, respectively. The specifications mirror those in Table 2, looking at overall spending, restaurant spending, and grocery spending across these different groups.

We noted previously that some categories did see differences in spending changes according to political leanings. Indeed, Figure 9 shows that there was significant heterogeneity in social

Covid Economics 18, 15 May 2020: 73-108

distancing between more Republican and Democrat leaning states. The figure shows, for each state and the District of Columbia, the overall drop in movement as measured from Unacast cell phone records by the share of the electorate voting for Donald J. Trump in the 2016 US Presidential Election. The figure shows a sharp negative relationship between social distancing and the share of Trump voters. States with more Trump voters indicate lower levels of staying at home and social distancing.

We see sharp increases in spending, for both predicted Republicans and Democrats. Contrary to much of the discussion in the popular press and evidence from surveys suggesting that Democrats were more concerned with the virus, we actually see slightly more overall spending between February 26 and March 10 among Republicans relative to Democrats. This is particularly true for grocery spending, which is shown in Figure 10. While we see significant evidence of stockpiling for both groups, the percentage increase in grocery spending by Republicans is approximately twice as large as the increase among Democrats.

The observed differences between predicted Republican and Democrats could be both due to differences in beliefs, and differences in risk exposure. The differences in risk exposure between different partisan groups are not obvious. For example, Republicans are more likely to live in rural areas, while Democrats are more likely to live in urban areas which are at higher risk in a contagion. On the other hand, Republicans also tend to be older, and older individuals are at higher mortality risk from COVID-19.

Figure 3 shows additional categorical spending, broken down by predicted political affiliation. We see a large rise in spending across most categories in early to mid-March, consistent with stockpiling. Republicans are more likely to continue to spend at shops, and while this difference persists, it may be driven by differential geographic patterns if Republicans live in more rural areas that offer fewer home delivery services, and more drive-up options. Consistent with some differential spending patterns being driven by geographic and urbanization patterns, the drop in public transportation and air travel is driven almost entirely by Democrats, as Republicans are much less likely to use public transportation ex ante. All groups increase their utilization of food delivery services.

In Table 4, we examine how user spending responses differed across some key demographic and financial characteristics. We again perform a similar regression analysis, here interacting the

Covid Economics 18, 15 May 2020: 73-108

weekly indicators with indicators of whether a household possessed a demographic or financial characteristic. Notably, we include interactions for whether the user is under 30 years old, whether they have children, whether they are male, and whether they have an annual income above $40,000. Across the three panels, we again turn to looking at a wide measure of users' spending, just restaurant spending, and just spending at grocery stores and supermarkets.

In the first column, we see that younger users tended to cut back on spending by a smaller amount than older users. This coincides with reports that younger individuals were obeying the shelter-in-place orders less strictly than older Americans. We see the same pattern in restaurant spending, though the interaction is not significantly different than zero.

In the second column, we find that households with children tended to have the largest declines in spending in recent days, with overall spending falling around twice as fast as among households without children. We also note that, in Panel C, we find that households with children tended to increase grocery spending in the earlier weeks of the outbreak by significantly more than users with no children.

In column (3), we see that male users tended to have more muted responses in most categories. That is, men generally 'stocked up' less than women in the early weeks of March, and also cut back spending less than women did in the later weeks. Finally, the last column looks at differential behavior among users with higher income. In general, here we see few differences. Users with high income tended to behave quite similarly in their patterns of spending behavior to users with lower income. This is largely consistent with work by Kaplan, Violante and Weidner (2014) and Kaplan and Violante (2014) and there being a significant number of "wealthy-hand-to-mouth" consumers.

Finally, in Table 5 we also split by pre-corona liquidity of households and find more pronounced effects in the first week of the pandemic. We do not find a reversal pattern in the second week for more liquid households. The split by the log number of reported corona cases by county in which a household lives in Table 6 shows that patterns depend on the number of reported cases. In the first week the stockpiling effects are larger, while in the second and third week the reduction in expenditures is stronger in the log number of cases.

Covid Economics 18, 15 May 2020: 73-108

CEPR PRESS

6 Conclusion

This paper provides a first view of household spending during the recent weeks of the COVID-19 outbreak in the United States. Using transaction-level household financial data from a personal financial website, SaverLife, we illustrate how Americans' spending responded to the rise in disease cases as well as to the policy responses put in place by many city and state governments, namely shelter-in-place orders. We show that users' spending was radically altered by these events across a wide range of categories, and that the strength of the response partly depended on how severe the outbreak was in a user's state. Demographic characteristics such as age and family structure provoked larger levels of heterogeneity in spending responses to COVID-19, while income did not. Moreover, we demonstrate users of all political orientation increased spending prior to the epidemic, and at the same time there were some differences across political orientation in some categories indicative of differential beliefs or risk exposure.

We caution that these are very short term responses, meant to illustrate as close to a real-time view of consumer spending as possible. In part, this paper demonstrates the utility of household transaction level data in providing a window into not just household finance, but also aggregate trends, as well. Additionally, we caution that our data are skewed towards younger users, who have lower risk exposure. Older individuals with very high risk exposure may have behave differently, and cut consumption more substantially.

The COVID-19 outbreak has upended economies around the world and we are surely just at the beginning of understanding the full impact at both a household and national level. We anticipate large amounts of future work examining the impact of COVID-19 using household transaction data. Questions about how households went about rearranging spending, shifted from brick and mortar to online retailers, and utilized liquidity and credit are all at the forefront. Moreover, the ability to observe household-level income and the sources of this income may be fruitful in analyzing how households who faced sudden unemployment were able to substitute to new types of work and new employers. For example, disemployed retail workers might find fast employment in sectors with newly elevated demand, such as home delivery services.

Covid Economics 18, 15 May 2020: 73-108

References

Agarwal, Sumit, Chunlin Liu, and Nicholas S Souleles, "The Reaction of Consumer Spending and Debt to Tax Rebates– Evidence from Consumer Credit Data," *Journal of Political Economy*, 2007, *115* (6), 986–1019.

Baker, Scott R., "Debt and the Response to Household Income Shocks: Validation and Application of Linked Financial Account Data," *Journal of Political Economy*, 2018.

_ , "Debt and the Consumption Response to Household Income Shocks," *Journal of Political Economy*, forthcoming.

_ **and Constantine Yannelis**, "Income Changes and Consumption: Evidence from the 2013 Federal Government Shutdown," *Review of Economic Dynamics*, 2017, *23*, 99–124.

_ **, Lorenz Kueng, Steffen Meyer, and Michaela Pagel**, "Measurement Error in Imputed Consumption," *Working Paper*, 2020.

Baldauf, Markus, Lorenzo Garlappi, and Constantine Yannelis, "Does Climate Change Affect Real Estate Prices? Only If You Believe In It," *The Review of Financial Studies*, 2020, *33* (3), 1256–1295.

Barrios, John and Yael Hochberg, "Risk Perception Through the Lens Of Politics in the Time of the COVID-19 Pandemic," *Working Paper*, 2020.

Barro, Robert J, José F Ursua, and Joanna Weng, "The Coronavirus and the Great Influenza Epidemic," 2020.

Bhutta, Neila and Ben Keys, "Household Credit and Employment in the Great Recession," *American Economic Review*, 2016, *106* (7), 1742–74.

Blundell, Richard, Luigi Pistaferri, and Ian Preston, "Consumption Inequality and Partial Insurance," *American Economic Review*, 2006, *98* (5), 1887–1921.

Coibion, Olivier, Yuriy Gorodnichenko, and Michael Weber, "Labor Markets During the COVID-19 Crisis: A Preliminary View," *Fama-Miller Working Paper*, 2020.

Eichenbaum, Martin S, Sergio Rebelo, and Mathias Trabandt, "The Macroeconomics of Epidemics," Technical Report, National Bureau of Economic Research 2020.

Covid Economics 18, 15 May 2020: 73-108

Fuster, Andreas, Greg Kaplan, and Basit Zafar, "What Would You Do With $500? Spending Responses to Gains, Losses, News and Loans," Technical Report, National Bureau of Economic Research 2018.

Ganong, Peter and Pascal Noel, "Liquidity vs. Wealth in Household Debt Obligations: Evidence from Housing Policy in the Great Recession," Technical Report, National Bureau of Economic Research 2018.

Gormsen, Niels Joachim and Ralph SJ Koijen, "Coronavirus: Impact on Stock Prices and Growth Expectations," *University of Chicago, Becker Friedman Institute for Economics Working Paper*, 2020, (2020-22).

Gourinchas, Pierre-Olivier and Jonathan A. Parker, "Consumption Risk Over the Life-Cycle," *Econometrica*, 2002, *70* (1), 47–89.

Jappelli, Tullio and Luigi Pistaferri, "The Consumption Response to Income Changes," *Annual Review of Economics*, 2010, *2*, 479–506.

Johnson, David S., Jonathan A. Parker, and Nicholas Souleles, "Household Expenditure and the Income Tax Rebates of 2001," *American Economic Review*, 2006, *96* (5), 1589–1610.

Jones, Callum, Thomas Philippon, and Venky Venkateswaran, "Optimal Mitigation Policies in a Pandemic," *Working Paper*, 2020.

Kaplan, Greg and Gianluca Violante, "How Much Consumption Insurance beyond Self-Insurance?," *American Economic Journal: Macroeconomics*, 2010, *2* (4), 53–87.

_ **and** _ , "A Model of the Consumption Response to Fiscal Stimulus Payments," *Econometrica*, 2014, *82* (4), 1199–1239.

_ **, Giovanni L Violante, and Justin Weidner**, "The Wealthy Hand-to-Mouth," *Brookings Papers on Economic Activity*, 2014, p. 77.

Kempf, Elisabeth and Margarita Tsoutsoura, "Partisan Professionals: Evidence from Credit Rating Analysts," Technical Report, National Bureau of Economic Research 2018.

Keys, Benjamin, Amit Seru, and Vikrant Vig, "Lender Screening and the Role of Securitization: Evidence from Prime and Subprime Mortgage Markets," *Review of Financial Studies*, 2012, *25* (7), 2071–2108.

_ **, Tanmoy Mukherjee, Amit Seru, and Vikrant Vig**, "Did Securitization Lead to Lax Screening? Evidence from Subprime Loans," *Quarterly Journal of Economics*, 2008, *125* (1), 307–362.

Covid Economics 18, 15 May 2020: 73-108

Maggio, Marco Di, Amir Kermani, Benjamin J Keys, Tomasz Piskorski, Rodney Ramcharan, Amit Seru, and Vincent Yao, "Interest Rate Pass-through: Mortgage Rates, Household Consumption, and Voluntary Deleveraging," *American Economic Review*, 2017, *107* (11), 3550–88.

Malmendier, Ulrike and Stefan Nagel, "Depression Babies: Do Macroeconomic Experiences Affect Risk Taking?," *The Quarterly Journal of Economics*, 2011, *126* (1), 373–416.

Meeuwis, Maarten, Jonathan A Parker, Antoinette Schoar, and Duncan I Simester, "Belief Disagreement and Portfolio Choice," Technical Report, National Bureau of Economic Research 2018.

Meyer, Steffen and Michaela Pagel, "Fully Closed: Individual Responses to Realized Gains and Losses," *Working Paper*, 2019.

Mian, Atif and Amir Sufi, "House Prices, Home Equity-Based Borrowing and the US Household Leverage Crisis," *American Economic Review*, 2011, *101* (5), 2132–56.

_ , Kamalesh Rao, and Amir Sufi, "Household Balance Sheets, Consumption and the Economic Slump," *The Quarterly Journal of Economics*, 2013, *128* (4), 1687–1726.

Mian, Atif R, Amir Sufi, and Nasim Khoshkhou, "Partisan Bias, Economic Expectations, and Household Spending," *Fama-Miller Working Paper*, 2018.

Olafsson, Arna and Michaela Pagel, "The Liquid Hand-to-Mouth: Evidence from Personal Finance Management Software," *Review of Financial Studies*, 2018.

Pagel, Michaela and Arna Vardardottir, "The Liquid Hand-to-Mouth: Evidence from a Personal Finance Management Software," *Review of Financial Studies*, forthcoming.

Pistaferri, Luigi, "Superior Information, Income Shocks and the Permanent Income Hypothesis," *Review of Economics and Statistics*, 2001, *83* (3), 465–476.

Souleles, Nicholas, "The Response of Household Consumption to Income Tax Refunds," *American Economic Review*, 1999, *89* (4), 947–958.

Zeldes, Stephen, "Consumption and Liquidity Constraints: An Empirical Investigation," *Journal of Political Economy*, 1989, *97* (2), 1469–1513.

Covid Economics 18, 15 May 2020: 73-108

CEPR PRESS

Figure 1: Example of Platform

Notes: Screenshots of the SaverLife-app and its financial advice page. Source: SaverLife.

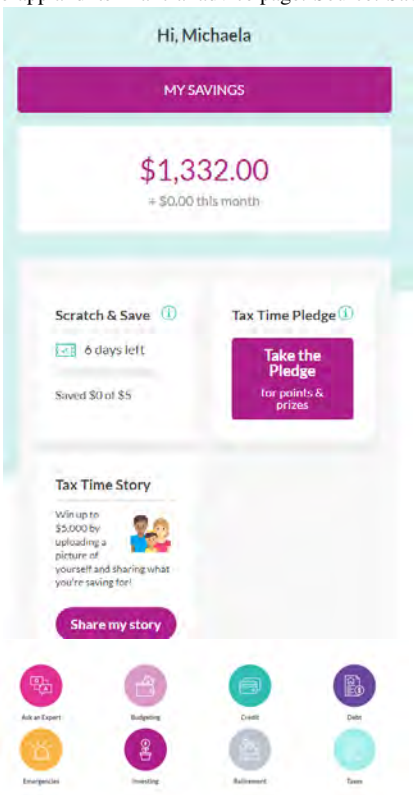

Covid Economics 18, 15 May 2020: 73-108

Covid Economics 18, 15 May 2020: 73-108

Figure 2: SaverLife Users

Notes: Panel A displays the number of SaverLife users by 5-digit zip code in the US. Panel B shows the average annual self-reported income of users by 5-digit zip code in the US (in 1,000 USD). Source: SaverLife.

Panel A: Number of Users

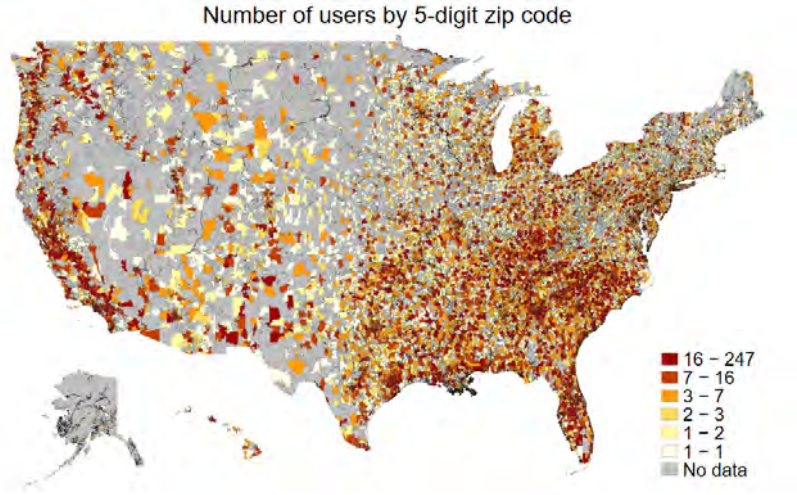

Panel B: Average User Income

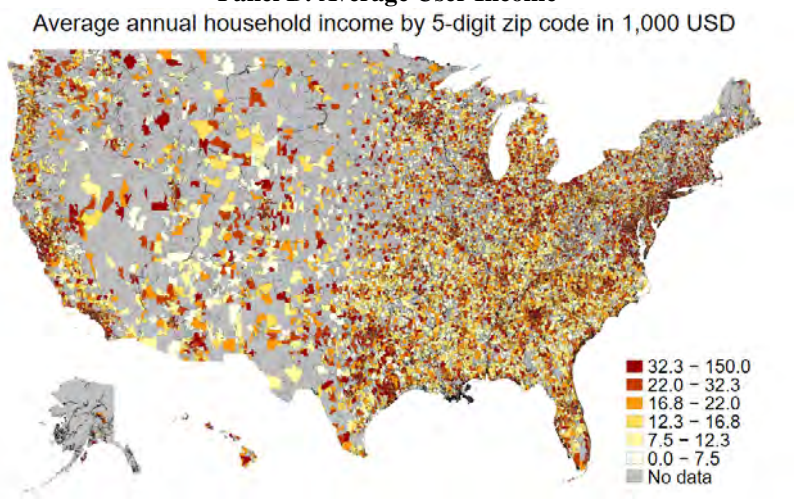

Covid Economics 18, 15 May 2020: 73-108

Figure 3: Household Grocery Spending Response

Notes: This graph displays how household spending changed by week in 2020. Spending is measured in daily dollars. Months are split into four periods equal in size across months. Individual fixed effects are removed prior to collapsing across individuals. Source: SaverLife.

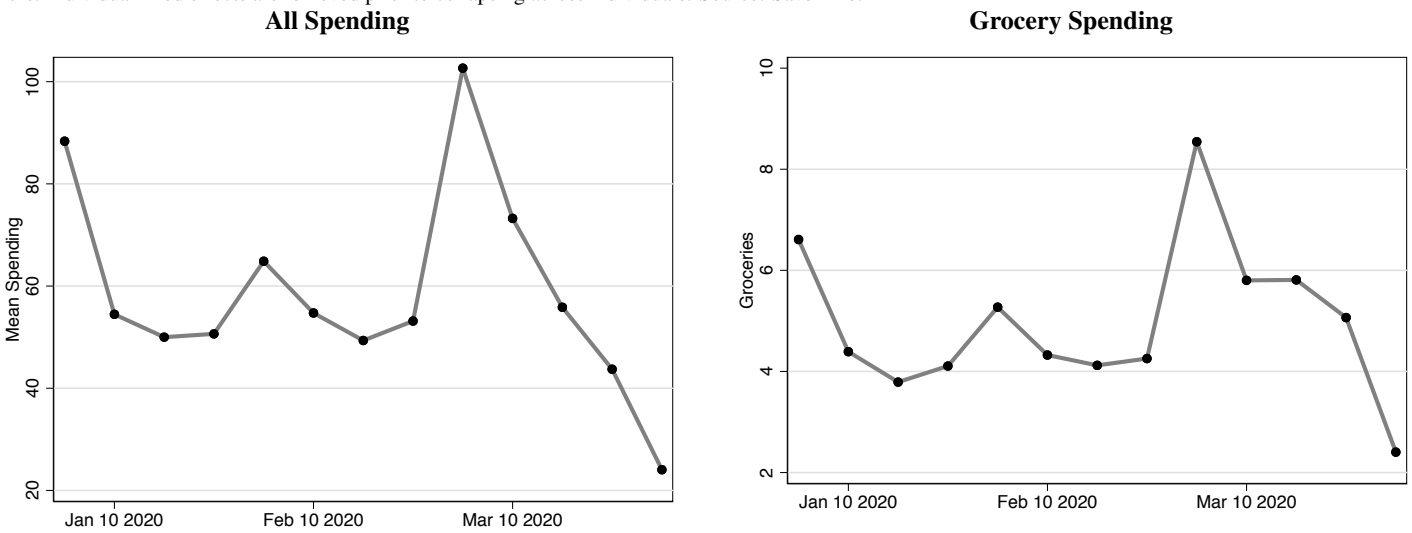

Covid Economics 18, 15 May 2020: 73-108

Figure 4: Household Spending Response Across Categories

Notes: This graph displays the response of household spending across a number of categories of spending. Spending is measured in daily dollars. Estimates are taken as the change in household spending from the first week of February to the first week of March. Source: SaverLife.

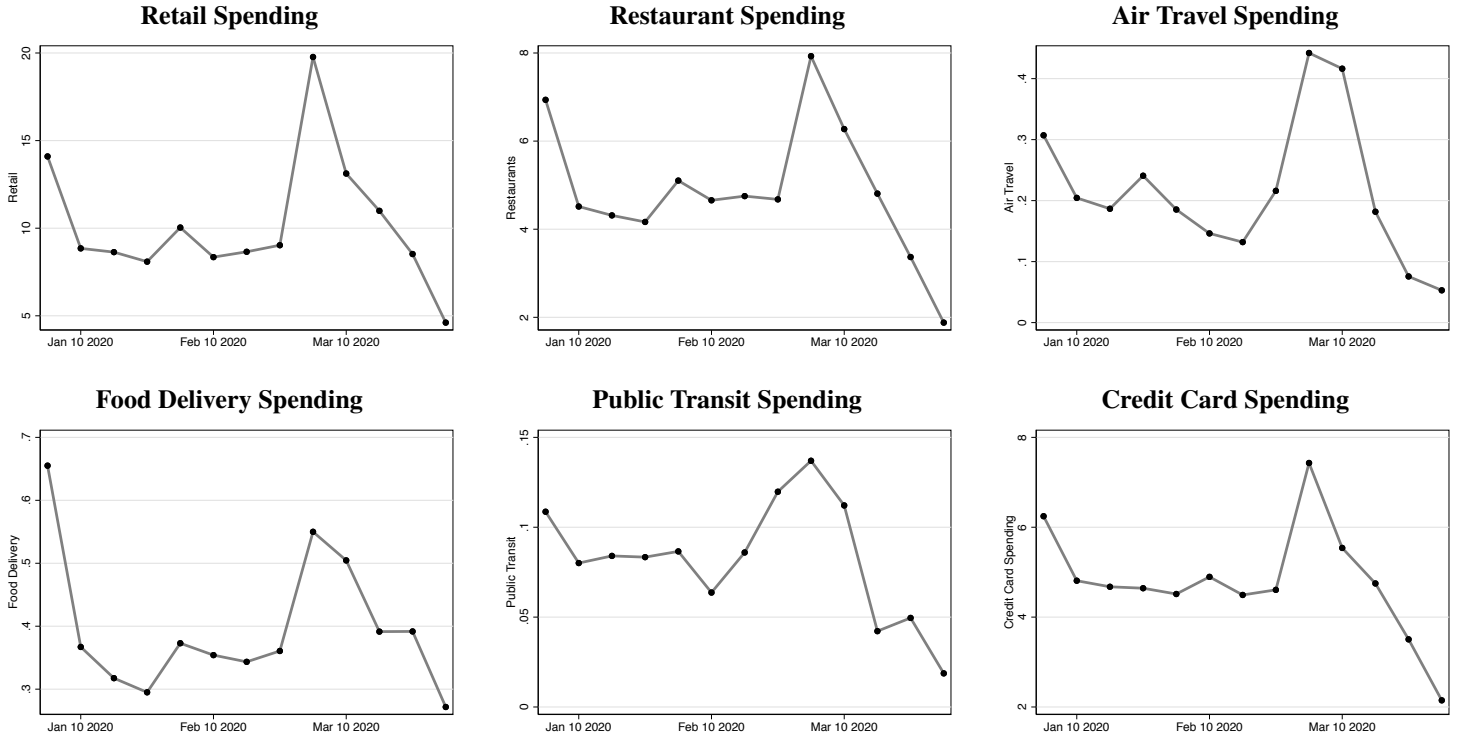

Figure 5: Household Spending Response Across Categories

Notes: This figure displays the percentage change in mean daily spending, across different categories relative to spending pre-February 26. Source: SaverLife.

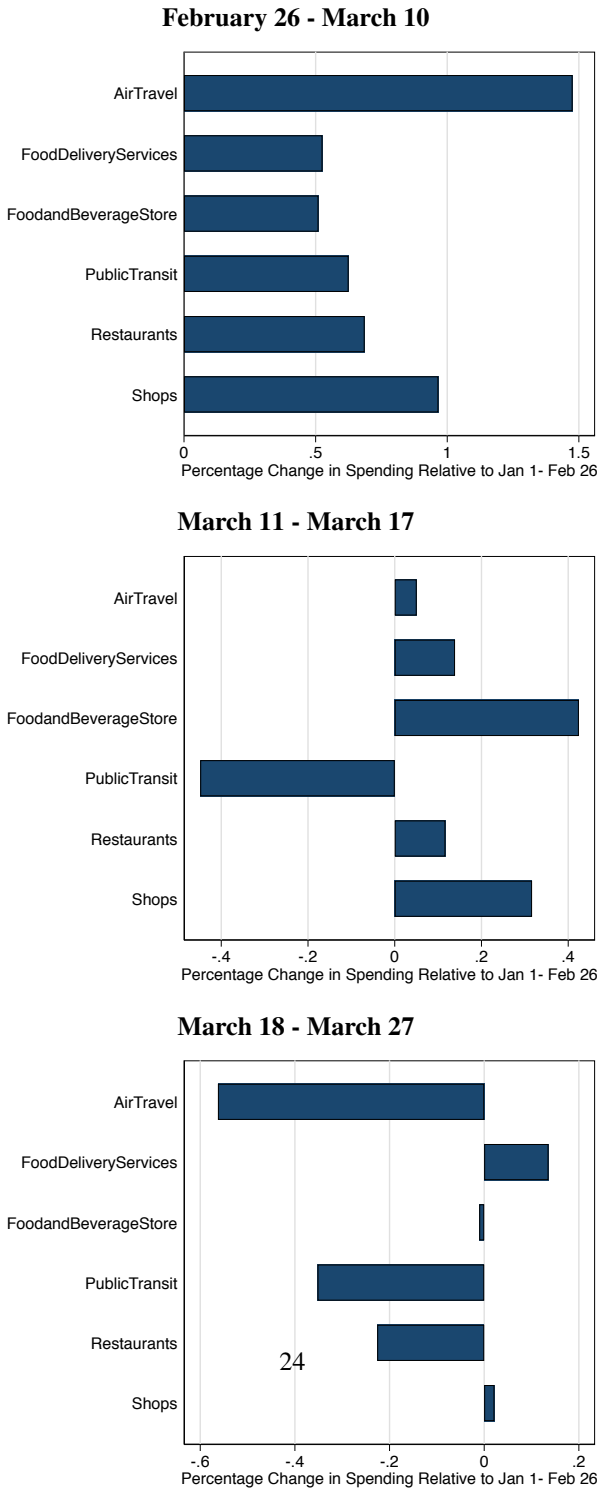

Covid Economics 18, 15 May 2020: 73-108

Covid Economics 18, 15 May 2020: 73-108

Figure 6: Household Spending and Social Distancing

Notes: This graph displaysf household spending across a number of categories of spending in bins of the daily difference in movement. Spending is measured in daily dollars. Source: SaverLife and Unacast.

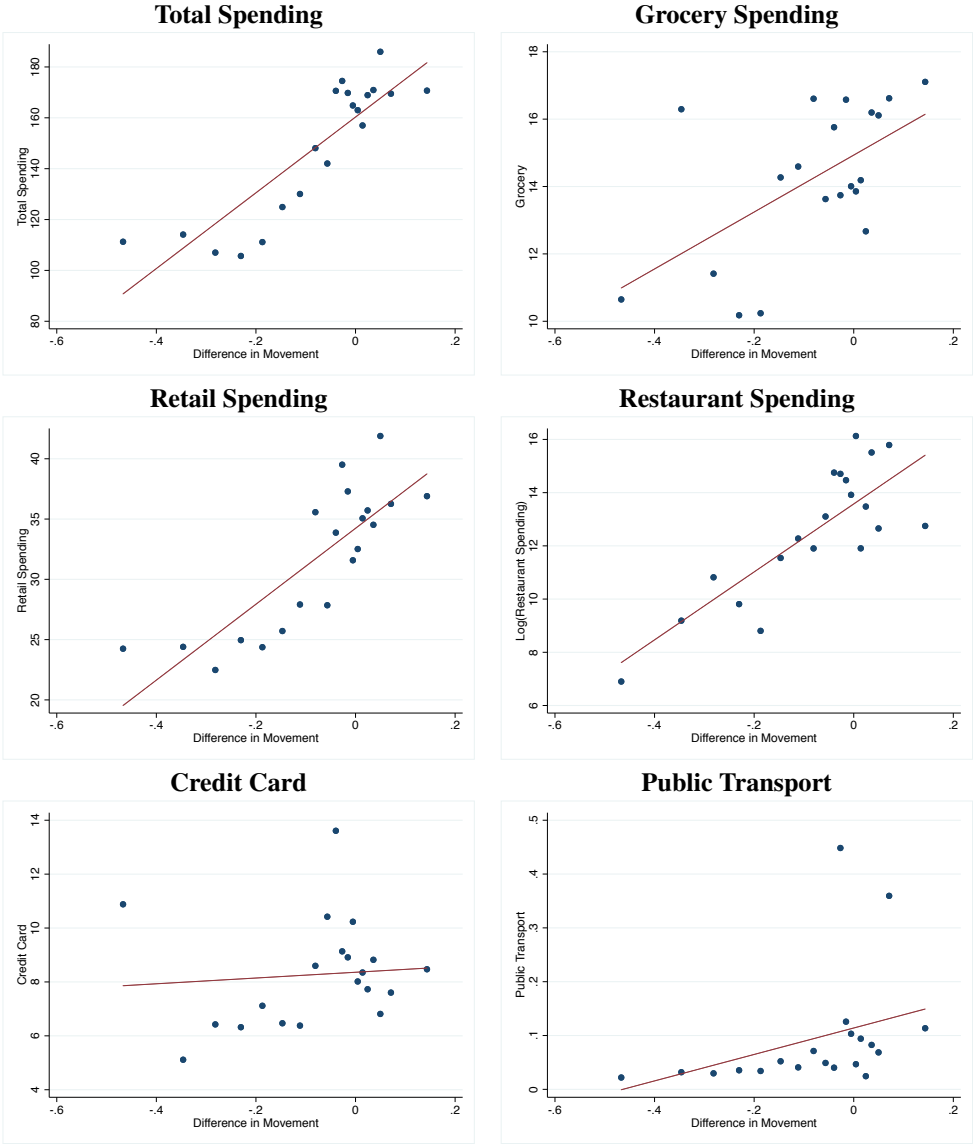

Figure 7: Newspaper Coverage of COVID-19, by State

Notes: This graph displays the fraction of newspaper articles in US newspapers that mentions a term related to COVID-19. Data shown for selected states. Nationwide, over 3,000 newspapers are utilized.

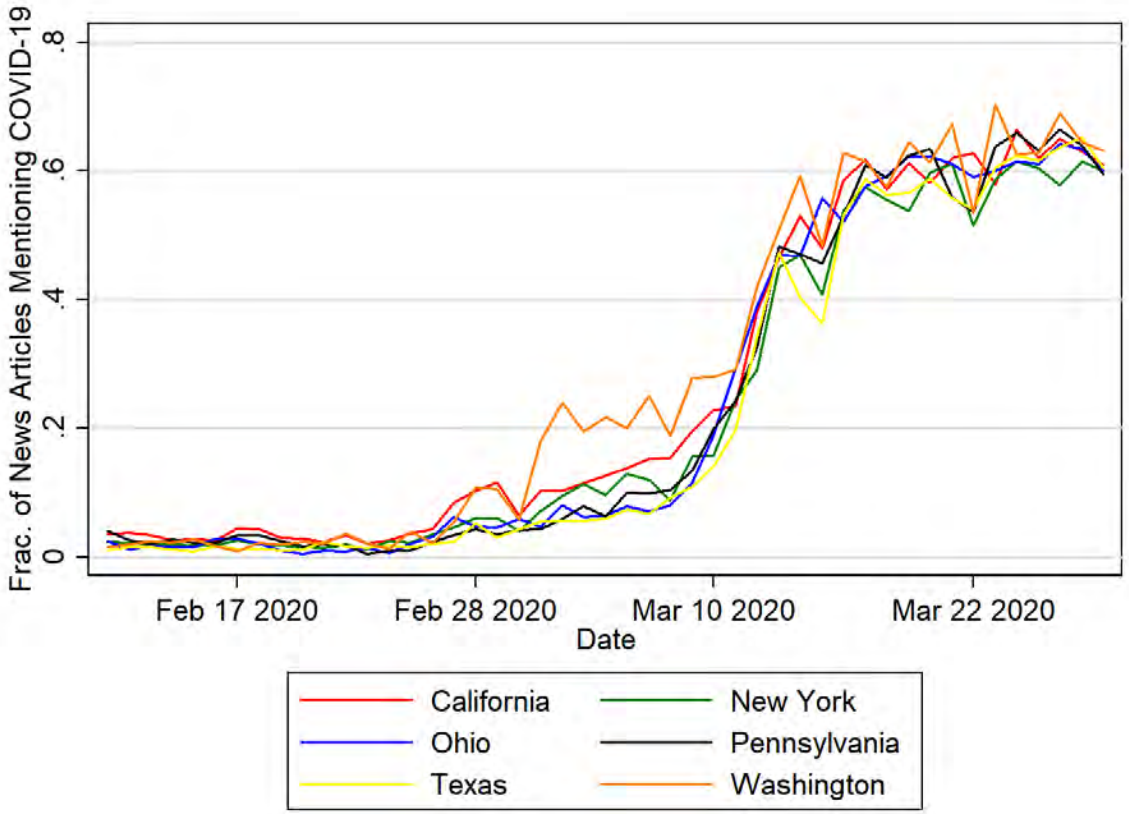

Covid Economics 18, 15 May 2020: 73-108

Covid Economics 18, 15 May 2020: 73-108

Figure 8: Map of Average Partisanship, by County

Notes: This figure shows the average predicted partisan scores in US counties. Darker red shapes indicates more Republican countries, while darker blue shades indicate more Democrat counties. Source: Gallup

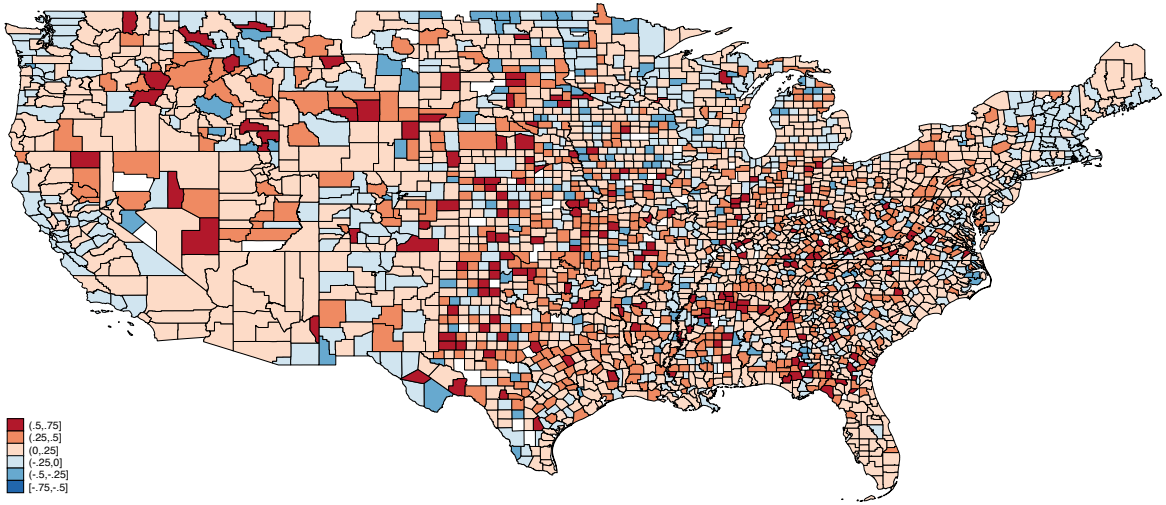

Figure 9: Vote Shares and Social Distancing Efforts

Notes: This figure shows a binned scatter plot of the drop in movement in all 50 US states and the District of Columbia, and the fraction of individuals who voted for Donald Trump in the 2016 US Presidential election. Source: MIT Election Data Lab and Unacast Social Distancing Scoreboard.

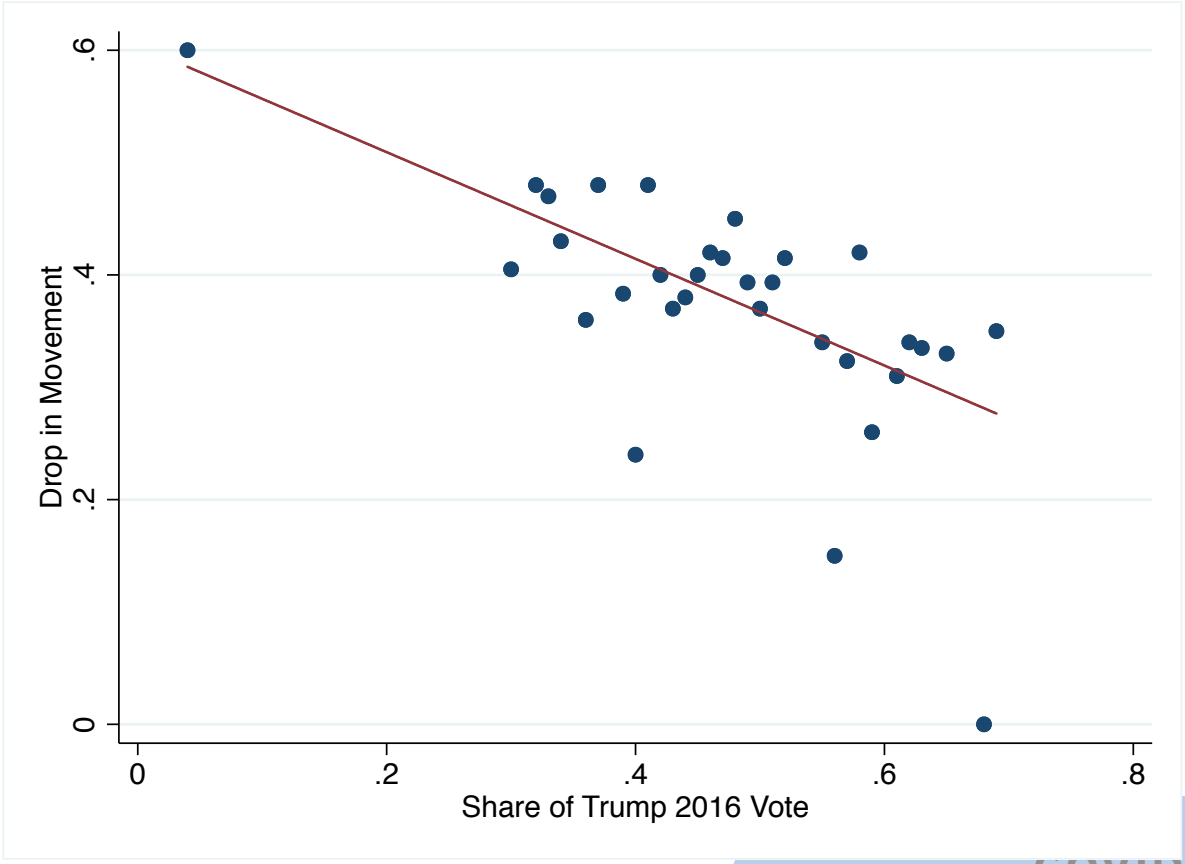

Covid Economics 18, 15 May 2020: 73-108

Figure 10: Grocery Spending and Political Scores in 2020

Notes: This figure displays the response of average household daily spending for groceries. Estimates are taken as the change in household spending from the first week of February to the first week of March. For each category, average response is plotted for three groups: the quartile of the sample with the highest predicted 'democrat' lean and the quartile of the sample with the highest predicted 'republican' lean and 'independents' who are in the middle two quartiles. Spending is measured in daily dollars. Source: SaverLife.

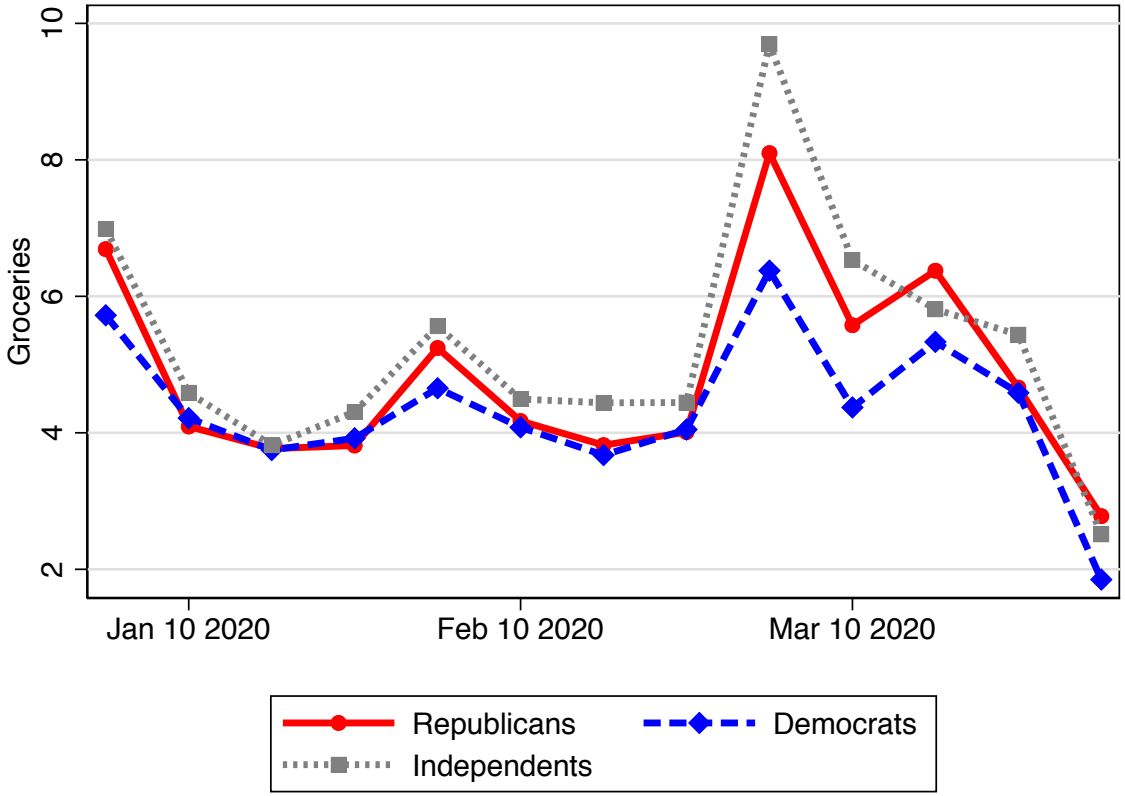

Covid Economics 18, 15 May 2020: 73-108

Covid Economics 18, 15 May 2020: 73-108

Figure 11: Household Spending Response Across Categories, by Predicted Partisanship

Notes: This figure displays the response of average household daily spending across a number of categories of spending. Estimates are taken as the change in household spending from the first week of February to the first week of March. For each category, average response is plotted for three groups: the quartile of the sample with the highest predicted 'democrat' lean and the quartile of the sample with the highest predicted 'republican' lean and 'independents' who are in the middle two quartiles. Spending is measured in daily dollars. Source: SaverLife.

Table 1: Monthly Summary Statistics

Summary statistics of the final sample of active users with complete data from March 27th. Data are monthly over users' entire smaple histories. All statistics are in USD.

			Percentiles				
	Mean	Std. Dev.	10%	25%	50%	75%	90%
Number of Linked Accts	2.61	2.92	1	1	2	3	5
Number of Txns	77.06	64.29	17	33	64	100	155
Payroll Income	$2,718.50	$3,789.80	$6.70	$410.64	$1,681.19	$3,629.03	$6,352.28
Groceries	$262.36	$351.75	$19.89	$48.01	$138.88	$351.75	$701.73
Restaurants	$318.97	$942.38	$16.32	$44.63	$124.66	$278.25	$652.35
Pharmacies	$53.39	$86.24	$6.47	$14.31	$30.78	$61.13	$114.26
Shopping	$165.15	$322.90	$8.55	$22.245	$69.995	$169.38	$371.31
Transaction-Level Obs.	691,542						
User-Week Obs.	61,555						
User-Month Obs.	14,205						

Covid Economics 18, 15 May 2020: 73-108

CEPR PRESS

Table 2: Spending by Week and Heterogeneity by State

Regression of spending on indicators for the different time periods. Dependent variables vary across columns, with columns (1)-(3) being on a wide metric of household spending including services, food and restaurants, entertainment, pharmacies, personal care and transportation. Columns (4)-(6) include only spending on restaurants, while the final set of columns include spending only at grocery stores and supermarkets. 'Shelter' indicates that the sample is limited to users in states that, as of March 27th, had a shelter in place order in place. 'No Shelter' restricts to users in states without such an order. Standard errors clustered at a user level. *$p < .1$, ** $p < .05$, *** $p < .01$. Source: SaverLife.

VARIABLES	(1) All	(2) Shelter	(3) No Shelter	(4) All - Rest	(5) Shelter - Rest	(6) No Shelter - Rest	(7) All - Groc	(8) Shelter - Groc	(9) No Shelter - Groc	N
February 26 - March 10	0.516***	0.584***	0.491***	0.371***	0.335***	0.337***	0.273***	0.284***	0.269***	0
	(0.0273)	(0.0452)	(0.0765)	(0.0212)	(0.0407)	(0.0626)	(0.0208)	(0.0390)	(0.0633)	
March 11 - March 17	-0.0437	0.134**	0.0701	0.0463*	0.0523	0.159**	0.189***	0.331***	0.187**	-
	(0.0318)	(0.0561)	(0.0957)	(0.0240)	(0.0455)	(0.0764)	(0.0255)	(0.0515)	(0.0827)	
March 18 - March 27	-0.477***	-0.245***	-0.159	-0.313***	-0.318***	-0.123	0.0745***	0.232***	0.0838	-0
	(0.0322)	(0.0558)	(0.0973)	(0.0235)	(0.0452)	(0.0784)	(0.0253)	(0.0519)	(0.0860)	
Observations	61,555	15,886	6,383	61,555	15,886	6,383	61,555	15,886	6,383	
R^2	0.397	0.431	0.443	0.397	0.428	0.443	0.398	0.415	0.440	
User FE	YES	YES	YES	YES	YES	YES	YES	YES	YES	

Robust standard errors in parentheses

*** p<0.01, ** p<0.05, * p<0.1

CEPR PRESS

Table 3: Spending by Week and Heterogeneity by Predicted Political Position

Regression of spending on indicators for the different time periods. Dependent variables vary across columns, with columns (1)-(3) being on a wide metric of household spending including services, food and restaurants, entertainment, pharmacies, personal care and transportation. Columns (4)-(6) include only spending on restaurants, while the final set of columns include spending only at grocery stores and supermarkets. 'Dem' indicates that the sample is limited to users who are predicted to be in the top quartile of most democratic leaning based on Demographic and financial indicators. 'Rep' indicates that the sample is limited to users who are predicted to be in the top quartile of most Republican leaning based on demographic and financial indicators. Standard errors clustered at a user level. *$p < .1$, ** $p < .05$, *** $p < .01$. Source: SaverLife.

VARIABLES	(1) All	(2) Dem	(3) Rep	(4) All - Rest	(5) Dem - Rest	(6) Rep - Rest	(7) All - Groc	(8) Dem - Groc	(9) Rep - Groc
February 26 - March 10	0.516***	0.401***	0.505***	0.371***	0.292***	0.379***	0.273***	0.120***	0.298***
	(0.0273)	(0.0524)	(0.0626)	(0.0212)	(0.0416)	(0.0480)	(0.0208)	(0.0393)	(0.0442)
March 11 - March 17	-0.0437	-0.0642	-0.0659	0.0463*	-0.0153	0.0638	0.189***	0.176***	0.238***
	(0.0318)	(0.0629)	(0.0729)	(0.0240)	(0.0491)	(0.0528)	(0.0255)	(0.0504)	(0.0562)
March 18 - March 27	-0.477***	-0.572***	-0.484***	-0.313***	-0.460***	-0.364***	0.0745***	0.0755	0.0595
	(0.0322)	(0.0661)	(0.0720)	(0.0235)	(0.0487)	(0.0496)	(0.0253)	(0.0504)	(0.0544)
Observations	61,555	15,080	12,922	61,555	15,080	12,922	61,555	15,080	12,922
R^2	0.397	0.388	0.386	0.397	0.392	0.381	0.398	0.397	0.393
User FE	YES	YES	YES	YES	YES	YES	YES	YES	YES

Covid Economics 18, 15 May 2020: 73-108

Table 4: Spending Response Heterogeneity by Demographic and Financial Indicators

Regression of spending on indicators for the different time periods. Dependent variables vary based on Panel. Panel A includes a wide metric of household spending including services, food and restaurants, entertainment, pharmacies, personal care and transportation. Panel B includes only spending on restaurants, while Panel C Includes spending only at grocery stores and supermarkets. In each panel, we interact indicators for the listed periods with indicators for demographic and financial characteristics, listed above the columns. Column (1) interacts with whether the user is under 30 years old. Column (2) interacts with an indicator for whether the user has children. Column (3) interacts with an indicator for whether the user is male. Column (4) interacts with an indicator for whether the user earns above $40,000 per year. Standard errors clustered at a user level. *$p < .1$, ** $p < .05$, *** $p < .01$. Source: SaverLife.

	(Young)	(Children)	(Male)	(High Income)
		Panel A. **All Spending**		
February 26 - March 10	0.550***	0.529***	0.567***	0.550***
	(0.0521)	(0.0365)	(0.0355)	(0.0384)
March 18 - March 27	-0.481***	-0.271***	-0.379***	-0.355***
	(0.0617)	(0.0460)	(0.0421)	(0.0451)
February 26 - March 10*Group	0.0364	0.111	-0.142*	0.0144
	(0.0675)	(0.0908)	(0.0759)	(0.0790)
March 18 - March 27*Group	0.234***	-0.329***	-0.0115	0.0243
	(0.0807)	(0.100)	(0.0912)	(0.102)
Observations	32,838	30,446	38,701	31,564
R^2	0.414	0.419	0.412	0.416
User FE	YES	YES	YES	YES
		Panel B. **Restaurant Spending**		
February 26 - March 10	0.307***	0.322***	0.407***	0.358***
	(0.0405)	(0.0321)	(0.0295)	(0.0321)
March 18 - March 27	-0.317***	-0.269***	-0.292***	-0.262***
	(0.0448)	(0.0371)	(0.0328)	(0.0358)
February 26 - March 10*Group	0.0812	0.0883	-0.200***	-0.0370
	(0.0554)	(0.0708)	(0.0611)	(0.0666)
March 18 - March 27*Group	0.0703	-0.0266	0.0239	-0.0452
	(0.0619)	(0.0750)	(0.0660)	(0.0765)
Observations	32,838	30,446	38,701	31,564
R^2	0.412	0.418	0.41	0.416
User FE	YES	YES	YES	YES
		Panel C. **Grocery Spending**		
February 26 - March 10	0.278***	0.245***	0.318***	0.304***
	(0.0419)	(0.0313)	(0.0298)	(0.0321)
March 18 - March 27	0.0169	0.140***	0.110***	0.129***
	(0.0532)	(0.0421)	(0.0371)	(0.0407)
February 26 - March 10*Group	0.0276	0.205***	-0.150***	-0.0491
	(0.0555)	(0.0721)	(0.0569)	(0.0659)
March 18 - March 27*Group	0.197***	-0.0273	-0.0412	0.0153
	(0.0706)	(0.0828)	(0.0705)	(0.0853)
Observations	32,838	30,446	38,701	31,564
R^2	0.408	0.411	0.41	0.407
User FE	YES	YES	YES	YES

Covid Economics 18, 15 May 2020: 73-108

Covid Economics 18, 15 May 2020: 73-108

Table 5: Spending Response Heterogeneity by Liquidity

Regression of spending on indicators for the different time periods interacted with the average monthly spending pre-crisis (period between September 2019 and February 2020). Column (1) uses all spending categories, column (2) only uses spending at restaurants and column (3) only looks at grocery spending. Standard errors clustered at a user level. *$p < .1$, ** $p < .05$, *** $p < .01$. Source: SaverLife.

VARIABLES	(1) All	(2) Restaurant	(3) Groceries
February 26 - March 10	0.385***	0.259***	0.150***
	(0.0330)	(0.0262)	(0.0253)
March 18 - March 27	-0.581***	-0.350***	0.0148
	(0.0408)	(0.0308)	(0.0326)
February 26 - March 10*Liquid	0.542***	0.367***	0.388***
	(0.0635)	(0.0508)	(0.0519)
March 18 - March 27*Liquid	0.358***	0.123**	0.116**
	(0.0725)	(0.0541)	(0.0592)
Observations	49,972	49,972	49,972
R^2	0.391	0.396	0.394
User FE	YES	YES	YES

Covid Economics 18, 15 May 2020: 73-108

Table 6: Spending Response Heterogeneity by Number of Cases

Regression of spending on indicators for the different time periods interacted with the natural logarithm of the number of cases per county. Column (1) uses all spending categories, column (2) only uses spending at restaurants and column (3) only looks at grocery spending. Standard errors clustered at a user level. *$p < .1$, ** $p < .05$, *** $p < .01$. Source: SaverLife.

VARIABLES	(1) All	(2) Restaurants	(3) Groceries
pre_stockpiling_weeks	0.0597**	0.0704***	0.0329
	(0.0276)	(0.0218)	(0.0216)
February 26 - March 10	0.625***	0.404***	0.308***
	(0.0351)	(0.0273)	(0.0272)
March 18 - March 27	-0.488***	-0.207***	0.0196
	(0.0689)	(0.0491)	(0.0530)
February 19 - February 25*ln(Cases)	0.131*	0.116*	0.0238
	(0.0791)	(0.0694)	(0.0601)
February 26 - March 10*ln(Cases)	-0.162***	-0.0420	-0.0763***
	(0.0330)	(0.0259)	(0.0266)
March 18 - March 27*ln(Cases)	0.00997	-0.0313**	0.0103
	(0.0188)	(0.0140)	(0.0150)
Observations	47,695	47,695	47,695
R^2	0.392	0.399	0.395
User FE	YES	YES	YES

The medium-run impact of non-pharmaceutical Interventions: Evidence from the 1918 influenza in US cities[1]

Guillaume Chapelle[2]

Date submitted: 11 May 2020; **Date accepted:** 12 May 2020

This paper uses a difference-in-differences framework to estimate the causal impact on the mortality rate of non-pharmaceutical interventions (NPIs) used to fight the 1918 inuenza pandemic. The results suggest that NPIs such as school closures and social distancing introduced a trade-off. While they could lower the fatality rate during the peak of the inuenza pandemic, they might also have reduced the herd immunity and significantly increased the death rate in subsequent years. There is no significant association between the implementation of NPIs and cities' growth.

Covid Economics 18, 15 May 2020: 109-156

1 An earlier version of this working paper (Chapelle, April 2020) is available at https://papers.ssrn.com/sol3/papers.cfm?abstract_id=3573562. The author acknowledges the support from ANR-11-LABX-0091 (LIEPP), ANR-11-IDEX-0005-02 and ANR-17-CE41-0008 (ECHOPPE). I thank Richard Baldwin, Sarah Cohen, Jean Benoit Eymeoud, Philippe Martin, Etienne Wasmer, Clara Wolf, Charles Wyplosz and a referee for their helpful comments on this working paper. The English was edited by Bernard Cohen, who I thank particularly. All errors remain mine.

2 Assistant Professor of Economics, University of Cergy Pontoise.

Covid Economics 18, 15 May 2020: 109-156

1 Introduction

Since the emergence of the global Covid-19 pandemic, a growing stream of contributions has sought to inform policy makers by analyzing past pandemics. In this context, the 1918 flu might offer an interesting opportunity to evaluate the potential impact of pandemics on economic activity (Barro, Ursúa, and Weng 2020) and the potential benefits of Non Pharmaceutical Interventions (NPIs) such as school closures and social distancing (Correia, Luck, and Verner 2020).

My first contribution is summarized in Figure 1. I estimate with a difference in differences approach the impact of Non Pharmaceutical Interventions to fight against pandemics on the aggregate death rate. I show that cities that responded more aggressively and rapidly to the 1918 pandemic with NPIs managed to decrease the death rate in 1918. However, these cities also ended with relatively higher mortality levels in the subsequent years, in particular when the intervention was long. The net benefit of Non Pharmaceutical Interventions thus seems smaller in terms of mortality. One potential explanation would be the lower immunity of the population generated by these measures making these cities more vulnerable during the following years. Indeed, the subsequent influenza epidemics, with the exception of avian influenza, have been caused by descendants of the 1918 virus (Taubenberger and Morens 2006) up to 1977 (Fine 1993). This finding seems to support that herd immunity[1], as initially advocated in Fox et al. (1971), allows to decrease the spread of influenza. Indeed, Fine (1993) reports that many epidemiological papers argued that herd immunity might be a convenient way to decrease the spread of influenza these include St Groth (1977) and Fine (1982).

I then investigate the impact of NPIs on cities' demographic structure and growth. Unsurprisingly in light of their limited impact on the death rate, I find no impact on their population growth or even on the share of population belonging to the most affected cohort. Moreover, a careful investigation of the long run dynamics of the manufacturing sector does not allow to establish any causal link of NPIs on economic growth given that cities that adopted longer NPIs had different economic dynamics (pre-trends) before 1909.

The paper is organized as follows. Section 2 presents the background and the current state of our knowledge on the 1918 pandemic including its potential effect on economic activity. Section 3 presents the data. Section 4 develops a difference in differences approach to estimate the impact of NPIs

1. *"The resistance of a group to attack by a disease to which a large proportion of the members are immune, thus lessening the likelihood of a patient with a disease coming into contact with a susceptible individual"* (Agnew 1965)

on the death rate. Section 5 discusses the impact of NPIs implemented in 1918 on cities' dynamics. Section 6 concludes.

Figure 1: Evolution of the yearly death rate before and after the 1918 flu in 43 cities that implemented Non Pharmaceutical Interventions in 1918 for different length

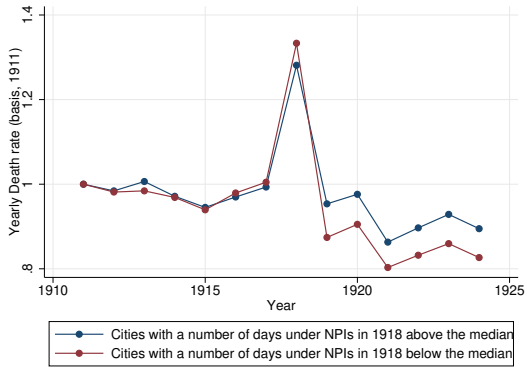

Reading notes:Cities that implemented NPIs for a longer time saw their death rates increase less than cities that had shorter NPIs in 1918. On the other hand the death rate remained relatively higher during the following years for these cities

Computation of the author from the Bureau of Census mortality Tables published in 1920 and 1925

Data on NPIs come from Markel et al. (2007)

Average death rate computed for a sample of 43 cities: Albany (NY), Baltimore, Birmingham, Boston, Buffalo, Cambridge, Chicago, Cincinnati, Cleveland, Columbus, Dayton, Denver, Fall River, Grand Rapid, Indianapolis, Kansas City, Los Angeles, Louisville, Lowell, Milkwaukee, Minneapolis, Nashville, New Haven, New Orleans, New York, Newark, Oakland, Omaha, Philadelphia, Pittsburgh, Portland, Providence, Richmond, Rochester, Saint Louis, Saintt Paul, San Fransisco, Seattle, Spokane, Syracuse, Toledo, Washington, Worcester.

2 Background and literature review

2.1 The Policy responses to the 1918 influenza

The year 2020 has seen a global health crisis with more than 50% of the world population under relatively strict NPIs. The closest crisis from which enough data is available is the 1918 flu that spread throughout the world at the end of the First World War and infected about a quarter of the world population at that time (Taubenberger and Morens 2006). It also

Covid Economics 18, 15 May 2020: 109-156

had long run consequences on children born during this period (Almond 2006). The flu mostly affected active people with an unusual casualty rate concentrated for the age groups between 15 and 45.
In the U.S., the flu was probably spread by troups coming back from Europe and increased dramatically the death rate in the autumn of 1918. It is also noteworthy that the death rate due to influenza decreased the next years but remained at higher levels when compared with previous years as illustrated in Figure 2. This might be because doctors were then more likely to report influenza as the cause of some death but also because the virus mutated and continued to affect people in the following years. Indeed, Taubenberger and Morens (2006) stress that the virus at the origin of the 1918 pandemic gave birth to most of the subsequent influenza strains, with the exception of avian flu. Fine (1993) states that *"prior to 1977 only a single major [influenza] virus (shift) subtype was found circulating in the human population worldwide at any time"*.

Figure 2: Evolution of the death rate caused by influenza and influenza and pneumonia

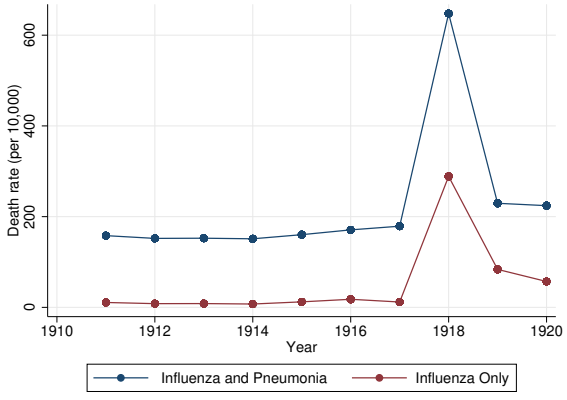

Author's computation from Bureau of the Census, Mortality Statistics 21st Annual Report published in 1920.
Average death rate computed for a sample of 43 cities: Albany, Baltimore, Birmingham, Boston, Buffalo, Cambridge, Chicago, Cincinnati, Cleveland, Columbus, Dayton, Denver, Fall River, Grand Rapids, Indianapolis, Kansas City, Los Angeles, Louisville, Lowell, Milkwaukee, Minneapolis, Nashville, New Haven, New Orleans, New York, Newark, Oakland, Omaha, Philadelphia, Pittsburgh, Portland, Providence, Richmond, Rochester, Saint Louis, Saint Paul, San Fransisco, Seattle, Spokane, Syracuse, Toledo, Washington, Worcester.

The Federal Government did not coordinate a national response (Correia, Luck, and Verner 2020) leaving cities to manage the pandemic by

Covid Economics 18, 15 May 2020: 109-156

Covid Economics 18, 15 May 2020: 109-156

implementing local measures. The timing of the response appears to be correlated with the geographical longitude suggesting that cities located in the West had more time to prepare using the experience of cities in the East that had been more rapidly overwhelmed. Indeed Markel et al. (2007) show that the pandemic waves started in the East during the second week of September 1918, in the Midwest in the last week of September and in the West in the second week of October. They show that all cities they investigated implemented some kind of NPI, such as quarantines, social distancing and school closures, but that some were stricter and faster to take action than others. Their data also documents some heterogeneity in the responses within each region. For example, New York responded rapidly to the pandemic and managed to flatten the epidemic curve implementing strictly enforced isolation and quarantine procedures. According to Markel et al. (2007) this allowed the city to experience the lowest death rate on the East Coast. On the other hand, Pittsburgh only took action on the beginning of October and closed schools at the end of the month. This resulted in the highest excess mortality burden in the sample studied.

2.2 Economic and health consequences of the 1918 pandemic

This paper is intended as a contribution to the economic literature and engages with the epidemiological literature as I study the impact of NPIs implemented in 1918 on health and economic outcomes. I try to extend the epidemiological literature documenting the impact of Non Pharmaceutical Policies (NPIs) as Markel et al. (2007), Bootsma and Ferguson (2007), and Hatchett, Mecher, and Lipsitch (2007) which was carefully reviewed in Aiello et al. (2010) using an econometric approach. My results confirm their estimated impact of the short run consequences of NPIs (i.e during the pandemic) and supplement their results by documenting the medium run impact of the policies once the main wave is over. My findings are in line with the literature on herd immunity (Fine 1993; Fine, Eames, and Heymann 2011) as I document a trade-off between short run benefits of NPIs and their medium run consequences. I show that cities that implemented NPIs incurred higher death rates in the following years. This paper also contribute to the literature documenting the evolution of mortality rates differential in US cities as Feigenbaum, Muller, and Wrigley-Field (2019), Clay, Lewis, and Severnini (2019), and Acuna-Soto, Viboud, and Chowell (2011).

I also contribute to the literature documenting the economic impact of pandemics. For example, Meltzer, Cox, and Fukuda (1999) estimated in 1999 the potential economic impact of the next pandemic without economic

Covid Economics 18, 15 May 2020: 109-156

disruption and analyzed the benefits of developing vaccines to prevent it. Smith et al. (2009) developed a general equilibrium model to measure the potential impact of a pandemic on the UK economy under different scenarios. The Covid-19 pandemic has also given rise to a wide range of estimates of its potential economic impact as Atkeson (2020), Kong and Prinz (2020), Takahashi and Yamada (2020), Barrot, Grassi, and Sauvagnat (2020), and Chen, Qian, and Wen (2020). This research is more precisely related to the literature that documented the impact of past pandemics and in particular the 1918 pandemic. Barro, Ursúa, and Weng (2020) used a panel of countries and estimate that the flu had negative impacts on GDP and consumption, estimated to be around 6 and 8 percent, respectively. The macroeconomic impact of the pandemic is also investigated in Lin and Meissner (2020) and Aassve et al. (2020) investigates the impact of this pandemic on trust. Dahl, Hansen Worm, and Sandholt Jensen (2020) and Carrillo and Jappelli (2020) investigate the impact of the 1918 pandemic on local growth in Denmark and Italy respectively. Velde (2020) study the short run dynamics of the US economy during the pandemic. I discuss more extensively the recent work of Correia, Luck, and Verner (2020) who document what kind of economic impact one can expect from nonpharmaceutical interventions and influenza pandemic on cities' manufacturing and banking sectors. My results argue for caution regarding any inferred causal links between economic activity and the mortality caused by the pandemic in US cities. I find that on the medium run, NPIs seem to have decreased the immunity of the population leaving individuals more sensitive to the following waves of the pandemic and strains of influenza. My findings can also contribute to the economic literature investigating the optimal policy responses to pandemics, e.g. Alvarez, Argente, and Lippi (2020), Jones, Philippon, and Venkateswaran (2020), and Toda (2020), as they suggest that optimal policy responses should include an exit strategy when implementing NPIs.

3 Data

I construct a panel of 43 cities with precise measures of NPIs in a spirit close to Correia, Luck, and Verner (2020). My data comes from the census bureau archives published online. I digitize the Statistical Abstract of the United States from the Census Bureau to extract information on the number of wage workers, aggregate wages, the total output and the added value for the 43 cities from 1899 to 1923. I end up with a balance panel of 43 cities for the years 1899, 1904, 1909, 1914, 1919 and 1920.
I supplement this dataset with the data compiled by Markel et al. (2007) on NPIs describing the number of days under NPIs and the speed of their

Table 1: Descriptive Statistics for the 43 US Cities

	Mean	Std.Dev.	Obs	min	max
Demographics					
Population (1900)	328018.60	576706.40	43	36800	3437200
Population (1910)	441201.02	776807.64	43	100292	4770082
Population growth (1900-1910)	0.50	0.56	43	0	2
Sex Ratio (men/women) 1910	1.03	0.12	43	1	1
average age (1910)	28.39	1.32	43	25	31
First decile age (1910)	5.09	0.92	43	4	7
Median Age (1910)	26.42	1.56	43	23	30
Ninth decile age (1910)	53.51	1.88	43	49	58
Health					
NPI days (1918)	88.28	46.43	43	28	170
NPI Speed (1918)	-7.35	7.84	43	-35	11
Death Rate (1917)	179.10	61.53	43	59	380
Death Rate (1918)	647.14	187.53	43	283	1244
Health Expenditures per head (1900)	0.19	0.11	43	0	1
Health Expenditures per head (1917)	1.84	0.61	43	1	3
Manufacturing sector					
Wage Workers (1899)	40886.84	70859.04	43	1060	388586
Value Produced (1899)	114844.51	217164.14	43	3756	1172870
Wages (1899)	18792.91	34528.14	43	616	196656

Author's computation from the Bureau of the Census, Mortality Statistics 21st Annual Report published in 1920 ,the US census Statistical Abstract and Manufacture Surveys (1900-1929) . NPI variables are from Markel et al. (2007).
The cities are Albany, Baltimore, Birmingham, Boston, Buffalo, Cambridge, Chicago, Cincinnati, Cleveland, Columbus, Dayton, Denver, Fall River, Grand Rapid, Indianapolis, Kansas City, Los Angeles, Louisville, Lowell, Milwaukee, Minneapolis, Nashville, New Haven, New Orleans, New York, Newark, Oakland, Omaha, Philadelphia, Pittsburgh, Portland, Providence, Richmond, Rochester, Saint Louis, Saint Paul, San Francisco, Seattle, Spokane, Syracuse, Toledo, Washington, Worcester.

implementation after the first case was reported in the city. I also use the mortality tables for large cities published by the Census Bureau from 1906 to 1924.
Finally, I use the exhaustive census for the years 1900, 1910, 1920 and 1930 downloaded on the IPUMS website and compiled by Ruggles et al. (2020). The main variables used are summarized in Table 1.

Covid Economics 18, 15 May 2020: 109-156

4 The impact of NPIs on the mortality rate in the medium run

4.1 Empirical specification

Epidemiological studies investigate how Non Pharmaceutical Interventions allow to flatten the epidemic curve by examining high frequency (weekly) data (Markel et al. 2007; Bootsma and Ferguson 2007). I follow a different approach in order to study their impact in the medium run. This is performed by an event study following a growing econometric literature (Duflo 2001; Autor 2003; De Chaisemartin and d'Haultfoeuille 2018; Fetzer 2019) to investigate the impact of NPIs on the death rate at the city level:

$$Deathrate_{i,t} = \delta_i + \gamma_t + \sum_{t \neq 1916} \beta^t \times 1_{t(i)=t} \times NPI_{1918,i} + \sum_{t \neq 1916} \lambda^t \times 1_{t(i)=t} \times X_i + \epsilon_{i,t} \quad (1)$$

where I use three different death rates : total death rate, death rate for influenza and pneumonia (used in Bootsma and Ferguson (2007), Markel et al. (2007), and Correia, Luck, and Verner (2020)) and death rate for influenza only. X_i controls for the population in 1910 and health expenditures per capital in 1917. There are two NPI terms reported in Markel et al. (2007). The first term, NPI Speed, measures the rapidity of the response after the first case was discovered in the city, and the second term, NPI Days, measures the duration that NPIs such as social distancing and school closures were implemented. β^t is used to describe if cities that responded more aggressively to the pandemic had different trends from 1911 to 1920.

To compute the net effect, I also estimate a simpler difference-in-differences specification:

$$Deathrate_{i,t} = \delta_i + \gamma_t + \beta \times Post \times NPI_{1918,i} + \sum_{t \neq 1916} \lambda^t \times 1_{t(i)=t} \times X_i + \epsilon_{i,t} \quad (2)$$

where $Post$ takes value one when the year is higher than 1917.β is used to measure the net impact of NPIs implemented in 1918 from year 1918 until the end of the observations (up to 1924 for the long run specifications). Both equations are estimated by ordinary least squares and standard errors are clustered at the city level.

4.2 Results of the event study

Figures 3 and 4 display the estimates of β^t. One can observe that the common trend assumption is fulfilled before the 1918 pandemic and that high

and low NPIs cities had similar mortality trends.These policies reduced the mortality rate in 1918, this is consistent with Markel et al. (2007). However, one also observes a significant rebound of mortality in these cities in 1919 and 1920. This tends to suggest that the herd immunity of the population is lower and that more people die from influenza and pneumonia in the two subsequent years than would have been the case with less aggressive NPIs. We observe the same patterns for the two measures of NPI policies with one difference that argues for the herd immunity interpretation. In 1919 and 1920, cities that implemented long NPIs experienced a dramatic increase in their death rate; while this is not so important when they responded rapidly after the first case appeared. This suggests that the longer people were isolated from the virus in 1918, the lower the herd immunity and the higher the death rate the next years. The figures for "death caused by influenza" could be recovered until 1920 but the series for the total death rate and deaths caused by pneumonia and influenza are available through 1924. I provide additional evidence in Figure B.1 and B.2 of the appendix that the total death rate appears to be higher through 1924 in cities that implemented long NPIs in 1918. It is possible that the impact of the influenza may be reflected more in the total death rate if those who die from influenza have other co morbidity factors.

These findings appear to be consistent with the literature on herd immunity. They suggest that the 1918 pandemic acted as a vaccine for the subsequent years in cities that did not implement NPIs. Indeed, Fine, Eames, and Heymann (2011) reported that *"one proposal has been to reduce community spread of [influenza] by concentrating on vaccination of schoolchildren, as transmission within crowded classrooms leads to rapid dispersal throughout the community, and into the homes where susceptible adults reside"*. As a consequence one might think that NPIs as school closures limited the spread of the virus during the pandemic but failed to raise the level of immunity within the city, making the population more susceptible. The impact of the length of NPIs appears to support this interpretation: the longer children stayed at home, the lower their exposure to the influenza and the subsequent immunity of the population.

Covid Economics 18, 15 May 2020: 109-156

Covid Economics 18, 15 May 2020: 109-156

Figure 3: Event study: Estimates of the aggregate impact of NPI implementation speed on death rates

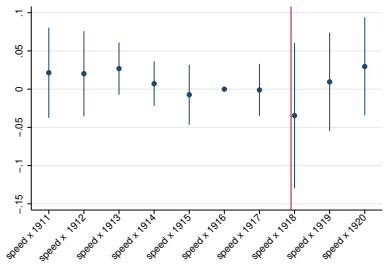

(a) All causes of death

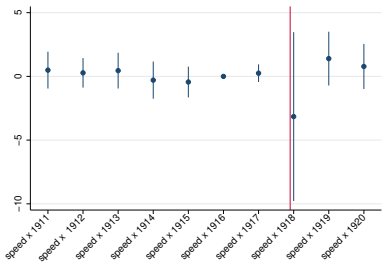

(b) Influenza and Pneumonia

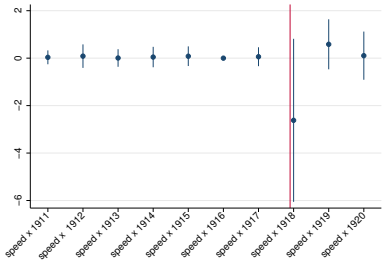

(c) Influenza Only

Reading notes: Cities having adopted more rapidly NPIs saw their death rates increase less than cities that were slower in 1918. On the other hand the death rate was relatively higher in 1919 and 1920 for these cities

Estimates of the difference in difference equation:

$Deathrate_{i,t} = \delta_i + \gamma_t + \sum_{t \neq 1916} \beta^t \times 1_{t(i)=t} \times NPI_{1918,i} + \sum_{t \neq 1916} \lambda^t \times 1_{t(i)=t} \times X_i + \epsilon_{i,t}$

Controls include health expenditures in 1917, population in 1910, years and city fixed effects

95% confidence Interval clustered at the city level

Covid Economics 18, 15 May 2020: 109-156

Figure 4: Event study: Estimates of the aggregate impact of NPI implementation duration on death rates

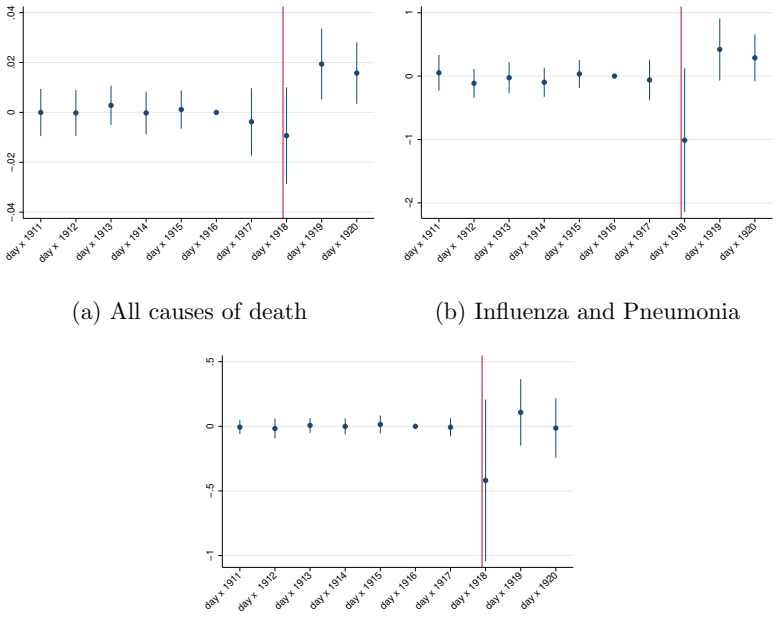

(a) All causes of death

(b) Influenza and Pneumonia

(c) Influenza Only

Reading notes: Cities that implemented NPIs for a longer time saw their death rates increase less than cities that had shorter NPIs in 1918. On the other hand the death rate was relatively higher in 1919 and 1920 for these cities

Estimates of the difference in difference equation:

$Deathrate_{i,t} = \delta_i + \gamma_t + \sum_{t \neq 1916} \beta^t \times 1_{t(i)=t} \times NPI_{1918,i} + \sum_{t \neq 1916} \lambda^t \times 1_{t(i)=t} \times X_i + \epsilon_{i,t}$

Controls include health expenditures in 1917, population in 1910, years and cities' fixed effects

95% confidence interval clustered at the city level

Covid Economics 18, 15 May 2020: 109-156

4.3 Robustness checks

I perform several robustness checks to verify the underlying hypothesis, to investigate the longer run impact of NPIs, and to control for the influence of the demographic structure of cities before and after the pandemic.

Additional tests of the common trend assumption. I gathered longer time series for the total death rate from 1906. Specific death rates for influenza alone or for influenza and pneumonia were not published in the sources that I consulted. Results remain unchanged as cities with a high and low level of NPIs in 1918 had common trends from 1906 as illustrated in Figure B.3 in the Appendix. I also extend the series for influenza and pneumonia and for the total death rate until 1924 in Figure B.1 and B.2. The results show that the length of NPIs still had a significant impact through 1924 while the impact of the speed of their implementation faded rapidly after 1919.

Cities' weights and differentiated trends between the East and the West. The observations are weighted according to their population in 1910. This does not affect the estimated trends. Moreover, as discussed in Correia, Luck, and Verner (2020) the pandemic spread from the East to the West, giving the West more time to adjust. One potential confounding factor could be that cities on the West Coast started to behave differently from the East Coast after the First World War due to some regional shocks. I control for this eventuality adding regional shocks, i.e., interacting years fixed effects with a fixed effect to indicate to which of the four regions the city belongs (West, South West, East, Midwest), results remain unchanged as illustrated in Figures C.3 and B.4 in the appendix.

Changing demographic structure. An alternate explanation would be that cities with an aggressive policy may undergone different demographic changes that could explain their divergence in terms of mortality after 1918. Appendix D compares the demographic structure of these cities (population, population growth, sex ratio, average age, age distribution, share of each cohort and age groups) in each census year. It is noteworthy that cities that implemented longer and earlier NPIs were younger, had higher population growth rates and had proportionally more males; these demographic trends continued unchanged after 1918. This reflects the fact that these cities tend to be located on the West Coast. If controlling for regional shocks might absorb these differences, I follow the epidemiological literature as Markel et al. (2007) and also control explicitly for the difference in sex ratio, median age and population growth in 1910, before the pan-

demic, or in 1920, immediately following the pandemic; in all such cases, the results remain unaffected, as illustrated in Figures B.6 and B.7.

4.4 Short run and long run impact of NPIs

In order to get an idea of the net benefits of NPIs, I run a difference in differences specification. The first one displayed in Table 2 only accounts for the year 1918 to estimate the short run impact of NPI, i.e. during their implementation. Columns (1) to (4) do not control for any characteristics beyond year and cities' fixed effects. Columns (5) to (8) also control for health expenditures per capita before the pandemic and city size. The inclusion of controls does not change the point estimate but makes it less precise and not significant. Columns (3), (4), (7) and (8) weight the observations by their population in 1910. Several comments are in order. First, speed appear to be more efficient than the duration of NPIs as the coefficient of the number of days is never statistically significant. Rapid implementation reduced the total death rate by 1.3 per 10,000 population, the death rate for pneumonia and influenza by 7 per 10,000 and the death rate for influenza only by 3 per 10,000. Note that the figures for the net number of lives saved by NPIs vary depending on the rate used. Their estimated impact is higher on the death rate caused by Influenza and Pneumonia than on the total death rate, suggesting that a portion of those saved from influenza by NPIs could have died from other diseases. Another interpretation could be that cities that implemented NPIs attributed a lower share of their deaths to influenza while the other cities tended to assign more deaths in 1918 to the ongoing pandemic.

In Table 3, I run the same specifications but including the year 1919 and 1920. One can observe that the point estimates are divided by two or three and are less significant. Rapid implementation of NPIs reduced the total death rate by 0.06 per 1,000 population, the death rate for pneumonia and influenza by 4 per 10,000 and the death rate for influenza only by 1.1 per 10,000. The impact of the number of days under NPIs is never significant. This suggests that a portion of the people saved by NPIs in 1918 were lost during the following two years.

Finally, Table 4 presents the estimates extending the series through 1924. Data for deaths caused by influenza alone were not available. The impact of speed remains significant in one specification but is even smaller. More interestingly, the impact of the length of the NPIs on the total death rate now turns positive and statistically significant in most of the specifications. This suggests that cities that implemented long periods of NPIs ultimately lost more people, increasing their death rate by 1.2 per 10,000. One potential interpretation of the finding could be that NPIs should not last too long and that their exit strategy should include specific policies to avoid

Covid Economics 18, 15 May 2020: 109-156

that having a lower herd immunity lead to higher death rates in the subsequent years.

Table 2: Short Run Impact of NPIs (1911-1918)

	(1)	(2)	(3)	(4)	(5)	(6)	(7)	(8)
Panel a) Dependant variable: Death rate for all causes (per 1,000)								
speed NPI x Post	-0.0570		-0.132***		-0.0627		-0.167*	
	(0.0388)		(0.0339)		(0.0427)		(0.0785)	
days NPI x Post		-0.00982		-0.0149		-0.00935		-0.0231
		(0.00683)		(0.0108)		(0.00766)		(0.0126)
N	343	343	343	343	343	343	343	343
R^2	0.915	0.915	0.908	0.888	0.915	0.915	0.910	0.902
Panel b) Dependant variable: Death rate for Influenza and pneumonia (per 10,000)								
speed NPI x Post	-1.829		-7.405**		-2.852		-11.49	
	(2.894)		(2.593)		(3.240)		(6.273)	
days NPI x Post		-0.867		-1.328		-0.958		-1.899*
		(0.549)		(0.784)		(0.557)		(0.934)
N	343	343	343	343	343	343	343	343
R^2	0.894	0.899	0.906	0.897	0.896	0.900	0.910	0.906
Panel b) Dependant variable: Death rate for Influenza only (per 10,000)								
speed NPI x Post	-2.455		-2.695*		-2.691		-4.475	
	(1.487)		(1.086)		(1.722)		(2.428)	
days NPI x Post		-0.306		-0.305		-0.416		-0.557
		(0.280)		(0.353)		(0.308)		(0.421)
N	343	343	343	343	343	343	343	343
R^2	0.922	0.921	0.945	0.938	0.924	0.923	0.948	0.943
Controls								
City FE	Y	Y	Y	Y	Y	Y	Y	Y
Year FE	Y	Y	Y	Y	Y	Y	Y	Y
Controls x Years FE	N	N	N	N	Y	Y	Y	Y
Weights	N	N	Y	Y	N	N	Y	Y

Clustered Standard errors in parentheses

* $p < 0.05$, ** $p < 0.01$, *** $p < 0.001$

Post is a dummy indicating observations after 1917 while speed NPI indicates the speed at which the city implemented their NPI. Days NPI describes the length the NPI measures were in place.

Estimates of the difference in difference equation:

$Deathrate_{i,t} = \delta_i + \gamma_t + \beta \times Post \times NPI_{1918,i} + \sum_{t \neq 1916} \lambda^t \times 1_{t(i)=t} \times X_i + \epsilon_{i,t}$

Controls include health expenditures in 1917, population in 1910, years and city fixed effects standard errors clustered at the city level. Cities are weighted with their population in 1910

Covid Economics 18, 15 May 2020: 109-156

Covid Economics 18, 15 May 2020: 109-156

Table 3: Medium Run Impact of NPIs (1911-1920)

	(1)	(2)	(3)	(4)	(5)	(6)	(7)	(8)
Panel a) Dependant variable: Death rate for all causes (per 1,000)								
speed NPI x Post	-0.0240		-0.0655***		-0.0284		-0.0569*	
	(0.0176)		(0.0114)		(0.0196)		(0.0217)	
days NPI x Post		0.00906*		0.00585		0.00846*		0.00151
		(0.00407)		(0.00552)		(0.00410)		(0.00535)
N	429	429	429	429	429	429	429	429
R^2	0.881	0.884	0.882	0.871	0.882	0.884	0.883	0.879
Panel b) Dependant variable: Death rate for Influenza and pneumonia (per 10,000)								
speed NPI x Post	-0.0163		-2.996**		-0.361		-3.315	
	(1.122)		(0.967)		(1.229)		(2.168)	
days NPI x Post		0.00828		-0.141		-0.0749		-0.448
		(0.237)		(0.326)		(0.242)		(0.357)
N	429	429	429	429	429	429	429	429
R^2	0.880	0.880	0.886	0.879	0.881	0.881	0.887	0.885
Panel b) Dependant variable: Death rate for Influenza only (per 10,000)								
speed NPI x Post	-0.604		-1.104**		-0.716		-1.256	
	(0.636)		(0.326)		(0.688)		(0.668)	
days NPI x Post		-0.0201		0.0311		-0.106		-0.103
		(0.133)		(0.149)		(0.136)		(0.149)
N	429	429	429	429	429	429	429	429
R^2	0.905	0.905	0.925	0.922	0.908	0.908	0.926	0.925
Controls								
City FE	Y	Y	Y	Y	Y	Y	Y	Y
Year FE	Y	Y	Y	Y	Y	Y	Y	Y
Controls x Years FE	N	N	N	N	Y	Y	Y	Y
Weights	N	N	Y	Y	N	N	Y	Y

Clustered Standard errors in parentheses

* $p < 0.05$, ** $p < 0.01$, *** $p < 0.001$

Post is a dummy indicating observations after 1917 while speed NPI indicates the speed at which the city implemented their NPI. Days NPI describes the length the NPI measures were in place.

Estimates of the difference in difference equation:

$Deathrate_{i,t} = \delta_i + \gamma_t + \beta \times Post \times NPI_{1918,i} + \sum_{t \neq 1916} \lambda^t \times 1_{t(i)=t} \times X_i + \epsilon_{i,t}$

Controls include health expenditures in 1917, population in 1910, years and city fixed effects standard errors clustered at the city level. Cities are weighted with their population in 1910

Covid Economics 18, 15 May 2020: 109-156

Table 4: Long Run Impact of NPIs (1911-1924)

	(1)	(2)	(3)	(4)	(5)	(6)	(7)	(8)
Panel a) Dependant variable: Death rate for all causes (per 1,000)								
speed NPI x Post	-0.0136		-0.0535***		-0.0140		-0.0268	
	(0.0256)		(0.00928)		(0.0261)		(0.0183)	
days NPI x Post		0.0143**		0.0123**		0.0128**		0.00813
		(0.00417)		(0.00456)		(0.00435)		(0.00415)
N	597	597	597	597	597	597	597	597
R^2	0.863	0.875	0.888	0.885	0.868	0.876	0.892	0.893
Panel b) Dependant variable: Death rate for Influenza and pneumonia (per 10,000)								
speed NPI x Post	0.0976		-2.131***		0.00578		-1.551	
	(0.652)		(0.565)		(0.620)		(1.112)	
days NPI x Post		0.180		0.143		0.0925		-0.123
		(0.132)		(0.195)		(0.127)		(0.197)
N	597	597	597	597	597	597	597	597
R^2	0.880	0.881	0.891	0.886	0.882	0.883	0.893	0.892
Controls								
City FE	Y	Y	Y	Y	Y	Y	Y	Y
Year FE	Y	Y	Y	Y	Y	Y	Y	Y
Controls x Years FE	N	N	N	N	Y	Y	Y	Y
Weights	N	N	Y	Y	N	N	Y	Y

Clustered Standard errors in parentheses

* $p < 0.05$, ** $p < 0.01$, *** $p < 0.001$

Post is a dummy indicating observations after 1917 while speed NPI indicates the speed at which the city implemented their NPI. Days NPI describes the length the NPI measures were in place.

Estimates of the difference in difference equation:

$Deathrate_{i,t} = \delta_i + \gamma_t + \beta \times Post \times NPI_{1918,i} + \sum_{t \neq 1916} \lambda^t \times 1_{t(i)=t} \times X_i + \epsilon_{i,t}$

Controls include health expenditures in 1917, population in 1910, years and city fixed effects standard errors clustered at the city level. Cities are weighted with their population in 1910

Covid Economics 18, 15 May 2020: 109-156

5 The impact of NPIs on city growth and demographics

One key measure of a city's dynamics is its demographic population growth, especially during a period of industrialization. It could thus be interesting to investigate the impact of NPIs on population growth in particular in the light of the higher death rates in the following decade. Moreover, the 1918 pandemic had an unusual characteristic in that, unlike earlier and later episodes of influenza, its death rate was particularly high for young workers aged between 24 and 35 years, as stressed in Taubenberger and Morens (2006) and illustrated in Figure 5. One can try to detect whether NPIs managed to preserve this demographic group and city's growth. An event study is conducted using the 1900 to 1930 censuses to document the relative demographic dynamics of cities that implemented NPIs.

Figure 5: Death rate from Influenza and Pneumonia in 1917 and 1918

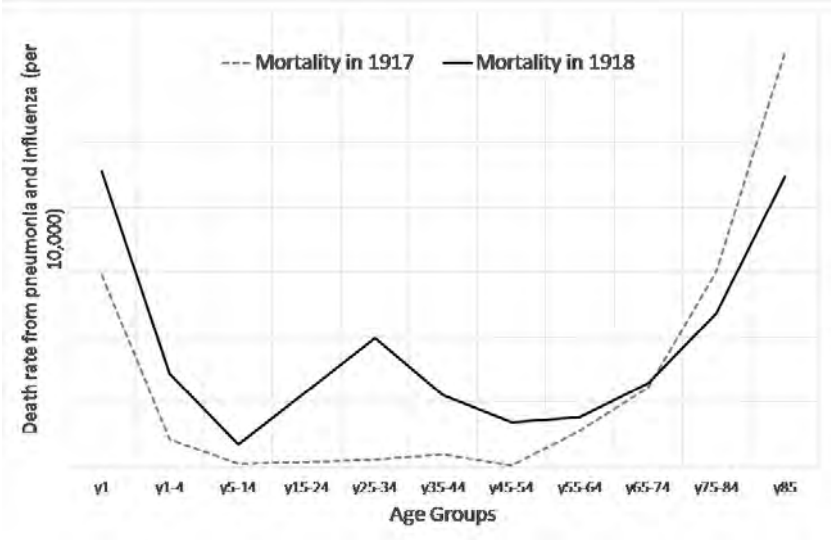

Source: Bureau of the Census, Mortality Statistics 21st Annual Report published in 1920

5.1 Empirical Specification

I conducted an event study in a spirit close to Correia, Luck, and Verner (2020) to investigate the impact of NPIs on a city's growth and the relative share of the cohort age 24 to 35 years in 1918 accounting for the different

levels of fatality rates in the first year of the pandemic.

$$y_{i,t} = \delta_i + \gamma_t + \sum_{t \neq 1910} \beta_1^t \times 1_{t(i)=t} \times Mortality_{1918,i} + \sum_{t \neq 1910} \beta_2^t \times 1_{t(i)=t} \times NPI_{1910,i} + \sum_{t \neq 1910} \lambda^t \times 1_{t(i)=t} \times X_i + \epsilon_{i,t} \quad (3)$$

where $y_{i,t}$ is the population growth rate of cities between year t and t-10 or the share of the cohort aged between 25 and 34 in the first year of the pandemic. β_1^t will estimate the differentiated trend between cities with high or low mortality in 1918. β_2^t will estimate the differentiated trends for cities with different levels of NPIs. X_i controls for the log population in 1900, the amount of health expenditures per capita in 1917 and regional shocks. Standard errors are clustered at the city level.

5.2 Results of the event study

Figure 6 displays the coefficients β_2. β_1s are reported in Figure B.8 in appendix. None is statistically significant at the standard levels. Cities that implemented NPIs appear to have had a slightly higher relative growth rate between 1900 and 1910 and, if anything, lower relative growth rates between 1910 and 1920 and between 1920 and 1930 as illustrated in panels a) and b). Moreover, there is no significant difference regarding the share of the birth cohort mostly affected by the 1918 pandemic.
These results are not so surprising in light of the limited impact of NPIs on mortality when one remembers that cities in the 1920s and 1930s experienced extremely large growth rates because of a massive rural exodus[2] and very high migration flows (with the exception of the period of the First World War) at least until the Immigration Act of 1924 that restricted immigrants from Southern and Eastern Europe. These massive flows of population may have soon erased the demographic impact of the 1918 pandemic on urban population even in the cities most affected. This is evident from the coefficients β_1 on mortality that are never significant as reported in Figure B.8 in the appendix.

On the other hand, given that population growth is usually a measure of cities' attractiveness and economic performance following the seminal

2. By 1890, twenty-eight percent of Americans lived in urban areas, and by 1920 more Americans lived in towns and cities than in rural areas (Kennedy and Cohen 2015)

Covid Economics 18, 15 May 2020: 109-156

Rosen and Roback model, these results seem at odds with the results provided in Correia, Luck, and Verner (2020). Appendix C extends their series at the city level back to 1899 and explores this issue in details. In a nutshell, their results at the city level might be driven by the fact that cities that implemented faster NPIs and that had lower mortality in 1918 had a different growth rate of their manufacturing sector and maintained that trend after the 1918 pandemic. Nevertheless, it should be noted that our main conclusion on the impact of NPIs on the economy is in line with their findings as Correia, Luck, and Verner (2020) argue that NPIs did not depress the local economy, which is also the result of Figure 6. It is possible that macroeconomic mechanisms still affected the performance of the national economy while leaving the relative growth of cities unaffected as suggested by the state level results in Correia, Luck, and Verner (2020) or the cross country evidence provided in Barro, Ursúa, and Weng (2020).

Covid Economics 18, 15 May 2020: 109-156

Figure 6: Event study: Estimates of the aggregate impact of NPI implementation duration on city population growth and the share of the cohort age 25 to 34 in 1918

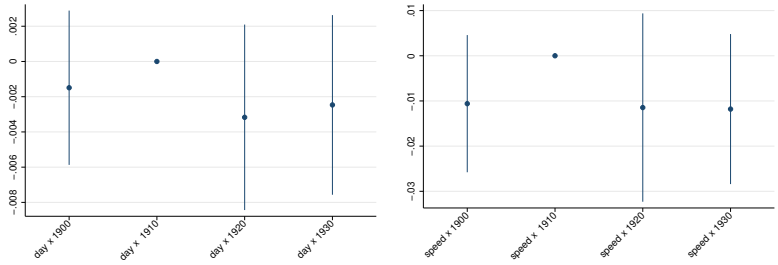

(a) Impact of NPI duration on population growth between year t and t-10

(b) Impact of NPI speed on population growth between year t and t-10

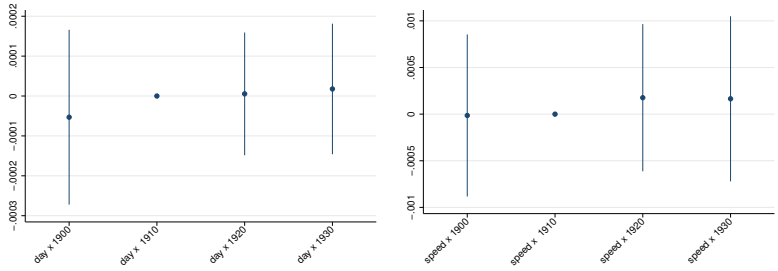

(c) Impact of NPI length on the cohort age 24 to 35 in 1918

(d) Impact of NPI speed on the cohort age 24 to 35 in 1918

Reading notes: Cities that implemented NPIs for a longer time or faster in 1918 were not found to have any specific population growth or change in the share of the cohort who was 25 to 34 1918.

Estimates of the difference in difference equation:

$y_{i,t} = \delta_i + \gamma_t + \sum_{t \neq 1910} \beta_1^t \times 1_{t(i)=t} \times Mortality_{1918,i} + \sum_{t \neq 1910} \beta_2^t \times 1_{t(i)=t} \times NPI_{1910,i} + \sum_{t \neq 1910} \lambda^t \times 1_{t(i)=t} \times X_i + \epsilon_{i,t}$

Controls include health expenditures in 1917, regional shocks, years and cities' fixed effects

95% confidence interval clustered at the city level

6 Conclusion

In this paper, I investigate the 1918 pandemic in the US to assess the potential economic and health benefits of non pharmaceutical interventions (NPIs) at the city level. My findings can be summarized as follows: first, in the medium run, I estimate that a significant share of the lives saved dur-

ing the pandemic might be lost during the subsequent years. A potential explanation of this could be that herd immunity becomes lower in cities that implemented NPIs over a long period of time. Second, I do not find any significant impact of these policies on city growth. These findings do not deny the short run benefits of these policies that lower the death rate during the peak of the pandemic and prevent overcrowding of the health system (Markel et al. 2007). However, policy makers should prepare exit strategies to prevent NPIs from leading to higher deaths when they end.

The last word is a word of caution. As any study based on an historical natural experiment, this paper has limited external validity and thus applicability to current public health policies. It would be difficult to draw any inference regarding the predicted impact of NPIs as implemented during the Covid-19 crisis, not least because their magnitude and scale are different. Today NPIs are mainly implemented on a national (or state) scale, rather than at the city level. Moreover, pharmaceutical technologies were less developed than today, and the capacity to produce a new vaccine within a reasonable time was much lower(Ni et al. 2020; Callaway 2020). Finally, the 1918 pandemic was an unprecedented event in the history of health provided that it gave birth to most strains of seasonal influenza until 1977 and which continue to kill up to 650,000 people yearly worldwide (World Health Organization 2007; Paget et al. 2019).

References

Aassve, Arnstein, Guido Alfani, Francesco Gandolfi, and Marco Le Moglie. 2020. "Epidemics and trust: the case of the spanish flu." *IGIER Working Paper,* no. 661.

Acuna-Soto, Rodolfo, Cecile Viboud, and Gerardo Chowell. 2011. "Influenza and pneumonia mortality in 66 large cities in the United States in years surrounding the 1918 pandemic." *PLoS One* 6 (8).

Agnew, LR. 1965. *Dorland's illustrated medical dictionary.* Saunders.

Aiello, Allison E, Rebecca M Coulborn, Tomas J Aragon, Michael G Baker, Barri B Burrus, Benjamin J Cowling, Alasdair Duncan, Wayne Enanoria, M Patricia Fabian, Yu-hui Ferng, et al. 2010. "Research findings from nonpharmaceutical intervention studies for pandemic influenza

Covid Economics 18, 15 May 2020: 109-156

and current gaps in the research." *American journal of infection control* 38 (4): 251–258.

Almond, Douglas. 2006. "Is the 1918 influenza pandemic over? Long-term effects of in utero influenza exposure in the post-1940 US population." *Journal of political Economy* 114 (4): 672–712.

Alvarez, Fernando E, David Argente, and Francesco Lippi. 2020. "A simple planning problem for covid-19 lockdown." *Covid Economics,* no. 14.

Atkeson, Andrew. 2020. *What will be the economic impact of COVID-19 in the US? Rough estimates of disease scenarios.* Technical report. National Bureau of Economic Research.

Autor, David H. 2003. "Outsourcing at will: The contribution of unjust dismissal doctrine to the growth of employment outsourcing." *Journal of labor economics* 21 (1): 1–42.

Barro, Robert J, José F Ursúa, and Joanna Weng. 2020. *The coronavirus and the great influenza pandemic: Lessons from the "spanish flu" for the coronavirus's potential effects on mortality and economic activity.* Technical report. National Bureau of Economic Research.

Barrot, Jean-Noel, Basile Grassi, and Julien Sauvagnat. 2020. "Sectoral effects of social distancing." *Covid Economics,* no. 3.

Bootsma, Martin CJ, and Neil M Ferguson. 2007. "The effect of public health measures on the 1918 influenza pandemic in US cities." *Proceedings of the National Academy of Sciences* 104 (18): 7588–7593.

Callaway, E. 2020. "The race for coronavirus vaccines: a graphical guide." *Nature* 580 (7805): 576.

Carrillo, Mario, and Tullio Jappelli. 2020. "Pandemic and Local Economic Growth: Evidence from the Great Influenza in Italy." *Covid-Economics,* no. 10.

Chapelle, Guillaume. April 2020. *The Medium Run impact of Non Pharmaceutical Interventions. Evidence from the 1918 Influenza in US cities.* Technical report.

Covid Economics 18, 15 May 2020: 109-156

Chen, Haiqiang, Wenlan Qian, and Qiang Wen. 2020. "The impact of the COVID-19 pandemic on consumption: Learning from high frequency transaction data." *Available at SSRN 3568574*.

Clay, Karen, Joshua Lewis, and Edson Severnini. 2019. "What explains cross-city variation in mortality during the 1918 influenza pandemic? Evidence from 438 US cities." *Economics & Human Biology* 35:42–50.

Correia, Sergio, Stephan Luck, and Emil Verner. 2020. "Pandemics Depress the Economy, Public Health Interventions Do Not: Evidence from the 1918 Flu."

Dahl, Christian Moller, Casper Hansen Worm, and Peter Sandholt Jensen. 2020. "The 1918 Epidemic and a V-shaped Recession: Evidence from Municipal Income Data." *Covid economics,* no. 6.

De Chaisemartin, Clément, and Xavier d'Haultfoeuille. 2018. "Fuzzy differences-in-differences." *The Review of Economic Studies* 85 (2): 999–1028.

Duflo, Esther. 2001. "Schooling and labor market consequences of school construction in Indonesia: Evidence from an unusual policy experiment." *American economic review* 91 (4): 795–813.

Feigenbaum, James J, Christopher Muller, and Elizabeth Wrigley-Field. 2019. "Regional and Racial Inequality in Infectious Disease Mortality in US Cities, 1900–1948." *Demography* 56 (4): 1371–1388.

Fetzer, Thiemo. 2019. "Did austerity cause Brexit?" *American Economic Review* 109 (11): 3849–86.

Fine, Paul EM. 1982. "Herd immunity." In *Influenza Models: Prospects for Development and Use,* edited by Philip Selby, 189–194. Lancaster, England: MTP Press Ltd.

———. 1993. "Herd immunity: history, theory, practice." *Epidemiologic reviews* 15 (2): 265–302.

Fine, Paul, Ken Eames, and David L Heymann. 2011. ""Herd immunity": a rough guide." *Clinical infectious diseases* 52 (7): 911–916.

Covid Economics 18, 15 May 2020: 109-156

Fox, John P, Lila Elveback, William Scott, LAEL GATEWOOD, and Eugene Ackerman. 1971. "Herd immunity: basic concept and relevance to public health immunization practices." *American Journal of Epidemiology* 94 (3): 179–189.

Garrett, Thomas A. 2007. "Economic effects of the 1918 influenza pandemic."

Hatchett, Richard J, Carter E Mecher, and Marc Lipsitch. 2007. "Public health interventions and epidemic intensity during the 1918 influenza pandemic." *Proceedings of the National Academy of Sciences* 104 (18): 7582–7587.

Jones, Callum J, Thomas Philippon, and Venky Venkateswaran. 2020. "Optimal Mitigation Policies in a Pandemic: Social Distancing and Working from Home." *Covid Economics,* no. 4.

Kennedy, David M, and Lizabeth Cohen. 2015. *American pageant.* Cengage Learning.

Kong, Edward, and Daniel Prinz. 2020. "The Impact of Non-Pharmaceutical Interventions on Unemployment During a Pandemic." *Available at SSRN 3581254.*

Lilley, Andrew, Matthew Lilley, and Gianlucca Rinaldi. May 2020. *Public Health Interventions and Economic growth: revisiting the Spanish Flu Evidence.* Technical report.

Lin, Zhixian, and Christopher M Meissner. 2020. "A Note on Long-Run Persistence of Public Health Outcomes in Pandemics." *Covid-Economics,* no. 14.

Markel, Howard, Harvey B Lipman, J Alexander Navarro, Alexandra Sloan, Joseph R Michalsen, Alexandra Minna Stern, and Martin S Cetron. 2007. "Nonpharmaceutical interventions implemented by US cities during the 1918-1919 influenza pandemic." *Jama* 298 (6): 644–654.

Meltzer, Martin I, Nancy J Cox, and Keiji Fukuda. 1999. "The economic impact of pandemic influenza in the United States: priorities for intervention." *Emerging infectious diseases* 5 (5): 659.

Covid Economics 18, 15 May 2020: 109-156

Ni, Ling, Fang Ye, Meng-Li Cheng, Yu Feng, Yong-Qiang Deng, Hui Zhao, Peng Wei, et al. 2020. "Detection of SARS-CoV-2-specific humoral and cellular immunity in COVID-19 convalescent individuals." *Immunity*. ISSN: 1074-7613.

Paget, John, Peter Spreeuwenberg, Vivek Charu, Robert J Taylor, A Danielle Iuliano, Joseph Bresee, Lone Simonsen, Cecile Viboud, et al. 2019. "Global mortality associated with seasonal influenza epidemics: New burden estimates and predictors from the GLaMOR Project." *Journal of global health* 9 (2).

Ruggles, Steven, Sarah Flood, Ronald Goeken, Josiah Grover, Erin Meyer, Jose Pacas, and Matthew Sobek. 2020. *IPUMS USA: Version 10.0 [dataset]*. Minneapolis, MN: IPUMS.

Smith, Richard D, Marcus R Keogh-Brown, Tony Barnett, and Joyce Tait. 2009. "The economy-wide impact of pandemic influenza on the UK: a computable general equilibrium modelling experiment." *Bmj* 339:b4571.

St Groth, SF de. 1977. "The control of influenza." *Bulletin der Schweizerischen Akademie der Medizinischen Wissenschaften* 33 (4-6): 201.

Takahashi, Hidenori, and Kazuo Yamada. 2020. "When Japanese Stock Market Meets COVID-19: Impact of Ownership, Trading, ESG, and Liquidity Channels." *mimeo.*

Taubenberger, Jeffery K, and David M Morens. 2006. "1918 Influenza: the mother of all pandemics." *Emerging infectious diseases* 12 (1): 15.

Toda, Alexis Akira. 2020. "Susceptible-infected-recovered (sir) dynamics of covid-19 and economic impact." *arXiv preprint arXiv:2003.11221.*

Velde, Francois R. 2020. "What Happened to the US Economy During the 1918 Influenza Pandemic? A View Through High-Frequency Data."

World Health Organization. 2007. "Up to 650 000 people die of respiratory diseases linked to seasonal flu each year." Accessed April 11, 2020. `https://www.who.int/en/news-room/detail/14-12-2017-up-to-650-000-people-die-of-respiratory-diseases-linked-to-seasonal-flu-each-year`.

Covid Economics 18, 15 May 2020: 109-156

A Additional Series

Figure A.1: Evolution of the death rates by level of NPI in 1918

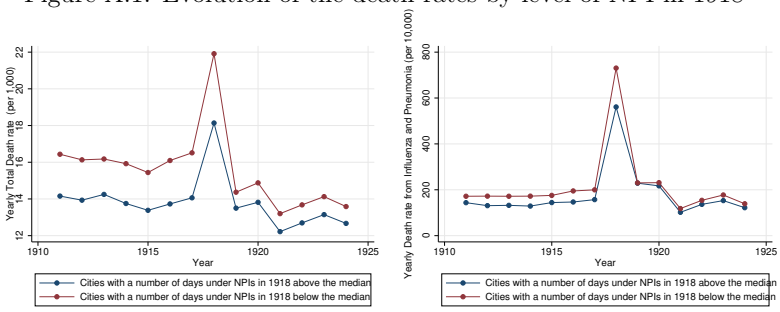

(a) All causes of death

(b) Influenza and Pneumonia

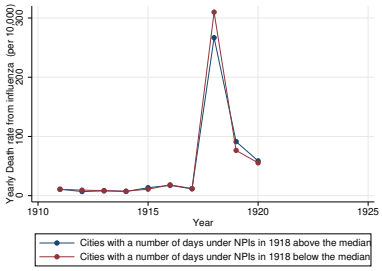

(c) Influenza Only

Reading notes: Cities that implemented NPIs for a longer time saw their death rates increase less than cities that had shorter NPIs in 1918. On the other hand the death rate was relatively higher in the next years for these cities

B Robustness Checks

B.1 Evidence until 1924 and from 1906

Covid Economics 18, 15 May 2020: 109-156

Covid Economics 18, 15 May 2020: 109-156

Figure B.1: Event study: Estimates of the aggregate impact of NPI implementation speed on death rates

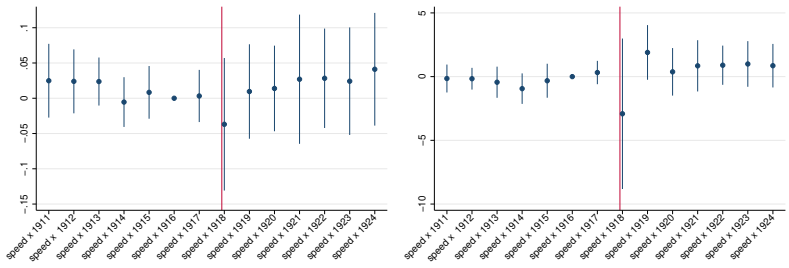

(a) All causes of death (b) Influenza and Pneumonia

Reading notes: Cities having adopted more rapidly NPIs saw their death rates increase less than cities that were slower in 1918. On the other hand the death rate was relatively higher in 1919 and 1920 for these cities

Estimates of the difference in difference equation:

$Deathrate_{i,t} = \delta_i + \gamma_t + \sum_{t \neq 1916} \beta^t \times 1_{t(i)=t} \times NPI_{1918,i} + \sum_{t \neq 1916} \lambda^t \times 1_{t(i)=t} \times X_i + \epsilon_{i,t}$

Controls include health expenditures in 1917, population in 1910, years and city fixed effects

95% confidence Interval clustered at the city level

Figure B.2: Event study: Estimates of the aggregate impact of NPI implementation length on death rates

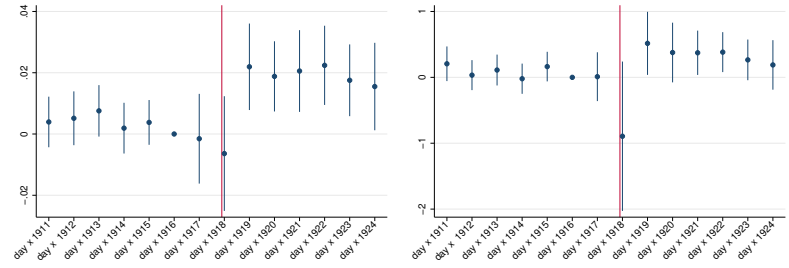

(a) All causes of death (b) Influenza and Pneumonia

Reading notes: Cities that went through long NPIs period saw their death rates increase less than cities that had shorter NPIs in 1918. On the other hand the death rate was relatively higher from 1919 for these cities

Estimates of the difference in difference equation:

$Deathrate_{i,t} = \delta_i + \gamma_t + \sum_{t \neq 1916} \beta^t \times 1_{t(i)=t} \times NPI_{1918,i} + \sum_{t \neq 1916} \lambda^t \times 1_{t(i)=t} \times X_i + \epsilon_{i,t}$

Controls include health expenditures in 1917, population in 1910, years and city fixed effects

95% confidence Interval clustered at the city level

Covid Economics 18, 15 May 2020: 109-156

Figure B.3: Event study: Estimates of the aggregate impact of NPI implementation length on death rates from 1906

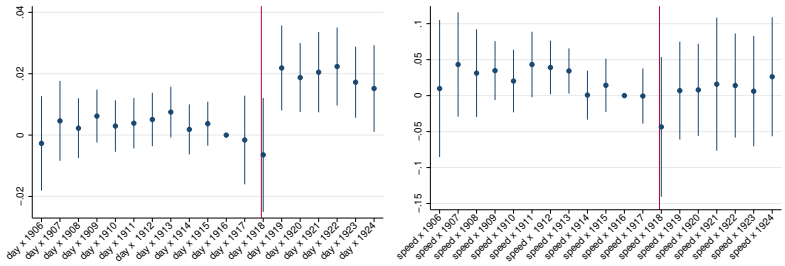

(a) All causes of death, number of days

(b) All causes of death, speed of implementation

Reading notes: Cities that implemented NPIs for a longer time saw their death rates increase less than cities that implemented shorter NPIs in 1918. On the other hand the death rate was relatively higher from 1919 for these cities

Estimates of the difference in difference equation:

$Deathrate_{i,t} = \delta_i + \gamma_t + \sum_{t \neq 1916} \beta^t \times 1_{t(i)=t} \times NPI_{1918,i} + \sum_{t \neq 1916} \lambda^t \times 1_{t(i)=t} \times X_i + \epsilon_{i,t}$

Controls include health expenditures in 1917, population in 1910, years and city fixed effects

95% confidence Interval clustered at the city level

B.2 Weighting the observation by their population and adding regional shocks

Figure B.4: Event study: Estimates of the aggregate impact of NPI implementation speed on death rates

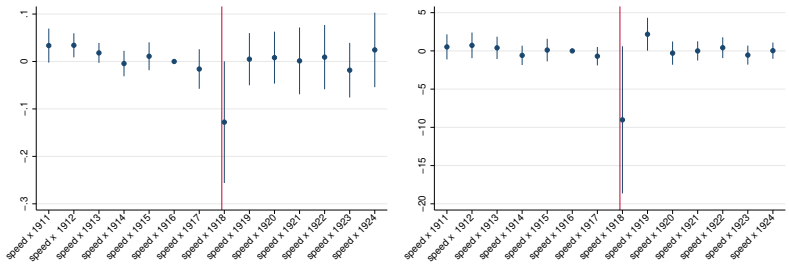

(a) All causes of death (b) Influenza and Pneumonia

Reading notes: Cities having adopted more rapidly NPIs saw their death rates increase less than cities that were slower in 1918. On the other hand the death rate was relatively higher in 1919 and 1920 for these cities

Estimates of the difference in difference equation:

$Deathrate_{i,t} = \delta_i + \gamma_t + \sum_{t \neq 1916} \beta^t \times 1_{t(i)=t} \times NPI_{1918,i} + \sum_{t \neq 1916} \lambda^t \times 1_{t(i)=t} \times X_i + \epsilon_{i,t}$

Controls include health expenditures in 1917, population in 1910, regional shocks, years and city fixed effects

Observations are weighted by their 1910 population

95% confidence Interval clustered at the city level

Covid Economics 18, 15 May 2020: 109-156

Figure B.5: Event study: Estimates of the aggregate impact of NPI implementation length on death rates

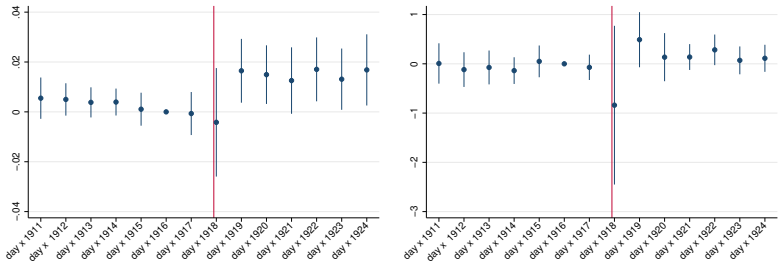

(a) All causes of death (b) Influenza and Pneumonia

Reading notes:Cities that implemented NPIs for a longer time saw their death rates increase less than cities that had shorter NPIs in 1918. On the other hand the death rate was relatively higher in 1919 and 1920 for these cities

Estimates of the difference in difference equation:

$Deathrate_{i,t} = \delta_i + \gamma_t + \sum_{t \neq 1916} \beta^t \times 1_{t(i)=t} \times NPI_{1918,i} + \sum_{t \neq 1916} \lambda^t \times 1_{t(i)=t} \times X_i + \epsilon_{i,t}$

Controls include health expenditures in 1917, population in 1910, regional shocks, years and city fixed effects

Observations are weighted by their 1910 population

95% confidence Interval clustered at the city level

B.3 Controlling for differences in the demographic structures

Covid Economics 18, 15 May 2020: 109-156

Covid Economics 18, 15 May 2020: 109-156

Figure B.6: Event study: Estimates of the aggregate impact of NPI implementation speed on death rates

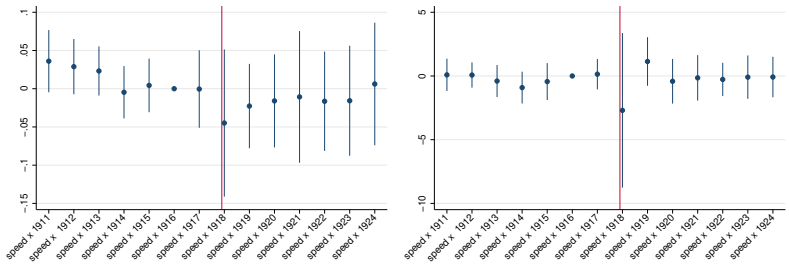

(a) All causes of death

(b) Influenza and Pneumonia

Reading notes: Cities having adopted more rapidly NPIs saw their death rates increase less than cities that were slower in 1918. On the other hand the death rate was relatively higher in 1919 and 1920 for these cities

Estimates of the difference in difference equation:

$Deathrate_{i,t} = \delta_i + \gamma_t + \sum_{t \neq 1916} \beta^t \times 1_{t(i)=t} \times NPI_{1918,i} + \sum_{t \neq 1916} \lambda^t \times 1_{t(i)=t} \times X_i + \epsilon_{i,t}$

Controls include health expenditures in 1917, population in 1910, average age, population growth and the sex ratio in 1910, years and city fixed effects

95% confidence Interval clustered at the city level

Covid Economics 18, 15 May 2020: 109-156

Figure B.7: Event study: Estimates of the aggregate impact of NPI implementation length on death rates

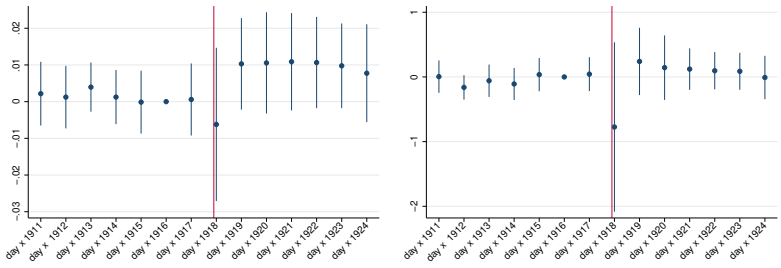

(a) All causes of death (b) Influenza and Pneumonia

Reading notes: Cities that implemented NPIs for a longer time saw their death rates increase less than cities that had shorter NPIs in 1918. On the other hand the death rate was relatively higher in 1919 and 1920 for these cities

Estimates of the difference in difference equation:

$Deathrate_{i,t} = \delta_i + \gamma_t + \sum_{t \neq 1916} \beta^t \times 1_{t(i)=t} \times NPI_{1918,i} + \sum_{t \neq 1916} \lambda^t \times 1_{t(i)=t} \times X_i + \epsilon_{i,t}$

Controls include health expenditures in 1917, population in 1900, average age, population growth and the sex ratio in 1920, years and city fixed effects

95% confidence Interval clustered at the city level

B.4 Coefficient on 1918 Mortality

Figure B.8: Event study: Estimates of the aggregate impact of the 1918 death rate on cities' demographic growth and the share of the cohort aged between 25 and 34 in 1918

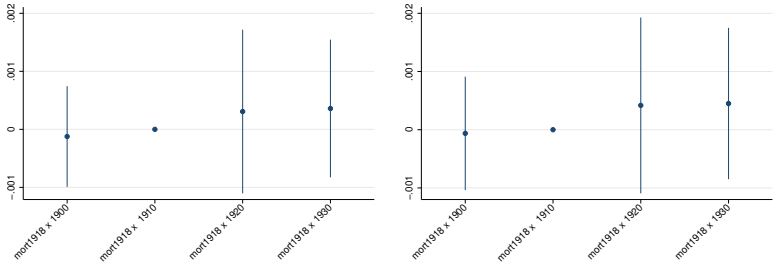

(a) Impact of the mortality in 1918 on Population growth between year t and t-10 ,controlling for the speed of implementation of NPIs

(b) Impact of the mortality in 1918 on Population growth between year t and t-10 ,controlling for the length of implementation of NPIs

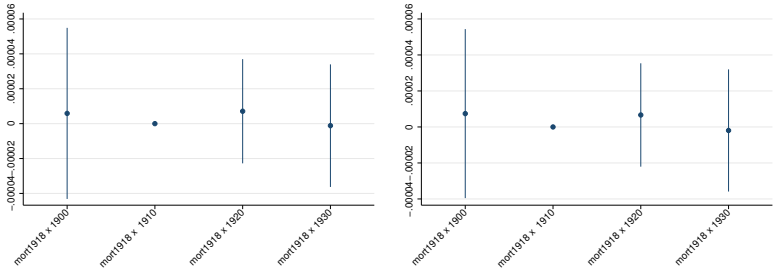

(c) Impact of the mortality in 1918 on the cohort aged between 24 and 35 in 1918,controlling for the speed of implementation of NPIs

(d) Impact of the mortality in 1918 on the cohort aged between 24 and 35 in 1918,controlling for the length of implementation of NPIs

Reading notes: Cities that implemented NPIs for a longer time saw their death rates increase less than cities that had shorter NPIs in 1918. On the other hand the death rate was relatively higher in 1919 and 1920 for these cities

Estimates of the difference in difference equation:

$Deathrate_{i,t} = \delta_i + \gamma_t + \sum_{t \neq 1916} \beta^t \times 1_{t(i)=t} \times NPI_{1918,i} + \sum_{t \neq 1916} \lambda^t \times 1_{t(i)=t} \times X_i + \epsilon_{i,t}$

Controls include health expenditures in 1917, population in 1910, years and city fixed effects

95% confidence Interval clustered at the city level

Covid Economics 18, 15 May 2020: 109-156

C Revisiting the impact of the 1918 flu on local output and employment growth

C.1 Purpose of the section

This section revisits a recent study that exploits the 1918 flu and the policies implemented in large US cities to document the impact of pandemics on the economic activity at the state and the city level and assess the benefits of NPIs. They use a difference-in-difference framework to compare cities that aggressively fought against the pandemic with these that adopted a more passive behaviour. Their main finding can be summarized in panel a) of Figure D.1. They show that there is a correlation between NPIs and Mortality suggesting that NPIs might have mitigated mortality. Moreover, they also show that cities that applied stricter NPIs didn't suffer from an economic loss and tended to grow faster in the medium term. My first contribution is summarized in panel b) of Figure D.1 where I show that the correlation between NPIs, growth and mortality in 1918 was the same before the flu. This suggests that cities that applied stricter NPIs had different trends from laxer cities even before the flu. As a consequence the common trend assumption to estimate the impact of NPIs comparing both group of cities might be violated making any inference much more challenging.

C.2 Empirical Specifications

I follow Correia, Luck, and Verner (2020) and run an event study at the city level in order to compare the growth rate of cities with high or low fatality rate before and after the 1918 flu. I estimate the following equation.

$$log(y_{i,t}) = \delta_i + \gamma_t + \sum_{t \neq 1918} \beta^t \times 1_{t(i)=t} \times Mortality_{1918,i} + \sum_{t \neq 1918} \lambda^t \times 1_{t(i)=t} \times X_{i,1900} + \epsilon_{i,t} \tag{D.1}$$

where $y_{i,t}$ are the different outcomes gathered from 1899 to 1923 as total output, total added valued of the manufacturing sector, number of wage workers or the sum of wages for each city i at time t. β^t will estimate the differentiated trend between placed that faced a high or a low mortality in 1918. The added value is not available for 1923. X_i control for the log population in 1900, the amount of health expenditures per capita in 1917, the mortality in 1917, the ratio of manufacturing job to population in 1900. Standard errors are clustered at the city level.

CEPR PRESS

I proceed similarly to identify the impact of NPIs:

$$log(y_{i,t}) = \delta_i + \gamma_t + \sum_{t \neq 1918} \beta^t \times 1_{t(i)=t} \times NPI_{1918,i} + \sum_{t \neq 1918} \lambda^t \times 1_{t(i)=t} \times X_{i,1900} + \epsilon_{i,t} \tag{D.2}$$

I use the same controls as in equation D.1

Figure D.1: Correlation between change in employment before and after 1918 with Mortality in 1918 in 43 US cities

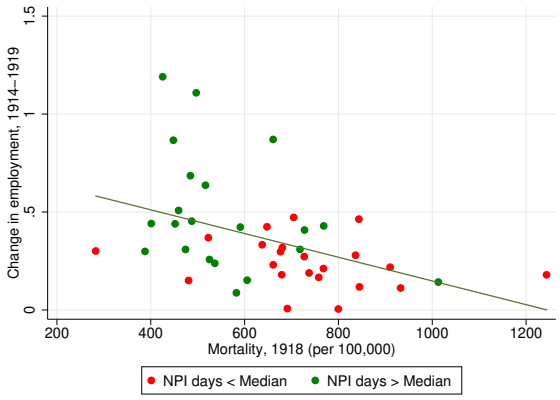

(a) Change in employment from 1914 to 1919, after the Flu and the implementation of NPIs

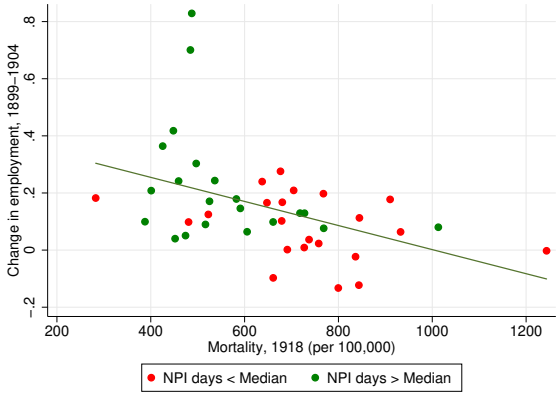

(b) Change in employment from 1899 and 1904, before the Flu and the implementation of NPIs

Covid Economics 18, 15 May 2020: 109-156

C.3 Balance tests for economic structure

I control for the comparability of low and high NPI cities with balance tests reported in Table D.1 and D.2. Overall, there are few significant differences between the two groups, apart from their level of NPI (by construction) and their level of mortality.

Table D.1: Balance test, manufacturing and health by length of NPIs

	Below the Median			Above the Median			Difference		
variable	Average	Standard Deviation	Obs	Average	Standard Deviation	Obs	Difference	Tstat	pvalue
citypop1900	246259	274059	22	413671	777509	21	-167412	-0.950	0.347
NPI_day	49.82	10.09	22	128.6	32.99	21	-78.75	-10.69	0
NPI_SPEED	-12.09	7.374	22	-2.381	4.631	21	-9.710	-5.142	7.09e-06
MORT_1917	199.7	65.79	22	157.5	49.53	21	42.13	2.363	0.0229
MORT_1918	730.2	184.8	22	560.1	149.8	21	170.2	3.307	0.00197
MANUF_1899	34965	44458	22	47091	91596	21	-12126	-0.556	0.581
VP_1899	84172	111908	22	146978	289427	21	-62807	-0.947	0.349
Wages_1899	15149	18083	22	22611	46156	21	-7462	-0.704	0.485
Health_perhead	0.203	0.125	22	0.184	0.105	21	0.0189	0.535	0.595
HEALTH_17	1.989	0.656	22	1.689	0.519	21	0.301	1.660	0.104

Table D.2: Balance test, manufacturing and health by length of NPIs

	Below the Median			Above the Median			Difference		
variable	Average	Standard Deviation	Obs	Average	Standard Deviation	Obs	Difference	Tstat	pvalue
citypop1900	257736	270547	22	401648	781318	21	-143911	-0.815	0.420
NPI_day	56.86	24.94	22	121.2	40.63	21	-64.33	-6.290	1.68e-07
NPI_SPEED	-12.82	6.558	22	-1.619	4.080	21	-11.20	-6.685	4.59e-08
MORT_1917	197.2	67.14	22	160.2	49.83	21	36.99	2.044	0.0475
MORT_1918	723.1	184.2	22	567.5	158.8	21	155.6	2.961	0.00509
MANUF_1899	35092	44287	22	46958	91701	21	-11867	-0.544	0.589
VP_1899	86974	110528	22	144042	290619	21	-57069	-0.859	0.396
Wages_1899	15274	17965	22	22479	46226	21	-7205	-0.680	0.501
Health_perhead	0.194	0.121	22	0.193	0.111	21	0.00123	0.0348	0.972
HEALTH_17	1.940	0.674	22	1.740	0.521	21	0.200	1.085	0.284

C.4 Results of the event study

C.4.1 Differentiated trends between cities with different mortality in 1918

Figure D.2 presents the coefficients estimated using equation D.1. These figures are in line with the results presented in Correia, Luck, and Verner (2020) for states and cities, as we observe a stronger decline in employment after the influenza of 1918 in cities with higher mortality rate and there is no particular trend between 1909 and 1914. However, the addition of data

points from 1899 and 1904 changes the picture. One can observe than the cities with lower mortality rates in 1918 used to behave differently in 1899 and 1904 with a growth rate significantly higher than cities with higher mortality in 1918. This findings is in line with panel b) of Figure D.1. While one potential interpretation of the change of sign of the growth rate could be the impact of the 1918 flu, this differentiated trend casts doubt on the possibility of treating the two groups of cities as comparable and of deriving any causal link. Panel b) has no counterpart in Correia, Luck, and Verner (2020) did not include any result on wages. One can observe that the sign of the growth rate of the sum of the wages also becomes negative. While this could be attributed to the impact of the flu, the differentiated positive growth rates at the beginning of the century would also cast serious doubts on this interpretation. Moreover, the sign of the impact is not in line with previous studies; Garrett (2007)for instance finds a positive impact on wages potentially explained by a shortage of labor. Panels c) and d) offer a very similar picture, as employment, total output and value added decline but their trends were also different in 1899 and 1904. To summarize, cities more affected by the flu had different trends before 1918 when compared with those less affected. It is thus difficult to infer any causal relationship between the 1918 pandemics and cities' manufacturing sector dynamics. These conclusions can be found in Chapelle (April 2020) and were confirmed in a working paper published after the first version of my working paper (Lilley, Lilley, and Rinaldi, May 2020).

Covid Economics 18, 15 May 2020: 109-156

Covid Economics 18, 15 May 2020: 109-156

Figure D.2: Event study: Estimates of the differentiated trends in the manufacturing sector between cities with High mortality and low mortality in 1918

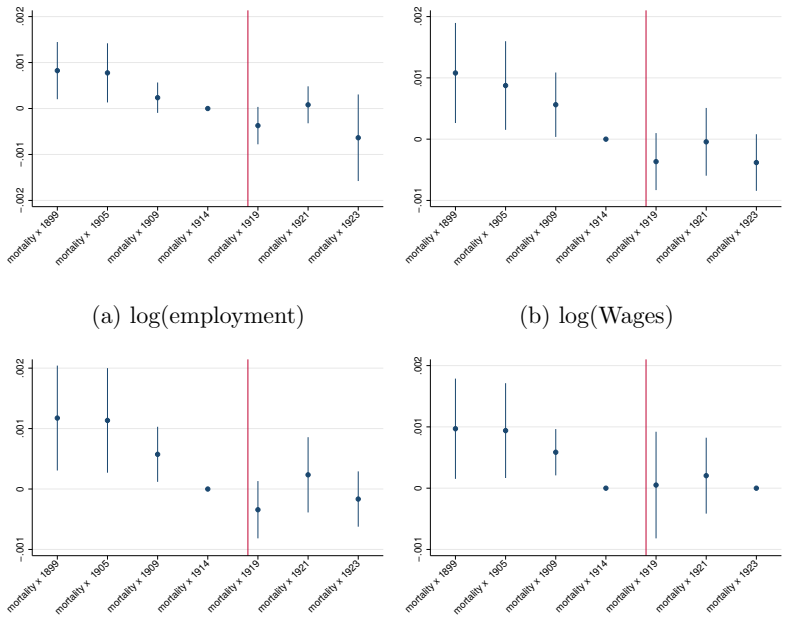

(a) log(employment)

(b) log(Wages)

(c) log(Total Output)

(d) log(Added Value)

Reading notes: Cities having higher mortality rate had higher growth rate for employment, wage bills, output and added value in 1899 and 1805 and lower in 1819. The growth rates were declining before

Estimates of the difference in difference equation:

$log(y_{i,t}) = \delta_i + \gamma_t + \sum_{t \neq 1918} \beta^t \times 1_{t(i)=t} \times Mortality_{1918,i} + \sum_{t \neq 1918} \lambda^t \times 1_{t(i)=t} \times X_{i,1900} + \epsilon_{i,t}$

Controls include health expenditures in 1917, population in 1900, the ratio for wage workers to population in 1900, and the mortality in 1917, years and city fixed effects

95% confidence Interval clustered at the city level

C.5 Differentiated trends between cities with different NPIs policies

Figures D.3 and D.4 respectively the differentiated trends of cities that adopted NPIs either earlier or for a longer period of time, and cities with laxer policies. There is no particular trend in mortality between 1909 and 1914, but for all dependant variables a clear trend of the opposite sign

Covid Economics 18, 15 May 2020: 109-156

appears before the flu, casting doubt on the causal interpretation of the impact of NPIs on economic activity. Moreover the evidence presented in the previous section documents that these cities also experienced higher death rates in 1919 and 1920 casting doubt on the potential channels that might explain the rebound, given that part of the human capital preserved in 1918 was lost in the subsequent years.

Figure D.3: Event study: Estimates of the differentiated trends in the manufacturing sector between cities High number of days and low number of days under NPIs in 1918

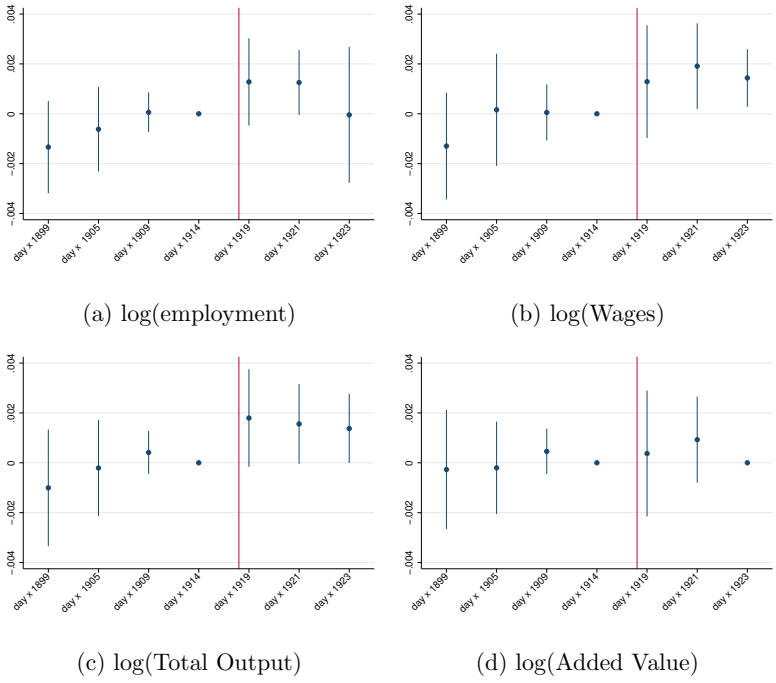

(a) log(employment) (b) log(Wages)

(c) log(Total Output) (d) log(Added Value)

Reading notes:Cities that implemented NPIs for a longer time in 1918 had lower growth rates for employment, wage bills, output and added value in 1899 and 1805 and higher in 1819. The growth rates were rising before 1918

Estimates of the difference in difference equation:

$log(y_{i,t}) = \delta_i + \gamma_t + \sum_{t \neq 1918} \beta^t \times 1_{t(i)=t} \times NPI_{1918,i} + \sum_{t \neq 1918} \lambda^t \times 1_{t(i)=t} \times X_{i,1900} + \epsilon_{i,t}$

Controls include health expenditures in 1917, population in 1900, the ratio for wage workers to population in 1900, and the mortality in 1917, years and city fixed effects

95% confidence Interval clustered at the city level

Covid Economics 18, 15 May 2020: 109-156

Figure D.4: Event study: Estimates of the differentiated trends in the manufacturing sector between cities which were faster and slower to implement NPIs in 1918

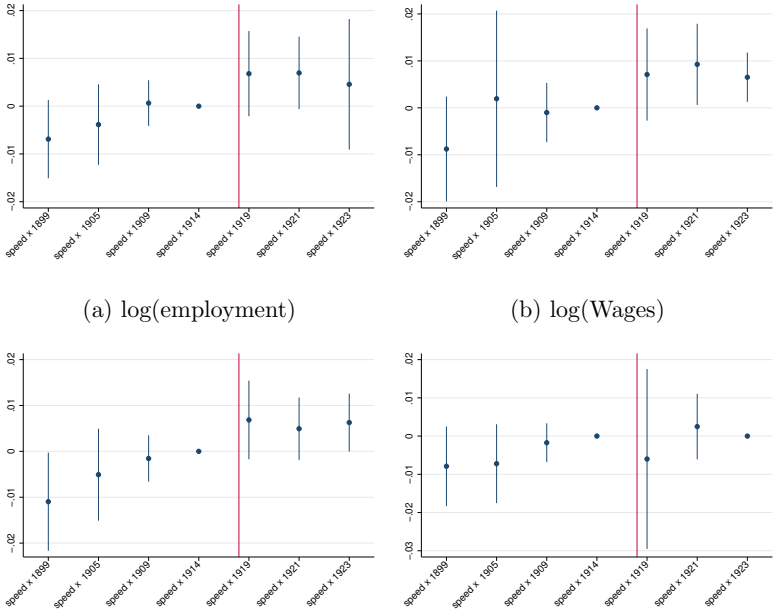

(a) log(employment) (b) log(Wages)

(c) log(Total Output) (d) log(Added Value)

Reading notes: Cities having adopted NPIS faster in 1918 had lower growth rates for employment, wage bills, output and added value in 1899 and 1805 and higher in 1918. The growth rates were rising before 1918

Estimates of the difference in difference equation:

$log(y_{i,t}) = \delta_i + \gamma_t + \sum_{t \neq 1918} \beta^t \times 1_{t(i)=t} \times NPI_{1918,i} + \sum_{t \neq 1918} \lambda^t \times 1_{t(i)=t} \times X_{i,1900} + \epsilon_{i,t}$

Controls include health expenditures in 1917, population in 1900, the ratio for wage workers to population in 1900, and the mortality in 1917, years and city fixed effects

95% confidence Interval clustered at the city level

D The demographic structure

CEPR PRESS

Covid Economics 18, 15 May 2020: 109-156

Table C.1: Balance test, demographics in 1900 by length of NPIs

		Below the Median			Above the Median			Difference		
variable	year	Average	Standard Deviation	Obs	Average	Standard Deviation	Obs	Difference	Tstat	pvalue
POP	1900	247074	274906	22	415965	782282	21	-168891	-0.953	0.346
POPgrowth	1900	.	.	.	.	.	.	.	.	.
ratio	1900	0.961	0.0675	22	1.068	0.218	21	-0.106	-2.186	0.0346
average_age	1900	27.34	1.267	22	27.43	1.335	21	-0.0909	-0.229	0.820
age_q1	1900	4.591	0.666	22	5.048	0.921	21	-0.457	-1.870	0.0686
age_q5	1900	25.32	1.323	22	25.76	1.868	21	-0.444	-0.902	0.372
age_q9	1900	53.05	2.126	22	52.10	2.071	21	0.950	1.483	0.146
share_a0001	1900	0.0207	0.00310	22	0.0184	0.00349	21	0.00229	2.279	0.0280
share_a0104	1900	0.0786	0.00875	22	0.0743	0.0120	21	0.00429	1.345	0.186
share_a0514	1900	0.185	0.0159	22	0.186	0.0201	21	-0.00121	-0.219	0.828
share_a1524	1900	0.200	0.0157	22	0.193	0.0109	21	0.00667	1.612	0.115
share_a2534	1900	0.192	0.0119	22	0.198	0.0198	21	-0.00588	-1.184	0.243
share_a3544	1900	0.142	0.00896	22	0.156	0.0213	21	-0.0138	-2.789	0.00799
share_a4554	1900	0.0915	0.00768	22	0.0914	0.00959	21	0.000129	0.0489	0.961
share_a5564	1900	0.0534	0.00782	22	0.0501	0.00836	21	0.00324	1.314	0.196
share_a6574	1900	0.0264	0.00484	22	0.0240	0.00567	21	0.00248	1.542	0.131
share_a7584	1900	0.00887	0.00207	22	0.00759	0.00192	21	0.00128	2.101	0.0418
share_a8500	1900	0.00193	0.000713	22	0.00144	0.000358	21	0.000492	2.841	0.00698
share_c0001	1900	.	.	.	.	.	.	.	.	.
share_c0104	1900	.	.	.	.	.	.	.	.	.
share_c0514	1900	.	.	.	.	.	.	.	.	.
share_c1524	1900	0.127	0.0139	22	0.120	0.0192	21	0.00697	1.370	0.178
share_c2534	1900	0.181	0.0160	22	0.182	0.0194	21	-0.00104	-0.192	0.849
share_c3544	1900	0.206	0.0170	22	0.197	0.0111	21	0.00884	2.006	0.0515
share_c4554	1900	0.184	0.0110	22	0.192	0.0195	21	-0.00814	-1.693	0.0981
share_c5564	1900	0.132	0.00773	22	0.144	0.0179	21	-0.0123	-2.945	0.00530
share_c6574	1900	0.0842	0.00804	22	0.0829	0.00897	21	0.00130	0.500	0.620
share_c7584	1900	0.0480	0.00755	22	0.0447	0.00806	21	0.00324	1.363	0.180
share_c8500	1900	0.0300	0.00623	22	0.0265	0.00678	21	0.00350	1.766	0.0848
share_c99999	1900	0.00819	0.00558	22	0.0106	0.0132	21	-0.00238	-0.774	0.443

Covid Economics 18, 15 May 2020: 109-156

Table C.2: Balance test, demographics in 1910 by length of NPIs

		Below the Median			Above the Median			Difference		
variable	year	Average	Standard Deviation	Obs	Average	Standard Deviation	Obs	Difference	Tstat	pvalue
POP	1910	310610	326523	22	578011	1.057e+06	21	-267402	-1.132	0.264
POPgrowth	1910	0.346	0.436	22	0.655	0.630	21	-0.309	-1.878	0.0675
ratio	1910	0.988	0.0923	22	1.073	0.138	21	-0.0844	-2.364	0.0229
average_age	1910	28.15	1.321	22	28.65	1.300	21	-0.505	-1.262	0.214
age_q1	1910	4.818	0.795	22	5.381	0.973	21	-0.563	-2.081	0.0437
age_q5	1910	26.05	1.463	22	26.81	1.601	21	-0.764	-1.635	0.110
age_q9	1910	53.82	1.967	22	53.19	1.778	21	0.628	1.096	0.280
share_a0001	1910	0.0208	0.00309	22	0.0184	0.00294	21	0.00240	2.607	0.0127
share_a0104	1910	0.0750	0.00850	22	0.0684	0.00924	21	0.00659	2.435	0.0193
share_a0514	1910	0.169	0.0170	22	0.154	0.0201	21	0.0146	2.575	0.0137
share_a1524	1910	0.200	0.0129	22	0.202	0.0108	21	-0.00230	-0.632	0.531
share_a2534	1910	0.192	0.0158	22	0.207	0.0198	21	-0.0154	-2.827	0.00722
share_a3544	1910	0.148	0.00971	22	0.154	0.0113	21	-0.00640	-1.999	0.0522
share_a4554	1910	0.101	0.00769	22	0.105	0.00807	21	-0.00389	-1.619	0.113
share_a5564	1910	0.0553	0.00708	22	0.0541	0.00717	21	0.00125	0.575	0.568
share_a6574	1910	0.0286	0.00536	22	0.0265	0.00490	21	0.00213	1.358	0.182
share_a7584	1910	0.00947	0.00206	22	0.00863	0.00177	21	0.000838	1.431	0.160
share_a8500	1910	0.00157	0.000372	22	0.00138	0.000312	21	0.000198	1.888	0.0661
share_c0001	1910	.	.	.	.	.	.	.	.	.
share_c0104	1910	.	.	.	.	.	.	.	.	.
share_c0514	1910	0.131	0.0153	22	0.119	0.0162	21	0.0124	2.585	0.0134
share_c1524	1910	0.168	0.0156	22	0.156	0.0197	21	0.0127	2.344	0.0240
share_c2534	1910	0.209	0.0143	22	0.217	0.0127	21	-0.00721	-1.743	0.0889
share_c3544	1910	0.183	0.0145	22	0.196	0.0181	21	-0.0129	-2.588	0.0133
share_c4554	1910	0.137	0.00942	22	0.143	0.0104	21	-0.00627	-2.078	0.0440
share_c5564	1910	0.0905	0.00773	22	0.0935	0.00792	21	-0.00298	-1.249	0.219
share_c6574	1910	0.0495	0.00700	22	0.0477	0.00707	21	0.00178	0.830	0.411
share_c7584	1910	0.0236	0.00460	22	0.0218	0.00422	21	0.00177	1.312	0.197
share_c8500	1910	0.00763	0.00173	22	0.00689	0.00143	21	0.000743	1.531	0.134
share_c99999	1910	.	.	.	.	.	.	.	.	.

Covid Economics 18, 15 May 2020: 109-156

Table C.3: Balance test, demographics in 1920 by length of NPIs

		Below the Median			Above the Median			Difference		
variable	year	Average	Standard Deviation	Obs	Average	Standard Deviation	Obs	Difference	Tstat	pvalue
POP	1920	369174	385078	22	711416	1.249e+06	21	-342242	-1.226	0.227
POPgrowth	1920	0.187	0.110	22	0.282	0.191	21	-0.0949	-2.003	0.0518
ratio	1920	0.968	0.0607	22	1.015	0.0519	21	-0.0465	-2.693	0.0102
average_age	1920	29.01	1.330	22	29.98	1.520	21	-0.964	-2.216	0.0323
age_q1	1920	4.955	0.899	22	5.476	0.928	21	-0.522	-1.872	0.0683
age_q5	1920	27.18	1.593	22	28.71	1.793	21	-1.532	-2.966	0.00501
age_q9	1920	55.41	1.894	22	55.81	2.089	21	-0.400	-0.659	0.513
share_a0001	1920	0.0198	0.00268	22	0.0167	0.00220	21	0.00307	4.086	0.000199
share_a0104	1920	0.0759	0.0102	22	0.0680	0.00961	21	0.00789	2.607	0.0127
share_a0514	1920	0.173	0.0183	22	0.160	0.0149	21	0.0134	2.624	0.0122
share_a1524	1920	0.176	0.0142	22	0.171	0.0115	21	0.00519	1.315	0.196
share_a2534	1920	0.185	0.0127	22	0.196	0.0105	21	-0.0112	-3.141	0.00312
share_a3544	1920	0.151	0.0114	22	0.161	0.0112	21	-0.0106	-3.083	0.00365
share_a4554	1920	0.112	0.00899	22	0.115	0.0115	21	-0.00349	-1.113	0.272
share_a5564	1920	0.0647	0.00843	22	0.0684	0.00930	21	-0.00374	-1.381	0.175
share_a6574	1920	0.0307	0.00476	22	0.0311	0.00548	21	-0.000414	-0.265	0.793
share_a7584	1920	0.0105	0.00202	22	0.0106	0.00214	21	-8.32e-05	-0.131	0.897
share_a8500	1920	0.00218	0.000378	22	0.00217	0.000447	21	9.49e-06	0.0753	0.940
share_c0001	1920	0.0193	0.00279	22	0.0171	0.00256	21	0.00221	2.706	0.00989
share_c0104	1920	0.0751	0.00934	22	0.0682	0.00865	21	0.00686	2.496	0.0167
share_c0514	1920	0.167	0.0171	22	0.154	0.0137	21	0.0127	2.676	0.0107
share_c1524	1920	0.186	0.0158	22	0.184	0.0113	21	0.00236	0.562	0.578
share_c2534	1920	0.180	0.0126	22	0.194	0.0105	21	-0.0137	-3.875	0.000377
share_c3544	1920	0.142	0.0105	22	0.150	0.0109	21	-0.00758	-2.324	0.0252
share_c4554	1920	0.100	0.00890	22	0.105	0.0116	21	-0.00417	-1.327	0.192
share_c5564	1920	0.0574	0.00757	22	0.0606	0.00864	21	-0.00321	-1.297	0.202
share_c6574	1920	0.0256	0.00424	22	0.0259	0.00491	21	-0.000293	-0.210	0.835
share_c7584	1920	0.00740	0.00145	22	0.00756	0.00157	21	-0.000153	-0.333	0.741
share_c8500	1920	0.00145	0.000337	22	0.00145	0.000339	21	7.99e-07	0.00774	0.994
share_c99999	1920	0.0386	0.00510	22	0.0336	0.00450	21	0.00503	3.421	0.00143

Covid Economics 18, 15 May 2020: 109-156

Table C.4: Balance test, demographics in 1930 by length of NPIs

		Below the Median			Above the Median			Difference		
variable	year	Average	Standard Deviation	Obs	Average	Standard Deviation	Obs	Difference	Tstat	pvalue
POP	1930	408033	411836	22	887415	1.545e+06	21	-479382	-1.404	0.168
POPgrowth	1930	0.115	0.118	22	0.238	0.219	21	-0.123	-2.313	0.0258
ratio	1930	0.952	0.0509	22	0.978	0.0372	21	-0.0262	-1.918	0.0621
average_age	1930	30.33	1.342	22	31.14	1.378	21	-0.808	-1.948	0.0583
age_q1	1930	5.773	0.813	22	6.286	0.644	21	-0.513	-2.288	0.0274
age_q5	1930	28.50	1.739	22	29.81	1.692	21	-1.310	-2.501	0.0165
age_q9	1930	57.59	2.039	22	57.86	1.905	21	-0.266	-0.442	0.661
share_a0001	1930	0.0149	0.00168	22	0.0140	0.00169	21	0.000988	1.922	0.0616
share_a0104	1930	0.0639	0.00686	22	0.0590	0.00648	21	0.00495	2.431	0.0195
share_a0514	1930	0.174	0.0194	22	0.158	0.0127	21	0.0163	3.232	0.00243
share_a1524	1930	0.177	0.0112	22	0.174	0.00867	21	0.00283	0.920	0.363
share_a2534	1930	0.169	0.0159	22	0.179	0.00991	21	-0.00904	-2.227	0.0315
share_a3544	1930	0.155	0.0106	22	0.165	0.00791	21	-0.00930	-3.246	0.00233
share_a4554	1930	0.117	0.00937	22	0.122	0.0104	21	-0.00501	-1.657	0.105
share_a5564	1930	0.0748	0.00966	22	0.0748	0.00897	21	-2.73e-05	-0.00959	0.992
share_a6574	1930	0.0393	0.00626	22	0.0405	0.00686	21	-0.00116	-0.581	0.564
share_a7584	1930	0.0122	0.00213	22	0.0127	0.00263	21	-0.000491	-0.674	0.504
share_a8500	1930	0.00207	0.000453	22	0.00208	0.000436	21	-3.50e-06	-0.0258	0.980
share_c0001	1930	0.0178	0.00226	22	0.0158	0.00155	21	0.00199	3.349	0.00175
share_c0104	1930	0.0675	0.00758	22	0.0616	0.00516	21	0.00594	2.987	0.00474
share_c0514	1930	0.179	0.0138	22	0.181	0.00886	21	-0.00145	-0.407	0.686
share_c1524	1930	0.169	0.0145	22	0.178	0.00916	21	-0.00885	-2.378	0.0222
share_c2534	1930	0.148	0.0102	22	0.157	0.00872	21	-0.00949	-3.280	0.00212
share_c3544	1930	0.108	0.00938	22	0.111	0.0103	21	-0.00302	-1.007	0.320
share_c4554	1930	0.0674	0.00939	22	0.0676	0.00862	21	-0.000279	-0.101	0.920
share_c5564	1930	0.0324	0.00525	22	0.0339	0.00626	21	-0.00154	-0.878	0.385
share_c6574	1930	0.00869	0.00169	22	0.00906	0.00196	21	-0.000371	-0.666	0.509
share_c7584	1930	0.00113	0.000243	22	0.00115	0.000250	21	-1.88e-05	-0.250	0.804
share_c8500	1930	8.54e-05	4.32e-05	22	7.90e-05	2.41e-05	21	6.30e-06	0.587	0.561
share_c99999	1930	0.201	0.0216	22	0.184	0.0163	21	0.0171	2.921	0.00566

CEPR PRESS

Covid Economics 18, 15 May 2020: 109-156

Table C.5: Balance test, demographics in 1900 by speed of NPIs

		Below the Median			Above the Median			Difference		
variable	year	Average	Standard Deviation	Obs	Average	Standard Deviation	Obs	Difference	Tstat	pvalue
POP	1900	258556	271404	22	403936	786094	21	-145380	-0.818	0.418
POPgrowth	1900	.	.	.	.	.	.	.	.	.
ratio	1900	0.968	0.0657	22	1.061	0.221	21	-0.0936	-1.899	0.0646
average_age	1900	27.28	1.221	22	27.49	1.373	21	-0.207	-0.523	0.604
age_q1	1900	4.500	0.598	22	5.143	0.910	21	-0.643	-2.750	0.00883
age_q5	1900	25.36	1.329	22	25.71	1.875	21	-0.351	-0.710	0.482
age_q9	1900	52.91	2.022	22	52.24	2.234	21	0.671	1.034	0.307
share_a0001	1900	0.0208	0.00300	22	0.0183	0.00351	21	0.00248	2.496	0.0167
share_a0104	1900	0.0791	0.00852	22	0.0738	0.0119	21	0.00532	1.689	0.0988
share_a0514	1900	0.185	0.0167	22	0.185	0.0194	21	-0.000401	-0.0726	0.942
share_a1524	1900	0.198	0.0155	22	0.195	0.0119	21	0.00330	0.778	0.441
share_a2534	1900	0.193	0.0121	22	0.197	0.0200	21	-0.00411	-0.819	0.417
share_a3544	1900	0.143	0.0112	22	0.154	0.0211	21	-0.0110	-2.143	0.0381
share_a4554	1900	0.0914	0.00767	22	0.0915	0.00960	21	-5.34e-05	-0.0202	0.984
share_a5564	1900	0.0529	0.00738	22	0.0507	0.00895	21	0.00220	0.882	0.383
share_a6574	1900	0.0259	0.00460	22	0.0246	0.00607	21	0.00134	0.817	0.419
share_a7584	1900	0.00858	0.00190	22	0.00789	0.00224	21	0.000689	1.090	0.282
share_a8500	1900	0.00179	0.000527	22	0.00160	0.000693	21	0.000192	1.024	0.312
share_c0001	1900	.	.	.	.	.	.	.	.	.
share_c0104	1900	.	.	.	.	.	.	.	.	.
share_c0514	1900	.	.	.	.	.	.	.	.	.
share_c1524	1900	0.127	0.0137	22	0.119	0.0190	21	0.00827	1.641	0.108
share_c2534	1900	0.181	0.0165	22	0.182	0.0190	21	-0.000922	-0.170	0.865
share_c3544	1900	0.204	0.0170	22	0.199	0.0123	21	0.00483	1.061	0.295
share_c4554	1900	0.185	0.0113	22	0.191	0.0198	21	-0.00572	-1.168	0.249
share_c5564	1900	0.133	0.00944	22	0.143	0.0178	21	-0.0101	-2.344	0.0240
share_c6574	1900	0.0839	0.00773	22	0.0832	0.00929	21	0.000684	0.263	0.794
share_c7584	1900	0.0474	0.00709	22	0.0453	0.00868	21	0.00214	0.886	0.381
share_c8500	1900	0.0292	0.00579	22	0.0274	0.00751	21	0.00180	0.883	0.382
share_c99999	1900	0.00888	0.00605	22	0.00985	0.0131	21	-0.000963	-0.311	0.757

Covid Economics 18, 15 May 2020: 109-156

Table C.6: Balance test, demographics in 1910 by speed of NPIs

		Below the Median			Above the Median			Difference		
variable	year	Average	Standard Deviation	Obs	Average	Standard Deviation	Obs	Difference	Tstat	pvalue
POP	1910	326922	320429	22	560922	1.063e+06	21	-234001	-0.987	0.329
POPgrowth	1910	0.365	0.436	22	0.636	0.639	21	-0.271	-1.635	0.110
ratio	1910	0.994	0.0903	22	1.067	0.143	21	-0.0736	-2.028	0.0491
average_age	1910	28.10	1.259	22	28.70	1.342	21	-0.603	-1.519	0.136
age_q1	1910	4.864	0.834	22	5.333	0.966	21	-0.470	-1.709	0.0949
age_q5	1910	26.05	1.430	22	26.81	1.632	21	-0.764	-1.635	0.110
age_q9	1910	53.64	1.733	22	53.38	2.061	21	0.255	0.441	0.662
share_a0001	1910	0.0208	0.00311	22	0.0184	0.00294	21	0.00239	2.586	0.0134
share_a0104	1910	0.0750	0.00853	22	0.0684	0.00924	21	0.00653	2.408	0.0206
share_a0514	1910	0.170	0.0173	22	0.154	0.0194	21	0.0157	2.805	0.00767
share_a1524	1910	0.199	0.0122	22	0.203	0.0114	21	-0.00399	-1.108	0.274
share_a2534	1910	0.192	0.0160	22	0.206	0.0203	21	-0.0135	-2.433	0.0194
share_a3544	1910	0.149	0.0101	22	0.153	0.0114	21	-0.00454	-1.384	0.174
share_a4554	1910	0.101	0.00795	22	0.105	0.00774	21	-0.00411	-1.716	0.0937
share_a5564	1910	0.0548	0.00646	22	0.0547	0.00781	21	9.90e-05	0.0454	0.964
share_a6574	1910	0.0281	0.00485	22	0.0270	0.00559	21	0.00108	0.675	0.503
share_a7584	1910	0.00922	0.00188	22	0.00889	0.00204	21	0.000331	0.553	0.583
share_a8500	1910	0.00151	0.000348	22	0.00144	0.000365	21	7.47e-05	0.687	0.496
share_c0001	1910	.	.	.	.	.	.	.	.	.
share_c0104	1910	.	.	.	.	.	.	.	.	.
share_c0514	1910	0.131	0.0154	22	0.119	0.0161	21	0.0126	2.628	0.0120
share_c1524	1910	0.169	0.0160	22	0.155	0.0191	21	0.0133	2.489	0.0170
share_c2534	1910	0.209	0.0138	22	0.217	0.0128	21	-0.00876	-2.156	0.0370
share_c3544	1910	0.184	0.0147	22	0.195	0.0186	21	-0.0111	-2.167	0.0361
share_c4554	1910	0.138	0.00971	22	0.142	0.0106	21	-0.00424	-1.368	0.179
share_c5564	1910	0.0902	0.00790	22	0.0938	0.00760	21	-0.00358	-1.512	0.138
share_c6574	1910	0.0489	0.00629	22	0.0483	0.00784	21	0.000595	0.275	0.785
share_c7584	1910	0.0231	0.00417	22	0.0223	0.00480	21	0.000816	0.596	0.555
share_c8500	1910	0.00740	0.00158	22	0.00713	0.00169	21	0.000279	0.561	0.578

Covid Economics 18, 15 May 2020: 109-156

Table C.7: Balance test, demographics in 1920 by speed of NPIs

		Below the Median			Above the Median			Difference		
variable	year	Average	Standard Deviation	Obs	Average	Standard Deviation	Obs	Difference	Tstat	pvalue
POP	1920	388825	377175	22	690830	1.257e+06	21	-302005	-1.078	0.287
POPgrowth	1920	0.193	0.106	22	0.275	0.197	21	-0.0828	-1.729	0.0913
ratio	1920	0.978	0.0609	22	1.005	0.0588	21	-0.0262	-1.433	0.159
average_age	1920	29.04	1.402	22	29.95	1.469	21	-0.911	-2.080	0.0438
age_q1	1920	5	0.976	22	5.429	0.870	21	-0.429	-1.517	0.137
age_q5	1920	27.27	1.723	22	28.62	1.746	21	-1.346	-2.545	0.0148
age_q9	1920	55.27	1.882	22	55.95	2.061	21	-0.680	-1.130	0.265
share_a0001	1920	0.0196	0.00290	22	0.0169	0.00221	21	0.00264	3.340	0.00180
share_a0104	1920	0.0751	0.0107	22	0.0689	0.00974	21	0.00622	1.994	0.0528
share_a0514	1920	0.172	0.0192	22	0.160	0.0145	21	0.0119	2.296	0.0269
share_a1524	1920	0.177	0.0137	22	0.170	0.0116	21	0.00682	1.753	0.0871
share_a2534	1920	0.186	0.0127	22	0.195	0.0115	21	-0.00942	-2.549	0.0146
share_a3544	1920	0.151	0.0115	22	0.161	0.0115	21	-0.00988	-2.821	0.00734
share_a4554	1920	0.112	0.0106	22	0.115	0.0102	21	-0.00243	-0.769	0.446
share_a5564	1920	0.0644	0.00889	22	0.0687	0.00871	21	-0.00426	-1.587	0.120
share_a6574	1920	0.0303	0.00448	22	0.0316	0.00566	21	-0.00126	-0.814	0.421
share_a7584	1920	0.0104	0.00187	22	0.0107	0.00227	21	-0.000378	-0.597	0.554
share_a8500	1920	0.00218	0.000384	22	0.00216	0.000442	21	2.19e-05	0.174	0.863
share_c0001	1920	0.0191	0.00287	22	0.0173	0.00263	21	0.00182	2.161	0.0366
share_c0104	1920	0.0743	0.00987	22	0.0691	0.00866	21	0.00520	1.833	0.0741
share_c0514	1920	0.166	0.0177	22	0.155	0.0133	21	0.0119	2.491	0.0169
share_c1524	1920	0.187	0.0154	22	0.183	0.0115	21	0.00419	1.004	0.321
share_c2534	1920	0.181	0.0125	22	0.193	0.0115	21	-0.0122	-3.316	0.00192
share_c3544	1920	0.142	0.0104	22	0.150	0.0111	21	-0.00723	-2.202	0.0334
share_c4554	1920	0.101	0.0111	22	0.104	0.00964	21	-0.00282	-0.885	0.381
share_c5564	1920	0.0571	0.00772	22	0.0609	0.00834	21	-0.00388	-1.585	0.121
share_c6574	1920	0.0252	0.00390	22	0.0263	0.00514	21	-0.00106	-0.763	0.450
share_c7584	1920	0.00735	0.00139	22	0.00761	0.00162	21	-0.000264	-0.575	0.569
share_c8500	1920	0.00146	0.000351	22	0.00143	0.000324	21	2.34e-05	0.227	0.821
share_c99999	1920	0.0383	0.00546	22	0.0340	0.00445	21	0.00430	2.820	0.00736

Covid Economics 18, 15 May 2020: 109-156

Table C.8: Balance test, demographics in 1930 by speed of NPIs

		Below the Median			Above the Median			Difference		
variable	year	Average	Standard Deviation	Obs	Average	Standard Deviation	Obs	Difference	Tstat	pvalue
POP	1930	430678	403520	22	863691	1.555e+06	21	-433013	-1.263	0.214
POPgrowth	1930	0.111	0.112	22	0.242	0.220	21	-0.131	-2.479	0.0174
ratio	1930	0.952	0.0496	22	0.977	0.0393	21	-0.0252	-1.844	0.0725
average_age	1930	30.29	1.351	22	31.18	1.341	21	-0.890	-2.167	0.0361
age_q1	1930	5.682	0.780	22	6.381	0.590	21	-0.699	-3.304	0.00199
age_q5	1930	28.45	1.654	22	29.86	1.740	21	-1.403	-2.710	0.00979
age_q9	1930	57.55	2.110	22	57.90	1.814	21	-0.359	-0.598	0.553
share_a0001	1930	0.0150	0.00159	22	0.0139	0.00176	21	0.00105	2.060	0.0458
share_a0104	1930	0.0644	0.00678	22	0.0585	0.00613	21	0.00589	2.985	0.00477
share_a0514	1930	0.174	0.0193	22	0.158	0.0129	21	0.0163	3.249	0.00231
share_a1524	1930	0.177	0.0104	22	0.175	0.00974	21	0.00226	0.732	0.469
share_a2534	1930	0.170	0.0161	22	0.178	0.0103	21	-0.00707	-1.701	0.0965
share_a3544	1930	0.155	0.0100	22	0.165	0.00857	21	-0.00949	-3.331	0.00184
share_a4554	1930	0.116	0.00896	22	0.123	0.0104	21	-0.00650	-2.204	0.0332
share_a5564	1930	0.0746	0.00994	22	0.0750	0.00863	21	-0.000464	-0.163	0.871
share_a6574	1930	0.0392	0.00670	22	0.0406	0.00638	21	-0.00146	-0.731	0.469
share_a7584	1930	0.0122	0.00226	22	0.0127	0.00251	21	-0.000536	-0.737	0.465
share_a8500	1930	0.00207	0.000455	22	0.00208	0.000434	21	-1.91e-05	-0.141	0.888
share_c0001	1930	0.0176	0.00231	22	0.0160	0.00167	21	0.00168	2.729	0.00930
share_c0104	1930	0.0670	0.00766	22	0.0621	0.00558	21	0.00497	2.421	0.0200
share_c0514	1930	0.179	0.0129	22	0.181	0.0103	21	-0.00157	-0.440	0.663
share_c1524	1930	0.170	0.0147	22	0.177	0.00972	21	-0.00701	-1.837	0.0735
share_c2534	1930	0.148	0.00938	22	0.158	0.00935	21	-0.00995	-3.485	0.00119
share_c3544	1930	0.107	0.00913	22	0.112	0.0102	21	-0.00465	-1.577	0.122
share_c4554	1930	0.0672	0.00969	22	0.0678	0.00826	21	-0.000571	-0.208	0.837
share_c5564	1930	0.0324	0.00568	22	0.0339	0.00585	21	-0.00156	-0.885	0.381
share_c6574	1930	0.00866	0.00176	22	0.00909	0.00188	21	-0.000434	-0.781	0.439
share_c7584	1930	0.00113	0.000251	22	0.00115	0.000240	21	-1.74e-05	-0.232	0.818
share_c8500	1930	8.70e-05	4.38e-05	22	7.74e-05	2.24e-05	21	9.60e-06	0.899	0.374
share_c99999	1930	0.202	0.0211	22	0.183	0.0158	21	0.0191	3.351	0.00174

CEPR PRESS

Covid Economics **Issue 18, 15 May 2020**

Who can live without two months of income?[1]

Catarina Midões[2]

Date submitted: 8 May 2020; **Date accepted:** 8 May 2020

Looking at 342 million residents in 21 EU countries, we estimate that 99 million individuals live in households which cannot cover for two months of the most basic expenses – food at home, utilities and rent/mortgage on their single main residence - only from their savings in bank accounts. Without privately earned income but with (pre-covid19) pension income and public transfers, 57 million have savings for less than 2 months. Government support in the form of employment protection schemes and beyond is thus fundamental to ensure livelihood during the covid19 shock, yet many individuals would remain vulnerable if ensured 50% of their gross privately earned income. We estimate mortgage and rent suspension can decrease in half the number of individuals at risk. We find there are stark differences between countries and that individuals born outside of the EU are particularly vulnerable. Those dependent on their income will be forced to resume work earlier and take higher health risks.

Covid Economics 18, 15 May 2020: 157-169

1 I thank Enrico Bergamini, Tanja Linta, Mateo Sere and Guntram Wolff for helpful comments.
2 Research Analyst, Bruegel.

Covid Economics 18, 15 May 2020: 157-169

1. Introduction

As a result of the covid19 pandemic, millions of individuals have stopped working or had to substantially reduce working hours, either due to health restrictions or to suppressed demand. Even with state support, many of the affected individuals are witnessing substantial shocks to their income.

How many households in different EU countries could live without an income for one and two months? In this piece, we simulate two scenarios: living without privately earned income and living with 50% of gross privately earned income[1]. Using the ECB Household Finance and Consumption Survey (HFCS) we estimate, under each scenario, whether households can cover their typical basic monthly expenses (utilities and food consumption at home) by using their bank deposits and their pre-covid19 pooled monthly pensions and pooled public transfers.[2] The numbers reported are estimates of the number of individuals living in households which cannot face these expenses.

Our second scenario can be interpreted as government support which guarantees individuals take home 50% of their gross privately earned income. Such scheme is more generous than it might at first seem since we are dealing with gross incomes.

We extend the analysis to include monthly mortgages and rents on main residences, but only for individuals who own no other residences. We discuss implications for covid19 policy measures, specifically, whether they are fine-tuned to ensure the livelihood of individuals.

The analysis is based on the ECB Household Finance and Consumption survey (HFCS) wave 3, conducted in 2017, which covers 21 countries: Croatia, Poland and Hungary and the Euro Area except for Spain[3]. The survey provides information on households and individuals[4].

The survey does not provide information on precautionary savings individuals might hold in cash instead of in bank accounts. We restrict the analysis to households who own bank accounts, as they are more likely to use it as their main source of savings. When explicitly stated we also resort to a sensitivity analysis where we include simulated holdings of cash in available savings, a sensitivity analysis using a different ECB survey[5].

The exact variables used and calculations are described in the Technical Appendix.

2. Results

2.1. Facing utilities and food expenses

We estimate there are 29.6 million individuals who cannot cover for one month of expenses with food at home and utilities without privately earned income. When taking home 50% of

[1] By privately earned income, we refer to income other than pensions and public transfers. It encompasses salary income, self-employed income, rental income, income from financial assets and regular private transfers.
[2] Utilities comprise electricity, water, gas, telephone, internet and television.
[3] Data on Spain will only be available later in the year.
[4] The HFCS represents the total number of households in each country, not the total number of individuals, but does consider household composition in its sampling design. As result, there are (small) differences in the number of individuals represented in the survey and the number of individuals of the country.
[5] More details are provided in the Technical Appendix.

Covid Economics 18, 15 May 2020: 157-169

their gross privately earned income, the number of vulnerable individuals decreases substantially, to 4.4 million.

Once we look at two months instead, we estimate there are 41.6 million and 5.5 million individuals who would not be able to cover for these expenses, or 12.2% and 1.6% of individuals analysed:

Figure 1. Millions of individuals who cannot cover for food and utilities expenses during one and two months without privately earned gross income and with 50% of their privately earned gross income

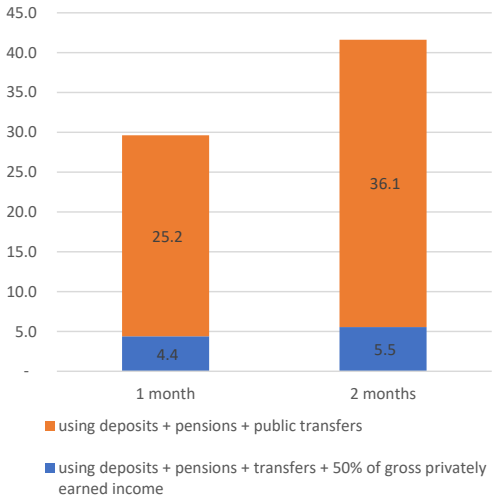

Differences across countries are substantial. In Slovenia, Lithuania, Latvia and Croatia more than 8% of individuals are unable to withstand expenses with 50% of their gross income for two months while in Belgium, Austria, Finland and Malta, there are less than 0.5% of individuals in such vulnerable positions (see Figure 2).

Covid Economics 18, 15 May 2020: 157-169

Figure 2. Percentage of individuals who cannot cover for two months of expenses with food at home and utilities with 50% of gross privately earned income

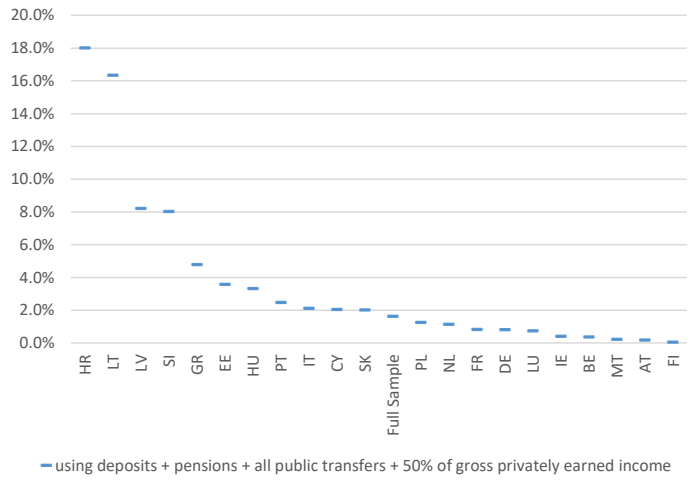

Percentages are informative to make cross-country comparisons, but it is also relevant to assess in absolute numbers where individuals are located.

Even if in Italy, only 2.1% of the individuals considered are vulnerable when taking home 50% of their gross privately earned income, it is the country with the highest absolute number of vulnerable individuals: 1.2 million[6]. Germany, Croatia and France follow, all with more than half a million vulnerable individuals (see Figure 6 in the annex).

With our allocation of precautionary cash savings, the numbers decrease, yet, we still estimate 1.03 million individuals at risk in Italy, and 482 thousand in France (see Figure 6 B in the Annex).

2.2. The relative importance of savings, pensions, public transfers and income

Households able to face these expenses must resort to a combination of savings, pensions, public transfers, and the proportion of income we assumed they retain. We provide a breakdown by these categories, to identify their relative importance for ensuring household livelihood.

The importance of private income even in the short horizon considered (2 months) is clear: in the countries analysed, we estimate 12.2% individuals cannot cover for food at home and utilities without privately earned income. Such percentage is highly variable across countries, being below 6% in Malta, the Netherlands and Austria, but above 30% in Greece, Slovenia, Latvia, Lithuania and Croatia. (see Figure 4, series 'deposits + pensions + all public transfers'). In the first month, 8.7% of individuals are already dependent on their monthly income.

[6] The number is slightly below 2.1% of the Italian population because we are only considering households with a bank account and because the survey is representative of households and not of individuals directly. The technical appendix provides further details.

Covid Economics 18, 15 May 2020: 157-169

When looking purely at deposits, 25% of individuals in the countries considered cannot cover for two months of food and utilities - and 17.4% cannot for the first month. Differences between European countries are striking: in Latvia, 71% cannot pay for two months with their bank deposits, while in Austria and the Netherlands, the percentage is 11% and 12.5% respectively.

Fig 3. Percentage of individuals who cannot cover two months of expenses with food and utilities, resorting to their deposits and different sources of income

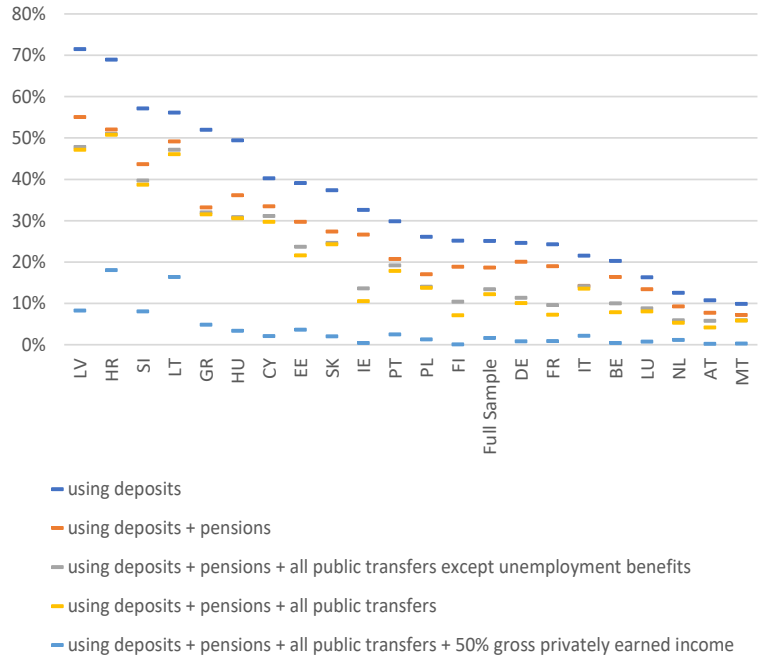

The welfare state provides coverage for millions of otherwise vulnerable individuals. Pensions are a fundamental source of income in all countries, substantially reducing the number of vulnerable individuals.

Public transfers (other than pensions) are crucial in France, Ireland, Finland and Germany. In Italy, Greece and Portugal, they do not provide substantial added social protection beyond pensions. Unemployment benefits are particularly important in Finland, Belgium and France.

2.3. Facing housing expenses

We now turn to households who cannot cover for food, utilities and housing expenses (rent or mortgages) on their main residence and own no other residences.

Through deposits and (pre-covid19) pensions and public transfers, 57.5 million individuals cannot cover for two months, and 41.1 cannot cover for the first month.

If ensured 50% of their gross privately earned income, numbers reduce considerably, yet, we estimate there are still 8.4 million people who cannot handle one month of expenses and 11.3 million who cannot handle two months:

Figure 4. Millions of individuals who cannot cover for food, utilities and housing expenses on their main residence (rent/mortgage) during one and two months without privately earned gross income and with 50% of their privately earned gross income

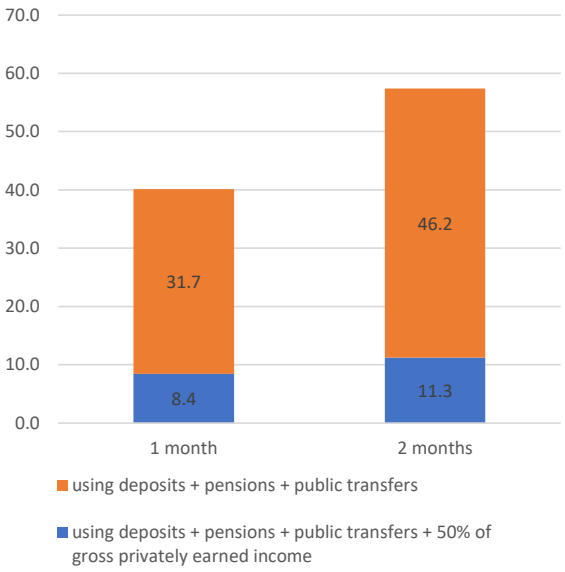

Expenses for a main (single) residence more than double the number of individuals who cannot pay for two months of expenses with 50% of their gross privately earned income (see Figure 3).

The addition of rents increases the number of vulnerable individuals from 5.5 million (when considering only utilities and food at home) to 9.8 million, and the addition of mortgages, to 11.3.

The corollary is that rent and mortgage suspension can indeed be an effective support for vulnerable households. It is important to assess landlords' income vulnerability as well and develop measures which do not safeguard certain individuals at the expenses of others; even so, we estimate fewer than 220,000 landlords who would not be able to cover for their expenses for two months without rental income and earning 50% of their other private gross income.

Covid Economics 18, 15 May 2020: 157-169

Covid Economics 18, 15 May 2020: 157-169

Figure 5. Percentage of individuals who cannot cover for two months of food and utilities with and without main residence expenses (rent or mortgage) with bank deposits, pensions, public transfers and 50% of their gross privately earned income

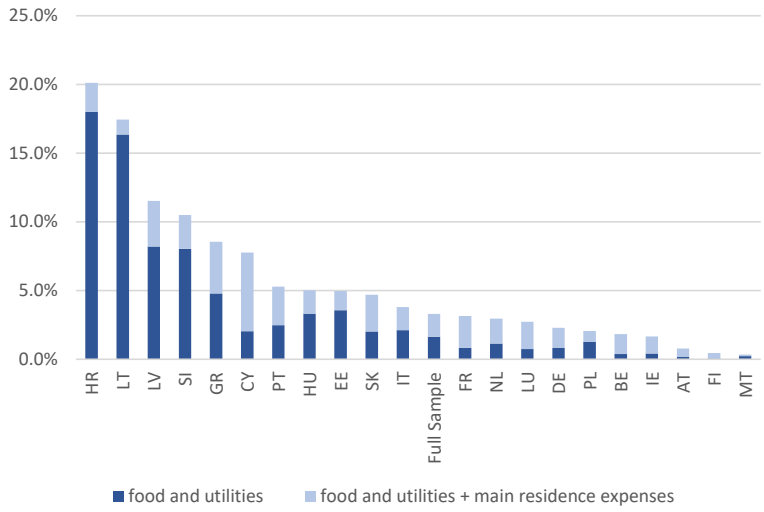

For certain countries, the measures can be particularly effective. While only 0.8% of the French population cannot face monthly expenses of food and utilities, 3.1% cannot pay their monthly expenses once rents and mortgages are accounted for. In Finland, the percentage of vulnerable individuals jumps from 0.1% to 0.5%. and in Belgium, from 0.4% to 1.8%. Germany, Ireland and Cyprus are also countries where such measures can be highly beneficial.

2.4. Migration background

We find that individuals born outside of their country of residence and particularly those born outside of Europe are substantially more at risk of not being able to cover for their food, utilities and housing expenses.

For individuals living in their country of birth, the probability of not being able to cover such expenses for 2 months under a 100% privately earned income shock is 16.3%, while for those born elsewhere in the EU it is 24.7% and for those born outside Europe, 29.6%. Individuals born elsewhere in the EU are 1.5 (24.7 / 16.3) times more at risk, while individuals born outside the EU are 1.8 (29.6 / 16.3) times more at risk.

Performing this calculation country by country reveals individuals born outside the EU are always at greater risk, except in Portugal and Slovenia[7]. The group born abroad is anything but homogeneous, since countries receive working age individuals from abroad, but also retirees from other countries and individuals whose parents had immigrated themselves.

[7] We have only considered countries for which they were more than 100 sampled individuals born outside of Europe and more than 100 sampled individuals born in the EU but outside the country.

Table 1. Risk of not being able to cover for 2 months of expenses without any privately earned income having been born outside the country, relative to those born in the country

	Relative risk, born outside the EU	Relative risk, born elsewhere in the EU	Risk for those born in the country
AT	3.4	2.3	5%
BE	3.1	2.3	13%
DE	2.3	1.3	14%
EE	2.2	1.5	25%
FI	2.2	1.8	12%
FR	2.1	2.0	14%
GR	1.9	1.1	32%
HR	1.8	1.6	52%
HU	1.8	1.6	33%
IE	1.8	1.1	16%
IT	1.7	1.0	15%
LT	1.4	0.7	44%
LU	1.3	0.9	11%
LV	1.0	1.0	49%
NL	1.0	0.9	10%
PT	0.8	0.8	22%
SI	0.7	0.6	40%

Note: 'Relative risk, born elsewhere in the EU' is the ratio between the percentage of individuals born elsewhere in the EU who cannot cover for two months of food, utilities and housing expenses and the percentage of individuals born in the country who cannot cover for said expenses. 'Relative risk, born outside the EU' is the ratio between the percentage of individuals born outside the EU who cannot cover for two months of food, utilities and housing expenses and the percentage of individuals born in the country who cannot. Countries with fewer than 100 sampled individuals born outside the country were not analysed.

Despite heterogeneity, there are important migrant groups who might also be more susceptible to higher private income shocks under covid19, due to precarious labour conditions and prevalence of informal work. These hinder access to social security and thus to government assistance policies in the case of income downfall.

3. Conclusion

We have found how resilience of individuals to income shocks is highly differentiated across the 21 EU countries analysed. Pensions are an important buffer for households who receive them. The effect of other public transfers is more heterogeneous, having little effect beyond pensions in reducing the number of vulnerable individuals in some countries, namely Portugal, Italy and Greece, but playing an important role in France, Belgium or Germany.

The stark differences in vulnerability might explain different perceptions of urgency and hinder EU cooperation. Measures such as mortgage and rent deferrals are generally helpful to support people in need, though to what extent depends on country characteristics. Policies on rent should safeguard tenants without jeopardizing the livelihood of landlords. Such measures appear feasible since an income shock threatens the livelihood of substantially more tenants than landlords.

Covid Economics 18, 15 May 2020: 157-169

Providing substantial income support is fundamental even in the very short term (2 months), since 57 million individuals cannot withstand their most basic expenses with savings and (pre-covid19) pensions and public transfers. Importantly, even when covid19 policy responses are in place, namely rent and mortgage deferrals and employment protection schemes, there might still be pockets of vulnerability. Individuals with a migration background are a particularly vulnerable group, possibly more likely to suffer income shocks and with difficult access to social assistance in the case of income downfall.

The shock simulated might be for some individuals in line with employment protection schemes in some countries. For instance, in France and Belgium schemes cover 70% of gross salaries and in Portugal 66%, on which individuals pay social security contributions and income tax. Importantly, schemes provide minimum amounts such as the minimum wage, which ought to decrease the number of vulnerable individuals. In future work, measures could be considered country by country to provide estimates of how much current policies might have reduced vulnerabilities. Resorting to net incomes instead of gross incomes would also allow for more accurate estimation of vulnerabilities.

Different levels of vulnerability will translate to different levels of health risk particularly as countries start lifting social distancing and allowing companies to return to normality. Individuals who are dependent on their income will be forced to leave their homes and resume work earlier, taking higher health risks than they might otherwise choose.

References

Esselink, H. and L. Hernández (2017), 'The use of cash by households in the euro area', *ECB Occasional Paper Series No. 201*, available at: https://www.ecb.europa.eu/pub/pdf/scpops/ecb.op201.en.pdf

Covid Economics 18, 15 May 2020: 157-169

Covid Economics 18, 15 May 2020: 157-169

Annex

Figure 6. Thousands of individuals who cannot cover two months of basic expenditures (food at home and utilities) with 50% of their gross privately earned income, by country

A. With deposits, pensions and public transfers

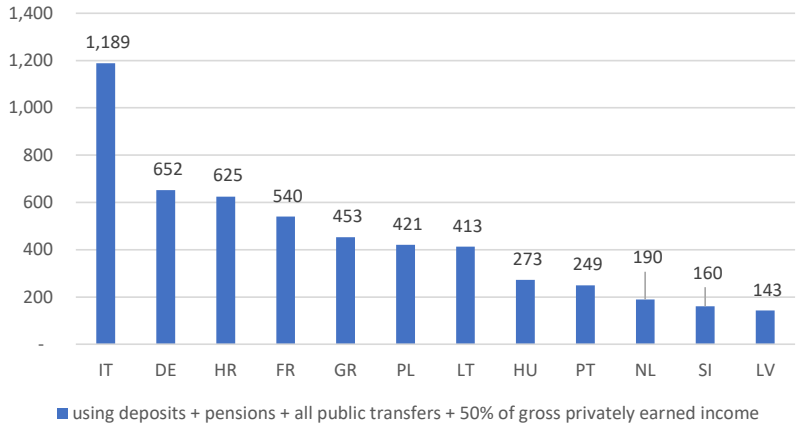

Note: Only countries with more than 100 thousand individuals at risk under a 50% income shock are depicted.

B. With deposits, pensions, public transfers and simulated cash savings

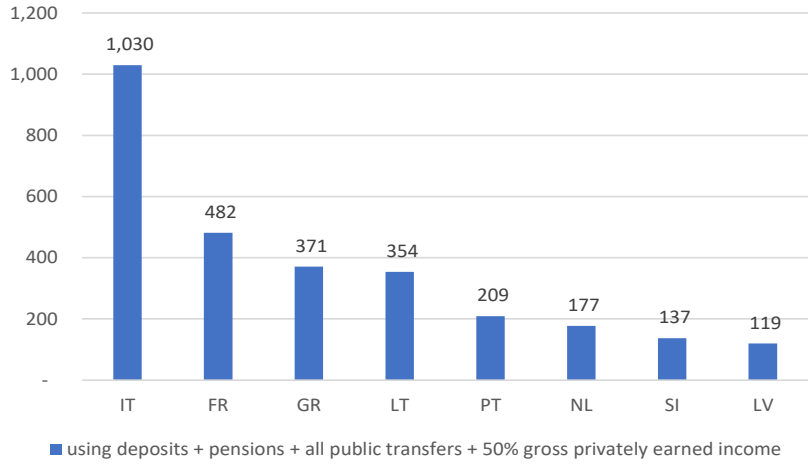

Note: We do not have information on precautionary cash held in Germany, Croatia, Hungary and Poland, thus such sensitivity analysis is not performed.

Technical Appendix

The analysis uses the ECB Household Finance and Consumption Survey (HFCS) wave 3, conducted in 2017, to estimate how many individuals live in households which cannot cover

for one and two months of basic expenses resorting to their bank deposits, pension income and (precovid19) public transfers, and 50% of their gross privately earned income.

The survey is representative of households residing in each of the 21 EU countries covered: Croatia, Poland and Hungary and the Euro Area excluding Spain. Weights provided ensure the number of households matches the total number of households in the country. The survey provides information on all individuals within each household sampled.

We determine which households in the sample cannot afford their typical expenses (as explained below) with certain types of resources (e.g., only with their bank deposits) and count the number of individuals living in such households. We then extrapolate for the country's population by weighing each individual within a household by that household's weight, as suggested in the HFCS user guide (provided by the ECB alongside the HFCS data), given that weight construction takes into account household composition.

Data has been multiple imputed by the ECB to correct for non-response. The HFCS data thus consists of 5 implicates – datasets with small differences between them in the imputed variables. As described in the HFCS user guide, we resort to averages across the 5 implicates. We calculate, on each implicate, the weighted number of individuals living in households which cannot afford expenses, and report the average number across the five implicates. More information on the sampling design, weighting and multiple imputation is available in the ECB HFCS Wave 3 Methodological Report.

Determining whether households cannot afford expenses

We divide the resources a household has available in m months (pooled resources of all household members) by a basket of expenses in m months (pooled expenses of all household members) and whenever the ratio is below one, we conclude the household cannot withstand expenses.

We thus construct a dummy variable $cannot\_afford\_expenses_h^m$, which, for each household h in an m-month time horizon, is a simple indicator function:

$$cannot\_afford\_expenses_h^m = 1\left\{resources\_to\_expenses_h^m = \frac{pooled\_resources_h(m)}{pooled\_expenses_h(m)} < 1\right\}$$

We change the numerator in an additive way keeping the denominator fixed, and thus identify fewer and fewer households not able to afford expenses. We use variables directly available from the HFCS (further description of the variables used is provided in the HFCS User Database Documentation) and calculate the following ratios:

1. With deposits: $resources\_to\_expenses_h^m = \frac{DA2101}{m\times(HI0100+HI0210)}$
2. With deposits and pension income: $resources\_to\_expenses_h^m = \frac{DA2101+ m\times\frac{DI1500}{12}}{m\times(HI0100+HI0210)}$
3. With deposits, pension income and public transfers but unemployment benefits: $resources\_to\_expenses_h^m = \frac{DA2101+ m\times\frac{DI1500}{12}+ m\times\frac{DI1620}{12}}{m\times(HI0100+HI0210)}$
4. With deposits, pension income and all public transfers: $resources\_to\_expenses_h^m = \frac{DA2101+ m\times\frac{DI1500}{12}+ m\times\frac{DI1600}{12}}{m\times(HI0100+HI0210)}$

Covid Economics 18, 15 May 2020: 157-169

5. With deposits, pension income, all public transfers and 50% of other privately earned income: $resources\_to\_expenses_h^m = \frac{DA2101 + m \times \frac{DI1500}{12} + m \times \frac{DI1600}{12} + 0.5 \times m \times \frac{other\ income}{12}}{m \times (HI0100 + HI0210)}$

Where:

$m = 1,2$ is the number of months considered

HI0100 is the amount spent by the household on food and beverages at home on a typical month;

HI0210 is the amount spent by the household on utilities such as electricity, water, gas, telephone, internet and television on a typical month;

DA2101 is the amount held in deposits, calculated as the total amount in sight and saving accounts the household owns;

DI1500 is gross income the household received from public pensions over the last 12 months;

DI1620 is gross income the household received from social transfers other than unemployment benefits over the last 12 months;

DI1600 is regular social transfers (except pensions), computed as the sum of DI1620 and the sum of gross income from unemployment benefits the household received over the last 12 months;

$other\ income$ is DI1100 + DI1200 + DI1300 + DI1400 + DI1700 + DI1800, which are, respectively, employee income, self-employment income, rental income from real estate property, income from financial assets, regular private transfers and income from other sources over the last 12 months. It excludes income from public pensions (DI1500) and income from public transfers other than pensions (DI1600).

Expenses with rent and mortgages

To determine whether households can afford expenses once housing expenses are considered, we increase the denominator $pooled\_expenses_h(m)$, of all ratios described above.

We add monthly rent (HFCS variable HB2300) and monthly mortgage payments (HFCS variable HB200) on the household's main residence. For the latter, we consider loans contracted to purchase, construct, refurbish or renovate the household's main residence (the purpose of the loan is described in HFCS variable HB120).

We change the denominator in this way only for households which own no other residential properties, that is, no flat, houses or apartment buildings, (based on HFCS variable HB250). The objective is to capture only the most vulnerable individuals, who would not have an alternative residence in case they were not able to face housing expenses. Some of the individuals we exclude might also have no alternative residence if their properties are for instance rented out, so the exercise is conservative.

Cash savings

The survey does not provide information on savings individuals might hold in cash. The analysis overall is performed considering only households which have a bank account, based on HFCS variable DA2101i 'has deposits'. These households are less likely to use cash as an important source of savings.

Covid Economics 18, 15 May 2020: 157-169

As a sensitivity analysis, we keep only households which have a bank account, but we allocate cash to all individuals above 18, and add them to their household available savings, that is, we increase the numerator $pooled\_resources_h(m)$. We use Table 5 from Esselink and Hernandez (2017), transcribed below, which provides percentages of individuals in different precautionary cash savings brackets, by country:

Precautionary cash reserves by value ranges, by country (Esselink and Hernández (2017))

	0-99	100-250	251-500	501-1000	Total < 1000	Total > 1000	Refusal
AT	14%	22%	20%	14%	70%	18%	12%
BE	20%	25%	26%	12%	82%	9%	8%
CY	31%	34%	11%	8%	84%	4%	12%
EE	19%	24%	15%	13%	72%	14%	14%
GR	15%	18%	16%	20%	69%	18%	14%
ES	17%	20%	21%	17%	75%	15%	10%
FI	20%	25%	19%	14%	79%	12%	10%
FR	30%	22%	17%	11%	80%	12%	8%
IE	20%	26%	21%	17%	83%	8%	9%
IT	17%	23%	22%	19%	82%	10%	8%
LT	16%	16%	18%	14%	64%	20%	16%
LU	13%	18%	27%	15%	73%	15%	11%
LV	20%	20%	17%	15%	72%	13%	16%
MT	20%	25%	29%	13%	87%	3%	10%
NL	36%	21%	13%	7%	77%	4%	19%
PT	32%	23%	16%	9%	80%	7%	13%
SI	15%	16%	17%	13%	60%	23%	17%
SK	27%	20%	20%	14%	80%	9%	11%

Source: Table 5 of Esselink and Hernández (2017).

'Refusal to answer' percentages were distributed in proportion of the respondents' brackets.

We then allocated cash savings randomly among all individuals aged 18 or above to match the country percentages, modified to accommodate for those who refused to answer. Individuals are randomly assigned to each bracket of precautionary savings in cash and allocated the midpoint of the interval. Individuals assigned to the bracket 'above 1000' were assigned 1500 euros.

Results are without allocated cash savings unless stated otherwise.

Migration background

The ECB HFCS survey provides information on the country of birth of each sampled individual, specifically, whether he was born in his current country of residence, elsewhere in the EU, or elsewhere in the World (variable RA0400). We compare the percentage of individuals residing in their country of birth who cannot afford two months of expenses with the percentage of individuals residing in the same country but born elsewhere in the EU and in the World who cannot.

Covid Economics 18, 15 May 2020: 157-169

Covid Economics **Issue 18, 15 May 2020**

Internal migration and the spread of Covid-19[1]

Michele Valsecchi[2]

Date submitted: 10 May 2020; **Date accepted:** 11 May 2020

In this paper, I hypothesize that internal migrants are key agents in the diffusion of viruses. Self-isolation and closure of economic activities in outbreak areas generate many people jobless or socially isolated. Recently settled migrants might therefore choose to return to their home towns, thus spreading the virus further. To test the existence and the quantitative importance of this mechanism, I use subnational data for Italy. I use panel data at the regional-daily level and exploit detailed data on individuals' changes of residence between Italian regions before Covid to measure, for each region, the number of potential of return migrants from outbreak areas. The results suggest that regions with more exposed to return migration experienced more Covid deaths throughout nearly all stages of diffusion of the virus. A back-of-the-envelope calculation suggests that, had all regions had the same number of migrants in outbreak areas as the one at the tenth percentile, Italy would have experienced around 2000 fewer Covid deaths, i.e, 22-24 percent fewer deaths than the regions outside the outbreak areas actually experienced.

Covid Economics 18, 15 May 2020: 170-195

1 I received useful comments from Douglas Campbell, Ruben Enikopolov, Tatiana Mikhailova, Maria Petrova and participants at the NES brown bag seminar.
2 Department of Economics, New Economic School.

Covid Economics 18, 15 May 2020: 170-195

1 Introduction

Covid-19 has claimed more than 200,000 lives so far[1]. It is also generating massive and unprecedented economic costs in terms of health care (e.g., hospitalization of sick people, testing of sick and healthy, quick expansion of intensive care health capacity), in terms of missed work, both direct (e.g., lost work due to sickness) and indirect (e.g., lost work due to quarantine measures), and in terms of lost human capital (e.g., lost education due to quarantine measures). Some economists expect the worst recession since the 1930s.[2]

In this paper, I hypothesize that internal migrants are key agents in the diffusion of viruses. This is because migration is a natural response in the face of disaster (Boustan et al 2012, Hornbeck 2020). This is be especially true if the government's main responses, *i.e*, self-isolation, social distancing and the shut-down of major economic activities is expected to last for a long time, or if the effect of these measures on the economy is so disruptive as to leave people jobless (Topel 1986). The people most likely to migrate away from the outbreak areas will be those with weak ties locally and strong ties elsewhere,[3] like recent internal migrants.[4] Unless potential return migrants realize they could be asymptomatic carriers (or interpret their symptoms correctly as signs of Covid) and internalize the effect of their actions on others, they will migrate and thus spread the virus further.

To test the existence and the quantitative importance of this mechanism, I use sub-national data for Italy. Covid, in Italy alone, has claimed more than 19,000 lives:[5] until recently, it was the worst hit European country by absolute number of deaths and by deaths per capita. Sadly, this provides me with substantial statistical power to test my hypothesis. I use panel data at the regional-daily level and exploit detailed data on individuals' changes of residence between Italian regions before Covid to measure the number of potential of internal migrants in outbreak areas who might return to their home towns (thus spreading the virus) as Covid restrictions leave them jobless or socially isolated. The results suggest that a standard deviation increase in the share of recent migrants to outbreak regions is associated with around 110 additional deaths over the two months period of available data. A variety of robustness tests and placebo estimations supports

[1] 238,628 lives at the 3^{rd} May 2020, according to the World Health Organization Situation Report - 104.

[2] There are obvious difficulties in predicting the effect of Covid on the macroeconomy. Goldman Sachs (2020) predicts a GDP loss of 9 percent in Q1 and 34 percent in Q2. Estimates that rely on the Spanish flu suggest it might generate a 6 percent GDP loss (Barro et al, 2020). See Eichenbaum et al (2020) and references therein for alternative approaches.

[3] Reasons for weak ties where they reside could be social (e.g., family somewhere else) or economic (e.g., not owning the house they live in, having informal employment or a short-term contract).

[4] These could be temporary migrants (who would have gone back anyway) anticipating their return, or permanent migrants changing their plans. Dustmann and Görlach (2016) provide a review of theory and evidence on return migration. Yang (2006) provides evidence of a negative economic shock increasing return migration, even though that was in the context of international migration at the time of the Asian financial crisis.

[5] 19,899 lives at the 12^{th} April 2020, according to the Italian Health Minister daily report.

this finding. A back-of-the-envelope calculation suggests that, had all regions had the same number of migrants in outbreak areas as the one at the tenth percentile, Italy would have experienced around 2000 fewer Covid deaths, *i.e*, 22-24 percent fewer deaths than the regions outside the outside the outbreak areas actually experienced.[6]

This paper makes three contributions. First, it contributes to the growing literature on Covid-19 and viruses in general. Such literature may be grouped into three strands. The first one focuses on estimating the effect of restrictions.[7] The second one focuses on the determinants of compliance to self-isolation measures.[8] The third one focuses on the determinants of the spreading of viruses other than government imposed restrictions, like railways (Adda 2016), trade (Oster 2012), paid sick leave (Barmby and Larguen 2009; Pichler and Ziebarth 2019) and Facebook connections (Kuchler et al 2020). I suggest a novel diffusion mechanism (internal migration) and find that it is not only statistically but also quantitatively very important. Future research should test the existence and quantitative importance of this mechanism in other countries.

The second contribution has to do with the Black Death (1347-1351). At that time, cities were death traps: both in absence of the virus (Woods 2003, Clark and Cummins 2009, Voigtländer and Voth 2013) and especially when the virus started spreading. To escape the virus (and secure some food), many escaped to the countryside (Boccaccio 1352, Carmichael 2014). It is not hard to imagine that some of those people brought the virus with them, and that such escape might have been more likely for people born in the countryside to start with (since they might have had a home town to go back to). However, to the best of my knowledge, no paper in the literature on the Black Death has investigated this possibility. Jedwab et al (2019) is the only attempt to analyse the spatial dimension of the Black death, albeit only for cities. Future research could try to gather similar data for rural areas and estimate the dynamics of the spreading of the disease.[9]

The third contribution is to the literature on the effect of migration on countries and locations of origin. Such literature may be grouped into two strands. The first one focuses

[6]Return migration is a choice. Hence, rather than framing the back of the envelope calculation in terms of what would have happened had regions had less migrants, one could think about it in terms of what would have happened had all regions managed to persuade migrants to stay in outbreak areas as much as the region at the tenth percentile. I will come back to this point towards the end of the paper.

[7]Here the most important contribution is probably Adda (2016), who analyzes the effect of school and public transportation closure for many (pre-Covid19) viruses using French data. Litvinova et al (2019) instead look at school closure using Russian data. For Covid-19, Bayham and Fenichel (2020) look at school closure using US data, while Fang et al (2020), Qui et al (2020), Chinazzi et al (2020) and Kraemer et al (2020) look at city lock down using Chinese data. Gatto et al (2020) instead use an epidemiological model to estimate the combined effect of all restrictions on the spread of infections using Italian data.

[8]Briscese et al (2020) estimate the effect of expected duration of restrictions on intention to comply, while Durante et al (2020) estimate the effect of social capital on compliance. Chudik et al (2020) look at voluntary and mandatory social distancing in Chinese provinces.

[9]Another historical episode lending credit to this mechanism may be the Spanish flu (1918-1919) and the role of soldiers' coming back from the front at the end of WWI (1914-1918), since the two overlapped for nine months. See Beach et al (2018) and references therein for recent work on the Spanish flu using micro-data. See Barro et al (2020) for a recent cross-country analysis.

Covid Economics 18, 15 May 2020: 170-195

on the overall effects of migration on countries[10] and areas[11] of origin. The channel of transmission in this literature is typically information, network effect, return migration or a combination of the three. The second strand of literature focuses instead specifically on return migration.[12] None of these papers considers the role of migration in spreading diseases back home. This is surprising, because the threat that migration poses in terms of health risk is well known not just from the time of Ellis Island and the age of mass migration to the US, but also by Diamond's description of how colonizers spread diseases during the colonization of the Americas (Diamond 1997).

Besides contributing to the economic literature on Covid and other viruses, this paper aims to inform policy-making on the dynamics of the spreading of Covid and therefore help governments enact more effective tracing and testing policies. Specifically, the evidence provided here suggests that, rather than passively tracing the contacts of positive cases, governments could anticipate potential super-spreaders, persuade them not to migrate and anyway tracking them before even having evidence of their positivity. This could be done using information that are already public (like the changes of residences). It could be used not only in future pandemics, but possibly already during the second wave of the Covid pandemic, since various commentators expect a second wave in Europe during the fall of 2020. Indeed, Surico and Galeotti (2020) stress that one should not forget that the effort we are making now to respect quarantine measures is not aimed at erasing the virus. It is aimed at buying ourselves time to prepare for the second wave of contagion.

2 Context

The first confirmed cases in Italy date back to the 30^{th} January 2020. By the end of February, the confirmed cases were in the hundreds. On the 21^{st} February, Italy had the first Covid death. The country recorded more than 77,000 cases (and 12,000 deaths) by the end of March and more than 100,000 cases (28,000 deaths) by the end of April.

During the health crisis, the Government took unprecedented measures, which started

[10]This literature suggests that international migration may have the following effects on countries of origin: greater bilateral trade (Parsons and Vezina 2014), FDI (Burchardi et al 2018), economic development (Burchardi and Hassan 2013), innovation (Kerr 2008), greater membership to labour unions, voting and public expenditure (Karadja and Prawitz 2019) and democratic capital at large (Pfutze 2012, Docquier et al 2016), greater collectivism (Knudsen 2019), religiosity (Rahman 2020) and a change in fertility norms (Beine et al 2013). See also Anelli and Peri (2017) for evidence democratic capital that stand in constrast with some of the other papers.

[11]This literature suggests that internal migration may have the following effects on areas of origin: greater risk spreading (Gröger and Zylberberg 2016 and references therein), which might also be a determinant of migration itself, greater support for right wing parties (Mantovani 2019) and different fertility norms (Daudin et al 2016).

[12]This literature suggests that the return migration may foster democratic capital among the population at large (Chauvet and Mercier 2014, Barsbai et al 2017) and among leaders (Spilimbergo 2009, Mercier 2016, Grewal 2020); may foster local development (Chauvet et al 2014); may be profitable (Abramitzy et al 2019); may lead to greater entrepreneurship (Yang 2008); and may be associated with newer attitudes and beliefs (Clingsmith et al 2009).

Covid Economics 18, 15 May 2020: 170-195

with an initial lock-down in the province of Lodi (21^{st} February)[13] and school closure in Lombardia, Veneto, Emilia-Romagna and Friuli-Venezia Giulia (24 February), continued with the expansion of the lock-down to most of northern areas (08^{th} March) for a total coverage of 16 million people, and finally reached the national level (9^{th} March).[14]
As the news of the expansion of the lock-down leaked (Saturday 7^{th} March),[15] people rushed to take night trains from Milan to the rest of the country to escape the quarantine measures. It was common wisdom in the media at that time that such mass departure would helped spreading the disease.[16]

People leaving Milan are presumably internal migrants who had come to Milan for studies or work. Hence, the higher the number of out-migrants (to Lombardy) a region has, the higher should be the number of return migrants the same region experienced on the 8^{th} March (or later), and the higher should be the number of infected cases and deaths by Covid-19 later on.

3 Data and research design

3.1 Data

To measure the exposure of Italian regions to return migration from outbreak areas, I use yearly data on changes of residence between any two Italian regions.[17] The data are available up until 2018 and are structured as a full matrix, *i.e*, the data provide the number of people who de-registered themselves from, say, Sicilia, and registered themselves in one of the outbreak regions (Lombardia, Veneto and Emilia-Romagna; henceforth, LVE) in a given year.[18] I focus on changes of residence to LVE regions and collapse the data by time. Specifically, to capture to full set of potential return migrants, I aggregate up changes of residence for the last three available years (2018, 2017 and 2016) to have the share of people who migrated to LVE between 2015 and 2018 for each 1000 inhabitants.[19]

To measure the number of Covid-19 deaths,[20] I use daily data from the Italian Ministry of Health elaborated by the Department of Civil Protection.[21]

[13]Decreto del presidente del consiglio dei ministri 22 febbraio 2020
[14]Decreto del presidente del consiglio dei ministri 09 marzo 2020
[15]Severgnini (8 March 2020). Corriere della Sera
[16]Giuffrida and Tondo (8 March 2020). The Guardian.
[17]Data provided by the Italian National Institute of Statistics (ISTAT).
[18]People have an incentive to register themselves in their new residence to get access to some basic services like, among others, the family doctor.
[19]The analysis does not seem sensitive to the precise choice of temporal window, because I ran the analysis using 2017-2018 and 2013-2018 migrants and obtained results that are very similar to those presented here.
[20]Throughout the entire paper, I focus on Covid deaths, rather than Covid infections, because the Italian government, along many other central governments around the world, tested primarily people showing symptoms of infection, rather than pursuing quasi-random testing (as in Iceland and South Korea).
[21]Data and description are available at: https://github.com/pcm-dpc/COVID-19

Covid Economics 18, 15 May 2020: 170-195

Covid Economics 18, 15 May 2020: 170-195

3.2 Descriptive statistics

Table 1 shows the descriptive statistics. Between 23^{rd} February and the 4^{th} of May, the average number of Covid deaths (per million inhabitants) outside the outbreak regions was 4.65. Figure 1.a) shows the evolution of Covid deaths over time: Covid deaths peaked between the 27^{th} March and the 3^{rd} April, and slowly decreased thereafter.

Table 1: Descriptive statistics

Variable	N	Mean	Std. Dev.	Min.	Max.
Covid deaths (region-daily level)					
deaths per mln people	1224	4.29	7.93	0.00	95.09
Migrants (region level)					
to LVE (per 1000 inh.)	17	7.13	1.82	4.66	11.46
to Lombardia (per 1000 inh.)	17	3.56	1.30	1.97	6.76
to Veneto (per 1000 inh.)	17	1.42	1.17	0.69	5.48
to Emilia-Romagna (per 1000 inh.)	17	2.15	0.99	1.05	3.64
to any region (per 1000 inh.)	17	19.37	5.37	12.06	30.79
Controls (region level)					
Distance to Milano (km)	17	606	375	144	1466
People with High School or higher	17	0.45	0.05	0.40	0.57
People with Bachelor degree or higher	17	0.14	0.02	0.11	0.20
Newspaper readership (at least once a week)	17	0.38	0.09	0.26	0.58
Newspaper readership (five times a week)	17	0.32	0.07	0.22	0.45
Trust in others	17	0.21	0.06	0.13	0.37
Unemployment	17	0.12	0.05	0.04	0.22
Regional GDP	17	0.03	0.01	0.02	0.04
Intensive care beds (per 100,000 inh.)	17	8.43	1.45	5.75	11.56

Source: LVE stands for Lombardia, Veneto and Reggio-Emilia. Migration computed from changes of residence between 2015 and 2018. All control indicators are per capita unless otherwise indicated. Control variables based on 2018 data except intensive care beds (2019).

Figure 1.a) also shows the evolution of Covid deaths in the outbreak regions. Covid clearly arrived later in non-outbreak regions and had a much lower intensity throughout the entire period, even though there is a clearly a convergence over time between outbreak and non-outbreak regions. The hypothesis in this paper is that internal migration might be a driver of such convergence.

Non-outbreak regions have an average of 7.13 migrants (per 1000 inhabitants) to the outbreak regions. This measure captures regional exposure to return migration and it is the key indicator of this paper. Migrants to Lombardia are the highest number (3.56), followed by Emilia-Romagna (2.15) and Veneto (1.42). Figure 1.b) shows how exposure to return migration varies across regions. Southern regions are more exposed than Northern regions, which is not surprising for anybody familiar with Italian migration. Yet, the map shows interesting heterogeneity in exposure even among regions that have a similar

Covid Economics 18, 15 May 2020: 170-195

Figure 1: Evolution of Covid-19 deaths and distribution of migrants to outbreak

(a) Deaths inside and outside outbreak regions

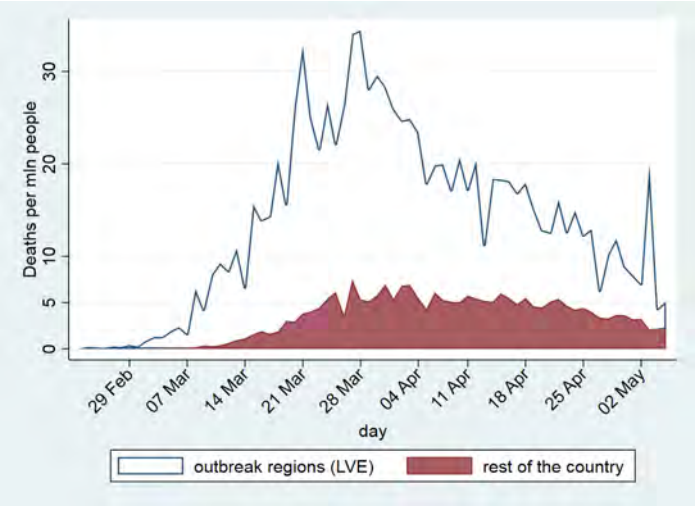

(b) Distribution of potential return migrants

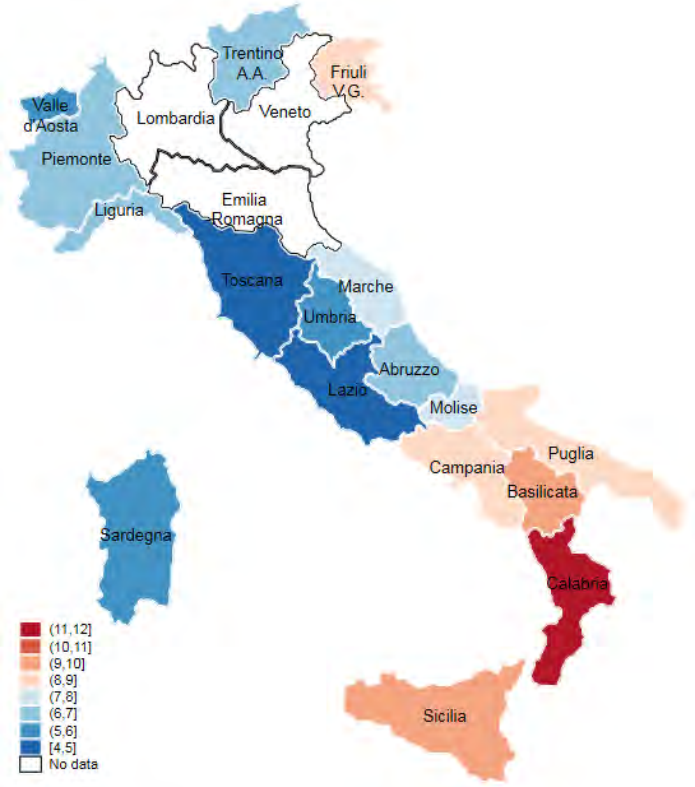

Notes: data on Covid deaths from the Italian Ministry of Health, provided by the Department of Civil Protection; data on number of migrants to outbreak areas by ISTAT; dates in panel a) are the mid-points in the week. LVE stands for Lombardia, Veneto and Emilia-Romagna.

distance to the outbreak. This is an important point for identification and I will discuss it further in the next section.

Table 1 also shows that non-outbreak regions have an average of 19.37 migrants to the rest of the country. This means that, while LVE constitute an important migration hub, it is by no means the only one. Besides LVE, the regions with the greatest internal migration are Lazio (2.29), Piemonte (1.86), Campania (1.38), Toscana (1.33) and Puglia (0.97). Having alternative migration destinations is important because it provides me with opportunities for placebo estimations.

3.3 Econometric specification

To test the relationship between return migration and the spread of Covid-19, I would need regional-daily data on the number of return migrants. Such information does not exist. Even if it did, return migration would likely be endogenous to the spread of Covid-19, because the migrant's decision to return to her hometown would likely depend also on health capacity and health conditions in the region of origin.[22]

I replace regional-daily data on return migrants with interactions between regional data on the number of potential return migrants in the outbreak areas in 2018 (*i.e*, well before Covid-19) and week dummies. Here we estimate the simple specification:

$$\text{arcsinh}(CovidDeaths_{r,day}) = \alpha_r + d_{day} + \beta_{week} ln(migrantsToLVE_r) \times d_{week} + X'_{r,week}\Gamma + \epsilon_{r,day}$$

where $CovidDeaths_{r,day}$ is the number of Covid-19 deaths in region r in a given day. The number of potential return migrants from outbreak areas is proxied by the number of migrants who left region r and settled in one of the outbreak areas (LVE) between 2015 and 2018:[23] $migrantsToLVE_r$. The other elements are region fixed effects (α_r), day fixed effects (d_{day}), a set of interactions between (pre-determined) time-invariant controls and week indicators ($X_{r,week}$) and an error term ($\epsilon_{r,day}$). I cluster standard errors at the regional level to take into account serial correlation in the error term.[24] Since I am interested in how the number of potential return migrants affects the Covid-related death risk for the average Italian resident (rather than the average region), I weigh observations by population size.

The challenge of this empirical strategy is that, even after controlling for region fixed effects and avoiding the obvious endogeneity of return migration, there might be time-varying characteristics correlated with both the number of migrants to outbreak areas and the latent risk of Covid deaths in a given region. To address this concern, I ex-

[22]This would presumably work as an attenuation bias, since potential return migrants facing nasty conditions in the region of origin would presumably stay in the outbreak area

[23]Data on changes of residence for 2019 are not yet available.

[24]Because of the limited number of clusters (17), I will report also the p-values associated with wild cluster bootstrap standard errors (Cameron, Gelbach and Miller 2008).

Covid Economics 18, 15 May 2020: 170-195

ploit the richness of data on Italian regions and control for a wide range of potential confounders (each interacted with week dummies).[25] The first one is distance to Milano, which should be correlated with migration to LVE (because of the South-North internal migration route) and might be correlated with Covid deaths. The correlation with Covid deaths would exist if distance to Milano captured the gradual spreading of Covid through mechanisms other than migration, like work activities and social interactions.[26] The second control is a proxi for compliance with social distancing and other quarantine measures. I construct this proxi by taking the first principal component of several indicators for people's education and social capital: share of people with at least high school education, share of people at least a bachelor degree, newspaper readership (at least once a week and, separately, five times a week or more), trust in others.[27] If this measure is correlated with Covid deaths (which seems reasonable) and migration to LVE (which one cannot exclude a priori), then this might turn out to be an important control. Along similar lines, I control for a proxi for health and, more broadly, state capacity. I construct this proxi by taking the first principal component of the following measures: share of unemployed people (relative to the workforce), regional GDP per capita and number of intensive care beds for 100,000 inhabitants. The fourth control is the share of people at risk, measured by the share of people who are at least 70 years old. Finally, I control for total number of migrants to other Italian regions.

In absence of any prior on whether a log-log, linear-log or linear-linear specification might be most appropriate, I will estimate all three models. For the sake of brevity, I report coefficient estimates for the log-log specification here, and report the coefficient estimates for the other two models in the Appendix. Results are very similar anyway. Since Table 1 showed that the number of Covid deaths at the region-daily level has many zeros, an inverse hyperbolic sine transformation seems better than a log transformation. The interpretation of the coefficients with an arcsinh-log specification is similar to what we would have with a log-log specification (Bellemare and Wichman 2020).

[25] In addition, I plan to extend the analysis with an instrumental variable strategy.

[26] Since Milano is the economic center of the Northern regions, highway and railway infrastructures are designed to optimize the traffic to and from it. In addition, the worst outbreak areas are located around Lodi, which is just a few kilometres south of the city. For these reasons, controlling for distance to Milano seems the best way to control for effective distance to the outbreak areas. Nonetheless, I experimented using the minimum of the distance to Lombardia, Veneto and Emilia-Romagna and results are very similar.

[27] Durante, Guiso and Gulino (2020) build a similar measure based on newspaper readership, trust in others and blood donations and show that it is correlated with mobility during the Covid period.

Covid Economics 18, 15 May 2020: 170-195

Covid Economics 18, 15 May 2020: 170-195

4 Results

Table 2 shows the main results. The number of potential return migrants from the outbreak regions has no effect on Covid deaths when controlling for region and day fixed effects but no additional control (Column 1): the coefficient estimates are negative and nowhere near statistical significance. However, as soon as one controls for distance to Milan (Column 2), the post-11^{th} March coefficient estimate becomes positive, large and precisely estimated. A one percent increase in the number of potential return migrants (per 1000 inhabitants) is associated with a 0.7 percent increase in the number Covid deaths (per million inhabitants). This is exactly consistent with the scenario described in Section 2: as Covid deaths started to appear in the outbreak regions, and the local and central government started locking down more and more provinces, recent migrants started returning to their regions of origin, either because they could not work any more, either because they forecasted forthcoming restrictions to economic activities and possibly to mobility across regions.

The inclusion of additional controls, like compliance with social distance and quarantine measures (Column 3), state and health capacity (Column 4), share of the population at risk (Column 5) and total number of potential return migrants (Column 6) changes slightly the magnitudes, but does not change neither their precision nor the overall take-away message. The coefficient estimates are even robust to the inclusion of all controls in the same specification (Column 7).

It is useful to look at how the effect evolves over time. Figure 2.a) plots the coefficient estimates associated with the specification with full week interactions for the migration indicator and all other controls.[28] Interestingly, regions more exposed to return migration suffered more deaths already during the week running from the 11^{th} to the 17^{th} of March, and then again more systematically with the week starting on the 25^{th} of March. This is consistent with the migration having started in late February, and having being reinforced by the exodus of the 7^{th} of March.[29] This said, the coefficient estimates associated with the linear-log and linear-linear specifications (Figures A.2 and A.3) show that the early effect is relatively small in terms of additional deaths.

[28]The coefficient estimates associated with Figure 2 can be found in Table A.1, Column 7. The coefficient estimates associated with the controls can be found in Figure A.1.

[29]In fact, it is very possible that most of the migration took place immediately on the 23^{th} and 24^{th} February, when schools and universities in the North closed (Jaime D'Alessandro, Repubblica of the 23^{rd} of March).

Table 2: Internal migration and Covid deaths by period.

	(1)	(2)	(3)	(4)	(5)	(6)	(7)
ln(migrantsToLVE)							
× (26^{th}Feb.-10^{th}Mar.)	-0.058	0.112	0.166	0.166	0.119	0.116	0.127
	(0.070)	(0.074)	(0.143)	(0.107)	(0.089)	(0.087)	(0.138)
	0.405	0.053	0.196	0.084	0.095	0.141	0.352
× (11^{th}Mar.-4^{th}May)	-1.010	0.702***	1.167**	1.201***	0.732***	1.048***	1.300***
	(0.818)	(0.232)	(0.462)	(0.405)	(0.215)	(0.273)	(0.427)
	0.307	0.063	0.020	0.009	0.063	0.033	0.023
Mean	1.295	1.295	1.295	1.295	1.295	1.295	1.295
R-squared	0.780	0.849	0.850	0.851	0.850	0.851	0.853
Number of regions	17	17	17	17	17	17	17
Observations	1,224	1,224	1,224	1,224	1,224	1,224	1,224
Day FE	Yes	Yes	Yes	Yes	Yes	Yes	Yes
Region FE	Yes	Yes	Yes	Yes	Yes	Yes	Yes
Distance to Milano	-	Yes	Yes	Yes	Yes	Yes	Yes
Compliance to quarantine	-	-	Yes	-	-	-	Yes
State capacity	-	-	-	Yes	-	-	Yes
Pop. at risk	-	-	-	-	Yes	-	Yes
Total emigrants	-	-	-	-	-	Yes	Yes

Notes: Dependent variable is the the Inverse Hyperbolic Sine (IHS) of the number of Covid-19 deaths (Italian Health Ministry). LVE stands for Lombardia, Veneto and Emilia-Romagna (the outbreak regions). The number on migrants is the number of people who changed their residence to one of the outbreak regions between 2015 an 2018 (three years) according to the Italian National Institute of Statistics (ISTAT). Control for "compliance with quarantine" is the first principal component of: share with higher school education, share with university education, newspaper readership (at least once a week), newspaper readership (at least five times a week), trust in others. Control for "state capacity" is the first principal component of: unemployment share, regional GDP per capita, number of intensive care beds per 100,000 inhabitants. Control for "population at risk" is the share of people with 70 years old or more. Control for "total emigrants" is the number of people who changed residence to another Italian region between 2015 and 2018. All controls are in logarithms. For each interaction, the table reports coefficient estimates on the first row, standard errors clustered at the region level (in brackets), and p-values for wild cluster bootstrap standard errors la Cameron, Gelbach and Miller 2008). *** p<0.01, ** p<0.05, * p<0.1.

Figure 2: Migrants to outbreak and Covid-19 deaths

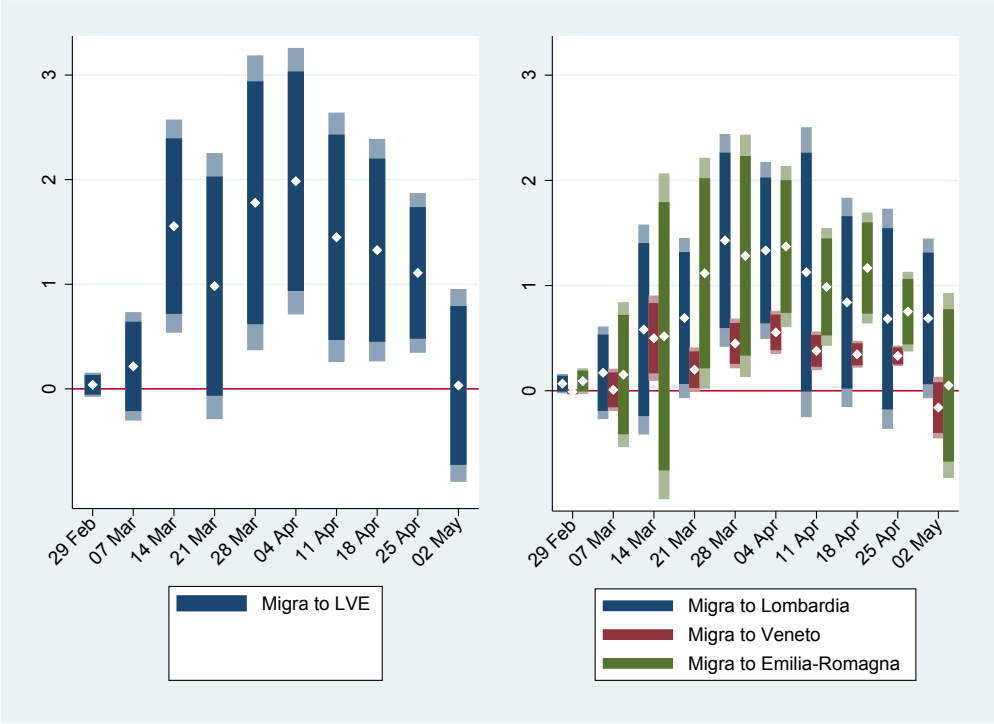

Notes: dark colors represent 90 percent confidence intervals; light colors represent 95 percent confidence intervals; dates are the mid-points in the week. LVE stands for Lombardia, Veneto and Emilia-Romagna.

Two additional tests strengthen the confidence towards these results. First, the estimates are robust to dropping one region at a time (Figure A.4). Second, and most importantly, I can exploit the data on the number of potential return migrants to any region other than LVE to estimate a whole set of placebo estimations. If what drives the main effect is migration from the outbreak regions, rather than general migration, then I should not observe any effect for migration to, say, Liguria or Piemonte.

Figure 3 shows the coefficient estimates associated with this exercise. The results are fairly striking: migration to any of the non-outbreak regions is never associated with an increase in the number of Covid deaths except perhaps for the cases of Friuli-Venezia-Giulia and Trentino Alto Adige. The fact that 15 out of 17 placebo estimations show no effect is very reassuring. In addition, it is easy to note from Figure 1.b) that the two regions showing a positive effects are located at the extreme North-East of the country, above Veneto and Lombardia. Indeed, Friuli-Venezia Giulia was among the regions that imposed school closure at the same time as LVE already on the 24^h February. Hence, it could well be that the effect they show is still a consequence of migrants bringing back to the regions of origin some of the virus that spilled over from the outbreak areas.

Covid Economics 18, 15 May 2020: 170-195

Figure 3: Placebo estimates: effect of migration outside outbreak regions

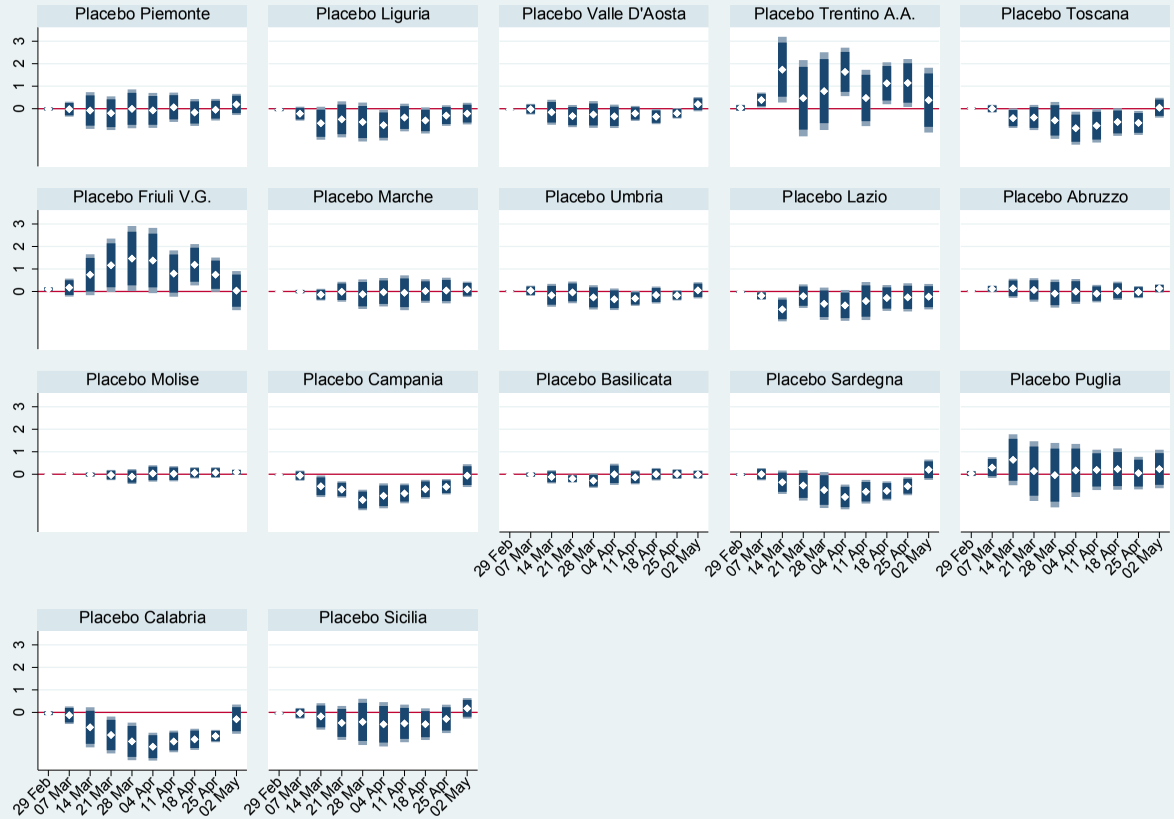

Notes: dark colors represent 90 percent confidence intervals; light colors represent 95 percent confidence intervals; dates are the mid-points in the week. LVE stands for Lombardia, Veneto and Emilia-Romagna.

Finally, estimating the relationship between the number of potential return migrants and Covid deaths using a linear-log and a linear-linear model provides also positive and precisely estimated effects.[30]. The results for the linear-linear specification suggest that a one standard deviation increase in number of migrants per 1000 inhabitants (1.82) leads to an additional 5.6 Covid deaths (per million inhabitants) during the 2^{nd} week of March, 8.5 during the 3^{rd} week, 21.7 during the 4^{th} week, 24.9 during the 1^{st} week of April, 16.0 during the 2^{nd} week, 15.8 during the 3^{rd} week, 9.6 during the 4^{th} week and 3.6 during the week starting at the end of April and ending in May. Altogether, it leads to an additional 106 Covid deaths per million inhabitants.[31]

A back of the envelope calculation suggests that, if all regions had had the same number of migrants per 1000 inhabitants as the 10^t percentile (*i.e*, 5), there would have been between 2,083 and 2,261 fewer Covid deaths. Since during this period, outside the outbreak regions, Italy experienced 9,591 Covid deaths, the death toll would have been between 22 and 24 percent lower.

Another interesting exercise has instead to do with the disaggregation of the effect by number of migrants to each outbreak region. Figure 2.b) [32] shows that the effect of a one percent increase in migration is greatest for Lombardia and Emilia-Romagna,[33] while it is remarkably lower for Veneto. This is consistent with multiple reports arguing that the regional government in Veneto took much better decisions than its counterpart in Lombardia (Pisano, Sadun and Zanini 2020).[34]

5 Conclusions

In a moment when Covid-19 is rapidly spreading both across and within countries, and there is a pletora of (sometimes conflicting) policy recommendations provided to governments around the world, it is more important than ever to test the existence of diffusion

[30]For the linear-log model, see Figures A.1 and Table A.2. For the linear-linear model, see Figure A.2 and Table A.3.

[31]The coefficient estimates for the ihs-log and linear-log specifications provide very similar magnitudes. A one standard deviation in the linear-linear specification corresponds to a 25.6 percent increase. Based on this, the ihs-log specification suggests 114 deaths, while the linear-log specification suggests 105 deaths.

[32]The coefficient estimates associated with Panel B are obtained by replacing the interactions between log(number of migrants to LVE per 1000 inhabitants) and week dummies with three sets of interactions: log(number of migrants to Lombardia), log(number of migrants to Veneto) and log(number of migrants to Emilia-Romagna), each interacted with week dummies.

[33]Since Lombardia is the region with the highest number of migrants, the disaggregated effects suggest that, for a similar increase in the number of migrants, the effect would be larger in Emilia-Romagna than in Lombardia. This is confirmed by the disaggregation for the linear-linear specification (Figure A.2.b)).

[34]Both Lombardia and Veneto took similar measures regarding social distancing and closure of retail shops. Yet, Veneto took a very different approach regarding testing and decentralized health care: tested started early and covered both symptomatic and asymptomatic individuals; co-residents and neighbours of positive cases were tested systematically (and home quarantine was imposed on co-residents when testing was not available); testing took place at individuals' homes rather than in hospitals; special care was devoted to the systematic testing of health operators and workers at risk.

Covid Economics 18, 15 May 2020: 170-195

mechanisms and to quantify their magnitude. This is what this paper attempts to do. I hypothesize that recently settled workers in outbreak regions might help spread the virus to other areas of the country. I then test for this hypothesis using regional-daily data on Covid-19 deaths and data on recent changes of residence for any two Italian regions. The results suggest that regions more exposed to return migration experience more Covid deaths than less exposed regions during all weeks in which Covid sows death except the starting and the ending weeks. The likely mechanism seems to be return migration.

The present analysis suggests that this effect seems not only statistical but also quantitatively important. A back of the envelope exercise suggests that, had all regions had the same number of emigrants as the tenth percentile at the peak of the crisis, Italy would have experienced around 2000 fewer Covid deaths. Given that the country experienced around 9,500 deaths during the period (outside the outbreak areas), this corresponds to a 22-24 percent decrease.

While there is no guarantee that these results replicate in other countries, some facts suggest they might. First, big cities are typically the location with the highest risk of an outbreak, because of high population density and links to internal trade and tourism. Second, internal migration is a common phenomenon across countries (Young 2013, United Nations 2013, Bell and Charles-Edwards 2014). Third, internal migrants in big cities often have informal jobs and lack formal social insurance mechanisms that make them one of the most vulnerable categories of workers in case of lockdown.[35] This is true in Italy, where recently settled internal migrants might have informal jobs (or short-term contracts) in bars, restaurants and cafes. It is even truer in developing countries, where internal migrants in big cities have the same (or higher) job instability (Kwakwa, 2020) and also often live in informal settlements where the risk of contagion might be even higher.

The results reported in this paper suggest that recent internal migrants in outbreak areas are more likely than others to become super-spreaders, *i.e*, individuals who directly infected a dozen or more people, not because of some medical condition, but because of the likelihood that they will go back to their hometowns and spread the virus in a relatively virgin territory. The good news is that, to the extent our registry-based measures captures a good share of them (rather than being only a proxi), they are easily traceable even in absence of sophisticated technologies or voluntary consent to install an app in their phone: the municipality where they reside knows their status. This is true for Italy but it must be true for other countries as well. A decently functioning central government could even centralize the information, send them targeted information to persuade them not to live the outbreak areas, and alert the municipalities in their hometowns for their potential arrival.

[35]Such risk is highlighted work by Mikhailova and Valsecchi (2020), where we provide some preliminary results for Italy and describe the case of Russia.

Covid Economics 18, 15 May 2020: 170-195

Covid Economics 18, 15 May 2020: 170-195

Finally, these results constitute a red flag as the end of the May 2020 comes closer. This is when the Ramadan finishes and people typically go back to their regions of origin to celebrate Eid al-Fitr.[36] Especially in countries with weak testing capacity, central government authorities might want to consider restricting altogether internal migration related to such festivities even in absence of precise data on the diffusion of the Covid-19.

6 References

Abramitzky, Ran, Leah Boustan, and Katherine Eriksson. 2019. "To the New World and Back Again: Return Migrants in the Age of Mass Migration." ILR Review 72 (2):300-322.

Adda, Jrme. 2016. "Economic Activity and the Spread of Viral Diseases: Evidence from High Frequency Data *." The Quarterly Journal of Economics 131 (2):891-941.

Anelli, Massimo, and Giovanni Peri. 2017. "Does emigration delay political change? Evidence from Italy during the great recession." Economic Policy 32 (91):551-596.

Barmby, Tim, and Makram Larguem. 2009. "Coughs and sneezes spread diseases: An empirical study of absenteeism and infectious illness." Journal of Health Economics 28 (5):1012-1017.

Barro, Robert J., Jos F. Ursa, and Joanna Weng. 2020. "The Coronavirus and the Great Influenza Pandemic: Lessons from the Spanish Flu for the Coronaviruss Potential Effects on Mortality and Economic Activity." National Bureau of Economic Research Working Paper Series No. 26866.

Barsbai, Toman, Hillel Rapoport, Andreas Steinmayr, and Christoph Trebesch. 2017. "The Effect of Labor Migration on the Diffusion of Democracy: Evidence from a Former Soviet Republic." American Economic Journal: Applied Economics 9 (3):36-69.

Bayham, Jude, and Eli P. Fenichel. "Impact of school closures for COVID-19 on the US health-care workforce and net mortality: a modelling study." The Lancet Public Health.

Beach, Brian, Joseph P. Ferrie, and Martin H. Saavedra. 2018. "Fetal Shock or Selection? The 1918 Influenza Pandemic and Human Capital Development." National Bureau of Economic Research Working Paper Series No. 24725.

Beine, Michel, Frdric Docquier, and Maurice Schiff. 2013. "International migration, transfer of norms and home country fertility." Canadian Journal of Economics/Revue canadienne d'conomique 46 (4):1406-1430.

Bell, Martin, and Elin Charles-Edwards. 2014. "Measuring Internal Migration around the Globe: A Comparative Analysis." KNOMAD Working Paper 3.

Bellemare, Marc F., and Casey J. Wichman. 2020. "Elasticities and the Inverse Hyperbolic Sine Transformation." Oxford Bulletin of Economics and Statistics 82 (1):50-61.

[36] This is well documented at least for Indonesia (Wight, 2020).

Boustan, Leah Platt, Matthew E. Kahn, and Paul W. Rhode. 2012. "Moving to Higher Ground: Migration Response to Natural Disasters in the Early Twentieth Century." American Economic Review 102 (3):238-44.

Briscese, Guglielmo, Nicola Lacetera, Mario Macis, and Mirco Tonin. 2020. "Compliance with COVID-19 Social-Distancing Measures in Italy: The Role of Expectations and Duration." National Bureau of Economic Research Working Paper Series No. 26916.

Burchardi, Konrad B, Thomas Chaney, and Tarek A Hassan. 2018. "Migrants, Ancestors, and Foreign Investments." The Review of Economic Studies 86 (4):1448-1486.

Burchardi, Konrad B., and Tarek A. Hassan. 2013. "The Economic Impact of Social Ties: Evidence from German Reunification*." The Quarterly Journal of Economics 128 (3):1219-1271.

Cameron, A. Colin, Jonah B. Gelbach, and Douglas L. Miller. 2008. "Bootstrap-Based Improvements for Inference with Clustered Errors." The Review of Economics and Statistics 90 (3):414-427.

Carmichael, Ann G. 2014. "Plague and the Poor in Renaissance Florence," Cambridge University Press.

Chauvet, Lisa, Flore Gubert, Marion Mercier, and Sandrine Mespl-Somps. 2015. "Migrants' Home Town Associations and Local Development in Mali." The Scandinavian Journal of Economics 117 (2):686-722.

Chauvet, Lisa, and Marion Mercier. 2014. "Do return migrants transfer political norms to their origin country? Evidence from Mali." Journal of Comparative Economics 42 (3):630-651.

Chinazzi, Matteo, Jessica T. Davis, Marco Ajelli, Corrado Gioannini, Maria Litvinova, Stefano Merler, Ana Pastore y Piontti, Kunpeng Mu, Luca Rossi, Kaiyuan Sun, Ccile Viboud, Xinyue Xiong, Hongjie Yu, M. Elizabeth Halloran, Ira M. Longini, and Alessandro Vespignani. 2020. "The effect of travel restrictions on the spread of the 2019 novel coronavirus (COVID-19) outbreak." Science 368 (6489):395-400.

Chudik, A, M H Pesaran, and A Rebucci (2020), Voluntary and Mandatory Social Distancing: Evidence on COVID-19 Exposure Rates from Chinese Provinces and Selected Countries, CEPR Discussion Paper 14646.

Clark, G. and Cummins, N. (2009), Urbanization, Mortality and Fertility in Malthusian England, American Economic Review, Papers and Proceedings, 99, 242247.

Clingingsmith, David, Asim Ijaz Khwaja, and Michael Kremer. 2009. "Estimating the Impact of The Hajj: Religion and Tolerance in Islam's Global Gathering*." The Quarterly Journal of Economics 124 (3):1133-1170. doi: 10.1162/qjec.2009.124.3.1133.

Daudin, Guillaume and Franck, Raphael and Rapoport, Hillel, The Cultural Diffusion of the Fertility Transition: Evidence from Internal Migration in 19th Century France. IZA Discussion Paper No. 9945. Available at SSRN: https://ssrn.com/abstract=2786029

DECRETO DEL PRESIDENTE DEL CONSIGLIO DEI MINISTRI 22 February 2020.

Covid Economics 18, 15 May 2020: 170-195

Available at https://www.gazzettaufficiale.it/eli/id/2020/03/22/20A01806/sg

DECRETO DEL PRESIDENTE DEL CONSIGLIO DEI MINISTRI 09 March 2020. Available at https://www.gazzettaufficiale.it/eli/id/2020/03/09/20A01558/sg

Diamond, Jared M. Guns, Germs, and Steel : the Fates of Human Societies. New York: Norton, 2005.

Docquier, Frdric, Elisabetta Lodigiani, Hillel Rapoport, and Maurice Schiff. 2016. "Emigration and democracy." Journal of Development Economics 120:209-223.

Dustmann, Christian, and Joseph-Simon Görlach. 2016. "The Economics of Temporary Migrations." Journal of Economic Literature 54 (1):98-136.

Eichenbaum, Martin S., Sergio Rebelo, and Mathias Trabandt. 2020. "The Macroeconomics of Epidemics." National Bureau of Economic Research Working Paper Series No. 26882.

Fang, Hanming, Long Wang, and Yang Yang. 2020. "Human Mobility Restrictions and the Spread of the Novel Coronavirus (2019-nCoV) in China." National Bureau of Economic Research Working Paper Series No. 26906.

Gatto, Marino, Enrico Bertuzzo, Lorenzo Mari, Stefano Miccoli, Luca Carraro, Renato Casagrandi, and Andrea Rinaldo. 2020. "Spread and dynamics of the COVID-19 epidemic in Italy: Effects of emergency containment measures." Proceedings of the National Academy of Sciences:202004978.

Grewal, Sharan. 2020. "From Islamists to Muslim Democrats: The Case of Tunisias Ennahda." American Political Science Review 114 (2):519-535.

Gröger, André, and Yanos Zylberberg. 2016. "Internal Labor Migration as a Shock Coping Strategy: Evidence from a Typhoon." American Economic Journal: Applied Economics 8 (2):123-53.

Hornbeck, Richard. 2012. "The Enduring Impact of the American Dust Bowl: Short- and Long-Run Adjustments to Environmental Catastrophe." American Economic Review 102 (4):1477-1507.

Jaime D'Alessandro. (23 April 2020=. "Coronavirus, l'illusione della grande fuga da Milano. Ecco i veri numeri degli spostamenti verso sud",["Coronavirus, the illusion of the big escape from Milano. Here are the true numbers of the movemements towards the South"]. Repubblica, available at https://www.repubblica.it/tecnologia/2020/04/23/news/coronavirus_l_illusione_della_grande_fuga_da_milano_e_i_veri_numeri_degli_spostamenti_verso_sud-254722355/

Jedwab, R, N Johnson and M Koyama (2019), "Pandemics, Places, and Populations: Evidence from the Black Death, CEPR Discussion Paper 13523

Karadja, Mounir, and Erik Prawitz. 2019. "Exit, Voice, and Political Change: Evidence from Swedish Mass Migration to the United States." Journal of Political Economy 127

Covid Economics 18, 15 May 2020: 170-195

(4):1864-1925.

Kerr, William R. 2008. "Ethnic Scientific Communities and International Technology Diffusion." The Review of Economics and Statistics 90 (3):518-537.

Knudsen, Anne Sofie Beck, Those Who Stayed: Individualism, Self-Selection and Cultural Change During the Age of Mass Migration (January 24, 2019). Available at SSRN http://dx.doi.org/10.2139/ssrn.3321790

Kraemer, Moritz U. G., Chia-Hung Yang, Bernardo Gutierrez, Chieh-Hsi Wu, Brennan Klein, David M. Pigott, Louis du Plessis, Nuno R. Faria, Ruoran Li, William P. Hanage, John S. Brownstein, Maylis Layan, Alessandro Vespignani, Huaiyu Tian, Christopher Dye, Oliver G. Pybus, and Samuel V. Scarpino. 2020. "The effect of human mobility and control measures on the COVID-19 epidemic in China." Science 368 (6490):493-497.

Kuchler, Theresa, Dominic Russel, and Johannes Stroebel. 2020. "The Geographic Spread of COVID-19 Correlates with Structure of Social Networks as Measured by Facebook." National Bureau of Economic Research Working Paper Series No. 26990.

Kwakwa, Victoria. 2020. "Governments facing tough choices in COVID-19 crisis", published on the East Asia and Pacific World Bank blog. Available at https://blogs.worldbank.org/eastasiapacific/governments-facing-tough-choices-covid-19-coronavirus CID=WBW_AL_BlogNotification_EN_EXT

Litvinova, Maria, Quan-Hui Liu, Evgeny S. Kulikov, and Marco Ajelli. 2019. "Reactive school closure weakens the network of social interactions and reduces the spread of influenza." Proceedings of the National Academy of Sciences 116 (27):13174-13181.

Mercier, Marion. 2016. "The return of the prodigy son: Do return migrants make better leaders?" Journal of Development Economics 122:76-91.

Mikhailova, T. and Valsecchi M. (2020). "Internal migration and the Covid-19 virus" in Economic Policy During the Covid-19 (ebook). New Economic School.

Ministero della Salute. Dipartmento della Protezione Civile. 2020. "Monitoraggio 12 Aprile 2020". Retrieved on 13th April at http://www.salute.gov.it/imgs/C_17_notizie_4454_0_file.pdf

Oster, Emily. 2012. "ROUTES OF INFECTION: EXPORTS AND HIV INCIDENCE IN SUB-SAHARAN AFRICA." Journal of the European Economic Association 10 (5):1025-1058.

Parsons, Christopher, and Pierre-Louis Vzina. 2018. "Migrant Networks and Trade: The Vietnamese Boat People as a Natural Experiment." The Economic Journal 128 (612):F210-F234.

Pfutze, Tobias. 2012. "Does migration promote democratization? Evidence from the Mexican transition." Journal of Comparative Economics 40 (2):159-175.

Pichler, Stefan, and Nicolas Ziebarth. 2019. "Reprint of: The pros and cons of sick pay schemes: Testing for contagious presenteeism and noncontagious absenteeism behav-

Covid Economics 18, 15 May 2020: 170-195

ior." Journal of Public Economics 171 (C):86-104.

Pisano, Gary P., Raffaella Sadun and Michele Zanini. 2020. "Lessons from Italys Response to Coronavirus," Harvard Business Review (27 March), available at https://hbr.org/2020/03/lessons-from-italys-response-to-coronavirus

Severgnini, Chiara (8 March 2020). "Coronavirus, Conte: "Ecco il decreto con le nuove misure, in vigore fino al 3 aprile"" [Coronavirus, Conte: "Here is the decree with the new measures, in force until April 3"]. Corriere della Sera

Spilimbergo, Antonio. 2009. "Democracy and Foreign Education." American Economic Review 99 (1):528-43.

Surico, Paolo, and Andrea Galeotti. 2020. "A user guide to COVID-19", Vox (27 March 2020), available at https://voxeu.org/article/user-guide-covid-19

Topel, Robert H. 1986. "Local Labor Markets." Journal of Political Economy 94 (3):S111-S143.

Voigtländer, Nico, and Hans-Joachim Voth. 2012. "The Three Horsemen of Riches: Plague, War, and Urbanization in Early Modern Europe." The Review of Economic Studies 80 (2):774-811.

United Nations. 2013. "Cross-national comparisons of internal migration: An update on global patterns and trends," United Nations Department of Economic and Social Affairs, Population Division, Technical Paper 2013/1.

Wight, Andrew. 2020. "Will The Coronavirus Follow When 20 Million Indonesians Go Home For Mudik?," Forbes Magazine, available at https://www.forbes.com/sites/andrewwight/2020/04/08/will-the-coronavirus-follow-when-20-million-indonesians-go-h#49839a2efc13

Woods, Robert. 2003. "Urban-Rural Mortality Differentials: An Unresolved Debate." Population and Development Review 29 (1):29-46.

World Health Organization. 2020. "Corona Virus Disease 19 (COVID 19). Situation Report - 104". Retrieved online on the 3rd May at https://https://www.who.int/docs/default-source/coronaviruse/situation-reports/20200503-covid-19-sitrep-104.pdf?sfvrsn=53328f46_2

Yang, Dean. 2006. "Why Do Migrants Return to Poor Countries? Evidence from Philippine Migrants' Responses to Exchange Rate Shocks." The Review of Economics and Statistics 88 (4):715-735.

Yang, Dean. 2008. "International Migration, Remittances and Household Investment: Evidence from Philippine Migrants Exchange Rate Shocks*." The Economic Journal 118 (528):591-630.

Young, Alwyn. 2013. "Inequality, the Urban-Rural Gap, and Migration*." The Quarterly Journal of Economics 128 (4):1727-1785.

Covid Economics 18, 15 May 2020: 170-195

Appendix

Table A.1: IHS-log specification: interactions with week indicators

	(1)	(2)	(3)	(4)	(5)	(6)	(7)
$ln(migrantsToLVE)$							
× (26^{th}Feb.-3^{rd}Mar.)	0.003	0.025	0.063	0.048	0.028	0.015	0.039
	(0.013)	(0.020)	(0.060)	(0.040)	(0.022)	(0.024)	(0.054)
	0.807	0.267	0.300	0.239	0.213	0.521	0.509
× (4^{th}Mar.-10^{th}Mar.)	-0.120	0.198	0.268	0.285	0.211	0.217	0.215
	(0.129)	(0.140)	(0.243)	(0.186)	(0.166)	(0.166)	(0.245)
	0.355	0.076	0.247	0.106	0.146	0.155	0.411
× (11^{th}Mar.-17^{th}Mar.)	-0.393	0.925***	1.504***	1.370***	0.953**	1.237***	1.556***
	(0.546)	(0.314)	(0.495)	(0.419)	(0.359)	(0.341)	(0.481)
	0.517	0.016	0.023	0.010	0.007	0.007	0.007
× (18^{th}Mar.-24^{nd}Mar.)	-1.292	0.426	1.185*	0.995**	0.465*	0.435	0.982
	(0.892)	(0.290)	(0.640)	(0.465)	(0.237)	(0.390)	(0.600)
	0.233	0.412	0.018	0.031	0.241	0.443	0.123
× (25^{th}Mar.-31^{st}Mar.)	-0.662	0.909***	1.675**	1.580***	0.933***	1.128**	1.779**
	(0.749)	(0.247)	(0.673)	(0.482)	(0.232)	(0.413)	(0.665)
	0.451	0.045	0.007	0.002	0.027	0.069	0.018
× (1^{st}Apr.-7^{th}Apr.)	-0.603	1.160***	1.800***	1.692***	1.178***	1.515***	1.985***
	(0.895)	(0.267)	(0.611)	(0.472)	(0.251)	(0.369)	(0.601)
	0.593	0.022	0.009	0.001	0.013	0.019	0.025
× (8^{th}Apr.-14^{nd}Apr.)	-1.091	0.796	1.117	1.316*	0.838*	1.515***	1.449**
	(1.063)	(0.521)	(0.664)	(0.728)	(0.465)	(0.494)	(0.562)
	0.394	0.415	0.202	0.185	0.319	0.132	0.082
× (15^{th}Apr.-21^{st}Apr.)	-1.064	0.971**	1.069*	1.272**	0.991**	1.391***	1.326**
	(1.040)	(0.348)	(0.574)	(0.538)	(0.340)	(0.366)	(0.502)
	0.393	0.128	0.094	0.068	0.124	0.051	0.041
× (22^{nd}Apr.-28^{nd}Apr.)	-1.065	0.842**	0.964**	1.091**	0.872**	1.280***	1.108***
	(1.011)	(0.360)	(0.424)	(0.470)	(0.318)	(0.379)	(0.360)
	0.380	0.207	0.136	0.051	0.130	0.094	0.053
× (29^{th}Apr.-4^{th}May)	-2.061***	-0.594	-0.167	0.138	-0.557	-0.305	0.032
	(0.518)	(0.433)	(0.445)	(0.423)	(0.496)	(0.507)	(0.435)
	0.027	0.616	0.778	0.757	0.787	0.792	0.959
Mean	1.295	1.295	1.295	1.295	1.295	1.295	1.295
R-squared	0.789	0.864	0.868	0.868	0.866	0.870	0.879
Number of regions	17	17	17	17	17	17	17
Observations	1,224	1,224	1,224	1,224	1,224	1,224	1,224
Day FE	Yes	Yes	Yes	Yes	Yes	Yes	Yes
Region FE	Yes	Yes	Yes	Yes	Yes	Yes	Yes
Distance to Milano	-	Yes	Yes	Yes	Yes	Yes	Yes
Compliance to quarantine	-	-	Yes	-	-	-	Yes
State capacity	-	-	-	Yes	-	-	Yes
Pop. at risk	-	-	-	-	Yes	-	Yes
Total emigrants	-	-	-	-	-	Yes	Yes

Notes: Dependent variable is the Inverse Hyperbolic Sine (IHS) of the number of Covid-19 deaths per million inhabitants. Control for "compliance with quarantine" is the first principal component of: share with higher school education, share with university education, newspaper readership (at least once a week), newspaper readership (at least five times a week), trust in others. Control for "state capacity" is the first principal component of: unemployment share, regional GDP per capita, number of intensive care beds per 100,000 inhabitants. Control for "population at risk" is the share of people with 70 years old or more. Control for "total emigrants" is the number of people who changed residence to another Italian region between 2015 and 2018. For each interaction, the table reports coefficient estimates on the first row, standard errors clustered at the region level (in brackets), and p-values for wild cluster bootstrap standard errors la Cameron, Gelbach and Miller 2008).

Covid Economics 18, 15 May 2020: 170-195

Covid Economics 18, 15 May 2020: 170-195

Figure A.1: IHS-log specification, interactions with week indicators: controls

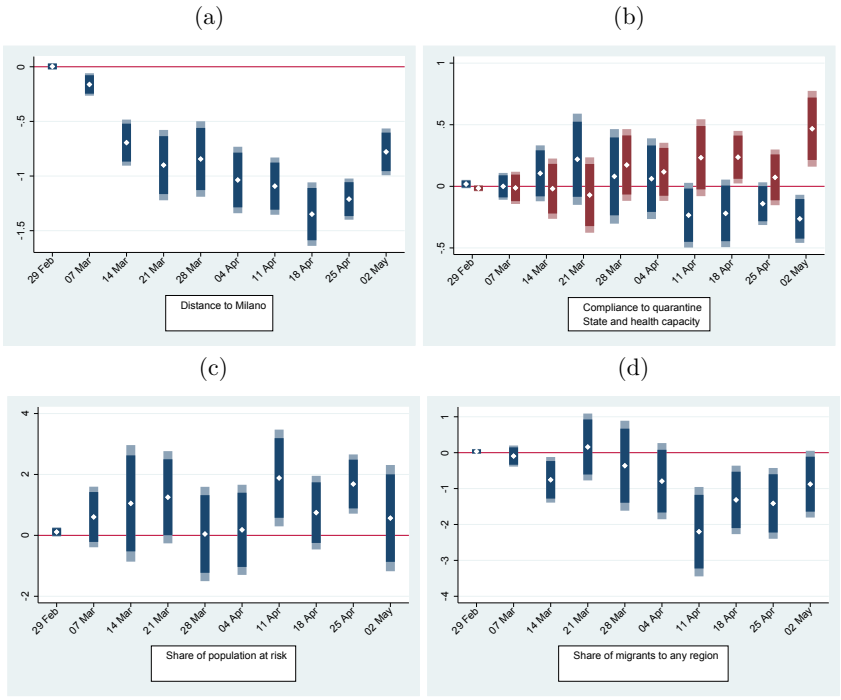

Figure A.2: linear-log specification: interactions with week indicators

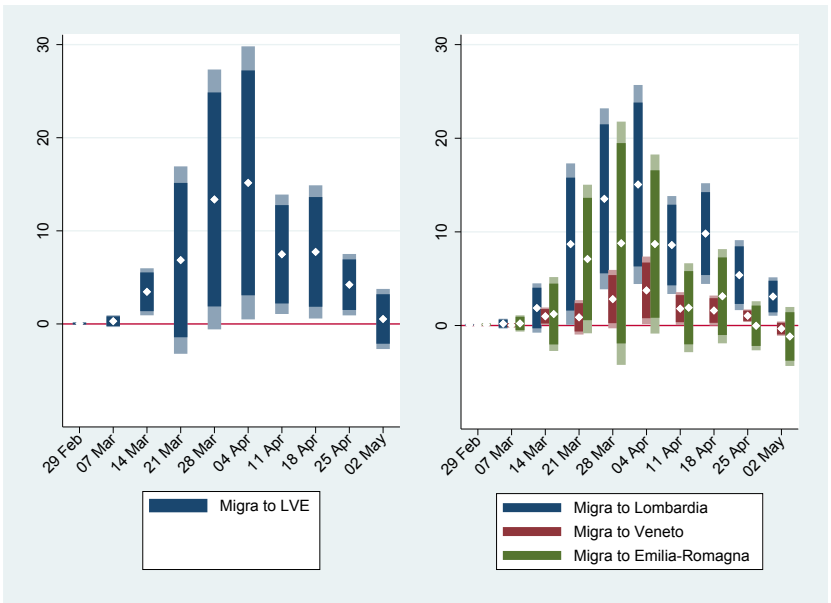

Notes: dark colors represent 90 percent confidence intervals; light colors represent 95 percent confidence intervals; dates are the mid-points in the week. LVE stands for Lombardia, Veneto and Emilia-Romagna.

Table A.2: linear-log specification: interactions with week indicators

	(1)	(2)	(3)	(4)	(5)	(6)	(7)
$ln(migrantsToLVE)$							
× (26^{th}Feb.-3^{rd}Mar.)	0.003	0.027	0.067	0.051	0.029	0.016	0.042
	(0.014)	(0.021)	(0.064)	(0.043)	(0.024)	(0.025)	(0.058)
	0.807	0.267	0.300	0.240	0.213	0.521	0.509
× (4^{th}Mar.-10^{th}Mar.)	-0.121	0.262	0.363	0.371	0.277	0.292	0.298
	(0.157)	(0.159)	(0.299)	(0.226)	(0.190)	(0.192)	(0.297)
	0.450	0.038	0.206	0.089	0.049	0.098	0.317
× (11^{th}Mar.-17^{th}Mar.)	-0.499	2.474***	3.649**	3.344***	2.551***	2.908***	3.454**
	(1.220)	(0.745)	(1.259)	(1.042)	(0.855)	(0.782)	(1.191)
	0.696	0.005	0.024	0.006	0.000	0.006	0.012
× (18^{th}Mar.-24^{nd}Mar.)	-3.134	4.302**	8.268	7.205**	4.497**	3.752	6.858
	(3.547)	(1.842)	(4.843)	(3.349)	(1.797)	(2.240)	(4.747)
	0.447	0.134	0.077	0.036	0.104	0.198	0.246
× (25^{th}Mar.-31^{st}Mar.)	-3.120	8.823***	12.536*	12.242**	8.917***	10.008***	13.372*
	(5.344)	(2.342)	(6.574)	(4.899)	(2.388)	(3.221)	(6.583)
	0.608	0.023	0.031	0.015	0.018	0.036	0.056
× (1^{st}Apr.-7^{th}Apr.)	-3.115	8.857***	13.255*	12.501**	8.852***	10.691***	15.152**
	(5.408)	(2.224)	(6.820)	(4.961)	(2.164)	(3.494)	(6.916)
	0.628	0.025	0.027	0.013	0.019	0.032	0.076
× (8^{th}Apr.-14^{nd}Apr.)	-4.902	7.877***	5.738*	7.836**	7.948***	10.438***	7.482**
	(5.778)	(2.312)	(2.733)	(3.639)	(2.294)	(2.769)	(3.025)
	0.471	0.063	0.032	0.058	0.074	0.060	0.119
× (15^{th}Apr.-21^{st}Apr.)	-4.273	8.250***	6.507**	8.082**	8.310***	10.179***	7.737**
	(5.326)	(1.936)	(3.068)	(3.398)	(1.978)	(2.371)	(3.375)
	0.495	0.021	0.007	0.029	0.019	0.037	0.160
× (22^{nd}Apr.-28^{nd}Apr.)	-3.565	6.098***	3.839***	5.420**	6.187***	7.222***	4.217**
	(4.160)	(1.503)	(1.254)	(2.231)	(1.527)	(1.919)	(1.556)
	0.463	0.031	0.019	0.013	0.033	0.052	0.106
× (29^{nd}Apr.-4^{th}May)	-4.546**	0.998	0.034	1.315	1.053	1.623	0.534
	(1.901)	(1.512)	(1.416)	(1.637)	(1.607)	(1.851)	(1.523)
	0.060	0.573	0.978	0.479	0.614	0.455	0.767
Mean	4.290	4.290	4.290	4.290	4.290	4.290	4.290
R-squared	0.617	0.780	0.792	0.787	0.782	0.784	0.804
Number of regions	17	17	17	17	17	17	17
Observations	1,224	1,224	1,224	1,224	1,224	1,224	1,224
Day FE	Yes	Yes	Yes	Yes	Yes	Yes	Yes
Region FE	Yes	Yes	Yes	Yes	Yes	Yes	Yes
Distance to Milano	-	Yes	Yes	Yes	Yes	Yes	Yes
Compliance to quarantine	-	-	Yes	-	-	-	Yes
State capacity	-	-	-	Yes	-	-	Yes
Pop. at risk	-	-	-	-	Yes	-	Yes
Total emigrants	-	-	-	-	-	Yes	Yes

Notes: Dependent variable is the number of Covid-19 deaths per million inhabitants. LVE stands for Lombardia, Veneto and Emilia-Romagna (the outbreak regions). The number on migrants is the number of people who changed their residence to one of the outbreak regions between 2015 an 2018 (three years). Control for "compliance with quarantine" is the first principal component of: share with higher school education, share with university education, newspaper readership (at least once a week), newspaper readership (at least five times a week), trust in others. Control for "state capacity" is the first principal component of: unemployment share, regional GDP per capita, number of intensive care beds per 100,000 inhabitants. Control for "population at risk" is the share of people with 70 years old or more. Control for "total emigrants" is the number of people who changed residence to another Italian region between 2015 and 2018. All controls are in logarithms. For each interaction, the table reports coefficient estimates on the first row, standard errors clustered at the region level (in brackets), and p-values for wild cluster bootstrap standard errors la Cameron, Gelbach and Miller 2008). *** p<0.01, ** p<0.05, * p<0.1.

Covid Economics 18, 15 May 2020: 170-195

Covid Economics 18, 15 May 2020: 170-195

Figure A.3: linear-linear specification: interactions with week indicators

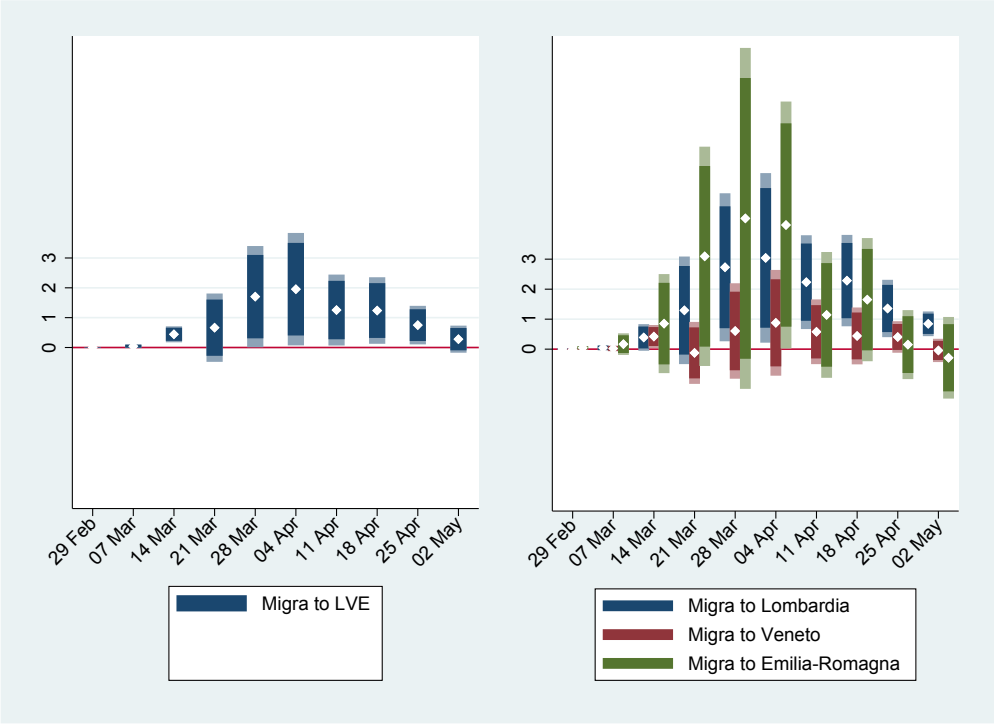

Notes: dark colors represent 90 percent confidence intervals; light colors represent 95 percent confidence intervals; dates are the mid-points in the week. LVE stands for Lombardia, Veneto and Emilia-Romagna.

Covid Economics 18, 15 May 2020: 170-195

Table A.3: linear-linear specification: interactions with week indicators

	(1)	(2)	(3)	(4)	(5)	(6)	(7)
migrantsToLVE							
× (26^{th}Feb.-3^{rd}Mar.)	-0.000	0.003	0.007	0.007	0.003	0.002	0.002
	(0.002)	(0.003)	(0.006)	(0.005)	(0.003)	(0.004)	(0.006)
	0.885	0.313	0.255	0.218	0.228	0.559	0.711
× (4^{th}Mar.-10^{th}Mar.)	-0.024	0.036	0.039	0.050*	0.035	0.044*	0.043
	(0.022)	(0.021)	(0.033)	(0.027)	(0.025)	(0.024)	(0.029)
	0.302	0.019	0.206	0.049	0.081	0.043	0.150
× (11^{th}Mar.-17^{th}Mar.)	-0.125	0.342***	0.439**	0.443**	0.341**	0.422***	0.442***
	(0.173)	(0.110)	(0.162)	(0.156)	(0.122)	(0.100)	(0.126)
	0.515	0.000	0.016	0.006	0.000	0.002	0.011
× (18^{th}Mar.-24^{nd}Mar.)	-0.581	0.576*	0.964*	0.922*	0.572**	0.487	0.664
	(0.479)	(0.276)	(0.524)	(0.454)	(0.257)	(0.336)	(0.540)
	0.313	0.147	0.073	0.024	0.104	0.237	0.317
× (25^{th}Mar.-31^{st}Mar.)	-0.662	1.205***	1.562*	1.524**	1.204***	1.372**	1.705**
	(0.744)	(0.361)	(0.749)	(0.645)	(0.366)	(0.479)	(0.800)
	0.448	0.033	0.028	0.005	0.028	0.044	0.110
× (1^{st}Apr.-7^{th}Apr.)	-0.661	1.212***	1.696*	1.553**	1.213***	1.444**	1.955**
	(0.753)	(0.359)	(0.835)	(0.657)	(0.363)	(0.515)	(0.889)
	0.471	0.034	0.029	0.006	0.026	0.035	0.137
× (8^{th}Apr.-14^{nd}Apr.)	-0.903	1.099**	0.852*	0.979*	1.099**	1.495***	1.255**
	(0.807)	(0.382)	(0.410)	(0.535)	(0.385)	(0.447)	(0.561)
	0.344	0.072	0.055	0.101	0.077	0.058	0.170
× (15^{th}Apr.-21^{st}Apr.)	-0.809	1.156***	0.938**	1.040*	1.155***	1.470***	1.239**
	(0.749)	(0.324)	(0.422)	(0.495)	(0.328)	(0.370)	(0.526)
	0.358	0.018	0.021	0.039	0.018	0.029	0.145
× (22^{nd}Apr.-28^{nd}Apr.)	-0.655	0.864***	0.591**	0.722**	0.862***	1.062***	0.750**
	(0.585)	(0.248)	(0.208)	(0.339)	(0.253)	(0.297)	(0.305)
	0.332	0.033	0.029	0.032	0.039	0.037	0.095
× (29^{th}Apr.-4^{th}May)	-0.714**	0.153	0.044	0.204	0.152	0.267	0.279
	(0.275)	(0.205)	(0.188)	(0.220)	(0.219)	(0.259)	(0.214)
	0.026	0.519	0.840	0.447	0.585	0.398	0.298
Mean	4.290	4.290	4.290	4.290	4.290	4.290	4.290
R-squared	0.621	0.778	0.787	0.782	0.780	0.782	0.798
Number of regions	17	17	17	17	17	17	17
Observations	1,224	1,224	1,224	1,224	1,224	1,224	1,224
Day FE	Yes	Yes	Yes	Yes	Yes	Yes	Yes
Region FE	Yes	Yes	Yes	Yes	Yes	Yes	Yes
Distance to Milano	-	Yes	Yes	Yes	Yes	Yes	Yes
Compliance to quarantine	-	-	Yes	-	-	-	Yes
State capacity	-	-	-	Yes	-	-	Yes
Pop. at risk	-	-	-	-	Yes	-	Yes
Total emigrants	-	-	-	-	-	Yes	Yes

Notes: Dependent variable is the number of Covid-19 deaths per million inhabitants. LVE stands for Lombardia, Veneto and Emilia-Romagna (the outbreak regions). The number on migrants is the number of people who changed their residence to one of the outbreak regions between 2015 an 2018 (three years). Control for "compliance with quarantine" is the first principal component of: share with higher school education, share with university education, newspaper readership (at least once a week), newspaper readership (at least five times a week), trust in others. Control for "state capacity" is the first principal component of: unemployment share, regional GDP per capita, number of intensive care beds per 100,000 inhabitants. Control for "population at risk" is the share of people with 70 years old or more. Control for "total emigrants" is the number of people who changed residence to another Italian region between 2015 and 2018. For each interaction, the table reports coefficient estimates on the first row, standard errors clustered at the region level (in brackets), and p-values for wild cluster bootstrap standard errors la Cameron, Gelbach, and Miller (2008). *** p<0.01, ** p<0.05, * p<0.1.

Figure A.4: IHS-log specification, robustness check: drop one region at a time

Notes: Dependent variable is the Inverse Hyperbolic Sine (IHS) of the number of Covid-19 deaths per million inhabitants. The explanatory variables of interest are the interactions between the log of the number of migrants to LVE during 2015-2018 (per 1000 inhabitants) and week dummies. Dark colors represent 90 percent confidence intervals. Light colors represent 95 percent confidence intervals. Dates are the mid-points in the week. LVE stands for Lombardia, Veneto and Emilia-Romagna.

Covid Economics **Issue 18, 15 May 2020**

The impact of pessimistic expectations on the effects of COVID-19-induced uncertainty in the euro area[1]

Giovanni Pellegrino,[2] Federico Ravenna[3] and Gabriel Züllig[4]

Date submitted: 8 May 2020; **Date accepted:** 8 May 2020

We estimate a nonlinear VAR model allowing for the impact of uncertainty shocks to depend on the average outlook of the economy measured by survey data. We find that, in response to the same uncertainty shock, industrial production and inflation's peak decrease is around three and a half times larger during pessimistic times. We build scenarios for a path of innovations in uncertainty consistent with the COVID-19-induced shock. Industrial production is predicted to experience a year-over-year peak loss of between 15.1% and 19% peaking between September and December 2020, and subsequently to recover with a rebound to pre-crisis levels between May and August 2021. The large impact is the result of an extreme shock to uncertainty occurring at a time of very negative expectations on the economic outlook.

1 We thank Efrem Castelnuovo for useful feedback. The viewpoints and conclusions stated are the responsibility of the individual contributors, and do not necessarily reflect the views of Danmarks Nationalbank. The authors alone are responsible for any remaining errors.
2 Assistant Professor, Aarhus University.
3 Head of Research, Danmarks Nationalbank; Professor, University of Copenhagen and HEC Montreal; CEPR.
4 Danmarks Nationalbank and PhD student, University of Copenhagen.

Covid Economics 18, 15 May 2020: 196-221

Covid Economics 18, 15 May 2020: 196-221

1 Introduction

The social distancing measures imposed worldwide to respond to the COVID-19 epidemic have resulted in the partial shutdown of economic activity, and immediate losses in output.[1] As countries started planning a gradual reopening of the economy in April 2020, expectations about the future were at their lowest, reflecting a pessimistic outlook for the future.[2] At the same time, measures of uncertainty were still very high, after having experienced levels comparable to those of the Great Financial Crisis.[3]

We assess what are the effects of heightened uncertainty in the presence of pessimistic expectations about the future economic outlook in the Euro Area, and estimate the macroeconomic impact of the COVID-induced uncertainty spike.

The observed increase in uncertainty measures can be interpreted as a perceived increase in the probability of very negative outcomes - for example, future waves of pandemic leading to protracted economic lockdowns – as well as very positive outcomes, such as the rapid procurement of a vaccine or effective antiviral drugs, and a fast rebound of economic activity. It is well known that unexpected surges or "shocks" in uncertainty have a negative effect on real activity (see, e.g., Bloom (2009), Leduc and Liu (2016), Baker, Bloom, and Davis (2016), Basu and Bundick (2017), Ludvigson, Ma, and Ng (2019)). This happens because risk-averse consumers increase precautionary savings against a rise in the risk of possible negative future outcomes and because firms postpone partially-irreversible investment to the future and adopt a "wait and see" behavior (see, e.g., Caballero (1990) and Bernanke (1983), respectively). Given the recent COVID-induced uncertainty shock, the same is expected to happen during this pandemic, with negative effects on output that will add to those given by the lockdowns, and may potentially last longer than the lockdowns. This is confirmed by recent Vector AutoRegression (VAR) studies on the impact of COVID-19 uncertainty by Baker, Bloom, Davis, and Terry (2020) – estimating a peak impact on year-over-year US GDP growth of about 5.5% – and Leduc and Liu (2020), estimating an impact on US unemployment peaking at one percentage points after 12 months. As regards the global effects of the COVID

[1] By the second half of April 2020, the Euro zone-wide composite Purchasing Manager Index (PMI) hit an all-time low of 13.5, implying the Eurozone economy had suffered the steepest ever fall in manufacturing and services activity (European Commission, 2020).

[2] The German ZEW sentiment index, and the consumer confidence indicator released by the European Commission in April 2020 signaled a confidence level approaching the number reached during the 2008-2009 financial crisis.

[3] Baker, Bloom, Davis, and Terry (2020) document the recent enormous increase in economic uncertainty as measured by several US indicators: the VIX index; the U.S. Economic Policy Uncertainty Index; several survey-based measures reporting uncertainty about the outlook among firms.

Covid Economics 18, 15 May 2020: 196-221

uncertainty shock, Caggiano, Castelnuovo, and Kima (2020) predict the cumulative loss in world output one year after the shock to be about 14%.

We provide two novel sets of results. First, we empirically study the role of pessimistic expectations about future outcomes for the historical propagation of uncertainty shocks in the Euro Area. Second, we make use of this novel finding to predict the expected propagation of the COVID-induced uncertainty shock.

We measure expectations about the economic outlook with consumer confidence and interpret plummeting consumer confidence as capturing pessimism about the future.[4] In principle, pessimism - that is , a negative outlook about the future of the economy- may influence the impact of uncertainty shocks. Given an average outlook, higher uncertainty increases the risks in the outlook: it implies a higher chance of more extreme outcomes, or an increased probability of large upside or downside risks.

At times of low prospects for future economic activity, an increase in the dispersion of future outcomes may have a larger impact on the economy: many more consumers, for example, may be closer to a worst-case scenario where they lose completely any income stream, and may optimally choose to change their behavior because of the increase in risk – even if there is an equally likely probability that the economy will rebound fast and demand growth will raise incomes. The same may be true for firms: with a very negative outlook, the same increase in uncertainty can – for example – dramatically raise the probability of bankruptcy for many firms, leading to a sharper change in behavior than what would be observed in normal times with a less extreme outlook. Several economists, including contributions by Fajgelbaum, Schaal, and Taschereau-Dumouchel (2014) and Cacciatore and Ravenna (2020) have suggested models able to explain the time-varying impact of uncertainty shocks.

We empirically test whether pessimism amplifies the impact of uncertainty shocks by modeling a vector of Euro area macroeconomic data with an Interacted VAR (IVAR) model for the period 1999m1-2020m1. The IVAR is a parsimonious nonlinear VAR model which augments a standard linear VAR model with an interaction term to determine how the effects of a shock on one variable depend on the level of another variable. We interact an uncertainty measure with a measure of consumer confidence to estimate the impact of an uncertainty shock at times when consumer

[4] Autonomous shifts in confidence have been documented to have powerful predictive implications for income and consumption. These shifts may operate through two possible channels: they may reflect changes in 'animal spirits', having a direct effect on the economy, or they may reflect fundamental information, or 'news', about the future state of the economy, available to consumers and not summarized by other measurable variables (Barsky and Sims (2012)).

Covid Economics 18, 15 May 2020: 196-221

confidence is in the bottom quantile of its historical distribution. Armed with this model, we build scenarios for a path of innovations in uncertainty consistent with the COVID-19-induced shock. In building the hypothetical response of the economy to the uncertainty shocks, we compute Generalized IRFs (GIRFs) à la Koop, Pesaran, and Potter (1996) to account for the endogenous evolution of the state of the economy – including its impact on uncertainty itself.[5]

Following the seminal work by Bloom (2009) we focus on financial uncertainty, that we measure by the VSTOXX index, a high-frequency measure of implied volatility for the EURO STOXX 50 stock market index (the European-analogue to the VIX index for the US). This is important since - as shown in Ludvigson, Ma, and Ng (2019) - indicators proxying this type of uncertainty are likely to capture movements in uncertainty which are relevant to explain the evolution of output at business cycle frequencies.

Our main results can be summarized as follows. First, we find that historically uncertainty shocks in the Euro area have had a significant impact on the economy only during pessimistic times. Industrial production and inflation decrease in both states of the economy, but their decrease is much larger and more persistent during pessimistic times. The peak response of industrial production (inflation) to a typical uncertainty shock is -1.28% (-0.11%) in pessimistic times and -0.36% (-0.04%) in normal times.

Second, our estimates imply that the COVID-19 shock via its uncertainty channel alone will induce a long and deep recession in the Euro area. In our first scenario, we hit the pessimistic-times state of our estimated IVAR with a 10 standard deviations uncertainty shock – corresponding to the unexpected rise in the level of the VSTOXX measure of uncertainty from February 2020 to March 2020. Industrial production is predicted to experience a year-over-year peak loss of 15.14% peaking after 7 months from the shock, in September 2020, and subsequently to recover with a rebound to pre-crisis levels in May 2021. In terms of GDP, a back-of-the-envelope calculation suggests a corresponding fall in year-over-year GDP of roughly 4.3% at peak.

We also consider two alternative scenarios where either uncertainty goes back to normal levels much more slowly in the current situation than in the past – given the persisting uncertainty in delivering a vaccine could span several months –, or where a second unexpected spike in uncertainty occurs following a possible new wave of the pandemic in the coming Fall. Both scenarios would delay the recovery and would prolong the recessionary impact by several months, yielding a larger

[5] Details on the estimation methodology for the IVAR model are in Caggiano, Castelnuovo, and Pellegrino (2017), Pellegrino (2017) and Pellegrino (2018).

total loss in industrial production. In the case of a new fall-2020 wave, our simulations predict the trough to happen in December 2020 and the rebound to start in July 2021.

Our findings lend support to the unprecedented policy responses to the pandemic, many of which can be interpreted as providing catastrophic insurance against worst-case outcomes.[6] Provided that the sole impact of the COVID-19 shock via its uncertainty channel will imply large losses as well as a slow and painful return to normality, policymakers are required to enact clear policies aimed not only at boosting confidence in the outlook, but specifically targeted at resolving the uncertainty.

The paper is structured as follows. Section 2 presents the empirical model and the data. Section 3 documents our empirical findings. Section 4 concludes.

Covid Economics 18, 15 May 2020: 196-221

2 Econometric setting

Interacted VAR The IVAR is a nonlinear VAR model which augments a standard linear VAR model with an interaction term to determine how the effects of a shock in one variable depend on the level of another variable. Our estimated IVAR reads as follows:

$$\mathbf{Y}_t = \boldsymbol{\alpha} + \sum_{j=1}^{L} \mathbf{A}_j \mathbf{Y}_{t-j} + \left[\sum_{j=1}^{L} \mathbf{c}_j unc_{t-j} \cdot conf_{t-j} \right] + \mathbf{u}_t \tag{1}$$

where $\mathbf{Y}_t$ is the vector of the endogenous variables, $\boldsymbol{\alpha}$ is a vector of constant terms, $\mathbf{A}_j$ are matrices of coefficients, $\mathbf{u}_t$ is the vector of error terms whose variance-covariance (VCV) matrix is $\boldsymbol{\Omega}$. The interaction term includes a vector of coefficients, $\mathbf{c}_j$, a measure of uncertainty, unc_t, i.e., the variable whose exogenous variations we aim at identifying, and a measure of consumer confidence, $conf_t$, that will serve as our conditioning variable. Both uncertainty and consumer confidence are treated as endogenous variables.

The vector of endogenous variables modeled by our IVAR reads as follows: $\mathbf{Y}_t = [unc_t, \Delta_{12} \ln IP_t, \pi_t, conf_t, i_t]'$, where unc stands for uncertainty, $\Delta_{12} \ln IP$ for year-over-year industrial production growth, π for year-over-year inflation, $conf$ for consumer confidence, and i for the policy rate. We proxy Euro area financial uncertainty with the monthly average of the VSTOXX index, which is the real-time measure of implied volatility for the EURO STOXX 50 stock

[6] A tracker of the unprecedented policy measures across the world to limit the human and economic impact of the COVID-19 pandemic is available at the ILO and IMF websites (https://www.ilo.org/global/topics/coronavirus/country-responses/) and https://www.imf.org/en/Topics/imf-and-covid19/Policy-Responses-to-COVID-19).

Covid Economics 18, 15 May 2020: 196-221

market index. The VSTOXX index is the European-analogue to the VXO index for the US, the index used in Bloom's (2009) seminal work. We use the Consumer Confidence Index provided by the European Commission, which provides an indication of next 12 months developments of households' consumption and saving, based upon answers regarding their expected financial situation, their sentiment about the general economic situation, unemployment and capability of savings.[7] To capture the stance of monetary policy, we use the overnight interest rate (EONIA), while industrial production (measured by the manufacturing sector) and inflation (measured by CPI index) are aggregates for the Euro area.[8] The Appendix reports plots of all the data series used in the model.

Relative to alternative nonlinear VARs like Smooth-Transition VARs and Threshold VARs, the IVAR is particularly appealing in addressing our research question. It enables us to model the interaction between uncertainty and consumer confidence in a parsimonious manner – as it does not require to estimate or calibrate any threshold/transition function –, and yet to precisely estimate the economy's response conditional on very low consumer confidence – as any regime is imposed before estimation, making the responses less sensitive to outliers in a particular regime. Our parsimonious specification follows Caggiano, Castelnuovo, and Pellegrino (2017), Pellegrino (2017) and Pellegrino (2018). To estimate our IVAR we use 4 lags as suggested by the AIC. The model is estimated by OLS. A multivariate LR test rejects the null of linearity against our I-VAR ($p - value = 0.00$).

We study the period 1999m1-2020m1. The starting date is dictated by the availability of the VSTOXX index and coincides with the establishment of the Euro area.

GIRFs for normal and pessimistic times We compute GIRFs à la Koop, Pesaran, and Potter (1996) to account for the endogenous response of consumer confidence to an uncertainty shock and the feedbacks this can have on the dynamics of the economy. GIRFs acknowledge the fact that, in a fully nonlinear model, responses depend on the sign of the shock, the size of the shock, and initial conditions. Theoretically, the GIRF at horizon h of the vector $\mathbf{Y}$ to a shock in date t, δ_t, computed conditional on an initial condition, $\boldsymbol{\varpi}_{t-1} = \{\mathbf{Y}_{t-1}, ..., \mathbf{Y}_{t-L}\}$, is given by the following

[7] The series is available at https://ec.europa.eu/info/business-economy-euro/indicators-statistics/economic-databases/business-and-consumer-surveys/download-business-and-consumer-survey-data/time-series_en (the mnemonic is CONS.EU.TOT.COF.BS.M)

[8] The use of synthetic European data is common among researchers (see, e.g., Smets and Wouters (2003) and Castelnuovo (2016)). The mnemonics for inflation and Eonia are respectively given by CPHPTT01EZM661N and FM.M.U2.EUR.4F.MM.EONIA.HSTA.

difference of conditional expectations:

$$GIRF_{Y,t}(h, \delta_t, \varpi_{t-1}) = \mathbb{E}\left[\mathbf{Y}_{t+h} \mid \delta_t, \varpi_{t-1}\right] - \mathbb{E}\left[\mathbf{Y}_{t+h} \mid \varpi_{t-1}\right]. \tag{2}$$

We are interested in computing the GIRFs to an uncertainty shock for normal and pessimistic times. We define the "Pessimistic times" state to be characterized by the initial quarters corresponding to the bottom 20% of the consumer confidence distribution, while the "Normal times" state is defined by all other initial quarters in the sample.[9] Figure 1 plots consumer confidence for the Euro area and provides a visual representation of the two states. Pessimistic times mostly capture the period of the Great Financial Crisis of 2008-2009 and the sovereign debt crisis of 2011-2013 but also capture the setback in confidence in 2003.

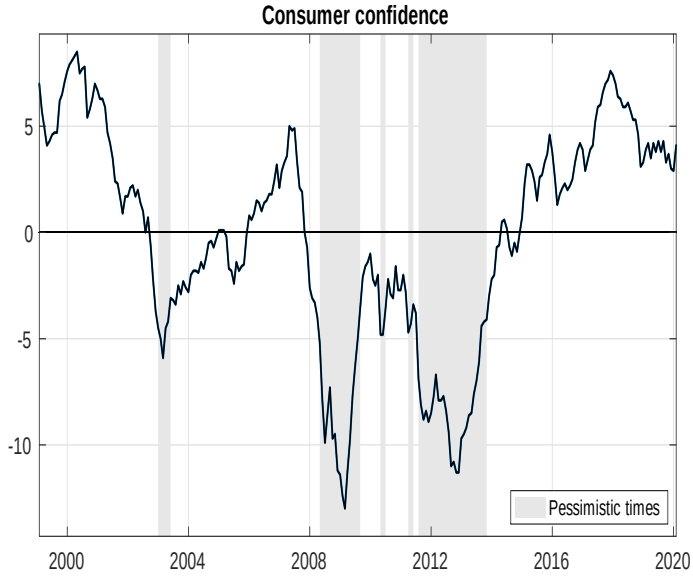

Figure 1: **European Commission Consumer Confidence Index (rescaled).** Solid line: European Commission Consumer Confidence Index. The series is obtained by subtracting the long-run average of the original series. Grey vertical bars: initial quarters in the bottom 20% of the consumer confidence distribution defining the Pessimistic times state.

Uncertainty shocks are identified by means of a Cholesky decomposition with recursive structure given by the ordering of the variables in the vector $\mathbf{Y}$ above, i.e., $[unc, \Delta_{12} \ln IP, \pi, conf, i]'$. Order-

[9] The algorithm at the basis of the simulation of our state-dependent GIRFs is provided in the Appendix.

ing the uncertainty proxy before macroeconomic aggregates in the vector allows real and nominal variables to react on impact, and it is a common choice in the literature (see, among others, Bloom (2009), Caggiano, Castelnuovo, and Groshenny (2014), Fernández-Villaverde, Guerrón-Quintana, Kuester, and Rubio-Ramírez (2015), Leduc and Liu (2016)). Moreover, it is justified by the theoretical model developed by Basu and Bundick (2017), who show that first-moment shocks in their framework exert a negligible effect on the expected volatility of stock market returns. This is in line with the findings in Ludvigson, Ma, and Ng (2019) according to which uncertainty about financial markets is a likely source of output fluctuations, rather than a consequence. Our Appendix documents that our results are robust to ordering uncertainty last.

3 Empirical results

3.1 The effects of uncertainty shocks in the Euro Area: The role of pessimism

We start by documenting the historical impact of uncertainty shocks in the Euro area during pessimistic and normal times. Figure 2 depicts the state-dependent GIRFs to a one standard deviation uncertainty shock along with 90% bootstrapped confidence bands. Figure 3 plots the 68% and 90% confidence bands of the statistical test on the difference of the impulse responses computed in the two states.[10]

[10] We compute differences between the impulse responses in the two states conditional on the same set of bootstrapped simulated samples. In this way, the construction of the test accounts for the correlation between the estimated impulse responses. The empirical density of the difference is based on 500 realizations for each horizon of interest.

Covid Economics 18, 15 May 2020: 196-221

Covid Economics 18, 15 May 2020: 196-221

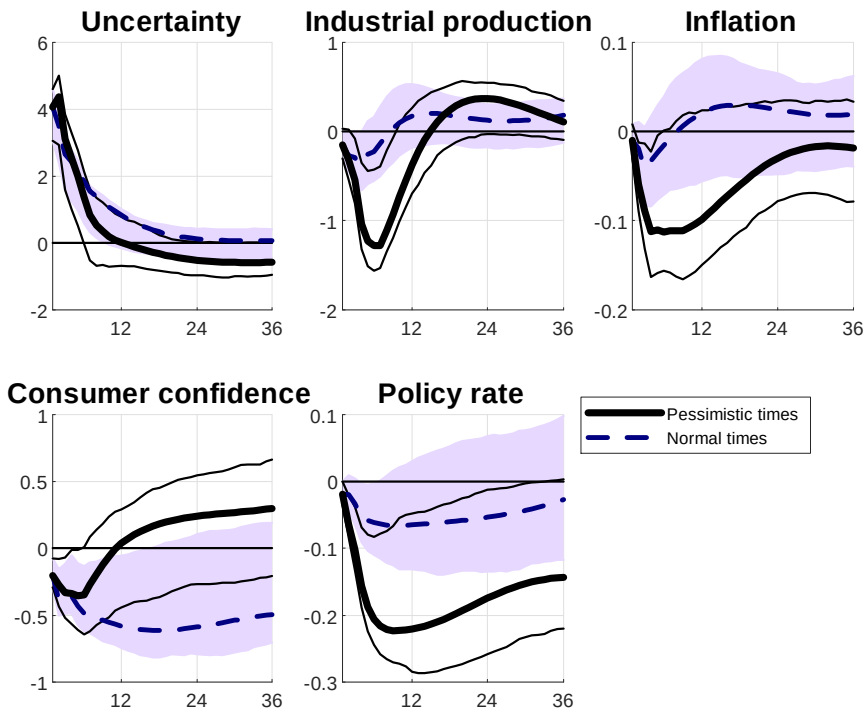

Figure 2: **Pessimistic vs. normal times state-conditional GIRFs**. Black solid lines: point estimates (bold lines) and 90% bootstrapped confidence bands for the GIRFs conditional to pessimistic times. Blue dashed lines and light blue areas: point estimates and 90% bootstrapped confidence bands for the GIRFs conditional to normal times. Monthly data.

We obtain three main results. First, real activity and inflation decrease in both states of the economy, but their decrease is much larger and more persistent during pessimistic times. The peak response of real activity is -1.28% in pessimistic times and -0.36% in normal times, i.e., around three and a half times bigger. The shock is deflationary, and the fall in inflation is three times as large in pessimistic times (-0.11%) compared to normal times (-0.04%). From a statistical standpoint, the decrease in real activity and inflation is significant only for pessimistic times, and their difference of responses across states is significant too (although for inflation at the 68% confidence level).

Covid Economics 18, 15 May 2020: 196-221

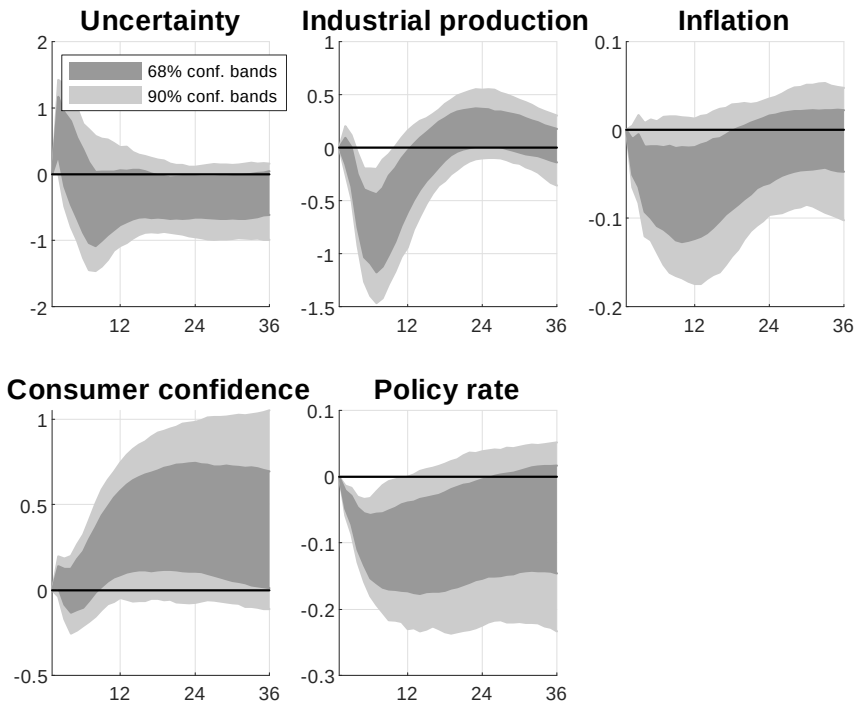

Figure 3: **Difference of state-conditional GIRFs between pessimistic and normal times**. Interior dark grey areas: 68 percent confidence bands for the difference between the pessimistic times conditional GIRF minus the normal times conditional GIRF. Confidence bands built with 500 bootstrap draws. Exterior light grey areas: 90 percent confidence bands. Monthly data.

Second, consumer confidence decreases for several months after the uncertainty shock hits before starting to grow again after 6 months in pessimistic times and after roughly one year and a half in normal times. Importantly, the response of consumer confidence is only marginally statistically significant, supporting the conclusion that shocks to uncertainty contain additional information relative to consumer confidence, and do not simply proxy for the average outlook of the economy.

Third, the difference in the reaction of consumer confidence across the "pessimistic" and "normal' states is significant (at the 68% confidence level). We find that this result is robust across all of the alternative specifications, reported in the Appendix. We attribute the faster estimated recovery in consumer confidence during pessimistic times to the estimated faster and larger cut in the policy rate engineered by the European Central Bank when the outlook is negative. The policy

rate is slashed in the first 5 months and reaches the peak response of about 20 basis points after 8 months from the shock.

Figures 4 and 5 document that the results above for industrial production and inflation are robust to: (i) the employment of either the US VIX index as a proxy for global uncertainty or the realized STOXX index volatility in place than our financial uncertainty indicator;[11] (ii) the use of either the OECD Euro area Consumer Confidence Index or the European Economic Sentiment Indicator in place of the European Commission Consumer Confidence Index; (iii) an alternative Cholesky-ordering that places uncertainty last rather than first; (iv) the use of a bond spread indicator as an omitted variable potentially relevant for the dynamics of real and nominal quantities (either ordered as second or last, in both cases just after the VSTOXX uncertainty measure);[12] (iv) the use of alternative thresholds for the definition of the pessimistic times state (bottom decile and bottom tertile); (v) the use of an alternative definition of the pessimistic times state based on the change in consumer confidence instead than its level to capture mood swings. Our main results are also robust to the use of alternative lag orders (3 and 6).

[11] The use of the VIX as a proxy of global uncertainty has recently been validated by Caggiano and Castelnuovo (2019), who show that an estimated global financial uncertainty factor is highly correlated with the VIX.

[12] Our credit spread measure is the ICE/BofA Euro High Yield Index Spread that tracks the performance of euro-denominated below-investment-grade corporate debt publicly issued in the euro markets with respect to a portfolio of Treasury bonds (source: Federal Reserve Bank of St. Louis).

Covid Economics 18, 15 May 2020: 196-221

Covid Economics 18, 15 May 2020: 196-221

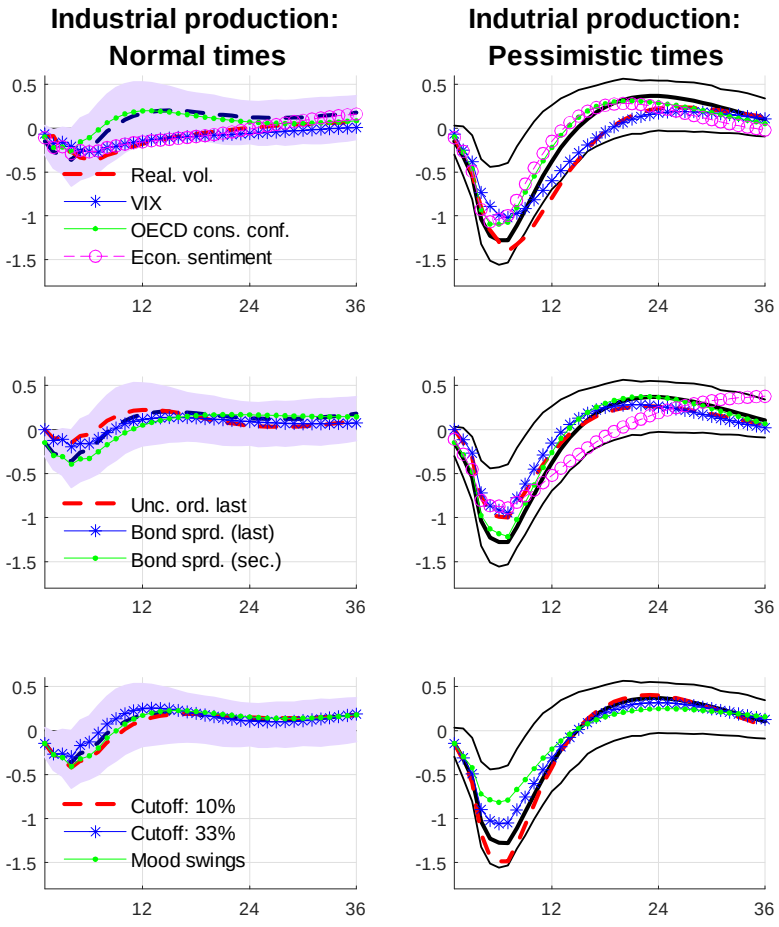

Figure 4: **Alternative IVAR models: Industrial Production GIRF.** Left-hand-side panels: Blue dashed lines and light blue areas represent the point estimates and 90% bootstrapped confidence bands for the baseline industrial production GIRFs conditional on normal times. Right-hand-side panels: Black solid lines represent the point estimates (bold lines) and 90% bootstrapped confidence bands for the baseline industrial production GIRFs conditional on pessimistic times. For the other lines refer to the legend and the main text. Monthly data.

Covid Economics 18, 15 May 2020: 196-221

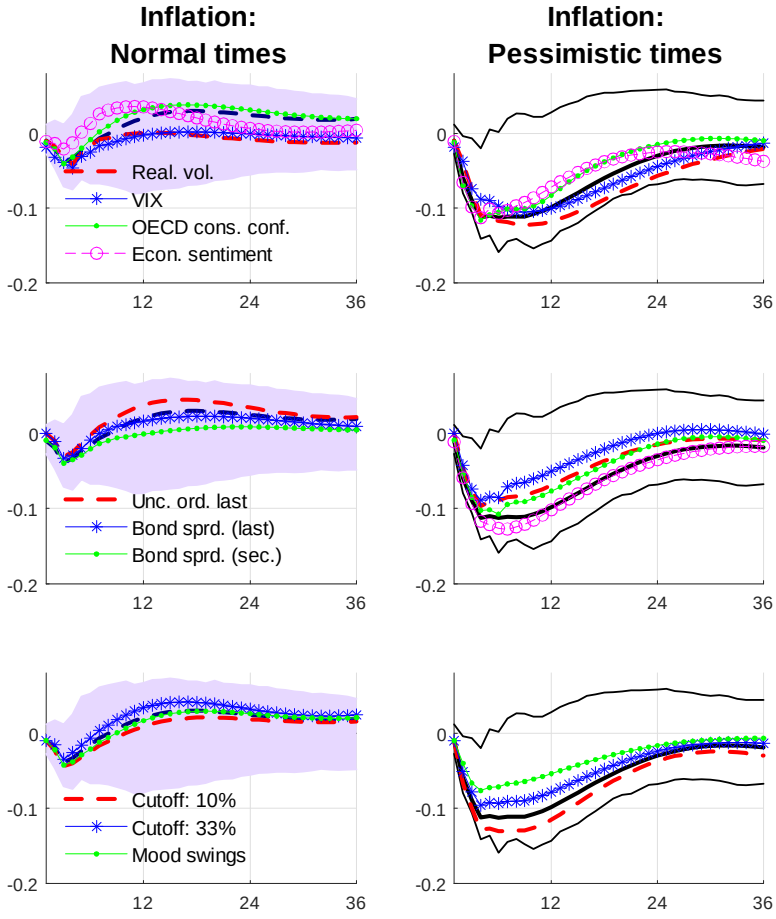

Figure 5: **Alternative IVAR models: Inflation GIRF.** Left-hand-side panels: Blue dashed lines and light blue areas represent the point estimates and 90% bootstrapped confidence bands for the baseline inflation GIRFs conditional on normal times. Right-hand-side panels: Black solid lines represent the point estimates (bold lines) and 90% bootstrapped confidence bands for the baseline inflation GIRFs conditional to pessimistic times. For the other lines refer to the legend and the main text. Monthly data

Covid Economics 18, 15 May 2020: 196-221

3.2 The uncertainty-channel of the COVID-19 shock

We predict the possible effects of the COVID-19 shock via its uncertainty channel. COVID-19 has caused enormous surges in financial uncertainty in the first half of 2020. Uncertainty has been surging since late February 2020, when the first cases in the Euro area not directly related to China were detected in Italy. During March the index has seen its biggest increase, in the period when the World Health Organization (WHO) declared a pandemic emergency on March 11. In the next few days most Euro area countries closed their schools and borders (e.g., Germany on March 13 and 15, respectively) and adopted a lockdown (Germany on March 22, the same date when Italy implemented the strictest measures for its lockdown already started on March 9). Since then the Euro area countries have been keeping their economies on hold to assess the evolution of the pandemic. Only in late April 2020 Euro area countries have been considering to start relaxing the restrictions.

As recently assessed by several surveys, consumers in April 2020 are highly pessimistic about the future. The April release of the European Commission consumer confidence indicator signaled a confidence level approaching the level reached during the 2008-2009 financial crisis. In the previous Section we computed the effects of a typical uncertainty shock occurring during pessimistic times and found that it has stronger effects than during normal times. The peak reaction of real activity is roughly 3.5 times stronger during pessimistic times than normal times. We now simulate the effects of the COVID-19 related surge in uncertainty by using the pessimistic-times state of our estimated IVAR.

On a monthly basis the Euro area has experienced a huge COVID-induced uncertainty shock in March 2020. According to our estimated IVAR, the unexpected rise in the level of the VSTOXX measure of uncertainty from February 2020 to March 2020 corresponds to roughly a 10 standard deviations shock. The black line in Figure 6 plots the effects of such an uncertainty shock during the average pessimistic state according to our estimated IVAR.[13] As Table 1 clarifies, industrial production experiences a year-over-year peak loss of 15.41% peaking after 7 months from the shock, in September 2020, and subsequently it recovers with a rebound to pre-crisis levels predicted to happen in May 2021. Given that our measure of industrial production is 2.8 times more volatile than

[13]Imposing a shock as big as 10 standard deviations causes our IVAR pessimistic times' response - which is based on the average of 50 initial quarters responses - to discard 5 particularly extreme initial histories which would lead to an explosive response. This implies that the estimated impact of the COVID-related uncertainty shock we report is conservative. However, our pessimistic times' response to a one standard deviation shock at the basis of Figure 2 did not discard any initial quarter.

Covid Economics 18, 15 May 2020: 196-221

the corresponding measure of GDP, a back-of-the-envelope calculation would translate the IVAR prediction for industrial production into a year-over-year fall in year-over-year GDP of roughly 4.3% at peak. Inflation year-over-year peak decrease is predicted to be −1.35% in August 2020.[14]

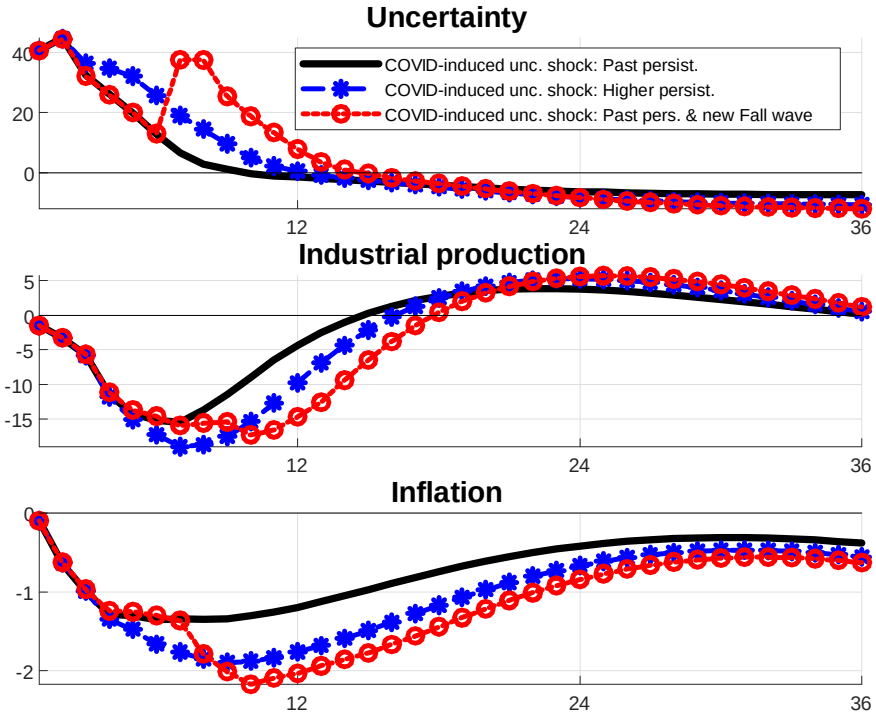

Figure 6: **The uncertainty-channel of the COVID-19 shock during pessimistic times: Alternative scenarios.** Solid black line: GIRF to a 10 standard deviation uncertainty shock hitting the economy during pessimistic times. Starred blue line: GIRF to the sequence of shocks $\boldsymbol{\delta} = [\delta_t, \delta_{t+2}, \delta_{t+3}, \delta_{t+4}, \delta_{t+5}, \delta_{t+6}, \delta_{t+7}] = [10, 1, 1, 1, 0.5, 0.5, 0.5]$ hitting the economy during pessimistic times (see equation 3). Circled red line: GIRF to the sequence of shocks $\boldsymbol{\delta} = [\delta_t, \delta_{t+6}] = [10, 7.5]$ hitting the economy during pessimistic times (see equation 3). The initial shock is assumed to hit in March 2020. Monthly data.

What if the COVID-19 related uncertainty shock propagated in a way different from the past Euro area experience? In performing the previous exercise we considered the persistence of a typical uncertainty shock as estimated by our IVAR on past data. Two alternative scenarios are plausible

[14]Note that this is a conservative estimate, since the actual drop in confidence in April 2020 is larger than the average drop in the "pessimistic" state over the sample.

Covid Economics 18, 15 May 2020: 196-221

Table 1: **Euro Area predicted response to the COVID-19-induced uncertainty shock.** 'Time to trough': number of months for the peak impact on industrial production to occur. 'Time to rebound': number of months for year-over-year growth in industrial production to go back to zero.

	March 2020 shock (historical shock persistence)	
	Industrial Production	Inflation
Peak y-o-y loss	−15.41%	−1.35%
Time to trough	7 months (September 2020)	6 months (August 2020)
Time to rebound	15 months (May 2021)	–
	March 2020 shock (increased shock persistence)	
Peak y-o-y loss	−18.96%	−1.90%
Time to trough	7 months (September 2020)	9 months (November 2020)
Time to rebound	17 months (July 2021)	–
	March 2020 shock (historical persistence) and Fall 2020 shock	
Peak y-o-y loss	−17.28%	−2.17%
Time to trough	10 months (December 2020)	10 months (December 2020)
Time to rebound	18 months (August 2021)	–

in the COVID-19 pandemics. We first assume that uncertainty can go back to normal levels much more slowly in the current situation than in the past, given the persisting uncertainty in delivering a vaccine could span several months. Alternatively, a second unexpected spike in uncertainty may occur following a new wave of the pandemic in the coming 6 to 9 months. In order to construct these two possible scenarios we compute GIRFs by feeding a sequence of shocks. We generalize the GIRF definition in equation (2) with the following:

$$GIRF_{Y,t}(h, \boldsymbol{\delta}, \boldsymbol{\varpi}_{t-1}) = \mathbb{E}\left[\mathbf{Y}_{t+h} \mid \boldsymbol{\delta}, \boldsymbol{\varpi}_{t-1}\right] - \mathbb{E}\left[\mathbf{Y}_{t+h} \mid \boldsymbol{\varpi}_{t-1}\right], \tag{3}$$

where now $\boldsymbol{\delta}$ is vector including several unexpected shocks hitting at different times, or $\boldsymbol{\delta} = [\delta_t, \delta_{t+1}, ..., \delta_{t+H}]$.

We operationalize the first scenario assuming our uncertainty indicator, on top of being hit by a 10 standard deviation shock in period 1, is also hit by a sequence of small shocks for six months so as to mimic a scenario in which uncertainty comes back to normal levels only slowly.[15] In the second scenario, our uncertainty indicator is also hit by a 7.5 standard deviation shock after 7 months, or in September 2020, so as to mimic the effects of a possible new epidemic wave.[16]

Figure 6 and Table 1 report the results of these two exercises. Both scenarios would exacerbate

[15] Specifically we use $\boldsymbol{\delta} = [\delta_t, \delta_{t+2}, \delta_{t+3}, \delta_{t+4}, \delta_{t+5}, \delta_{t+6}, \delta_{t+7}] = [10, 1, 1, 1, 0.5, 0.5, 0.5]$.

[16] In a recent interview on April 1 2020, Yale University Professor Nicholas Christakis (MD, PhD, MPH) states that in Fall 2020 the US will have a 75% chance of getting a second wave of the pandemic (the podcast by the *Journal of American Medical Association* (JAMA) Network is available at https://edhub.ama-assn.org/jn-learning/audio-player/18393767). We use this information to calibrate the size in standard deviations of our Fall shock: $75\% \cdot 10 = 7.5$.

the depth and length of the COVID-19 induced recession, by enlarging the maximum loss in industrial production and by shifting the time of the peak loss and the time of the rebound farther in future. In the case of a new fall wave, our simulations predict the trough to happen in December 2020 and the rebound in August 2021.

Surprisingly, the effect of the hypothetical September 2020 shock is small notwithstanding its size. This is because in the simulations consumer confidence endogenously subsides after the initial shock and hence the new uncertainty shock arrives in less pessimistic (or rather normal) times (Pellegrino (2017) discusses the effect of mean reversion in a fully nonlinear IVAR). This implies that we are conservative in our findings. In the Appendix we show that, in a situation in which consumer confidence is not allowed to mean revert for the first 6 months – a plausible case for the COVID pandemic –, even shocks of half size of those considered in this Section still imply a similar impact on real activity and inflation.

4 Conclusion

We analyze the impact of the COVID-19 shock via its uncertainty channel using an IVAR model for the Euro Area. The COVID-19 shock can be interpreted as a rare natural disaster shock that because of its long-term consequences also affects economic uncertainty, as documented by Ludvigson, Ma, and Ng (2020) and Baker, Bloom, Davis, and Terry (2020). As the latter studies, we rely on past historical data to predict the macroeconomic impact of the COVID-19 induced uncertainty shock, and as such appropriate caveats apply to our analysis. However, to try mitigating them, we considered alternative scenarios accounting for a possible different propagation of this huge uncertainty shock.

Our results suggest that the impact of an uncertainty shock in the Euro area is highly state-dependent, and varies according to the expectations for the economic outlook as measured by several confidence survey-measures. Using the estimated IVAR model, we assess that the rebound after the COVID-19 epidemics will be slow and painful - even if impact occurred only through the massive increase in uncertainty. This is caused by the uncertainty shock hitting the Euro area economy at a time of a severely negative economic outlook. Even when lockdowns will gradually be relaxed, there will still be a drag on the Euro Area economy given by the heightened level of uncertainty about the future.

The current experience is unique, in that measures of uncertainty registered surges in both the

Covid Economics 18, 15 May 2020: 196-221

US and the Euro Area equal to several standard deviations, and measures of economic sentiment simultaneously hit their record bottom. If the uncertainty-channel alone can explain up a substantial share of the overall cost of the COVID-19 disaster shock, policymakers ought to seriously consider enacting clear policies aimed not only at boosting confidence in the outlook, but specifically targeted at resolving the uncertainty, by providing to the public contingent scenarios and policies ready to be adopted if the worst-case outcomes materialize .

Covid Economics 18, 15 May 2020: 196-221

Covid Economics 18, 15 May 2020: 196-221

References

Andreasen, M. M., J. Fernández-Villaverde, and J. F. Rubio-Ramírez (2017): "The pruned state-space system for non-linear DSGE models: Theory and empirical applications," *The Review of Economic Studies*, 85(1), 1–49.

Baker, S., N. Bloom, and S. J. Davis (2016): "Measuring Economic Policy Uncertainty," *Quarterly Journal of Economics*, 131(4), 1539–1636.

Baker, S. R., N. Bloom, S. J. Davis, and S. J. Terry (2020): "Covid-induced economic uncertainty," Discussion paper, National Bureau of Economic Research.

Barsky, R. B., and E. R. Sims (2012): "Information, animal spirits, and the meaning of innovations in consumer confidence," *American Economic Review*, 102(4), 1343–77.

Basu, S., and B. Bundick (2017): "Uncertainty Shocks in a Model of Effective Demand," *Econometrica*, 85(3), 937–958.

Bernanke, B. S. (1983): "Irreversibility, Uncertainty, and Cyclical Investment," *Quarterly Journal of Economics*, 98(1), 85–106.

Bloom, N. (2009): "The Impact of Uncertainty Shocks," *Econometrica*, 77(3), 623–685.

Caballero, R. (1990): "Consumption Puzzles and Precautionary Savings," *Journal of Monetary Economics*, 25, 113–136.

Cacciatore, M., and F. Ravenna (2020): "Uncertainty, Wages, and the Business Cycle," HEC Montreal, mimeo.

Caggiano, G., and E. Castelnuovo (2019): "Global Uncertainty," Monash University and University of Melbourne, available at https://sites.google.com/site/efremcastelnuovo/.

Caggiano, G., E. Castelnuovo, and N. Groshenny (2014): "Uncertainty Shocks and Unemployment Dynamics: An Analysis of Post-WWII U.S. Recessions," *Journal of Monetary Economics*, 67, 78–92.

Caggiano, G., E. Castelnuovo, and R. Kima (2020): "The global effects of Covid-19-induced uncertainty," Monash University and University of Melbourne, available at https://sites.google.com/site/efremcastelnuovo/.

Caggiano, G., E. Castelnuovo, and G. Pellegrino (2017): "Estimating the Real Effects of Uncertainty Shocks at the Zero Lower Bound," *European Economic Review*, 100, 257–272.

Castelnuovo, E. (2016): "Modest Macroeconomic Effects of Monetary Policy Shocks During the Great Moderation: An Alternative Interpretation," *Journal of Macroeconomics*, 47, 300–314.

Christiano, L. J., M. Eichenbaum, and C. Evans (1999): "Monetary Policy Shocks: What Have We Learned and to What End?," In: J.B. Taylor and M. Woodford (eds.): Handbook of Macroeconomics, Elsevier Science, 65–148.

EuropeanCommission (2020): "Flash Consumer Confidence Indicator for EU and Euro Area, Press Release, 23 April 2020," Discussion paper.

Fajgelbaum, P., E. Schaal, and M. Taschereau-Dumouchel (2014): "Uncertainty Traps," Working Paper 19973, National Bureau of Economic Research.

Fernández-Villaverde, J., P. Guerrón-Quintana, K. Kuester, and J. Rubio-Ramírez (2015): "Fiscal Volatility Shocks and Economic Activity," *American Economic Review*, 105(11), 3352–84.

Kilian, L., and R. Vigfusson (2011): "Are the Responses of the U.S. Economy Asymmetric in Energy Price Increases and Decreases?," *Quantitative Economics*, 2, 419–453.

Koop, G., M. Pesaran, and S. Potter (1996): "Impulse response analysis in nonlinear multivariate models," *Journal of Econometrics*, 74(1), 119–147.

Leduc, S., and Z. Liu (2016): "Uncertainty Shocks are Aggregate Demand Shocks," *Journal of Monetary Economics*, 82, 20–35.

——— (2020): "The Uncertainty Channel of the Coronavirus," *FRBSF Economic Letter*, 2020(07), 1–05.

Ludvigson, S. C., S. Ma, and S. Ng (2019): "Uncertainty and Business Cycles: Exogenous Impulse or Endogenous Response?," *American Economic Journal: Macroeconomics*, forthcoming.

Ludvigson, S. C., S. Ma, and S. Ng (2020): "Covid19 and the Macroeconomic Effects of Costly Disasters," Working Paper 26987, National Bureau of Economic Research.

Pellegrino, G. (2017): "Uncertainty and Monetary Policy in the US: A Journey into Non-Linear Territory," Melbourne Institute Working Paper No. 6/17.

——— (2018): "Uncertainty and the Real Effects of Monetary Policy Shocks in the Euro Area," *Economics Letters*, 162, 177–181.

Smets, F., and R. Wouters (2003): "An Estimated Dynamic Stochastic General Equilibrium Model of the Euro Area," *Journal of the European Economic Association*, 1, 1123–1175.

Covid Economics 18, 15 May 2020: 196-221

Covid Economics 18, 15 May 2020: 196-221

Appendix

"The Effects of COVID-19-Induced Uncertainty in the Euro Area: The role of Pessimism" by Giovanni Pellegrino, Federico Ravenna and Gabriel Züllig

A Computation of the Generalized Impulse Response Functions

This Section documents the algorithm employed to compute the state-dependent GIRFs and their confidence intervals. The algorithm follows Koop, Pesaran, and Potter (1996), with the modification of considering an orthogonal structural shock, as in Kilian and Vigfusson (2011). The algorithm is the same used in Pellegrino (2017).

The theoretical GIRF of the vector of endogenous variables $\mathbf{Y}$, h periods ahead, for a starting condition $\varpi_{t-1} = \{\mathbf{Y}_{t-1}, ..., \mathbf{Y}_{t-L}\}$, and a structural shock in date t, δ_t, can be expressed – following Koop, Pesaran, and Potter (1996) – as:

$$GIRF_{Y,t}(h, \delta_t, \varpi_{t-1}) = \mathbb{E}\left[\mathbf{Y}_{t+h} \mid \delta_t, \varpi_{t-1}\right] - \mathbb{E}\left[\mathbf{Y}_{t+h} \mid \varpi_{t-1}\right], \quad h = 0, 1, \ldots, H$$

where $\mathbb{E}[\cdot]$ represents the expectation operator. We are interested in the state-dependent GIRFs for pessimistic and normal times, which can be defined as:

$$GIRF_{Y,t}\left(h, \delta_t, \mathbf{\Omega}_{t-1}^{pessimistic\ times}\right) = \mathbb{E}\left[GIRF_{Y,t}\left(h, \delta_t, \left\{\varpi_{t-1} \in \mathbf{\Omega}_{t-1}^{pessimistic\ times}\right\}\right)\right]$$

$$GIRF_{Y,t}\left(h, \delta_t, \mathbf{\Omega}_{t-1}^{normal\ times}\right) = \mathbb{E}\left[GIRF_{Y,t}\left(h, \delta_t, \left\{\varpi_{t-1} \in \mathbf{\Omega}_{t-1}^{normal\ times}\right\}\right)\right]$$

where $\mathbf{\Omega}_{t-1}^{i}$ denotes the set of histories characterizing the state $i = \{pessimistic\ times, \quad normal\ times\}$.

The algorithm to estimate our state-conditional GIRF reads as follows:

1. pick an initial condition $\varpi_{t-1} = \{\mathbf{Y}_{t-1}, ..., \mathbf{Y}_{t-L}\}$, i.e., the historical values for the lagged endogenous variables at a particular date $t = L+1, \ldots, T$. Notice that this set includes the values for the interaction terms;

2. draw randomly (with repetition) a sequence of (n-dimensional) residuals $\{\mathbf{u}_{t+h}\}^s$, $h = 0, 1, ..H = 19$, from the empirical distribution $d(\mathbf{0}, \widehat{\mathbf{\Omega}})$, where $\widehat{\mathbf{\Omega}}$ is the estimated VCV matrix. In order to preserve the contemporaneous structural relationships among variables, residuals are assumed to be jointly distributed, so that if date t' s residual is drawn, all n residuals for date t are collected;

Covid Economics 18, 15 May 2020: 196-221

3. conditional on ϖ_{t-1} and on the estimated model (1), use the sequence of residuals $\{\mathbf{u}_{t+h}\}^s$ to simulate the evolution of the vector of endogenous variables over the following H periods to obtain the path $\mathbf{Y}^s_{t+h}$ for $h = 0, 1 \dots H$. s denotes the dependence of the path on the particular sequence of residuals used;

4. conditional on ϖ_{t-1} and on the estimated model (1), use the sequence of residuals $\{\mathbf{u}_{t+h}\}^s$ to simulate the evolution of the vector of endogenous variables over the following H periods when a structural shock δ_t is imposed to $\mathbf{u}^s_t$. In particular, we Cholesky-decompose $\widehat{\mathbf{\Omega}} = \mathbf{C}\mathbf{C}'$, where $\mathbf{C}$ is a lower-triangular matrix. Then, we recover the structural innovation associated to $\mathbf{u}^s_t$ by $\boldsymbol{\varepsilon}^s_t = \mathbf{C}^{-1}\mathbf{u}^s_t$ and add a quantity $\delta < 0$ to the scalar element of $\boldsymbol{\varepsilon}^s_t$ that refers to the uncertainty measure, i.e. $\varepsilon^s_{t,unc}$. We then move again to the residual associated with the structural shock $\mathbf{u}^{s,\delta}_t = \mathbf{C}\boldsymbol{\varepsilon}^{s,\delta}_t$ to proceed with simulations as in point 3. Call the resulting path $\mathbf{Y}^{s,\delta}_{t+h}$;

5. compute the difference between the previous two paths for each horizon and for each variable, i.e. $\mathbf{Y}^{s,\delta}_{t+h} - \mathbf{Y}^s_{t+h}$ for $h = 0, 1 \dots, H$;

6. repeat steps 2-5 for a number of $S = 500$ different extractions for the residuals and then take the average across s. Notice that in this computation the starting quarter $t-1$ does not change. In this way we obtain a consistent point estimate of the GIRF for each given starting quarter in our sample , i.e. $\widehat{GIRF}_{Y,t}(\delta_t, \varpi_{t-1}) = \left\{\widehat{\mathbb{E}}\left[\mathbf{Y}_{t+h} \mid \delta_t, \varpi_{t-1}\right] - \widehat{\mathbb{E}}\left[\mathbf{Y}_{t+h} \mid \varpi_{t-1}\right]\right\}_{h=0}^{19}$. If a given initial condition ϖ_{t-1} brings an explosive response (namely if this is explosive for most of the sequences of residuals drawn $\{\mathbf{u}_{t+h}\}^s$, in the sense that the response of the variable shocked diverges instead than reverting to zero), it is discarded and not considered for the computation of state-conditional responses at the next step;[17]

7. repeat steps 2-6 to obtain an history-conditional GIRF for each initial condition ϖ_{t-1} of interest. In particular, we select two particular subsets of initial conditions related to the historical level of consumer confidence to define two states. An initial condition $\varpi_{t-1} = \{\mathbf{Y}_{t-1}, ..., \mathbf{Y}_{t-L}\}$ is classified to belong to the "pessimistic times" state if $conf_{t-1}$ is in the

[17] While we allow this to happen for bootstrapped simulated responses, we make sure that this does not happen for point-estimated responses (i.e. our responses estimated on actual data) so that to back up the stability of the estimated IVAR . The nonlinear DSGE literature has developed the pruning method in order to preserve stability (see Andreasen, Fernández-Villaverde, and Rubio-Ramírez (2017)) but this is not currently available for nonlinear VARs.

bottom 20% of the consumer confidence empirical distribution and to the "normal times" state if $conf_{t-1}$ is in not in its bottom 20%;

8. history-dependent GIRFs obtained in step 7 are then averaged over the state they belong to produce our estimate of the state-dependent GIRFs, i.e., our $\widehat{GIRF}_{Y,t}\left(\delta_t, \mathbf{\Omega}_{t-1}^{pessimistic\ \ times}\right)$ and $\widehat{GIRF}_{Y,t}\left(\delta_t, \mathbf{\Omega}_{t-1}^{normal\ times}\right)$;

9. confidence bands around the point estimates obtained in point 8 are computed through bootstrap[18]. In particular, we simulate $R = 500$ datasets statistically equivalent to the actual sample and for each of them interaction terms are constructed coherently with the simulated series. Then, for each dataset, (i) we estimate our Interacted-VAR model and (ii) implement steps 1-8. In implementing this procedure this time we have that the starting conditions and the VCV matrix used in the computation depend on the particular dataset r used, i.e. ϖ_{t-1}^r and $\widehat{\mathbf{\Omega}}^r$. Of the resulting distribution of state-conditional GIRFs, we take the 5th and 95th percentiles to construct the 90% confidence bands.

B Supplementary results

Figure A1 plots the time series that enter our baseline IVAR.

Figure A2 plots the daily VSTOXX index, our proxy for Euro area financial uncertainty, against its monthly average.

Figure A3 plots the consumer confidence indicator released by the European Commission in April – a leading indicator of future economic activity –, which signaled a confidence level approaching the number reached during the 2008-2009 financial crisis.

Figure A4 and Table A1 complement the findings in Figure 6 and Table 1. They show that, in a situation in which consumer confidence is not allowed to mean revert for the first 6 months, even shocks of half size of those considered in Section 3.2 still imply similar findings.[19] This means that in our findings in Section 3.2 we are conservative on the possible losses implied by the COVID-19-induced uncertainty shock.

[18] The bootstrap used is similar to the one used by Christiano, Eichenbaum and Evans (1999, footnote 23). Our code repeats the explosive artificial draws to be sure that exactly 2000 draws are used.

[19] We compute the GIRF for a counterfactual where the consumer confidence level (for each of the shocked paths behind the average shocked path in equation 2 of the main paper, $\mathbb{E}\left[\mathbf{Y}_{t+h} \mid \delta_t, \boldsymbol{\varpi}_{t-1}\right]$) is not allowed to increase if not after 6 months. If the consumer confidence would increase, a counterfactual shock keeps its level constant to the last value.

Covid Economics 18, 15 May 2020: 196-221

Covid Economics 18, 15 May 2020: 196-221

Table A1: **Euro Area predicted response to the COVID-19-induced uncertainty shock: Alternative case without a fast recovery in consumer confidence** 'Time to trough': number of months for the peak impact on industrial production to occur. 'Time to rebound': number of months for year-over-year growth in industrial production to go back to zero.

	March 2020 shock (with past persistence)	
	Industrial Production	Inflation
Peak y-o-y loss	−15.41%	−1.35%
Time to trough	7 months (September 2020)	6 months (August 2020)
Time to rebound	15 months (May 2021)	–
	March 2020 shock (with increased persistence and lower confidence)	
Peak y-o-y loss	−17.71%	−1.66%
Time to trough	7 months (September 2020)	9 months (November 2020)
Time to rebound	16 months (June 2021)	–
	March 2020 shock (with past persist. and lower conf.) & plus hypoth. Fall 2020 shock	
Peak y-o-y loss	−16.29%	−1.80%
Time to trough	7 months (September 2020)	10 months (December 2020)
Time to rebound	17 months (July 2021)	–

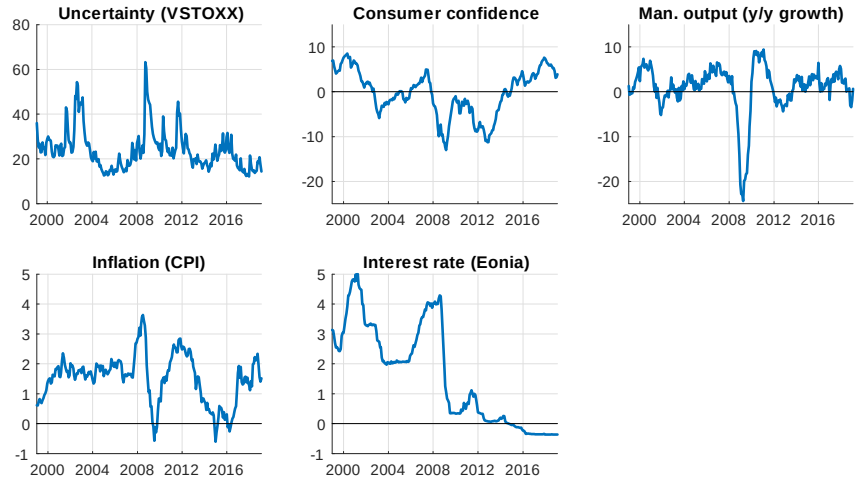

Figure A1: **Time series modeled in our baseline IVAR model.** Note: the series and their sources are given in Section 2 of the main paper. The sample period modeled is 1999m1-2020m1.

Covid Economics 18, 15 May 2020: 196-221

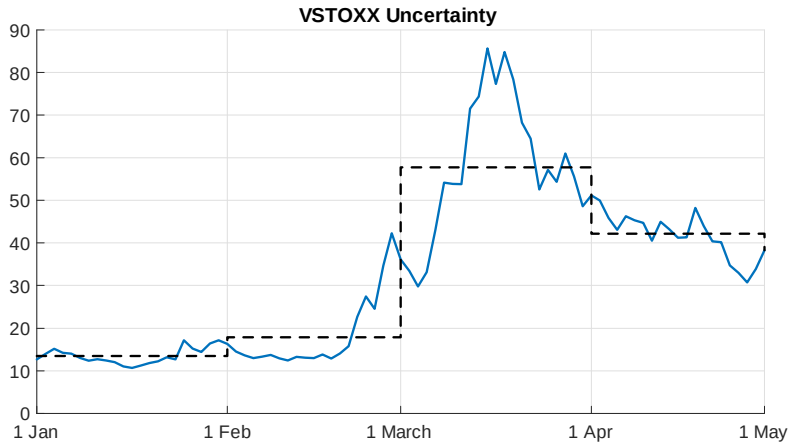

Figure A2: **VSTOXX index since January 2020.** Blue solid line: daily index. Black dashed line: monthly average.

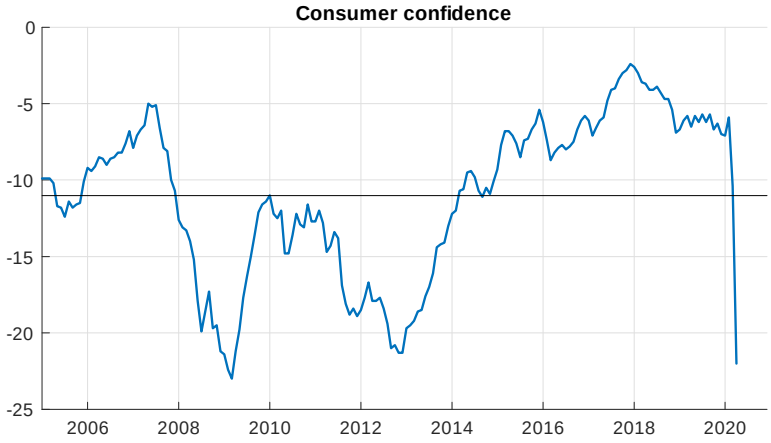

Figure A3: **European Commission consumer confidence indicator.** Blue line: time series of interest. Black line: average of the series over the period considered**.** Note: the series is available at https://ec.europa.eu/info/business-economy-euro/indicators-statistics/economic-databases/business-and-consumer-surveys/download-business-and-consumer-survey-data/time-series_en (the mnemonic is CONS.EU.TOT.COF.BS.M).

Covid Economics 18, 15 May 2020: 196-221

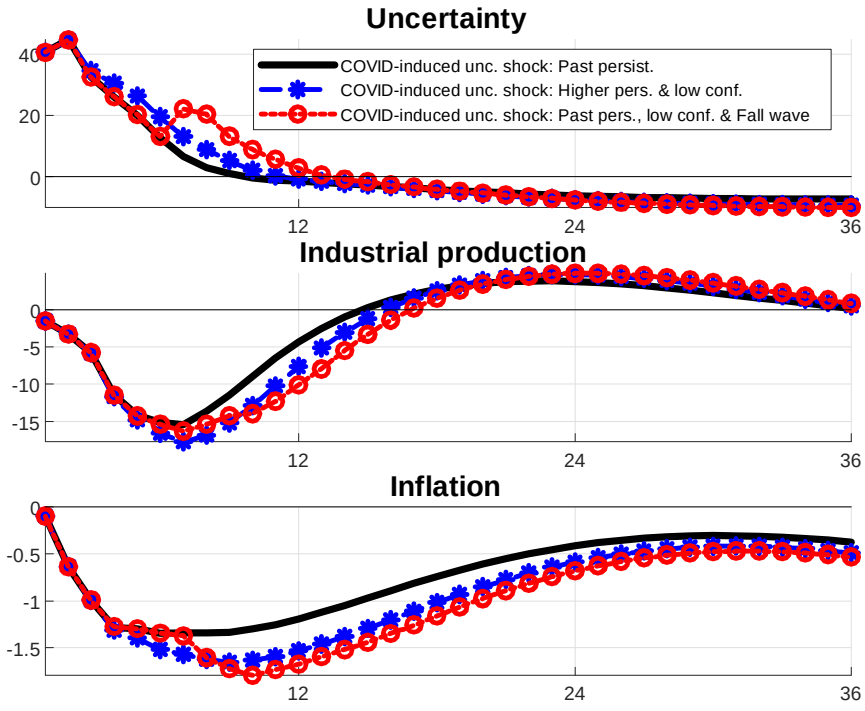

Figure A4: **The uncertainty-channel of the COVID-19 shock during pessimistic times: Alternative scenarios (case without a fast recovery in consumer confidence).** Solid black line: GIRF to a 10 standard deviation uncertainty shock hitting the economy during pessimistic times. Starred blue line: GIRF to the sequence of shocks $\boldsymbol{\delta} = [\delta_t, \delta_{t+2}, \delta_{t+3}, \delta_{t+4}, \delta_{t+5}, \delta_{t+6}, \delta_{t+7}] = [10, 0.5, 0.5, 0.5, 0.25, 0.25, 0.25]$ hitting the economy during pessimistic times (see equation 3 in the main paper). Circled red line: GIRF to the sequence of shocks $\boldsymbol{\delta} = [\delta_t, \delta_{t+6}] = [10, 3.75]$ hitting the economy during pessimistic times (see equation 3). Note: x-axis in months. The initial shock is assumed to hit in March 2020. The subsequent shocks are half of those considered for the exercise at the basis of Figure 4 in the main paper. For the computation of the counterfactual GIRF please see foonote 19.

Covid Economics Issue 18, 15 May 2020

Democracy, culture, and contagion: Political regimes and countries' responsiveness to Covid-19[1]

Carl Benedikt Frey,[2] Chinchih Chen[3] and Giorgio Presidente[4]

Date submitted: 12 May 2020; **Date accepted:** 13 May 2020; **Date revised:** 16 September 2020

A widely held belief is that autocratic governments have been more effective in reducing the movement of people to curb the spread of Covid-19. Using the Oxford COVID-19 Government Response Tracker (OxCGRT), and a real-time dataset with daily information on travel and movement across 111 countries, we find that autocratic regimes imposed more stringent lockdowns and relied more on contact tracing. However, we find no evidence that autocratic governments were more effective in reducing travel, and evidence to the contrary: countries with democratically accountable governments introduced less stringent lockdowns but were more effective in reducing geographic mobility at the same level of policy stringency. In addition, building on a large literature on cross-cultural psychology, we show that for the same policy stringency, countries with collectivist cultural traits experienced larger declines in geographic mobility relative to their more individualistic counterparts. We conclude that, in terms of reducing mobility, collectivist and democratic countries have implemented relatively effective responses to Covid-19.

1 Frey and Presidente gratefully acknowledge funding from Citi.
2 Oxford Martin School, Oxford University.
3 Oxford Martin School, Oxford University.
4 Oxford Martin School, Oxford University.

Covid Economics 18, 15 May 2020: 222-240

Covid Economics 18, 15 May 2020: 222-240

1 Introduction

The Covid-19 pandemic is unfolding at a time when democracy is in decline. Data from Freedom House (2020) shows that democracy has been in recession for over a decade, and the rate at which countries have lost civil and political rights has accelerated since the 2000s (Diamond, 2019). A key concern is that Covid-19 will exacerbate the decline of democracy. As the New York Times puts it, "China and some of its acolytes are pointing to Beijing's success in coming to grips with the coronavirus pandemic as a strong case for authoritarian rule" (Schmemann, 2020). Even the World Health Organization (WHO) has called its forceful lockdown "perhaps the most ambitious, agile and aggressive disease containment in history" (Kuo, 2020). This raises serious questions: have autocratic regimes generally been able to take more stringent policy measures to restrain people from moving around spreading the virus, and have their policies been more effective?

Governments around the world have introduced unprecedented measures to curb travel in order to halt the spread of Covid-19. Figure 1 shows how travel fell in a number of selected countries as time passed and more stringent policy measures were introduced. However, even at similar levels of policy stringency, there is a wide variation in cross-country mobility. In this paper, we examine the institutional and cultural underpinnings of this variation, tracing governments responses to the Covid-19 pandemic at the national level. By exploiting a real-time dataset with daily information on mobility trends and policy restrictions in 111 countries since the beginning of the lockdown, we estimate the differential responses and their effectiveness in democratic and authoritarian nation states.

We split the analysis in two stages. In the first stage, we regress an index of restrictions on mobility on daily confirmed cases of Covid-19 and their interaction with a proxy for whether a country is democratic.[1] Exploiting time variation in policy and infections, we are able to include country fixed effects and purge our estimates from country-specific characteristics potentially affecting the spread of the virus and the policy response.[2] We find that for a given number of infections, our policy stringency index was 11 percent lower in democratic countries.[3]

The second stage of our analysis regresses changes in people's mobility on policy stringency and its interaction with proxies for democracy. Again, we include country fixed effects that allows us to estimate the impact of institutions on the effectiveness of time-varying restrictions, while minimising the bias from country-specific characteristics. We find that although autocratic regimes tend to impose more stringent lockdowns, there is no evidence that they were more effective in reducing travel. On the contrary, we find robust evidence that countries

[1] Daily confirmed Covid-19 cases are assumed to be the main variable considered by policy makers when deciding on mobility restrictions.

[2] Given the daily frequency of our data and the relatively short time period under analysis, we deem it unlikely that unobserved time-varying characteristics would bias the estimated coefficients.

[3] The number refers to column 2 of Table 2 in Section 3.

Figure 1: Lockdown measures and cross-country reduction in mobility

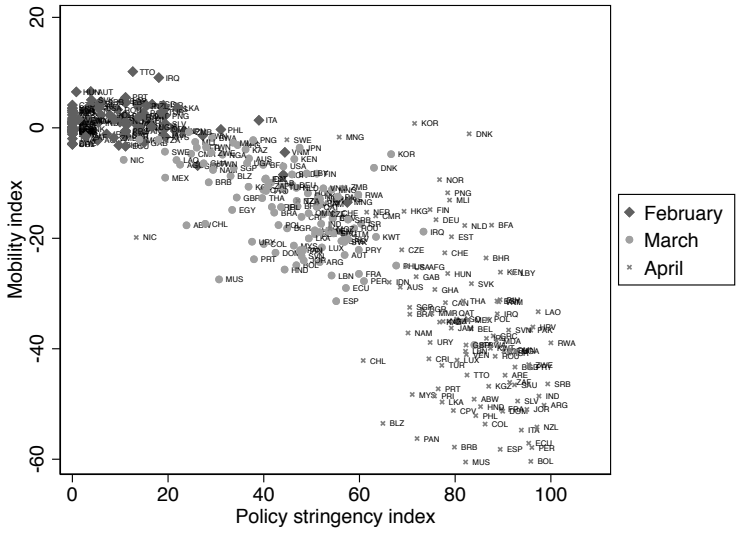

This figure shows, for each country, the monthly average mobility index (vertical axis) and the policy stringency index (horizontal axis). See Section 2 for details on the variables used.
Sources: OxCGRT; Google Community Mobility Reports

with democratically accountable governments introduced less stringent lockdowns but experienced 35% larger declines in geographic mobility at the same level of policy stringency. The positive correlation between an index of political and civil rights and our estimated elasticities of mobility to policy restrictions is presented in Figure 2. In our regression analysis, we find this relationship to be robust across a variety of specifications: in our baseline specification we find that on average, a ten percent increase in policy stringency corresponds to a 3.1% reduction in geographic mobility, while in countries with democratic government, the reduction is 4.1%.[4] In other words, governments policy measures appear to be less effective in autocratic countries in terms of reducing mobility.

It is of course possible that the capacity of the state to enforce the lockdown matters more than the political system in place. Indeed, a large literature emphasises the role the state's ability to implement a range of policies in order to effectively respond to a crisis as well as driving economic development (Besley and Persson, 2009; 2010; Fukuyama, 2011; 2015; Johnson and Koyama, 2017; Migdal, 1988).[5] To that end, we explore the role of state capacity, proxied by the percentage of armed forces in the total labour force, in shaping the effectiveness of governments responses to Covid-19. We find that at the same level of policy stringency, countries with greater state capacity saw steeper reductions in geographic mobility. However, the negative correlation between autocracy and declining mobility remains statistically significant, also

[4]The numbers refer to column 1 of Table 4 in Section 4.

[5]For instance, several scholars, including Amsden (1989); Wade (1990); and Evans (1995), have attributed the economic success of South Korea and Taiwan to state capacity.

Covid Economics 18, 15 May 2020: 222-240

Covid Economics 18, 15 May 2020: 222-240

Figure 2: Cross-country elasticities of mobility to changes in policy stringency and democracy

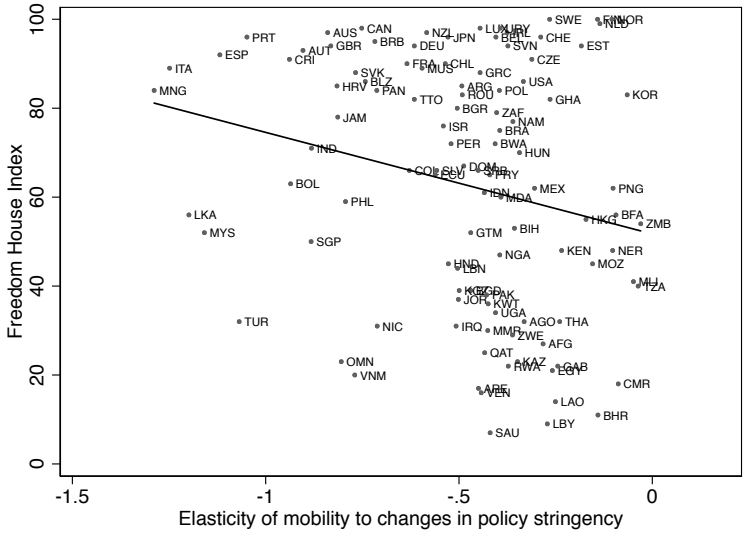

The figure shows the Freedom House Index (vertical axis) and the estimate elasticity of mobility to policy restrictions. The elasticities are calculated by estimating model (3) in Section 4 with OLS. Sources: authors' calculations based on OxCGRT, Google Community Mobility Reports and Freedom House

when accounting for state capacity.

Another complementary theory is that some cultures are more obedient than others, prompting people to better follow more stringent lockdown measures. For example, several studies have documented that Western Europeans and their cultural descendants in North America and Australia stand out as being particularly individualistic and independent, while revealing less conformity, obedience, in-group loyalty (see Heine, 2007; Henrich et al., 2010; Henrich, 2017; Schultz et al., 2019). Individualistic countries appear to have a dynamic advantage leading to higher economic growth by giving social status rewards to non-conformism and innovation (Gorodnichenko and Roland, 2011), and take out more patents for inventions (Gorodnichenko and Roland, 2017).[6] The flipside of an individualistic culture is that it can make collective action more difficult (Gorodnichenko and Roland, 2015), such as mounting a coordinated response to a pandemic. This hypothesis is supported by the positive correlation between the widely used Hofstede's (2001) scale, which we employ to measure the variation in individualism across countries, and the reduction in geographic mobility (Figure 3). Regression results show that at the same level of policy stringency, less individualistic countries experienced sharper declines in mobility, and that the relationship remains robust also when adding a full set of controls. We note that our findings are in line with research showing that individualistic cultural traits are associated with negative attitudes towards government interventions (Pitlik

[6]The observation that the United States is especially individualistic is not new and dates at least as far back as de Toqueville (1835).

and Rode, 2017).

The remainder of this paper is structured as follows. Section 2 outlines the construction of our dataset. In section 3, we discuss our empirical strategy and the determinants of policy stringency. Section 4 describes our methodology and explores the elasticity of geographic mobility to policy stringency. In section 4.2, we investigate the role of democratic institutions and state capacity in shaping the effectiveness of governments policy responses. Section 4.3 explores the role of cultural traits in understanding patterns of geographic mobility. Finally, in section 5, we outline our conclusions.

Figure 3: Cultural values and cross-country reduction in mobility

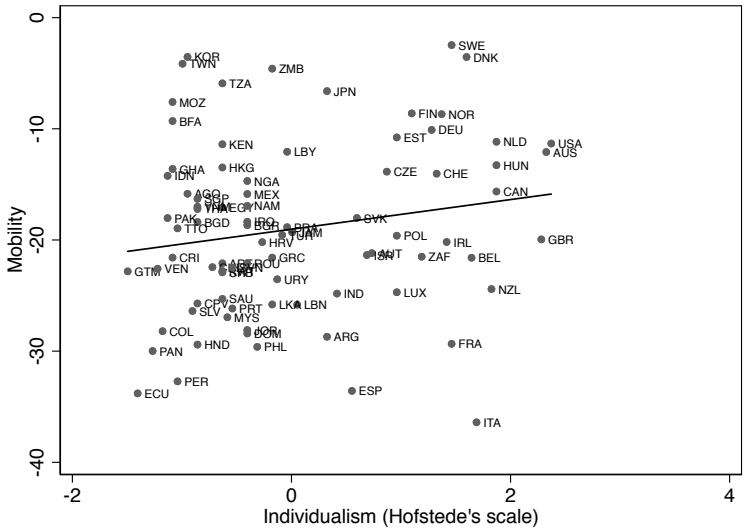

The figure shows the average mobility index (vertical axis) and a country-level measure of individualism (Hofstede's scale) on the horizontal axis. Sources: authors' own calculations based on Hofstede (2001); OxCGRT; Google's COVID-19 Community Mobility Reports

2 Data

We build a dataset allowing us to trace the daily spread of Covid-19 cases, government's response to the pandemic, and the movement of people across 111 countries over the entire lockdown period to date. Data on movement and travel were collected from Google's Community Mobility Reports, and matched with information on policy restrictions, testing, and tracing from the Oxford Covid-19 Government Response Tracker (OxCGRT) (Hale et al., 2020). Table 1 provides some summary statistics for the variables of interest in our analysis.

The Google Community Mobility Reports provide daily data on Google Maps users who have opted-in to the "location history" in their Google accounts settings across 132 countries. The reports calculate changes in movement compared to a baseline, which is the median value

Covid Economics 18, 15 May 2020: 222-240

for the corresponding day of the week during the period between the 3rd of January and the 6th of February 2020. The purpose of travel has been assigned to one of the following categories: retail and recreation, groceries and pharmacies, parks, transit stations, workplaces, and residential.

OxCGRT is a novel dataset which is published by the Blavatnik School of Government at the University of Oxford. It contains various lockdown measures, such as school and workplace closings, travel restrictions, bans on public gatherings, and stay-at-home requirements, etc. These measures are complied into a stringency index, which is constantly updated to reflect daily changes in policy. This allows us to analyse policy changes as well as geographic mobility patterns on a daily basis. Data on testing policy and contact tracing is also taken from OxCGRT.[7]

To measure democratic institutions, we collect data from three sources. Following BenYishay and Betancourt (2014), who argue that democracy constitutes both civil and political rights, we use the civil and political rights country score from Freedom in the World 2020, compiled by Freedom House. For robustness, we employ a second variable, which is a dummy variable equal to 1 if a country classified as authoritarian, taken from Dictatorship Countries Population 2020, compiled by the World Population Review. Finally, we use the revised combined POLITY Score, from Polity IV. The continuous variable captures ranges from -10 (hereditary monarchy) to +10 (consolidated democracy).

To examine the role of culture, we employ the widely used individualism-collectivism measure from Hofstede's (2001), which integrates questions about goals, achievement-orientation, and family ties.[8] One advantage with this measure is that it has been validated in a number of studies.[9] For robustness, we also create a novel measure of attitudes towards obedience and conformity using data from the World Value Survey (WVS), which is based on face-to-face interviews and uniformly structured questionnaires (Inglehart et al., 2014).[10] Inspired by the obedience and conformity dimensions highlighted by Schultz et al. (2019), we run a Principal Component Analysis (PCA) to construct an "obedience index".[11] The drawback of compiling the WVS variables into an index is that we lose observation if at least one of the subcomponents is missing for a certain country. However, we believe that this measure better captures the dimensions of obedience and conformity described by Schultz et al. (2019).

[7] See Hale et al. (2020) for more details on variable construction.

[8] A higher value on the scale corresponds to higher individualism.

[9] For an overview, see Gorodnichenko and Roland (2017)

[10] The variables are based on the percentage of respondents placing weight on the following values: obedience (respondents say whether obedience is an important value to be taught to children); proper behaviour; family ties; religiousness.

[11] The PCA shows that the first component has an eigenvalue of 2.7 and explains 54% of the variation, and that the second component has an eigenvalue of 0.97 and explains 20% of the variation. The first component has an eigenvalue larger than 1 and it explains more than half of the common variation across the variables, justifying our choice of using it as an obedience index.

Covid Economics 18, 15 May 2020: 222-240

Table 1: Summary statistics

Mobility rates	Country x Date	Mean	Std. Dev.	25%	50%	75%
Park	9375	-16.42	31.75	-38	-10	2
Retail and recreation	9459	-31.12	31.60	-61	-24	-1
Grocery & pharmacy	9424	-15.61	23.91	-30	-7	2
Workplaces	9477	-23.25	28.12	-48	-16	2
Transit	9426	-32.35	31.28	-60	-29	-2
Residential	9208	11.68	11.85	1	9	20
Policy	Country x Date	Mean	Std. Dev.	25%	50%	75%
Policy stringency index	18540	33.86	35.92	0	15.47	71.57
Contact tracing	16619	.83	0.83	0	0	2
Testing policy	16791	0.99	0.85	0	0	2
Confirmed cases	11680	6750.74	43014.02	1	61	950
Confirmed deaths	11680	437.87	2944.25	0	1	18
Democracy, state capacity, culture	N. of countries	Mean	Std. Dev.	25%	50%	75%
Civil and political rights (FH index)	210	56.70	30.64	29	61	86
Polity revised combined score	166	4.10	6.19	-1	7	9
Armed forces (%)	165	1.16	1.19	0.44	0.79	1.45
Cellphone subscriptions per 100 people	223	109.61	35.86	89.16	109.56	127.71
GDP per capita ($)	239	15122.49	22220.89	2028.18	6389.16	17277.97
Individualism (std)	102	0	1	-0.86	-0.40	0.87
Obedience (PCA index)	54	0	1.61	-1.09	0.21	1.07

The notation "std" indicates that a variable has been standardised. Sources: Google Community Mobility Reports (coverage period 15/02/2020-26/04/2020); OxCGRT (coverage period 01/01/2020-03/05/2020); Freedom House; Hofstede (2001); World Bank.

Covid Economics 18, 15 May 2020: 222-240

3 Political Regimes and Covid-19 Policy

To assess whether authoritarian governments tend to implement more stringent mobility restrictions, we estimate OLS regressions of the following form:

$$\Phi_{c,t} = \alpha_0 + \alpha_1 Covid_{c,t} + \alpha_2 \Big[Covid_{c,t} \times D_c \Big] + u_c + u_t + \eta_{c,t} \tag{1}$$

Specification (1) assumes that policy stringency $\Phi_{c,t}$ in country c and date t, depends on the contemporaneous impact of Covid-19, $Covid_{c,t}$. The variable $Covid_{c,t}$ is the log number of daily confirmed cases of infection. This specification allows policy to vary between democratic and authoritarian countries, which is proxied by D_c.[12] Because $\Phi_{c,t}$ varies by country and date, (1) allows for the inclusion of country fixed effect, u_c. Time fixed effects u_t, purge the estimates from the impact of confounders affecting all countries in the sample. Given the high frequency of the data, most country-specific confounders are absorbed by the country fixed effect. However, one possibility is that there are factors associated with economic development, which might be correlated with being a democracy, that also affects policy stringency. This would lead to omitted variable bias in our regressions. To mitigate such concerns, unless differently stated, all specifications control for the interaction between the $Covid_{c,t}$, the logarithm of real GDP per capita, and the number of mobile phone subscriptions per hundred people. Building

[12]Our baseline proxy for democracy is a continuous variable taking values between 0 and 100, with higher values corresponding to stronger democratic institutions (see Section 2 for details).

on the intuition that countries that were exposed to SARS or MERS have managed Covid-19 more effectively, we also include a dummy for experience with these past epidemics.

In (1), the coefficient of interest is α_2, which measures the differential policy stringency in response to the pandemic, in democracies relative to authoritarian countries. Because D_c varies at the country level, we cluster standard errors accordingly.

3.1 Main Results

Our OLS estimates speak to the popular perception that authoritarian governments have mounted stricter lockdowns and rely more on contact tracing to curb the spread of the Coronavirus. Specifically, we find that when the number of confirmed Covid-19 infections doubles, policy stringency increases by 11% less democratic countries.[13] Many commentators have noted that countries like Taiwan and South Korea might have benefited from greater experience with past epidemics. However, on average, we find no statistically significant differences in policy stringency in countries which have been more exposed to epidemics in the past.[14] Instead, countries that experienced SARS or MERS, were more likely to implement more comprehensive testing policies (column 4 of Table 2). For instance, South Korea has implemented open public testing, such as "drive through" testing available to asymptomatic people. This might explain why South Korea did not experience a larger drop in mobility (Figure 1): strict restrictions on movement might have been unnecessary so far as it managed to contain Covid-19 early on. Finally, we note that authoritarian countries were more likely to implement contact tracing (column 6 Table 2). While we are unable to disentangle the precise factors driving these relationships, our findings speak to the general perception that democracies with a stronger sense of liberal values and privacy have been more reluctant engage in tracking the movement of people. Examples include the United States and France, which did not implement large-scale contact tracing early on during the pandemic. Table 6 of the appendix shows that the results of Table 2 hold when using alternative measures of democracy.

4 The Determinants of Geographic Mobility

In this section, we explore the effectiveness of the lockdown measures taken in reducing geographic mobility across countries. We begin by elucidating the relationship between policy stringency and geographic mobility. We next proceed to examine whether autocratic regimes have been more effective in reducing movement and travel (section 4.2). Finally, in section 4.3, we explore how different cultural traits have shaped peoples compliance with the lockdown measures taken by their governments.

[13]This can be seen in column 2 of Table 2. The average sample value of the FH index is 58.9. Therefore, cases of infection increase stringency by 0.0885 - 0.00015*58.9 = - 0.079665.

[14]We flag a country as having experience with past epidemics if they experienced more than fifty SARS or MERS cases.

Covid Economics 18, 15 May 2020: 222-240

Table 2: Determinants of policy stringency, testing policy and contact tracing

	(1) Policy stringency	(2) Policy stringency	(3) Testing	(4) Testing	(5) Contact tracing	(6) Contact tracing
Log number of COVID-19 cases	0.0467***	0.0885***	0.0325	0.107	0.0317	0.0319
	[0.00910]	[0.0188]	[0.0284]	[0.0919]	[0.0257]	[0.0890]
Cases × civil and political rights (FH)		-0.000150**		4.47e-05		-0.000979**
		[7.38e-05]		[0.000390]		[0.000446]
Cases × experience with past epidemics		-0.00412		0.102***		-0.0214
		[0.00516]		[0.0265]		[0.0315]
Observations	11,576	10,212	10,046	9,010	9,819	8,914
R-squared	0.869	0.893	0.530	0.562	0.392	0.445
Number of countries	150	127	148	126	146	126
Policy x controls	no	yes	no	yes	no	yes
Country FE	yes	yes	yes	yes	yes	yes
Time FE	yes	yes	yes	yes	yes	yes

The table presents OLS estimates from regressing the policy stringency index (columns 1-2), categorical variables for the intensity of testing (columns 3-4) and contact tracing (columns 5-6) on the log number of COVID-19 infections. Columns 2, 4 and 6 include an interaction between infections and the Freedom House index and infections, and a dummy equal to 1 if a country has experienced more than fifty SARS or MERS cases. Columns 2, 4 and 6 include as controls the interaction between infections and: i) log GDP per capita, and ii) mobile phone subscriptions per hundred people. Errors are clustered at the country-level. The coefficients with * * * are significant at the 1% level, with * * are significant at the 5% level, and with * are significant at the 10% level.

Covid Economics 18, 15 May 2020: 222-240

Our analysis is based on the following specification:

$$M_{c,t,m} = \beta_0 + \beta_1 \Phi_{c,t} + \beta_2 \left[\Phi_{c,t} \times X_c \right] + u_{c,m} + u_t + \varepsilon_{c,t,m} \tag{2}$$

where, $M_{c,t,m}$ is the mobility index in country c, date t and mobility category m. As discussed in Section 2, mobility indexes are provided for different mobility categories,

$$m = \{\text{workplace, grocery, transit, retail and entertainment, residential, park}\}$$

One concern might be that mobility in parks, for example, could be systematically higher in countries with a larger number of parks, or a temperate climate. Thus, in (2) we include country-mobility category fixed effects, $u_{c,m}$, which allow to purge the estimates from constant unobserved characteristics of each particular mobility category in a given country. In (2), the coefficient of interest is β_2, which measures the differential impact of policy stringency for countries characterised by each variable in X_c. Unless differently stated, all specifications control for the interaction between policy stringency, the logarithm of real GDP per capita, mobile phone subscriptions, and a dummy for experience with epidemics.

To construct Figure 2, we also estimate country-specific mobility elasticities to changes in policy using the following linear model:

$$M_{c,t,m} = \delta_0 + \delta_1 \Phi_{c,t} + \sum_{k=1}^{C} \delta_{2k} \left[\Phi_{c,t} \times u_k \right]$$

$$+\delta_3\Big[\Phi_{c,t} \times X_c\Big] + u_{c,m} + u_t + \varepsilon_{c,t,m} \tag{3}$$

where, C is the total number of countries and $u_k = 1$ when $k = c$.[15] The elasticity of mobility to changes in policy stringency for country c' is given by:

$$\frac{dM_{c',t,m}}{d\Phi_{c',t}} = \delta_1 + \delta_{2c'} u_{c'}$$

4.1 Main Results

By how much did geographic mobility decline as lockdown measures were introduced? On average across all countries in our sample, a ten percent increase in policy stringency is associated with a 4.2% reduction in geographic mobility (column 1 of Table 3). To put these numbers in perspective, from February to the end of April, policy stringency increased by 34% on average, which corresponds to a reduction in mobility by roughly 14%.

To be sure, the average effects discussed above hide a great deal of heterogeneity, not least since people move around for different purposes. In the United Kingdom, for example, people are allowed to commute to work provided that the job cannot be done from home. The richness of the Google Mobility Reports, which categorises all travel according to its purpose, allows us to better distinguish between essential and non-essential activities. We deem mobility related to "grocery and pharma" as well as "workplaces" to be essential travel.[16] These categories can be distinguished from mobility related to "parks" and "retail and recreation", which captures trends for places like restaurants, cafes, shopping centres, theme parks, museums, libraries, and movie theatres. We label these activities as non-essential. Based on this distinction, we find that while both essential and non-essential declined markedly in response to increases in policy stringency, non-essential mobility was 15% more responsive (columns 2-3 of Table 3).[17]

4.2 Democracy and State Capacity

As noted, while authoritarian governments have introduced stricter lockdowns (Table 2), whether they have been effective in reducing movement and travel remains an open question. To that end, we turn to exploring the relationship between democracy and the ability of governments to implement policy to reduce geographic mobility. The relationship is a priori unclear. As Gorodnichenko and Roland (2015) point out, "one cannot claim that autocracy is more efficient than

[15] To account for the possibility that country-specific elasticities depend on complementary policies, in X_c we include a dummy equal to one if a country implemented aggressively testing and tracing during the first month of the sample.

[16] While we recognise that not all workplace travel might in fact be essential, most workplaces that are still open will fall into the essential category.

[17] In making the distinction between non-essential and essential travel, we exclude mobility categories "transit" and "residential", as they might capture both essential and non-essential travel. For instance, mobility in residential places might simply capture people taking out their rubbish or collecting their mail.

Covid Economics 18, 15 May 2020: 222-240

Table 3: Elasticities of mobility to policy stringency

	(1) Mobility	(2) Non-essential	(3) Essential
Policy stringency	-41.67***	-56.49***	-48.93***
	[3.627]	[5.335]	[4.560]
Observations	47,466	15,838	15,836
R-squared	0.476	0.656	0.703
Number of country_places	666	222	222
Policy x controls	yes	yes	yes
Country FE	yes	yes	yes
Time FE	yes	yes	yes

The table presents OLS estimates from regressing all mobility categories (column1), mobility to parks, retail and entertainment (column 2) and mobility in workplaces, grocery and pharmacies (column 3) on the policy stringency index. Errors are clustered at the country-level. The coefficients with * * * are significant at the 1% level, with * * are significant at the 5% level, and with * are significant at the 10% level.

Covid Economics 18, 15 May 2020: 222-240

democracy – or vice-versa – in dealing with pathogen prevalence." For example, March and Olsen (1984) and Fukuyama (2011; 2015) have emphasized the possibility of political gridlock in democracy, while Olson (1982) has argued that interest groups can stifle democracies, especially as interest groups become powerful and organized over time. In the context of Covid-19, it is possible that political divisions and strong business interests make it harder to introduce stringent lockdowns in democracies. At the same time, Xue and Koyama (2019) find that political repression reduces social capital, and Acemoglu et al. (2019) show that democracy causes faster economic growth, through the provision of more public goods and lower levels of social unrest, which might make restriction on movement and travel more acceptable.

Our findings show that while autocracies have taken more radical measures to reduce the movement of people relative to democracies (Table 2), they have been less effective in implementing them (Table 4). Specifically, restrictions on movement are around 35% less effective in reducing geographic mobility in authoritarian countries on average.[18] Of course, one concern is that the relative effectiveness of democracies simply reflects greater state capacity. Indeed, a large literature emphasises the role of state capacity in allowing governments to implement their policies (Besley and Persson, 2009; 2010; Fukuyama, 2011; Johnson and Koyama, 2017; Migdal, 1988). Consistent with this literature, we find that the state's ability to enforce the lockdown matters. The correlation between enforcement, proxied by the percentage of armed forces' officials in the total labor force, and mobility declines, is negative and strongly significantly (columns 1-3 of Table 4). A greater ability to enforce the restrictions seems to matter less for mobility related to groceries, pharma and workplaces (column 3 of 4). This speaks to the intuition that unlawful mobility to parks and social gatherings are more likely to be sanctioned by law enforcement officials.

However, we note that even when accounting for state capacity, the democracy variable

[18]This can be seen in column 1 of Table 4. In the sample used in the table, the average value of the FH index is 63.58. Therefore, in democratic countries stringency lowers mobility by -30.6 - 0.17*63.6 = - 41.41. Thus, an increase in stringency lowers mobility by 41.4/30.6-1 = 0.35 more in democratic countries.

remains strongly economically and statistically significant. This is confirmed by the results presented in Table 7 of the appendix, which uses our alternative measures of democracy. We conclude that greater protection of political and civil rights is associated with larger reductions in geographic mobility.

Table 4: Elasticities of mobility to policy stringency: the role of democracy and state capacity

	(1) Mobility	(2) Non-essential	(3) Essential
Policy stringency	-30.62**	-35.64	-49.88***
	[14.70]	[23.48]	[18.64]
Policy stringency × civil and political rights (FH)	-0.170**	-0.215*	-0.209**
	[0.0794]	[0.119]	[0.0989]
Policy stringency × % armed forces	-4.803***	-8.364***	-4.160*
	[1.495]	[2.385]	[2.248]
Observations	43,389	14,468	14,466
R-squared	0.479	0.658	0.712
Number of country_places	606	202	202
Policy x controls	yes	yes	yes
Country FE	yes	yes	yes
Time FE	yes	yes	yes

The table presents OLS estimates from regressing all mobility categories (column 1), mobility to parks, retail and entertainment (column 2) and mobility in workplaces, grocery and pharmacies (column 3) on the policy stringency index and an interaction between policy stringency index and the Freedom House index. All columns include the interaction between policy stringency and: i) the percentage of armed forces officials as a percentage of the total labor force; ii) dummy for experience with epidemics; iii) log-real GDP per capita, and iv) mobile phone subscriptions per hundred people. Errors are clustered at the country-level. The coefficients with *** are significant at the 1% level, with ** are significant at the 5% level, and with * are significant at the 10% level.

4.3 Culture

In addition, different cultural traits may have shaped the effectiveness of governments lockdown measures. While societies differ on many cultural dimensions (see Boyd and Richerson, 1988; 2005; Henrich, 2010; 2017), cross-cultural psychologists view the individualism-collectivism distinction as the main divider (Heine, 2007; Schultz et al., 2019).[19] Specifically, we build on the intuition of Gorodnichenko and Roland (2015), who argue that collectivist countries are more capable of solving collective action problems, such as mounting a coordinated response to a pandemic.

Table 5 shows how cross-cultural differences are related to peoples compliance with their government's lockdown measures. As expected, and as shown in column 1, people in more individualistic societies were less obedient to the lockdown, where movement fell by less at the same policy stringency. This is especially true of non-essential travel, where the individualist societies stand out.

Using our obedience index instead, Table 8 of the appendix shows that in more obedient

[19]Cross-cultural differences have deep historical roots. For example, scholars have compared herders and farmers, showing that the independence and mobility of herding make herding cultures more individualistic, whereas farming cultures are more collectivistic (Nisbett et al., 2001). This is especially true of rice farming (Talhem et al., 2014). Because rice paddies need standing water, people in rice regions needed to build elaborate irrigation systems—a labour-intensive burden that fell on villages, not isolated individuals. And the legacies of rice farming are continuing to affect people in the modern world. Even within China, Talhem et al. (2014) find that people in rice regions have a more collectivist psychology today still, relative regions growing wheat.

Covid Economics 18, 15 May 2020: 222-240

societies, mobility tends to declined more at a given level of policy stringency.[20] The coefficient in column 1 is negative but not significant at conventional levels (p-value = 0.13). However, as in Table 5, the largest elasticity of mobility to policy restrictions is found for non-essential travel. In column 2, the coefficient is large, negative and statistically significant.

Table 5: Elasticities of mobility to policy stringency: the role of cultural traits

	(1) Mobility	(2) Non-essential	(3) Essential
Policy stringency	-5.981	-1.133	-16.92
	[21.62]	[34.60]	[26.15]
Policy stringency × individualism	6.026***	12.44***	4.890*
	[2.256]	[3.858]	[2.605]
Observations	33,777	11,264	11,262
R-squared	0.472	0.647	0.701
Number of country_places	474	158	158
Policy x controls	no	yes	yes
Country FE	yes	yes	yes
Time FE	yes	yes	yes

The table presents OLS estimates from regressing all mobility categories (columns1-2), mobility to parks, retail and entertainment (column 3-4) and mobility in workplaces, grocery and pharmacies (column 5-6) on the policy stringency index. Columns 1, 3 and 5 include an interaction between policy stringency index and Hofstede' scale. Columns 2, 4 and 6 replace Hofstede' scale with an index of obedience. The index of obedience is the first component of a Principal Component Analysis (PCA) based on World Value Survey (WVS) data (see Section 2 for details). All columns include as controls the interaction between policy stringency and i) log GDP per capita, and ii) dummy for experience with epidemics. Errors are clustered at the country-level. The coefficients with * * * are significant at the 1% level, with * * are significant at the 5% level, and with * are significant at the 10% level.

5 Conclusion

Democracies can get trapped in institutional arrangements that make problem-solving harder (Fukuyama, 2011; 2015). Political divisions, checks and balances, and special interest groups can cause gridlock (March and Olsen 1984; Olson, 1982), and limit democratic governments ability to effectively respond to a crisis, like Covid-19. Yet so far, as noted by the New York Times, "it is hard to draw up a conclusive balance sheet on the relative disease-fighting abilities of autocracies and democracies" (Schmemann, 2020).

This paper constitutes a first partial assessment. Exploring governments policy responses across 111 countries over the whole lockdown period up until the latest Google Mobility Reports data release, we find that even though autocracies have introduced more stringent lockdowns and use more contact tracing, democracies have seemingly been more effective in meeting the policy objective of reducing geographic mobility in their countries. We also show that state capacity to enforce the lockdown is associated with sharper declines in movement and travel. That said, the negative correlation between autocracy and declining mobility remains statistically significant, also when accounting for state capacity. This is in line with studies showing that political repression reduces social capital and perceptions that support cooperation (Xue and Koyama, 2019), while democracies provide more public goods and experience

[20]The relatively low number of observations in Table 8 is due to the data limitations involved in the construction of the obedience index (see Section 2).

Covid Economics 18, 15 May 2020: 222-240

less social unrest (Acemoglu et al., 2019), making people more likely to follow and support government interventions in democratic societies. However, what drives this relationship is a line of enquiry that deserves further attention.

Finally, building on a growing literature showing that individualistic societies—where conformity, obedience, in-group loyalty are perceived to be less important—tend to be more dynamic and innovative, we provide evidence that for a given level of policy stringency, more conformist countries saw steeper declines in travel relative to their more individualistic counterparts. In other words, the flipside of the individualism that drives dynamism and inventiveness is that it makes collective action harder, such as a collective coordinated response to a pandemic. Indeed, countries with more individualistic cultural traits have more negative attitudes towards government interventions (Pitlik and Rode, 2017).

Our results lead us to conclude that collectivist and democratic countries have mounted relatively effective responses to Covid-19 in terms of reducing geographic mobility. However, cultural traits and the form of government in place are likely to be interrelated. For instance, Gorodnichenko and Roland (2015) have shown that collectivist countries are more likely to experience a transition towards autocracy while individualist countries are more likely to experience a transition towards democracy. Therefore, in light of our results, an interesting direction for future research is studying how compliance with mobility restrictions varies across the individualism-collectivism spectrum in countries with similar institutional arrangements.

Covid Economics 18, 15 May 2020: 222-240

References

[1] Acemoglu, D., Naidu, S., Restrepo, P., & Robinson, J. A. (2019). Democracy does cause growth. Journal of Political Economy, 127(1), 47-100.

[2] Amsden, A. H. (1989). Asia's next giant: South Korea and late industrialization. Oxford University Press.

[3] BenYishay, A., & Betancourt, R. (2014). Unbundling democracy: Political rights and civil liberties. Journal of Comparative Economics, 42(3), 552-568.

[4] Besley, T., & Persson, T. (2009). The origins of state capacity: Property rights, taxation, and politics. American economic review, 99(4), 1218-44.

[5] Besley, T., & Persson, T. (2010). State capacity, conflict, and development. Econometrica, 78(1), 1-34.

[6] Boyd, R., & Richerson, P. J. (1988). Culture and the evolutionary process. University of Chicago Press.

[7] Boyd, R., & Richerson, P. J. (2005). The origin and evolution of cultures. Oxford University Press.

[8] Chua, R. Y., Huang, K. G., & Jin, M. (2019). Mapping cultural tightness and its links to innovation, urbanization, and happiness across 31 provinces in China. Proceedings of the National Academy of Sciences, 116(14), 6720-6725.

[9] Diamond, L. (2020). Ill Winds: Saving Democracy from Russian Rage, Chinese Ambition, and American Complacency. Penguin Books.

[10] Evans, P. B. (1995). Embedded autonomy: States and industrial transformation. Princeton University Press.

[11] Fendos, J. (2020). Lessons From South Korea's COVID-19 Outbreak: The Good, Bad, and Ugly. The Diplomant, March 10.

[12] Freedom House (2020). Democracy Index. https://freedomhouse.org/countries/freedom-world/scores

[13] Fukuyama, F. (2011). The origins of political order: From prehuman times to the French Revolution. Farrar, Straus and Giroux.

[14] Fukuyama, F. (2015). Political order and political decay: From the industrial revolution to the globalization of democracy. Macmillan.

[15] Google LLC "Google COVID-19 Community Mobility Reports."

Covid Economics 18, 15 May 2020: 222-240

[16] Gorodnichenko, Y., & Roland, G. (2011). Which dimensions of culture matter for long-run growth?. American Economic Review, 101(3), 492-98.

[17] Gorodnichenko, Y., & Roland, G. (2015). Culture, institutions and democratization (No. w21117). National Bureau of Economic Research.

[18] Gorodnichenko, Y., & Roland, G. (2015). Are there cultural obstacles to democratisation?. VoxEU, May 14.

[19] Gorodnichenko, Y., & Roland, G. (2017). Culture, institutions, and the wealth of nations. Review of Economics and Statistics, 99(3), 402-416.

[20] Hale, Thomas, Sam Webster, Anna Petherick, Toby Phillips, and Beatriz Kira (2020). Oxford COVID-19 Government Response Tracker, Blavatnik School of Government. Data use policy: Creative Commons Attribution CC BY standard.

[21] Heine, S. (2007). Cultural Psychology. New York: Norton

[22] Henrich, J. (2017). The secret of our success: how culture is driving human evolution, domesticating our species, and making us smarter. Princeton University Press.

[23] Henrich, J., Heine, S. J., & Norenzayan, A. (2010). The weirdest people in the world?. Behavioral and Brain Sciences, 33(2-3), 61-83.

[24] Hofstede, G. (2001). Culture's consequences: Comparing values, behaviors, institutions and organizations across nations. Sage Publications.

[25] Inglehart, R., Haerpfer, C., Moreno, A., Welzel, C., Kizilova, K., Diez-Medrano, J., ... & Puranen, B. (2014). World values survey: Round six-country-pooled datafile version. Madrid: JD Systems Institute, 12.

[26] Johnson, N. D., & Koyama, M. (2017). States and economic growth: Capacity and constraints. Explorations in Economic History, 64, 1-20.

[27] Kuo, L. (2020). How did China get to grips with its coronavirus outbreak?. The Guardian, March 9.

[28] March, J. and Olsen, J.P. (1984). The new institutionalism: organizational factors in political life. The American Political Science Review, 78(3), 734-749.

[29] Migdal, J. S. (1988). Strong societies and weak states: state-society relations and state capabilities in the Third World. Princeton University Press.

[30] Nisbett, R. E., Peng, K., Choi, I., & Norenzayan, A. (2001). Culture and systems of thought: holistic versus analytic cognition. Psychological Review, 108(2), 291.

Covid Economics 18, 15 May 2020: 222-240

[31] Olsen, M. (1982). The rise and decline of nations: economic growth, stagflation, and social rigidities. Yale University Press.

[32] Pitlik, H., & Rode, M. (2017). Individualistic values, institutional trust, and interventionist attitudes. Journal of Institutional Economics, 13(3), 575-598.

[33] Wade, R. (1990). Governing the market: Economic theory and the role of government in East Asian industrialization. Princeton University Press.

[34] Schmemann, S. (2020) The Virus Comes for Democracy Strongmen think they know the cure for Covid-19. Are they right?, New York Times, April 2.

[35] Schulz, J. F., Bahrami-Rad, D., Beauchamp, J. P., & Henrich, J. (2019). The Church, intensive kinship, and global psychological variation. Science, 366(6466).

[36] Talhelm, T., Zhang, X., Oishi, S., Shimin, C., Duan, D., Lan, X., & Kitayama, S. (2014). Large-scale psychological differences within China explained by rice versus wheat agriculture. Science, 344(6184), 603-608.

[37] Tocqueville, A. D. (2000). Democracy in America. 1835. Trans. Harvey C. Mansfield and Delba Winthrop. Chicago: University of Chicago Press.

[38] Xue, M. M., & Koyama, M. (2019). Autocratic rule and social capital: evidence from imperial China. Working paper.

Covid Economics 18, 15 May 2020: 222-240

Covid Economics 18, 15 May 2020: 222-240

Table 6: Determinants of policy stringency, testing policy and contact tracing (alternative democracy variables)

	(1) Policy stringency	(2) Policy stringency	(3) Testing	(4) Testing	(5) Contact tracing	(6) Contact tracing
Log number of COVID-19 cases	0.0964***	0.0912***	0.116	0.137	0.0834	0.0936
	[0.0179]	[0.0189]	[0.0876]	[0.0842]	[0.0873]	[0.0840]
Cases × autocratic country (WPR)	0.00884*		0.00310		0.0259	
	[0.00465]		[0.0244]		[0.0321]	
Cases × Polity revised combined score		-0.000772***		-0.000707		-0.00345*
		[0.000265]		[0.00146]		[0.00181]
Cases × experience with past epidemics	-0.00245	-0.00441	0.103***	0.106***	-0.00837	-0.00930
	[0.00527]	[0.00483]	[0.0251]	[0.0272]	[0.0310]	[0.0294]
Observations	10,448	9,692	9,134	8,521	9,010	8,394
R-squared	0.890	0.905	0.560	0.571	0.431	0.456
Number of countries	131	119	129	118	128	117
Policy x controls	yes	yes	yes	yes	yes	yes
Country FE	yes	yes	yes	yes	yes	yes
Time FE	yes	yes	yes	yes	yes	yes

The table presents OLS estimates from regressing stringency index (columns 1-2), categorical variables for the intensity of testing (columns 3-4) and contact tracing (columns 5-6) on the log number of COVID-19 infections. Columns 1, 3 and 5 include an interaction between infections and a dummy equal to 1 if the World Population Review flags a country as a non-democracy. Columns 2, 4 and 6 include an interaction between infections and the revised combined polity score from Polity IV. All specifications include the interaction between infections and: i) a dummy equal to 1 if a country has experienced more than fifty SARS or MERS cases, ii) log GDP per capita, and iii) mobile phone subscriptions per hundred people. Errors are clustered at the country-level. The coefficients with *** are significant at the 1% level, with ** are significant at the 5% level, and with * are significant at the 10% level.

Table 7: Elasticities of mobility to policy stringency: the role of democracy and state capacity (alternative democracy variables)

	(1) Mobility	(2) Mobility	(3) Non-essential	(4) Non-essential	(5) Essential	(6) Essential
Policy stringency	-27.82*	-26.28*	-15.55	-13.31	-46.43**	-44.85**
	[14.90]	[13.99]	[21.64]	[20.59]	[19.00]	[17.79]
Policy stringency × autocratic country (WPR)	8.160*		8.980		9.908*	
	[4.210]		[6.338]		[5.635]	
Policy stringency × Polity revised combined score		-0.711**		-0.676		-0.935**
		[0.292]		[0.475]		[0.375]
Policy stringency × % armed forces	-3.795**	-5.018***	-8.630***	-9.544***	-2.909	-4.564**
	[1.485]	[1.489]	[2.154]	[2.183]	[2.204]	[2.290]
Observations	43,606	42,321	14,400	13,968	14,542	14,110
R-squared	0.478	0.477	0.668	0.664	0.711	0.711
Number of country_places	612	594	202	196	204	198
Policy x controls	yes	yes	yes	yes	yes	yes
Country FE	yes	yes	yes	yes	yes	yes
Time FE	yes	yes	yes	yes	yes	yes

The table presents OLS estimates from regressing all mobility categories (columns1-2), mobility to parks, retail and entertainment (column 3-4) and mobility in workplaces, grocery and pharmacies (column 5-6) on the policy stringency index. Columns 1, 3 and 5 include an interaction between policy stringency index and a dummy equal to 1 if the World Population Review flags a country as a non-democracy. Columns 2, 4 and 6 include an interaction between policy stringency index and the revised combined score from Polity IV. All columns include the interaction between policy stringency and: i) the percentage of armed forces officials as a percentage of the total labor force; ii) log GDP per capita, iii) mobile phone subscriptions per hundred people, and iv) dummy for experience with epidemics. Errors are clustered at the country-level. The coefficients with *** are significant at the 1% level, with ** are significant at the 5% level, and with * are significant at the 10% level.

Covid Economics 18, 15 May 2020: 222-240

Table 8: Elasticities of mobility to policy stringency: the role of cultural traits (obedience)

	(1) Mobility	(2) Non-essential	(3) Essential
Policy stringency	-24.59	4.047	-71.86***
	[21.55]	[37.30]	[25.39]
Policy stringency × obedience	-4.533	-11.82**	-1.252
	[2.926]	[4.930]	[3.516]
Observations	17,674	5,892	5,890
R-squared	0.471	0.633	0.719
Number of country_places	246	82	82
Policy x controls	yes	yes	yes
Country FE	yes	yes	yes
Time FE	yes	yes	yes

The table presents OLS estimates from regressing all mobility categories (column 1), mobility to parks, retail and entertainment (column 2) and mobility in workplaces, grocery and pharmacies (column 3) on the policy stringency index. All specifications include an interaction between the policy stringency index and an index of obedience. The index of obedience is the first component of a Principal Component Analysis (PCA) based on World Value Survey (WVS) data (see Section 2 for details). All columns include as controls the interaction between policy stringency and i) log GDP per capita, ii) mobile phone subscriptions per hundred people, and iii) dummy for experience with epidemics. Errors are clustered at the country-level. The coefficients with *** are significant at the 1% level, with ** are significant at the 5% level, and with * are significant at the 10% level.